
# SEDIMENTOLOGICAL AND STRATIGRAPHICAL ASPECTS OF THE SYN- TO POST-RIFT TRANSITION ON FULLY SEPARATED CONJUGATE MARGINS

Duarte Miguel Paulinha Soares

A thesis submitted in partial fulfilment of the requirements for the degree of Doctor of Philosophy at Cardiff University

September 2014

DECLARATION

This work has not been submitted in substance for any other degree or award at this or any other university or place of learning, nor is being submitted concurrently in candidature for any degree or other award.

Signed …… (candidate)

Date ……

STATEMENT 1

This thesis is being submitted in partial fulfilment of the requirements for the degree of PhD

Signed …… (candidate)

Date ……

STATEMENT 2

This thesis is the result of my own independent work/investigation, except where otherwise stated. Other sources are acknowledged by explicit references. The views expressed are my own.

Signed …… (candidate)

Date ……

STATEMENT 3

I hereby give consent for my thesis, if accepted, to be available online in the University's Open Access repository and for inter-library loan, and for the title and summary to be made available to outside organisations.

Signed …… (candidate)

Date ……

*To my mother and father.*

*In memory of Avô Zé and Avó Vidade.*

## Abstract

The integration of several industry and scientific 2D seismic surveys with various well data allowed for the first time a detailed analysis of the sedimentological, stratigraphic and architectural changes recorded during syn- to post-rift transitions on passive margins. The Northwest Iberia margin and its conjugate margin of Newfoundland formed the basis for an interpretive model. Comparison with the South Australia–East Antarctica conjugate margins enabled hypothesis testing and premise refinement.

The *breakup unconformity* concept is revised and a more comprehensive term is proposed for the stratigraphic surface recording the transition between syn- and post-rift: the lithospheric breakup surface. This new term: a) discriminates between continental crust breakup and complete lithospheric breakup as verified in several magma-poor margins, and b) takes into account the different character this surface can show according to its position on the margin. The concept of a breakup sequence is proposed as a sedimentary sequence showing a distinct architecture to strata deposited prior to the lithospheric breakup event. The breakup sequence records the depositional changes occurring across the lithospheric breakup surface due to lithospheric adjustments triggered by lithospheric breakup.

Contourites were identified for the first time as being associated with lithospheric breakup, supposedly being triggered by the lithospheric plate in-plane stress release occurring at the time of lithospheric breakup. Consequently, it is proposed that contourites can be used as an indicator for established lithospheric breakup.

On the East Antarctica margin, a surface usually dated as mid Eocene to early Oligocene by comparison with the conjugate South Australia margin, is dated as latest Maastrichtian–earliest Palaeocene using data from IODP Site 1356. This new date suggests that the surface is a lithospheric breakup surface, which can explain its generation and the overlying strong contouritic deposition.

## Author's note

Chapters 4 and 5 of this thesis were published as two papers in an international publication:

Chapter 4 has been published as: *The breakup sequence and associated lithospheric breakup surface: Their significance in the context of rifted continental margins (West Iberia and Newfoundland margins, North Atlantic)*. Soares, D.M., Alves, T.M., Terrinha, P., (2012), Earth and Planetary Science Letters 355–356, p. 311-326.

Chapter 5 has been published as: *Contourite drifts on early passive margins as indicators of established lithospheric breakup*. Soares, D., Alves T., Terrinha, P. (2014), Earth and Planetary Science Letters, 401, p. 116-131.

## Acknowledgments

My parents should be thanked in first place, as this thesis came to existence due to them, not only because they are my parents but as well because it was them who instilled in me the love for science/questioning in general (my mother) and rocks in particular (my father).

Thanks go to my three supervisors, Tiago Alves, Pedro Terrinha and Joe Cartwright, for their support during this project. Tiago Alves, as my first supervisor I want to thank for his crucial editorial work and being there when needed. Pedro Terrinha and Joe Cartwright are thanked for their help on key moments of this project. Fundação para a Ciência e a Tecnologia (FCT) is thanked for the SFRH/BD/64127/2009 PhD scholarship which allowed me to undertake this project.

I must thank DGEG/DPEP (Direcção Geral de Energia e Geologia/Divisão para a Pesquisa e Exploração de Petróleo), in particular Teresinha Abecassis, Carlos Moita, José Miguel Martins and Maria José Trindade for granting me access to their archives and use of their facilities. Cristina Roque is thanked for her help, discussions and confirmation of some of my interpretations. Carlos Kullberg is thanked for his support for my field work in Portugal. Gwenn Péron-Pinvidic and Tim Reston are thanked for providing the CAM survey. A big thank you goes to those persons behind the extremely useful projects and respective websites Academic Seismic Portal (ASP) at UTIG, the Antarctic Seismic Data Library System (SDLS), the International Ocean Discovery Program (IODP) database and the General Bathymetric Chart of the Oceans (GEBCO) from which so much data is available for researchers and without it this project would not be possible. Rafael Moura and Blueback Reservoirs are thanked for providing access to the Blueback Geophysics Toolbox plug-in for Petrel. University Centre in Svalbard (UNIS) is thanked for offering me a place on their 'Sequence Stratigraphy–A tool for basin analysis' course, one of the most enjoyable things I have done during this project. The Halifax 2008 Legacy Bursary 2008 (a big thanks to David Brown) and the organization of the Atlantic Conjugate Margins Conference 2014–St. John's are thanked for their generous financial support, which allowed me to attend this conference. I thank the reviewers of my papers, Javier Hernández-Molina, Adriano Viana and three anonymous reviewers, for their very useful comments who greatly helped improve

the quality of my work. The staff from Cardiff University is thanked, especially Gwen Pettigrew for her computer expertise and humour.

These years spent at the 3D Lab group in Cardiff University allowed me to meet many people that were important for several reasons during the completion of this project. With them, I had many scientific discussions, they helped me with my work, they provided moments of good fun, and in general they helped preserve my mental sanity intact while writing. They are Martino, Davide & Ana, Aldina (plus thanks for your house while doing work in Lisbon to avoid commuting–part 2), Bledd, Ricardo, Iqbal, Cristina, Chris, Kamal, and all the other colleagues from the 3D Lab. The above mentioned extends to people from other groups as well: Paola, Laura, Maggi, Anabel, Scott and Katie. Lesley Cherns is thanked for her friendship, her teachings while in the field in the Cantabria Mountains (I will miss that!) and her love for Palaeontology, which helped maintain mine on.

Of course, not only those associated with Geology are to be thanked, other people played an important role in my life at Cardiff to who I need to thank: Treena Huang (thank you very much! :), Adam & Ana, Katia (& Martino), Mafalda & Zé, Rita & Jon (plus Sarah & Sophie), Bei-Shan (Mei-mei), Hung-Chang, Jia-Hau, Hélio, Sara, Padmasimha (I will miss your great Yoga classes a lot).

During the completion of this thesis I went back to Portugal, not only on holidays but for work as well. Some friends should be thanked for hearing me complaining about the Welsh weather and the project in general: Alcobia, Paulo & Ana, Pedro & Karina, Alvaro, André, Gabi (thanks for your house while working in Lisbon to avoid commuting–part 1), Pastor and many others.

At last but most importantly, is the giant thank you I owe to my wife. Huiyu helped me through these years, while she was doing a PhD as well. She fed me (I have many meals to cook to pay you back!), supported me, wisely advised me on many things and gave me her love even during the many days I arrived home long after she was in bed and many weekends without resting. I could not have done this without her. Thank you, very much :)

# Table of Contents



## Chapter One

## Chapter Two



## Chapter Three



## Chapter Four

## Chapter Five



## Chapter Six

## Chapter Seven

## Chapter Eight

# Table of abbreviations

| | |
|---|---|
| BS | Breakup sequence |
| DSDP | Deep Sea Drilling Project |
| EEU | End of extension unconformity |
| GAB | Great Australian Bight |
| HST | Highstand systems tract |
| IODP | Integrated Ocean Drilling Program |
| LBS | Lithospheric breakup surface |
| LRS | Lithospheric rifting stage |
| LST | Lowstand systems tract |
| Ma | $10^6$ years ago |
| MTD | Massive transport deposit |
| myr | $10^6$ years duration |
| OAE | Oceanic anoxic event |
| OCTZ | Ocean–continent transition zone |
| ODP | Ocean Drilling Project |
| SRS | Southern Rift System |
| TST | Transgressive systems tract |
| TWT | Two-way travel time |
| ZECM | Zone of exhumed continental mantle |

Chapter One

# INTRODUCTION

# 1.1. Project rationale and objectives

## 1.1.1. Rationale

Since the advent of plate tectonics theory, rift development and its evolution is a topic extensively studied in Geology (*e.g.* Ziegler, 1988; Banda *et al.*, 1995; Mohriak *et al.*, 2012; Roberts & Bally, 2012). The process of formation of passive margins (Mitchell & Reading, 1969; also known as Atlantic-type margins) is the culmination of a long record of intra-plate continental rifting until an overstretched continental lithosphere fails, leading to its separation and the accretion of normal oceanic crust. This process can be divided in two main phases, the syn-rift and the post-rift stages. The transition between these two stages occurs when complete continental lithosphere separation is finally achieved (lithospheric breakup) and the definitive accretion of oceanic crust ensues (*e.g.* Wilson, 1965; Rosendahl, 1987; Buck, 2007).

A *breakup unconformity*, as defined by Falvey (1974), is a basin-wide angular unconformity generated at the time of breakup and onset of oceanic crust accretion, across which syn-rift deposits and basin bounding faults are overlapped by flat lying post-rift deposits. Not all rifted margins display this type of unconformity, but several do (Tankard & Welsink, 1987; Wernicke & Tilke, 1989; Embry & Dixon, 1990; Withjack *et al.*, 1998; Jungslager, 1999; Whitmarsh & Wallace, 2001; Kyrkjebø *et al.*, 2004; Dupré *et al.*, 2007; Autin *et al.*, 2010; Mohriak & Fainstein, 2012).

To understand the origin of such unconformities is crucial to the recognition of the mechanisms that control continental extension and rupture of conjugate margins. Nonetheless, the geological meaning of the *breakup unconformity* is still ambiguous. Is this unconformity a stratigraphic feature that marks the end of rifting and the beginning of drifting? Is the end of rifting a process that can generate a basin wide stratigraphic feature such as the so called *breakup unconformity*?

In fact, in recent years, with the ongoing paradigm shift caused by the discovery that in several margins continental breakup is not promptly associated with the generation of normal oceanic crust (resulting instead on the generation of a

transitional zone with exhumation and thinning of the lower lithosphere), led several authors to regard the existence of a '*breakup unconformity*' as doubtful (Manatschal, 2004; Péron-Pinvidic *et al.*, 2007; Sibuet *et al.*, 2007b; Tucholke *et al.*, 2007a).

In effect, the basinward migration of the extensional locus experienced on continental margins ongoing rifting is more strongly felt on a margin where exhumation of continental mantle occurs. Therefore, at the same time mantle exhumation occurs on distal margins, the thinned, ruptured continental crust records a period of relative tectonic quiescence (*e.g.* Pérez-Gussinyé *et al.*, 2003; Reston, 2005). As the classical main geometrical indicator for the presence of syn-rift sediments is their thickening (fanning) against footwalls (*e.g.* Prosser, 1993; Driscoll *et al.*, 1995), how can the latter stages of rifting and mantle exhumation be identified on most continental margins, as correlative syn-rift sediments are accumulating at this stage in a relative tectonic quiescent environment in shelf and slope basins?

The conjugate margins of West Iberia–Newfoundland are the best studied examples of rift evolution in a magma-poor rift system, (Wilson, 1975; Boillot *et al.*, 1980; Tucholke *et al.*, 1989; Pinheiro *et al.*, 1996; Manatschal & Bernoulli, 1998; Pérez-Gussinyé *et al.*, 2003; Péron-Pinvidic *et al.*, 2007; Tucholke *et al.*, 2007a; *e.g.* Afilhado *et al.*, 2008; Alves *et al.*, 2009; Miranda *et al.*, 2009; Ranero & Pérez-Gussinyé, 2010; Reston & McDermott, 2014). In particular, several reflection and refraction seismic surveys were acquired in West Iberia throughout the past 50 years exclusively with scientific purposes (*e.g.* Black *et al.*, 1964; Montadert *et al.*, 1974; Dean *et al.*, 2000; Tucholke & Holbrook, 2001; Henning *et al.*, 2004). In addition, the West Iberia–Newfoundland conjugate margins have been the target of six scientific drilling campaigns (five in West Iberia, one in Newfoundland), with the objective of studying their geological history and evolution (Sibuet *et al.*, 1979; Boillot *et al.*, 1987b; Sawyer *et al.*, 1994; Whitmarsh *et al.*, 1998; Tucholke *et al.*, 2004; Expedition 339 Scientists, 2012).

Given the abundance of published work, public available datasets and thorough scientific understanding of Iberia-Newfoundland, they are a privileged natural

laboratory to develop further work regarding the evolution of conjugate margins. Adding to the wealth of publicly available data—which are mainly from the distal margin of Northwest Iberia—for this project industry seismic and well data from the Northwest Iberia inner proximal and outer proximal margins were kindly made available by DGE/DPEP (Direcção Geral de Energia e Geologia/Divisão para a Pesquisa e Exploração de Petróleo).

This integration of industry and publicly available data allowed for the first time a holistic regional approach (from inner proximal to distal areas) to the rifting history of Northwest Iberia and, in particular, the analysis of sedimentary and stratigraphical changes triggered by the lithospheric breakup event.

### 1.1.2. Objectives

This thesis investigates how the complete separation of conjugate margins results in changes in the sedimentological and stratigraphic record of rifted margins from shallow marine to distal environments. Besides promoting the scientific advance of our society, the main objective of this research is to provide a better understanding in the way this transition is viewed in terms of its sedimentology, stratigraphy and depositional architecture. Another important objective of this research is to provide the scientific community with new tools to identify on seismic and well data the stratigraphic position of syn- to post-rift transitions.

## 1.2. Lithospheric extension – the rifting process

The formation of passive margins (Mitchell & Reading, 1969; also known as Atlantic-type margins) is the culmination of a long history of intra-plate continental rifting, in which an overstretched continental lithosphere fails leading to breakup and the formation of new oceanic crust (Bond & Kominz, 1988; Lister *et al.*, 1991).

This process can be separated in two main phases in terms of temporal span and processes, the syn-rift and the post-rift stages. These two stages have distinct aspects

in terms of sedimentation patterns and characteristic structural features, as they are conditioned by distinct rifting mechanisms and subsequent passive margin evolution.

The rift initiation is the first stage of a history of lithospheric extension that may eventually culminate in continental break-up. This stage is influenced not only by the triggering factors that initiated it, but also by conditioning factors imposed by the strain type and strain rates, the rheological layering and properties of the rocks affected by rifting, the character and extension of pre-existing structures and weaknesses, crustal thickness, the evolution of thermal anomalies (which can develop before or after the extension process), and earth-surface processes like erosion and sedimentation affecting the isostatic balance (Kooi & Cloetingh, 1992; Ziegler & Cloetingh, 2004; Allen & Allen, 2005; Buck, 2007). The prolongation of lithospheric extension after rift initiation can last until continental crust separation finally occurs (the so called *continental breakup*) and oceanic lithosphere starts to form. Yet, this extensional process can be stopped at any stage of is development, generating abandoned rift arms or aulacogens (Şengör, 1995; Ziegler & Cloetingh, 2004).

Since the advent of Plate Tectonics and the concept of Wilson cycle (Wilson, 1965) as a valid model to explain continental drifting and continental margin formation (see Dott Jr, 1978; Bond & Kominz, 1988 for a historical perspective on the pre-plate tectonics theory concepts of basin formation), several other models have been proposed to explain the driving mechanisms involved in rift initiation, development and continental breakup (*e.g.* Falvey, 1974; McKenzie, 1978; Wernicke, 1981; Lister *et al.*, 1986; Huismans & Beaumont, 2011). These models, which can be numerical and/or analogical, incorporate multiple outcrop, geological, petrological and geophysical data sets, providing insights on the physically inaccessible part of our planet that is the deep subsurface.

### 1.2.1. Rift initiation

Initial studies on the driving forces leading to lithospheric extension and rifting initiation led to an end-member classification based on the genetic characteristics of rifting dynamics, the so-called *active* and *passive* rifting (Şengör & Burke, 1978; Morgan & Baker, 1983; Turcotte & Emerman, 1983; Keen, 1985; Bott, 1992a; Olsen & Morgan, 1995; Ruppel, 1995; Lesne *et al.*, 1998; Corti *et al.*, 2003; Ziegler & Cloetingh, 2004) (Fig. 1.1).

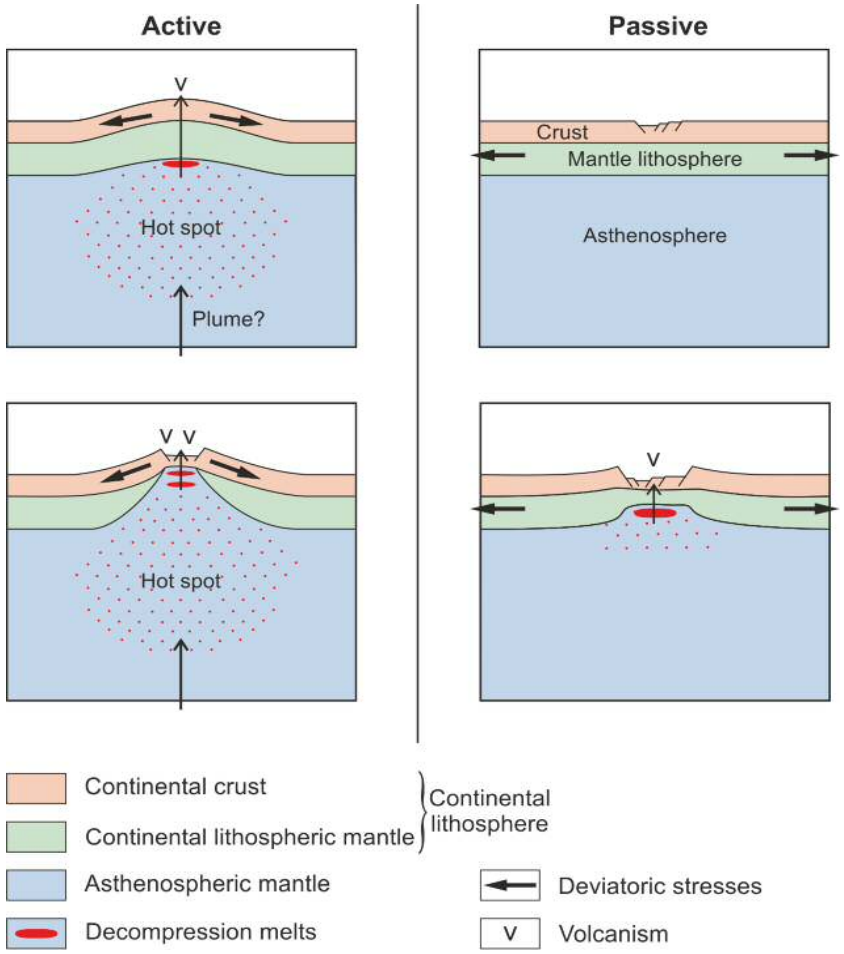


**Figure 1.1** Active and passive rifting. Redrafted and colour added from original in Bott (1995).

#### *1.2.1.1. Active rifting*

In active rifting (*e.g.* the East African Rift System) the installation of a mantle plume or the ascending margins of convection cells lead to thermal upwelling due to a lowering in density of the lithosphere, resulting in crustal doming (Fig. 1.1). Active rifting is generated due to thinning of the lithosphere via convective heating (displacing solid material upwards and recording a density loss) and adsorption into (diapiricaly rising) asthenosphere. Tensional stresses produced by thermal swelling of the crust ultimately result in rifting (Dewey & Burke, 1974; Şengör & Burke, 1978; Bott & Kusznir, 1979; Spohn & Schubert, 1982; Bott, 1992a; Storey, 1995; Corti *et al.*, 2007; Schmeling, 2010). Active rifting can explain some characteristics of rift areas such as: (1) a transition from crustal uplift to rifting; (2) rift development in zones of active compressive stresses; and (3) the association of narrow rifts with broad crustal doming and basaltic provinces (Corti *et al.*, 2003).

#### *1.2.1.2. Passive rifting*

In passive rifting the main trigger of extension is the lithospheric response to an already imposed extensional regional stress field (Fig. 1.1). Stresses acting over the plate boundaries, or imposed by differences in the gravitational potential energy, will trigger rifting. In this case, the doming and igneous intrusions generated by asthenosphere rising is a subsequent effect of the rifting process *per se*, and does not play a direct role on the rifting onset (McKenzie, 1978; White & McKenzie, 1989; Khain, 1992; Coblentz *et al.*, 1994; Corti *et al.*, 2003; Ziegler & Cloetingh, 2004; Rosenbaum *et al.*, 2008). The imposed extensional stress field is generated by distant plate boundary forces controlling the movement and interaction between tectonic plates. These forces are transmitted over large distances through the lithosphere generating an in-plane deviatoric tensional stress field (Ziegler & Cloetingh, 2004; Allen & Allen, 2005). The forces include trench pull, roll-back, ridge push and collisional resistance (Forsyth & Uyeda, 1975; Houseman & England, 1986; Bott, 1992b; Zoback, 1992; Bott, 1993; Ziegler, 1993; Cloetingh & Ziegler, 2007).

It is very likely that these forces have played a very important role in the rifting process of large continental plates such as Pangaea, as a response to the presence of

subduction zones on both sides of the supercontinent (Bott, 1992b, 1993; Ziegler, 1993). Another important mechanism generating intra-plate stresses is the presence of frictional forces exerted by the convective mantle on the base of the lithosphere (Fig. 1.2). These frictional forces are generated by shear traction when opposed to the general movement of the lithospheric plate (Ziegler & Cloetingh, 2004).

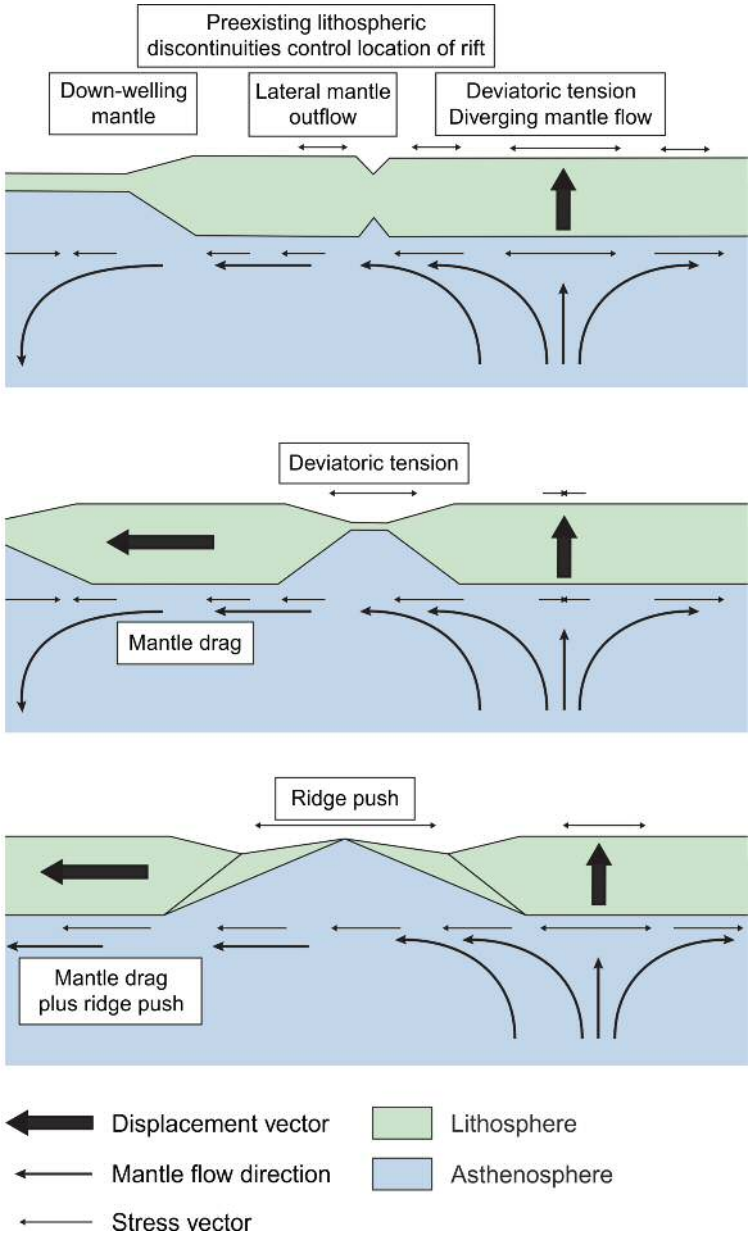


**Figure 1.2** Diagram depicting deviatoric forces due to in-plane stresses (ridge push) and frictional forces due to convective mantle upwelling. Redrafted from Ziegler & Cloetingh (2004).

According to Leeder (1995) characteristics such as (1) early rift subsidence due to normal faulting; (2) marine sediments being deposited in early rift stages (if rifting is taking place at an altitude close to sea level); (3) absence of evidence for thermal doming in the initial rifting phases and (4) profusion of igneous activity to be confined to the last stages of syn-rift, can indicate passive rifting (or *open-system* rifting as named by Leeder, 1995).

#### *1.2.1.3. Active vs. passive rifting*

Since *active* and *passive* rifting are the end members of a wider spectrum of possibilities, the most common process in nature is the generation of rifts that combine both processes and not exclusively one in isolation (Khain, 1992; Saunders *et al.*, 1992; White, 1992; Ingersoll & Busby, 1995; Leeder, 1995; Ruppel, 1995; Ziegler & Cloetingh, 2004; Allen & Allen, 2005). In fact, based on data from Phanerozoic rifts, Ziegler & Cloetingh (2004) (and again Cloetingh & Ziegler, 2007) question the need of such a rigid distinction as rift-related volcanism and associated doming is after all a consequence of the rifting process. Nevertheless, the authors also admit the possibility of using such distinction in practical terms, given the fact that the extrusion of igneous rocks early in the process of continental rifting should be related to the emplacement of a thermal anomaly under stretched crust (Fig. 1.1). Also, given the existence of completely non-volcanic rifts, one should consider the existence of totally passive rifts. It should be noted that the mentioned thermal anomaly emplacement plays a secondary role in the majority of rift systems, not driving the rifting process *per se* but instead defining the position of the future rift locus due to the weakening action (Ziegler & Cloetingh, 2004). Given this, it is likely that both mechanisms contribute to the process of rift initiation, with the predominance of one process over the other changing over time (Corti *et al.*, 2003).

Passive margins on which *active* rifting is the dominant process are named *volcanically-active margins,* being characterized by the presence of large amounts of intrusive and extrusive igneous rocks. They also record extensive seaward-dipping reflections, prominent magnetic anomalies, a short continent-ocean transition zone and considerable rift flank uplift during the rifting episode (Talwani *et al.*, 1995; Allen

& Allen, 2005). In contrast, passive margins dominantly affected by *passive* rifting—known as *non-volcanic* or *magma-poor margins*, *e.g.* the West Iberia margin—are characterized by the absence of significant igneous rocks, with magmatism being important only during the last stages of syn-rift. These margins also show a wider strip of thinned lithosphere, at times spanning over 1000 km (Keen *et al.*, 1987; Bott, 1995; Allen & Allen, 2005).

The initiation of any rifting process, active or passive, tends to exploit pre-inherited crustal weaknesses caused by the underlying mantle plumes or by pre-existing basement structures—such as transfer and deformation zones inherited from previous Wilson cycles (Dunbar & Sawyer, 1989; Lister *et al.*, 1991; Bott, 1992a; Ring, 1994; Ingersoll & Busby, 1995; Ziegler & Cloetingh, 2004; Henk, 2006; Huismans & Beaumont, 2007).

## 1.2.2. Rifting mechanisms and processes

Ingersol & Busby (1995) consider that continental rifting models should acknowledge contrasts in the character of the lithosphere, such as: (1) the rheology of different horizons, (2) contrasts in fabric, structure and composition between crust and mantle rocks, (3) contrasts between continental and oceanic crust, (4) contrasts between *active* versus *passive* rifting (considering *active* as asthenospherically driven and *passive* as lithospherically driven), (5) the presence of pre-existing crustal heterogeneities, and (6) the amount of time involved in continental rifting—a parameter influencing strain rates. More recently, models can include other factors such as thermal evolution and melt generation (*e.g.* Schmeling, 2010).

### *1.2.2.1. Rift extension modes*

From a structural point of view, three major modes of rift extension where described by Buck (1991): the narrow rifting mode; the wide rifting mode and the core complex rifting mode (Fig. 1.3). The development of each mode is dependent of parameters such as crustal thickness, differences in density between the crust and mantle, depth of the brittle-ductile transition in the crust, rheological properties of

the different lithospheric layers, thermal structure, crustal water content and extensional strain rate (Buck, 1991; Buck, 2007; Dyksterhuis *et al.*, 2007).

Considering the wide and narrow extension modes, the main difference in terms of recognisable morphologies is the width of the region affected by the extensional processes (Fig. 1.3). This width is pre-conditioned by the depth at which the fragile/ductile transition occurs, but is not particularly affected by the strain rates (Allemand & Brun, 1991; Buck, 1991; Brun, 1999).

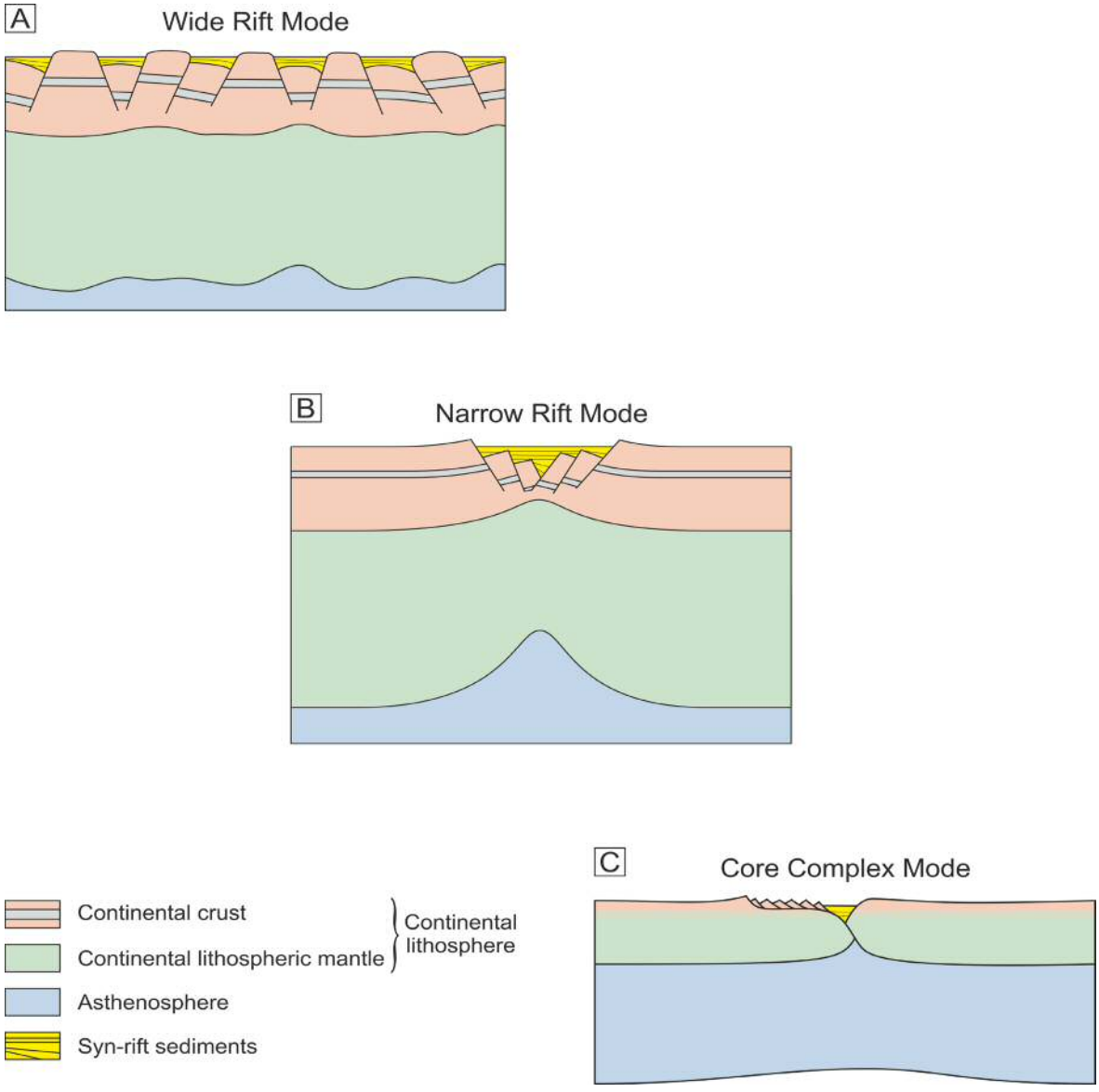


**Figure 1.3** Idealized lithospheric stretching modes. Modified from Buck (1991).

#### *1.2.2.2. Wide rifting*

Wide rifting (Fig. 1.3A) is characterized by the extension of overthickened continental crust, commonly hotter than average, over a wider region spanning over more than 800 km. Small lateral gradients in crustal thinning are observed in this case (Hamilton, 1987; Brun, 1999; Corti *et al.*, 2003; Buck, 2007). The resulting wide region of deformation is characterized by the presence of horst-and-graben systems and by a non-homogeneous partition of the total extension affecting the rift system (see Corti *et al.*, 2003 and references within).

The birth of wide rifts can be due to the lateral migration of the extensional locus from a previously weakened region of localized rifting (which become strengthened during the rifting process) to a weaker area. This 'jump' in the extensional locus can originate a wide rift if repeated several times, developing a wide rift (Buck, 2007).Several processes where proposed for this extensional jump such as (1) thermal diffusion strengthening (England, 1983; Sonder & England, 1989); (2) changes in gravitational stresses due to crustal buoyancy (Buck, 1991; Brun, 1999) (3) viscous stress strengthening (Bassi, 1991) and (4) the presence of lithospheric weaknesses (Dyksterhuis *et al.*, 2007).

The first explanation implies very low strain rates that allow for the replacement of a weaker thinning lithosphere by stronger mantle rocks (England, 1983). For this process to effectively strengthen the crust, the intruded mantle must cool down by thermal diffusion in a much more efficient way than the crustal weakening process (Buck, 2007).

The second process referred to above relies on the non-dominance of lithospheric advective weakening. Thus, given the ductile behaviour of the overheated lithosphere, the thinning can occur by means of lithospheric gravity spreading under a thick brittle upper crust due to isostatic adjustments (Brun, 1999; Buck, 2007). This way, crustal thickness heterogeneities resulting from localized thinning can promote a gravitational switching in the extension locus.

The 'viscous stress strengthening' hypothesis considers that wide rifts can be formed by a delocalization of deformation resulting from different strain rates acting on the lithosphere. This would lead to the developing of the so called *lithospheric boudinage* (Brun & Beslier, 1996; Müntener & Hermann, 2001; Buck, 2007; Reston, 2007).The presence of weaknesses over an area subjected to extensional stresses can generate several extensional loci, leading to wide rift formation (Dyksterhuis *et al.*, 2007).

#### *1.2.2.3. Narrow rifting*

Narrow rift systems (or discrete intercontinental rifts according to Ruppel, 1995) (Fig. 1.3B), occur when extension is focused on a narrow region (less than 100 km wide) of localized deformation in a region of normal crustal thickness and normal geotherms (England, 1983; Buck, 1991; Brun, 1999; Buck, 2007). Usually displaying low values of bulk extension and moderate rates of stretching (Buck *et al.*, 1999; Corti *et al.*, 2003), narrow rifting often results in large lateral changes in the amount of crustal thinning (Buck, 2007). Narrow rifting is characterized by crustal normal fault segmentation along its axis, displaying half-grabens arranged in an asymmetric way on both rift flanks (Buck, 1991; Ruppel, 1995; Brun, 1999). Towards the rift axis is commonly observed a reduction in the dimensions of the tilted blocks, as well as a decrease in the fault angle (Brun, 1999). Here, the lithosphere suffers localized necking with the Moho bending upward with a wavelength wider than the crustal expression of the rift (Brun, 1999; Buck *et al.*, 1999). This will originate high rift shoulder uplift, assumed to be generated due to intrusion of magmatic bodies lowering the crust density (Zeyen *et al.*, 1996; Ziegler & Cloetingh, 2004).

Considering the East African Rift as the archetypical example of narrow rifting, Ruppel (1995), presents a comprehensive and well referenced review of its characteristics in terms of rift segmentation, tectonics, magmatism and geophysical properties.

#### *1.2.2.4. Core complexes*

Core complexes (Figs. 1.3C, 1.4) occur where the extensional deformation is concentrated on the upper crust, accommodated by movement along low-angle detachment faults. At the same time, the lower crust is extended over a broader area by means of diffuse flow (Buck, 1988; Buck, 1991). A requirement for the occurrence of this mode is an extremely hot (and therefore weak) lithosphere in zones that were previously subjected to crustal thickening, like in post-orogenic regions (Coney, 1980; Lister & Davis, 1989; Buck, 1991; Buck *et al.*, 1999). A consequence of this extensional mode is the exhumation of middle to lower lithosphere rocks, displaying mid- to high-grade metamorphism in direct contact with low-grade or non-metamorphic rocks (Davis, 1983; Buck, 1991; Brun *et al.*, 1994; Rosenbaum *et al.*, 2005) (Fig. 1.4). Structures of this type where described from other extensional contexts, namely in oceanic crust (Blackman *et al.*, 1998; Karson, 1999; Ranero & Reston, 1999; Corti *et al.*, 2003; MacLeod *et al.*, 2009).

Given the close association between the modelled core complex formation and the wide rift mode, Brun (1999) considers core complexes as not a particular mode of extension but instead anomalies in wide rifts. Nevertheless later authors recognize it as a separated extensional mode (*e.g.* Rey *et al.*, 2001; Corti *et al.*, 2003; Rosenbaum *et al.*, 2005; Dyksterhuis *et al.*, 2007).

In practise, these three modes of rifting can be part of a continuum, representing end members of the transition that occurs among them (Ingersoll & Busby, 1995; Olsen & Morgan, 1995; Corti *et al.*, 2003; Huismans & Beaumont, 2007). In fact, the formation of wide rifts require multiple localized extensional locus that each in isolation characterize narrow rifting (Buck, 2007).

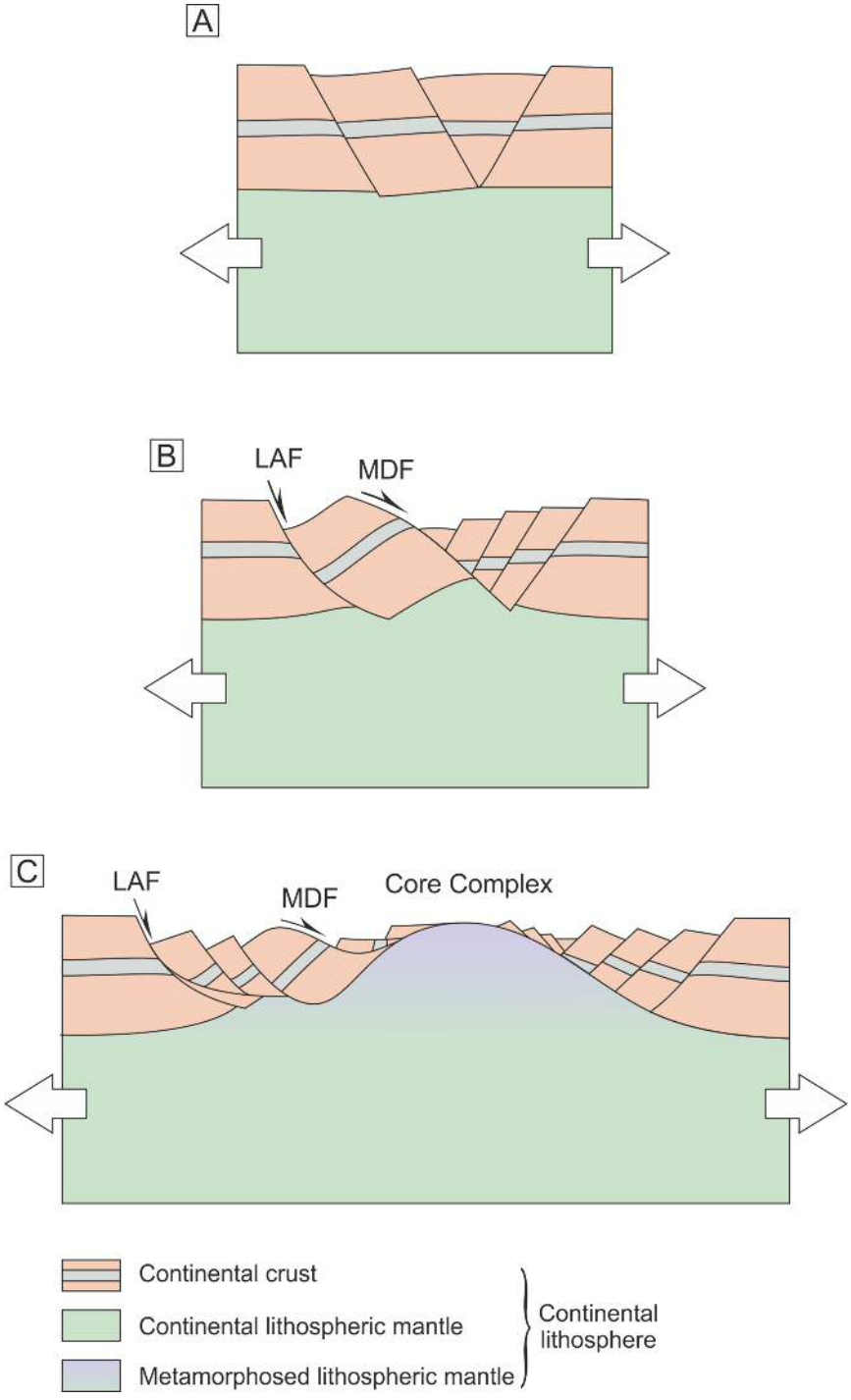


**Figure 1.4** Idealized evolution of a core complex. The last stage (C) show the juxtaposition of low grade to unmetamorphosed rocks on mid- to high grade metamorphosed rocks. LAF—listric accommodation fault; MDF—main detachment fault. Modified from Brun *et al.* (1994).

#### *1.2.2.5. Pure shear models*

The first quantitative model explaining lithospheric extension was proposed by McKenzie (1978). Using a mathematical approach for the concept of crustal stretching, McKenzie (1978) assumes instantaneous rifting and uniform stretching of the lithosphere, being usually named as *pure shear model* (Fig. 1.5). In this model, crustal extension occurs due to faulting and block rotation in the fragile upper crust, whereas the lower crust suffers ductile deformation. This configuration leads to the formation of a rift basin with symmetric rift structures and symmetric rift margins. If breakup occurs, conjugate continental margins will develop symmetric thermal subsidence. The limitations of this model are evident since it results from an oversimplification of the modelled structure of the crust. For example, it does not take into account vertical differences in the amounts of extension recorded on continental margins due to rheological stratification. In addition, extension is achieved by means of pure shear, assuming constant isostatic equilibrium. Magmatic activity is not considered at any point in this model. Another limitation of McKenzie's (1978) model is that it does not account for lateral heat flow and heat loss during the extensional process (Buck, 2007).

Despite these limitations, the McKenzie (1978) model is able to explain and predict several characteristics of extended terrains, such as post-extension crustal thickness and subsidence history, as it provides an accurate 1D description of the effect of lithospheric extension (*e.g.* Northeast Atlantic Armorican and Galicia continental margins: Le Pichon & Sibuet (1981); North Sea: Wood, (1981); Aegean area: Le Pichon *et al.*, (1982); Black Sea: Shillington *et al.*, (2008)).

In considering equal amounts of extension for both crust and under crustal lithospheric mantle, however, this model fails to explain structural asymmetries commonly observed in conjugated margins such as Iberia-Newfoundland (*e.g.* Lister *et al.*, 1986).

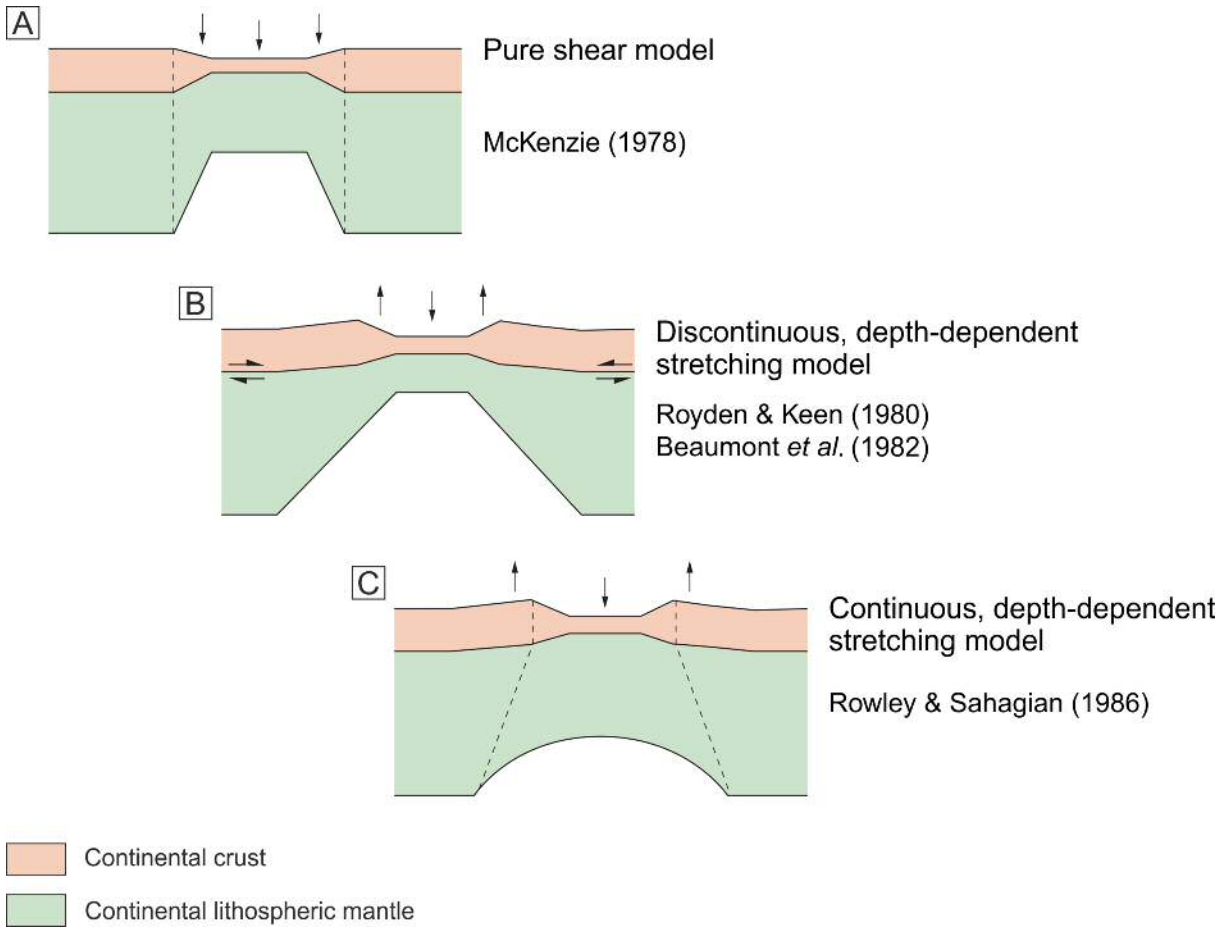


**Figure 1.5** Pure shear lithospheric extension models. Redraft from Ziegler & Cloetingh (2004).

Several modifications on this initial pure shear model emerged after 1978, and tried to add variables not considered in Mackenzie's original model (Fig. 1.5A). One of the parameters is the inclusion of the factor time in the previously instantaneous stretching, the *finite rifting* models (Jarvis & McKenzie, 1980; Ter Voorde & Cloetingh, 1996). From subsequent modifications two models stand out, both of them dealing with the heterogeneous aspect of lithospheric rheological composition. These two models are able to predict an important fact observed in nature, the flexural uplift of rift shoulders (or arch rims in Veevers, 1981).

The discontinuous (depth-dependent) stretching model of Beaumont *et al.* (1982) and Royden & Keen (1980) (Fig. 1.5B), add a discontinuity between the crust and the sub-crustal lithosphere, which materialises the rheological boundary between brittle

and ductile deformation. Given this intracrustal decoupling, different amounts of extension occur between the two layers. A higher amount of extension occurs in the ductile crustal lithosphere predicting the elevated levels of lithospheric and crustal melting observed in rift zones by imposition of a higher thermal anomaly (comparatively to the original pure shear model). During the lithospheric thinning, the amount of asthenosphere passively intruded in the space left by the lower lithosphere raises the thermocline position, increasing the lithospheric thinning by partial melting (Ziegler & Cloetingh, 2004). It is the increased amount of lower lithospheric thinning over the original pure shear model that allows these thermal induced events to be modelled and predicted. The rift flank uplift observed in this model is generated by the attenuated subcrustal lithosphere, which extends over a larger region than the crustal rift zone. The difference in densities between the mantle and the thinned crust generates an isostatic disturbance that will raise the crustal rift margins in other to re-establish the isostatic balance by flexural compensation (Royden & Keen, 1980; Zuber & Parmentier, 1986; Braun & Beaumont, 1989; Kusznir & Ziegler, 1992). Coupled with an upper crustal simple shear extensional behaviour is the *flexural cantilever model* (Kusznir *et al.*, 1991; Kusznir & Ziegler, 1992).

Other modification to the Mackenzie's pure shear model is the *continuous depth-dependent* model (Rowley & Sahagian, 1986) (Fig. 1.5C). The continuous depth-dependent model is a further refinement of the discontinuous depth dependent model, eliminating the presence of the (dubious) discontinuity between the fragile and ductile lithosphere and instead considering a gradational transition between them. In this way, it solves the space problems generated by the different amounts of extension across this brittle-ductile boundary.

#### *1.2.2.6. Simple Shear models*

After Mackenzie's pure shear model several models leading to the development of asymmetric rifting were proposed using the concept of simple shear to explain lithospheric extension (Fig. 1.6).

Simple shear models can explain and predict asymmetries observed in rift zones in terms of thermal doming and magmatic activity, the location of continental mantle exhumation, differences in rift flank uplift, asymmetries in terms of configuration, structural styles and stratigraphic patterns (Wernicke, 1981; Wernicke & Burchfiel, 1982; Lister *et al.*, 1986; Boillot *et al.*, 1987a; Ziegler & Cloetingh, 2004; Buck, 2007; Kusznir & Karner, 2007).

The development of models using simple shear to explain the formation of conjugated margins was initiated by Wernicke (1981) after studying the Basin and Range province in the United States. The resultant *simple shear model* proposed by Wernicke & Burchfiel (1982), deals with large asymmetric low-angle detachment faults reflecting simple shear through the lithosphere. Progressive thinning in the lithosphere eventually generates a large-scale low-angle shear zone (Fig. 1.6A). The shear zone effectively creates a lateral offset in the extension locus between the crust and the lower lithosphere. This way, the foot-wall of the rift system, is where the thinning of the lower lithosphere is more significant, promoting crustal doming due to thermal uplift and isostatic compensation. In this region (known as lower plate, Lister *et al.*, 1986) the lithospheric thinning is focused in the fragile upper crust by means of brittle failure generating highly extended terrains, dominated by listric faulting soling out in the brittle-ductile crustal transition (Ziegler & Cloetingh, 2004). Given the lateral offset of the crustal extension and lithospheric extension locus, the influence of tectonic subsidence will affect mainly the lower plate, while the influence of thermal subsidence will affect primarily the upper plate during the post-rift phase (Buck, 2007).

This asymmetric displacement leads to the formation of three main zones in the extensional shear zone (Wernicke, 1981, 1985): a zone where the upper crust is thinned by listric faults soling out in the detachment fault; the *discrepant* zone where the shear zone cuts through the lithosphere, extending and thinning the lower crust but with negligible action on the upper crust; and the zone where the shear zone extends through the lower lithosphere plunging into the asthenosphere.

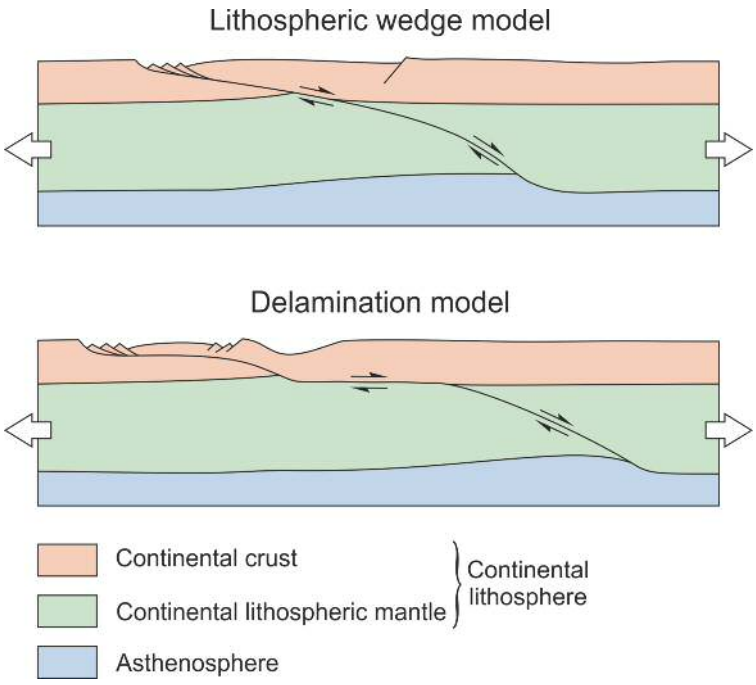


**Figure 1.6** Simple shear lithospheric extension models. Modified from Lister *et al.* (1991).

The study of Basin and Range province and the formation of core complexes gave birth to more models using the simple shear principle (*e.g.* Gans *et al.*, 1985; Lister *et al.*, 1986). The *delamination model* (Lister *et al.*, 1986) (Fig. 1.6B) differs from the original simple shear model by the inclusion of flat shear zones running at different crustal levels (delamination) and connected by ramps in analogy to the thrust flat-and-ramp geometry (Lister *et al.*, 1986, 1991). Lister *et al.* (1986) model predicts and explains the variation along strike of the upper and lower plate position (switching places by means of transfer faults) as a consequence of inherited geometry due to nucleation of detachments in different places along strike (Fig. 1.7).

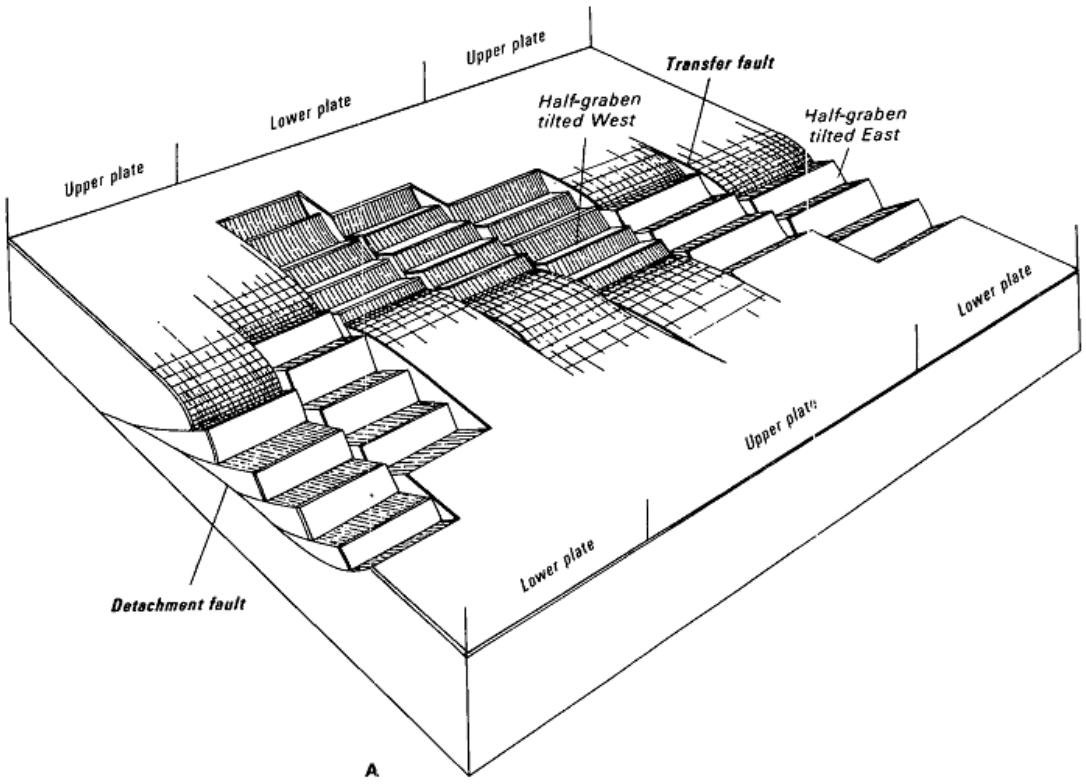


**Figure 1.7** Block diagram showing a simple shear model exhibiting changes in upper and lower plate position across strike bounded by transfer faults. From Lister *et al.* (1986).

### *1.2.2.7. Heterogeneous models*

Several models dealing with a combination of simple and pure shear extensional geometries (Fig. 1.8) are able to explain features observed on rifted margins that neither of them successfully address by themselves (*e.g.* Coward, 1986; Bell *et al.*, 1988; Kusznir & Egan, 1989; Kusznir & Ziegler, 1992; Brun & Beslier, 1996; Ter Voorde & Cloetingh, 1996; Manatschal *et al.*, 2001). In these models simple shear occurs invariably in the brittle upper crust and pure shear in the lower lithosphere and upper mantle. The presence of important detachment faults cutting the lithosphere can be present or absent in the models (Fig. 1.8). In the model proposed by Manatschal *et al.* (2001) for the Galicia and Adriatic margin evolution, the occurrence of pure and simple shear are separated in time. In the initial phases of extension, pure shear is the dominant extensional process changing to simple shear later on during the development of the thinning process.

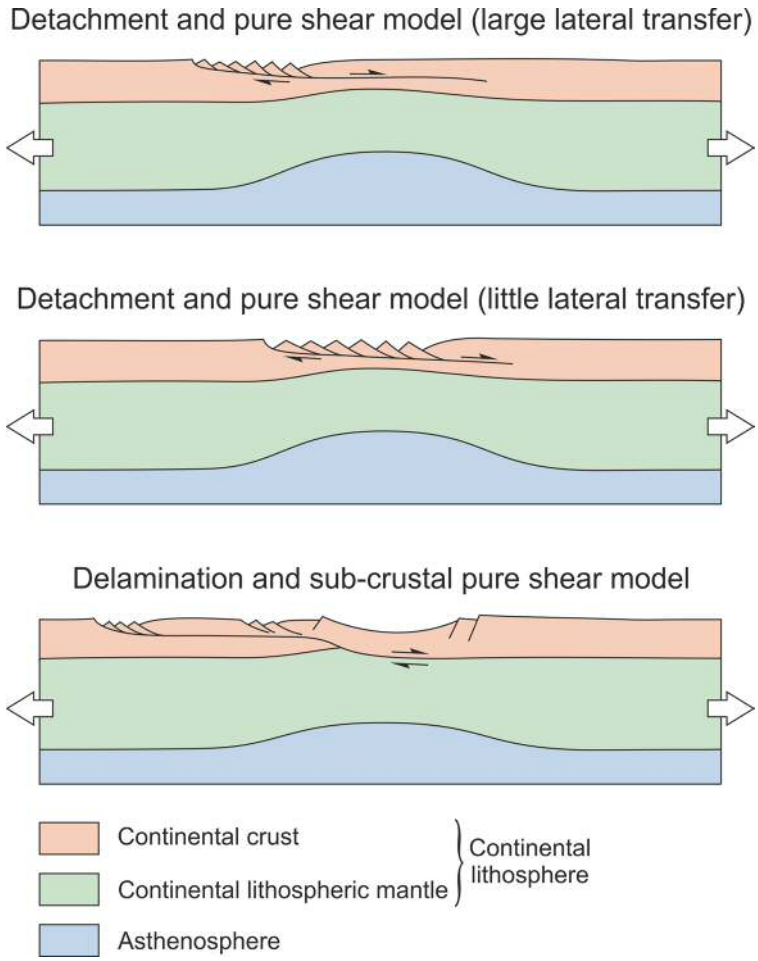


**Figure 1.8** Heterogeneous lithospheric extension models. Modified from Lister *et al.* (1991).

## *1.3.* Continental breakup and the *breakup unconformity*

The ultimate consequence of continental stretching is complete separation of conjugate rifted margins – the *lithospheric breakup* event. This event marks the onset of normal (*sensu* Penrose conference participants, 1972) oceanic crust accretion, and the generation of two conjugate passive margins (Wilson, 1965; Rosendahl, 1987; Busby & Ingersoll, 1995; Olsen & Morgan, 1995; Allen & Allen, 2005; Buck, 2007).

Falvey (1974) recognized the development of an unconformity at the time of continental breakup, coining the term *breakup unconformity*. According to him, the generation of the breakup unconformity was due to thermal expansion motivated by convection from the upwelling asthenosphere during the breakup event. This

thermal expansion would occur at a regional level, leading to a brief period of crustal uplift and erosion followed by post-rift subsidence due to thermal contraction (Fig. 1.9).

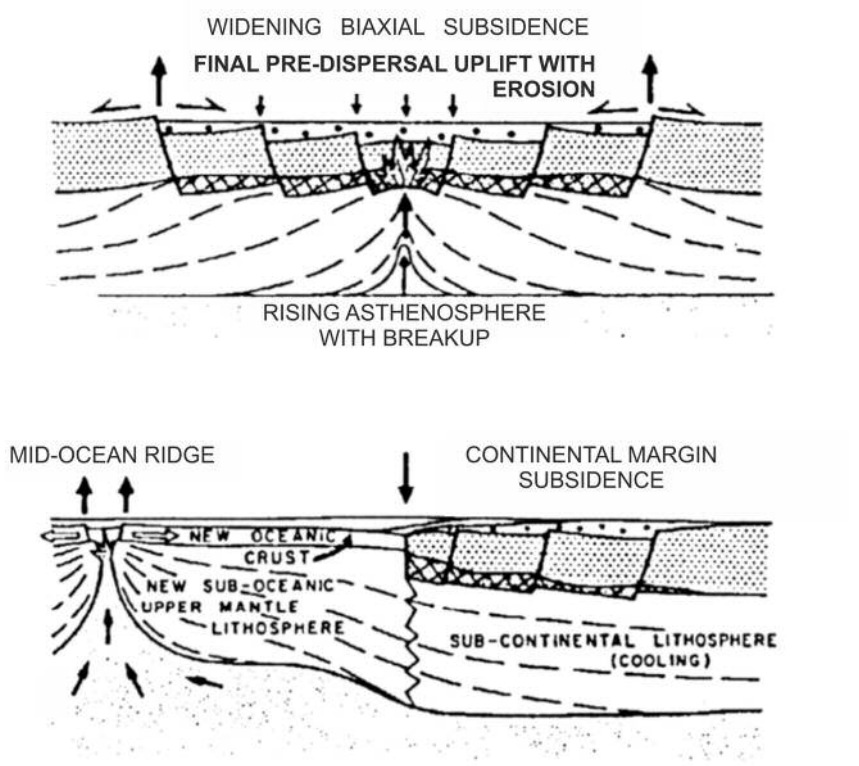


**Figure 1.9** Lithospheric breakup between conjugate margins. From Falvey 1974

The identification of the *breakup unconformity* as defined by Falvey (1974) was subsequently acknowledged by several authors and identified on numerous passive margins around the world as an ubiquitous feature (*e.g.* Veevers, 1986; Tankard & Welsink, 1987; Sinclair, 1988; Wernicke & Tilke, 1989; Embry & Dixon, 1990; Moore, 1992; O'Driscoll *et al.*, 1995; Whitmarsh & Wallace, 2001; Kyrkjebø *et al.*, 2004; Tucholke *et al.*, 2007a; Mohriak *et al.*, 2008).

The mechanism beyond the causes of the rift flank uplift at the time of lithospheric breakup was tentatively explained by several authors. It was proposed to be derived from: thermal uplift (Falvey, 1974; Coward, 1986; Favre *et al.*, 1991); the position of the extensional lower lithosphere locus in the upper plate (Issler *et al.*, 1989);

underplating (Lister *et al.*, 1991); or to the cessation (or decreasing) of extensional in-plane stresses acting on continental plates resulting in flexural rebound (Braun & Beaumont, 1989; Issler *et al.*, 1989; Kooi & Cloetingh, 1992). The later explanation is the one that is at present more widely accepted (Buck, 2007).

Not all the *breakup unconformities* are in fact a breakup unconformity *sensu stricto*, but instead composite unconformities generated by the imposition of successive erosional episodes. This is more common in the proximal parts of continental margins, having been referred by Ollier & Pain (1997) in this case as a *basal unconformity*.

According to the models previously described (pure-shear, simple-shear or a combination of both), complete lithospheric separation can be preceded by another breakup event where the breakup occur only in the upper crust, exposing the shear zone between the upper crust and the upper mantle. With the continuation of lithospheric thinning, the lithospheric mantle can be exposed, suffering brittle extensional tectonics that ultimately leads to a complete separation of the continental lithosphere (Lister *et al.*, 1986, 1991; Beslier *et al.*, 1993; Froitzheim & Manatschal, 1996; Boillot & Froitzheim, 2001; Whitmarsh & Wallace, 2001; Buck, 2007; Tucholke *et al.*, 2007a and many more).

### 1.3.1. Lithospheric vertical movements due to lithospheric breakup

Rather than a rapid tectonic event, lithospheric breakup has recently been proposed as reflecting a gradual process where extension on exhumed upper mantle and normal oceanic crust emplacement occur simultaneously until the later becomes predominant (Russell & Whitmarsh, 2003; Jagoutz *et al.*, 2007; Sibuet *et al.*, 2007b). Nevertheless, considering individual crustal segments on a rifted margin, numerical modelling shows that complete separation of exhumed mantle, with resulting cessation of lithospheric thinning, releases accumulated extensional in-plane stresses during an event considered to be instantaneous at a geological scale (Cloetingh, 1988; Braun & Beaumont, 1989; Bott, 1992b; Cloetingh & Ziegler, 2007). This release of in-

plane stress will generate a flexural rebound of the lithosphere in the form of large wavelength vertical and horizontal movements, thus creating localized uplift, subsidence and minor compression along the thinned lithosphere (Braun & Beaumont, 1989; Cloetingh *et al.*, 1989; Issler *et al.*, 1989; Cathles & Hallam, 1991; Egan, 1992; Kooi & Cloetingh, 1992; van Balen *et al.*, 1998).

Cloetingh *et al.* (1985) show for the first time that in-plane stresses can cause vertical motions at extensional basins: an increase in the level of compressive far-field in-plane stress causes flank uplift and basin centre subsidence, while an increase in extensional far-field in-plane stress causes flank subsidence and basin centre uplift.

The way the flexural rebound propagates along the lithosphere is much dependent on its initial state of flexure (Kooi & Cloetingh, 1992). Braun & Beaumont (1989) demonstrated that the depth of necking of the lithosphere (the depth at which the lithosphere is strongest and therefore more resistant to extensional strain), controls the state of flexure of the lithosphere during rifting (Fig. 1.10). In fact, it is the depth of necking that will condition the eventual departure from a hypothetical isostatic balanced lithosphere, or in the absence of isostatic forces, during rifting (Kooi & Cloetingh, 1992). In this way, rift basins with a deeply located necking and upward flexure will significantly uplift the rift zone, while shallow necking depths cause downward flexing of the rift zone (Braun & Beaumont, 1989; Weissel & Karner, 1989; Kooi & Cloetingh, 1992; Govers & Wortel, 1999) (Fig. 1.10B, C).

Following the pioneering work of Cloetingh *et al.* (1985) on how in-plane stress changes affect the lithosphere on a rift margin, Kooi & Cloetingh (1992) incorporated in their models a variable depth of necking ($Z_{neck}$, according to their notation). Kooi & Cloetingh (1992) show that in-plane stress signal changes recorded at the time of breakup (the relaxation of a tensional regime—promoted by lithospheric breakup—is equivalent to the instalment of compressive stresses) are much dependent on the state of flexure of the lithosphere during extension.

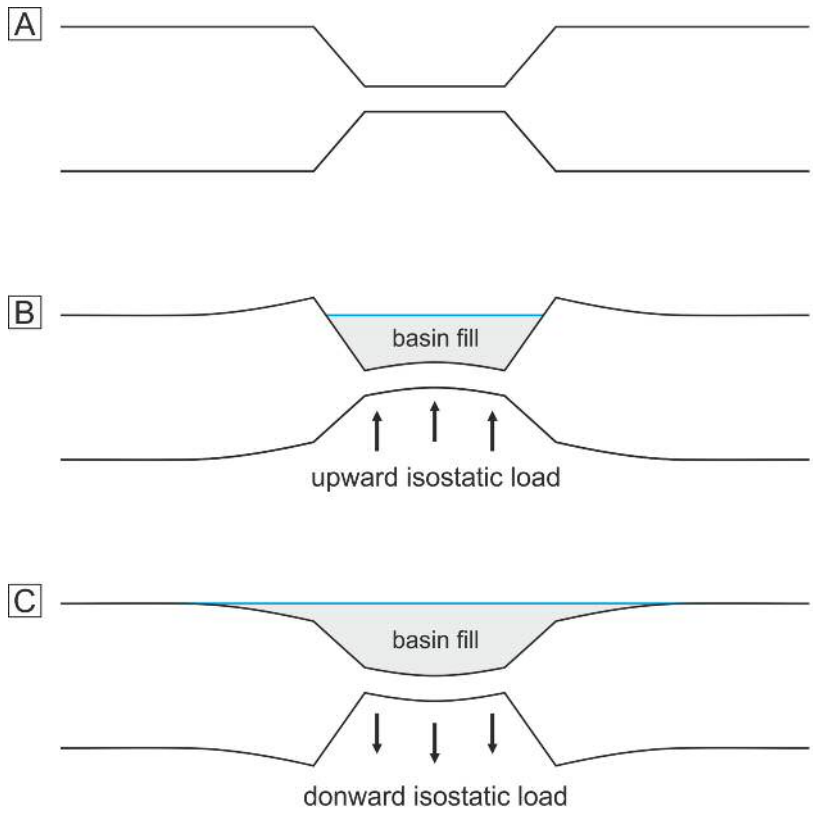


**Figure 1.10** Schematic illustration of the depth of necking concept in extensional settings. A—conceptual lithosphere necking occurring in the absence of gravity or isostatic forces (isostatically balanced). B—deep levels of necking create an upward isostatic load promoting flexural uplift. C—shallow levels of necking create downward isostatic forces leading to flexural subsidence.

With a more realistic approach, van Balen *et al.* (1998) modelled the vertical movements in a margin due to in-plane stress changes using a decoupled two-layer model of the lithosphere. They also took into account permanent brittle deformation of the lithosphere caused by extension (Fig. 1.11). They argue that the flexural response of the rifted lithosphere is mainly driven by the faulted shape of the upper crustal competent layer, assuming this character as predominating over the effect of overall depth of necking. In their model, the pre-existing midplane curvature of the upper crustal flexural plate is always in a downward state of flexure (Fig. 1.10C) which implies that a change in in-plane stresses from extensional to compressive stresses will promote rift flank uplift independently of the depth of necking.

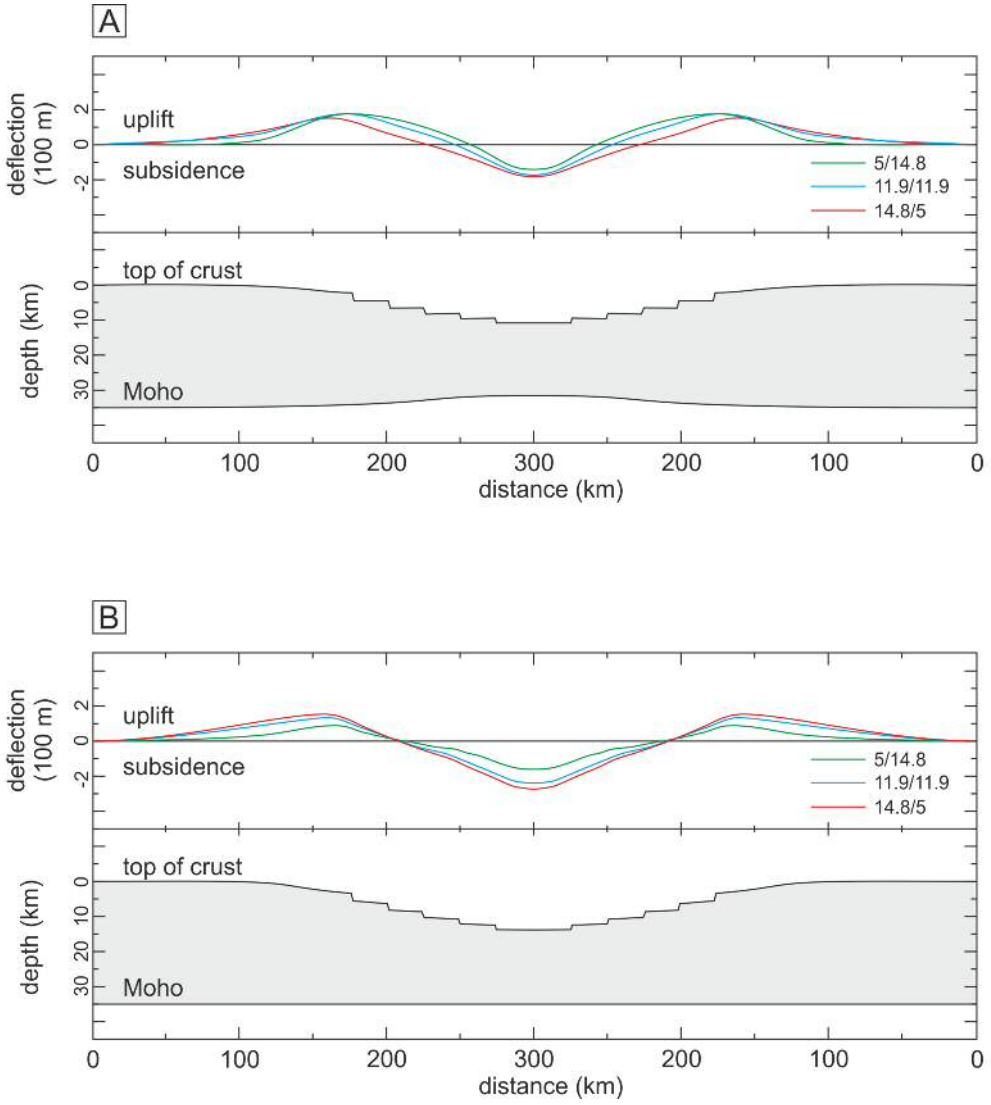


**Figure 1.11** Model results from van Balen *et al.* (1998) showing the calculated lithospheric vertical movements after the application of 100 MPa in-plane compressional stress. For each panel three modelled results are shown, with changing effective elastic thickness value combinations for the upper crustal and subcrustal competent layers: 5 km and 14.8 km; 11.9 km and 11.9; Km; 14.8 and 5 km. A—model with uplifted Moho representing an intermediate depth of necking. Notice that the Moho topography is only slightly uplifted, corresponding to a rift margin which did not undergo a significant amount of extension. B—model with a flat Moho. Modified from van Balen *et al.* (1998).

The Moho topography used by van Balen *et al.* (1998) corresponds of a rifted margin that underwent a small amount of extension. Unfortunately, these authors do not present results corresponding to a margin in a more advanced extensional stage. Nevertheless, they report that for a flat Moho (Fig. 1.11B), the amount of flank uplift

varies between 100 and 200 m, in contrast with the model with the uplifted Moho, where these values vary between 150 and 200 m. If this trend is maintained throughout further lithospheric thinning (and consequent increase in Moho complexity/uplift) probably the rift flank uplift is maintained on the transition from in-plane extensional stresses to compressional stresses as verified at lithospheric breakup. Furthermore, Figure 1.11A is the scenario with the thinnest upper crust effective elastic thickness values (green line in Figure 1.11) that shows the highest amount of uplift, suggesting that these values can be maintained with further thinning of the upper crust.

Another important cause for lithospheric vertical movements occurring at the time of final breakup is isostatic readjustment due to the relative loss of support given by the conjugate margin. Along with flexural vertical movements, the cessation of lithosphere extension should promote a measurable elastic retraction of the lithosphere (Kooi & Cloetingh, 1992). Changes in density along the newly separated plate due to the compressive stresses generated by lithospheric breakup can contribute for further isostatic imbalance (Cathles & Hallam, 1991). Furthermore, the continuing erosion of rift shoulder areas contributes to the persistence of uplift in time by erosional unloading (van Balen *et al.*, 1995; Burov & Cloetingh, 1997; Burov & Poliakov, 2003; Rouby *et al.*, 2013).

Chapter Two

# DATA AND METHODOLOGY

## 2.1. Introduction

The data used in this thesis consist of 2D multichannel seismic reflection profiles from multiple surveys, combined with borehole wireline data, and information (descriptions of core and cuttings) obtained from industry reports and publications. All these data sets were integrated and interpreted using Petrel software (Schlumberger).

This thesis follows the zonation of rifted margins proposed by Manatschal & Bernoulli (1998) and Alves *et al.* (2006). These authors divide rifted continental margins in: (1) inner proximal margin, comprising proximal offshore basins and exhumed aulacogens (*e.g.* Lusitanian Basin, Wilson *et al.*, 1989); (2) outer proximal margin, where the majority of the continental crust thinning occurs, and (3) distal margin, which comprises exhumed upper mantle rocks proximally overlain by highly-extended continental blocks within a ocean-continent transitional zone (Whitmarsh & Miles, 1995) (Fig. 2.1).

The bathymetric data used for the generation of the maps presented here is derived from GEBCO_08 Grid* (global grid at 30 arc-second intervals). The maps compiled in this thesis were projected using the Universal Transverse Mercator system, except those picturing East Antarctica. Due to its geographical position, the South Universal Polar Stereographic was used as the main projection system for the Antarctica data. The datum used in all maps was World Geodetic System 1984.

The stratigraphic nomenclature used in this work for the West Iberia inner proximal margin is based on published literature (Wilson *et al.*, 1989; Alves *et al.*, 2003b) and unpublished reports (Witt, 1977; GPEP, 1986). Stratigraphic ages are based on the geological timescale of Gradstein *et al.* (2005).

In this work, all seismic profiles in figures are shown in two-way travel time (TWT).

* The GEBCO_08 Grid, version 20100927, http://www.gebco.net, accessed during 2011-2014

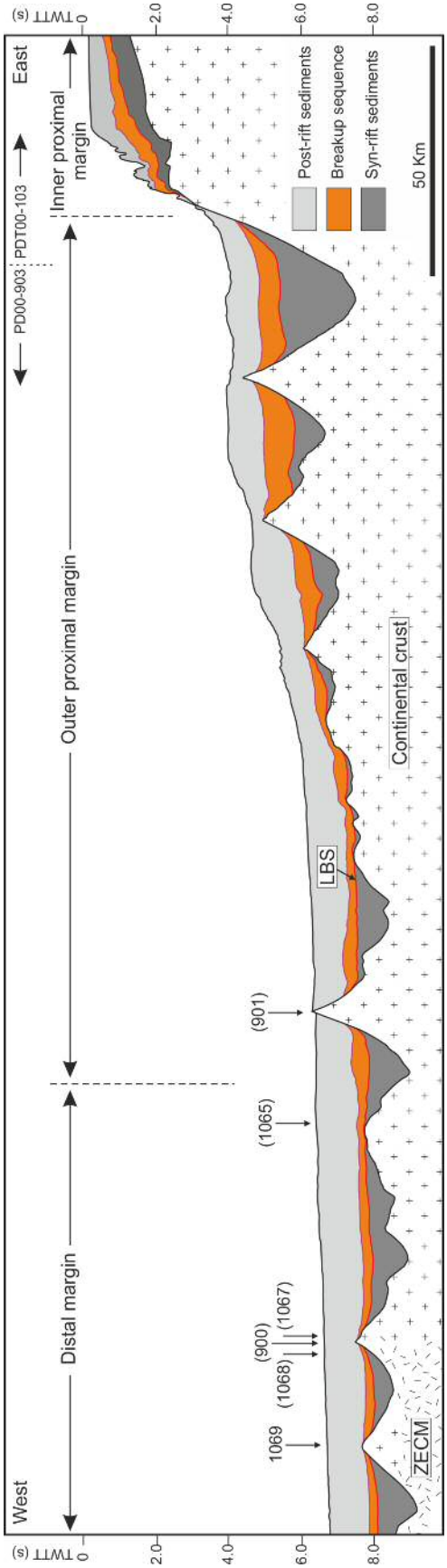


**Figure 2.1** Simplified interpretation of seismic reflection profiles (TGS-NOPEC PD00-903 and PDT00-103) showing the margin zonation adopted in this study. In parentheses are projected ODP sites. LBS—lithospheric breakup surface; ZECM—zone of exhumed continental mantle.

# 2.2. 2D Seismic reflection data

## 2.2.1. Datasets

Seismic data used in this work consists of multichannel reflection seismic from industry and scientific surveys (Table 2.1, Fig. 2.2). Industry 2D seismic surveys, covering the Northwest Iberian margin, were provided by DGEG/DPEP (Direcção Geral de Energia e Geologia/Divisão para a Pesquisa e Exploração de Petróleo) both in digital format and paper prints. In addition, multiple scientific surveys were downloaded from several sources online (Table 2.2) and the GP and GA280 surveys from the literature were high quality, and large format images were available.

**Table 2.1** Details of the several seismic datasets used in this study. Shaded in grey the industry datasets used in this study. See Figure 2.2 for the geographical location and distribution of the seismic surveys.

| Survey | Acquisition date | Type of data | Quality of seismic imaging | Number of seismic profiles | Number of kilometres covered | Used in Chapter | Region of coverage | References for acquisition parameters |
|---|---|---|---|---|---|---|---|---|
| **NESTE-PORTUGAL** | 1989 | SEG Y from paper scans | poor-good | 5 | ~170 | 4 | Iberia | — |
| **TGS-NOPEC** | 1999/2000 | SEG Y | excellent to good | 34 | ~3352 | 4 (*pro parte*)/ 5 | Iberia | — |
| **ISE** | 1997 | SEG Y | excellent to poor * | 26 | ~2920 | 4 / 5 | Iberia | Henning *et al.*, 2004 |
| **CAM** | 1995 | SEG Y | excellent | 31 | ~1411 | 5 | Iberia | Dean *et al.*, 2000 |
| **GP** | 1975 | SEG Y from paper scans | poor | 5 | ~564 | 5 | Iberia | — |
| **SCREECH** | 2000 | SEG Y | excellent to poor ** | 30 | ~2914 | 4 / 5 | Newfoundland | Tucholke & Holbrook, 2001 |
| **GA227** | 2001 | SEG Y | poor (non-migrated) | 15 | ~2010 | 6 | East Antarctica | Stagg *et al.* 2005 |
| **GA228** | 2001 | SEG Y | good (non-migrated) | 17 | ~5158 | 6 | East Antarctica | Stagg *et al.* 2005 |
| **GA229** | 2002 | SEG Y | good (non-migrated) | 11 | ~2469 | 6 | East Antarctica | Stagg *et al.* 2005 |
| **GA280** | 204 | PDF images | excellent | 12 | ~1300 | 6 | South Australia | Bradshaw, 2005 |

* Poor data on profiles located on the inner proximal margin
** Poor data only on the Flemish Cap

**Table 2.2** Source of the scientific surveys acquired online.

| Survey | Region of coverage | Online source | Website |
|---|---|---|---|
| **ISE** | Iberia | Academic Seismic Portal (ASP) at University of Texas Institute for Geophysics | www.ig.utexas.edu/sdc/ |
| **SCREECH** | Newfoundland | | |
| **GA227** | East Antarctica | Antarctic Seismic Data Library System (SDLS) | http://sdls.ogs.trieste.it |
| **GA228** | East Antarctica | | |
| **GA229** | East Antarctica | | |
| **GA280** | South Australia | Geoscience Australia | www.ga.gov.au |

The GP profiles and one profile from the NESTE survey were not available as SEG Y data files†, but only in large print format. High quality scans of the lines were used and vectorized (digitally transformed in SEG Y format) using the Blueback Toolbox plug-in for Petrel from Blueback Reservoirs. Navigation data was obtained using georeferenced maps where the seismic shot points were figured. This procedure involved some necessary small adjustments on the time-depth and on the navigation of the lines in order to match the interpreted data (i.e all the scanned profiles crossed digital data accurately positioned which served as reference points). The seismic data obtained in this way, displaying the old processing, cannot have its imaging quality increased after the vectorisation process. The other profiles from the NESTE-PORTUGAL survey are as well print-to-SEG Y conversions, but the vectorisation process and georeferencing was performed by DGEG/DPEP.

Nevertheless having its limitations in terms of detailed imaging when compared with the more modern surveys used (*e.g.* TGS-NOPEC, ISE and CAM), the vectorized seismic profiles are extremely useful regarding the reconstruction of the studied surfaces and for subsequent areal and thickness estimations (Chapter 5).

† SEG Y is the standard recording format adopted by the Society of Exploration Geophysicists (SEG) in 1975 for data exchange and the nowadays most used format for seismic data (Barry *et al.*, 1975)

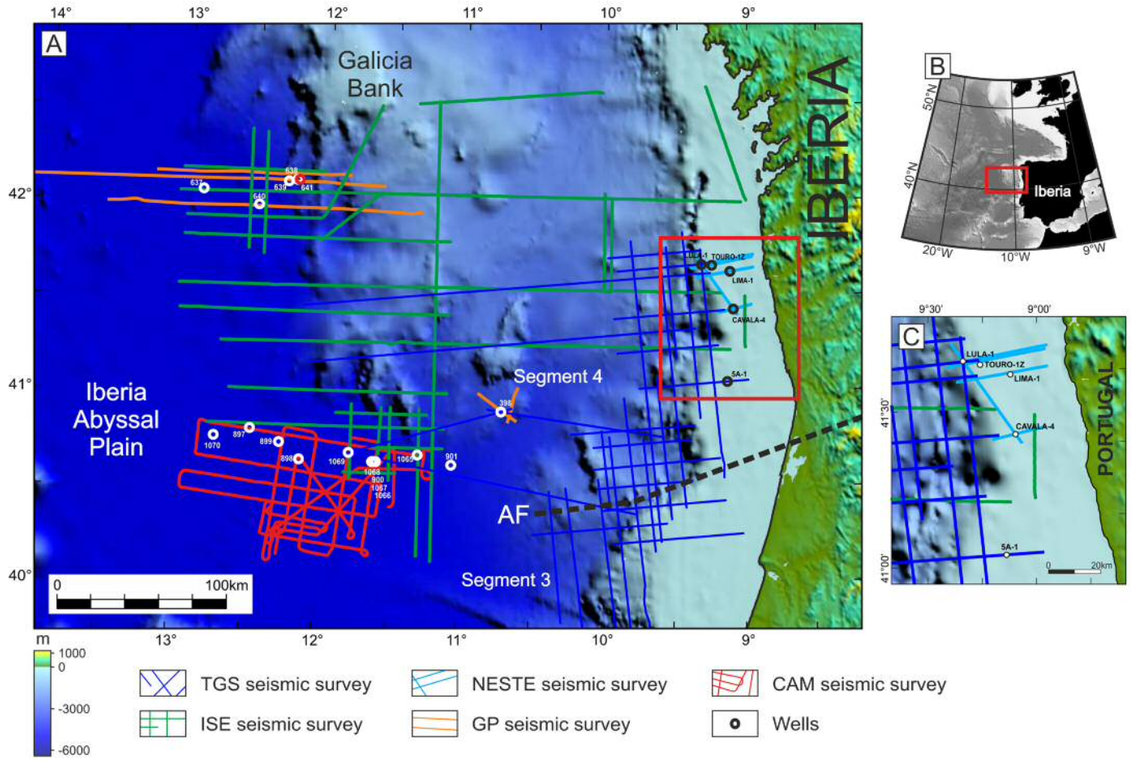
A
Galicia Bank
IBERIA
Iberia Abyssal Plain
Segment 4
Segment 3
AF
0 100km
B
Iberia
C
PORTUGAL
LULA-1
TOURO-1Z
LIMA-1
CAVALA-4
5A-1
m
1000
0
-3000
-6000
TGS seismic survey
ISE seismic survey
NESTE seismic survey
GP seismic survey
CAM seismic survey
Wells

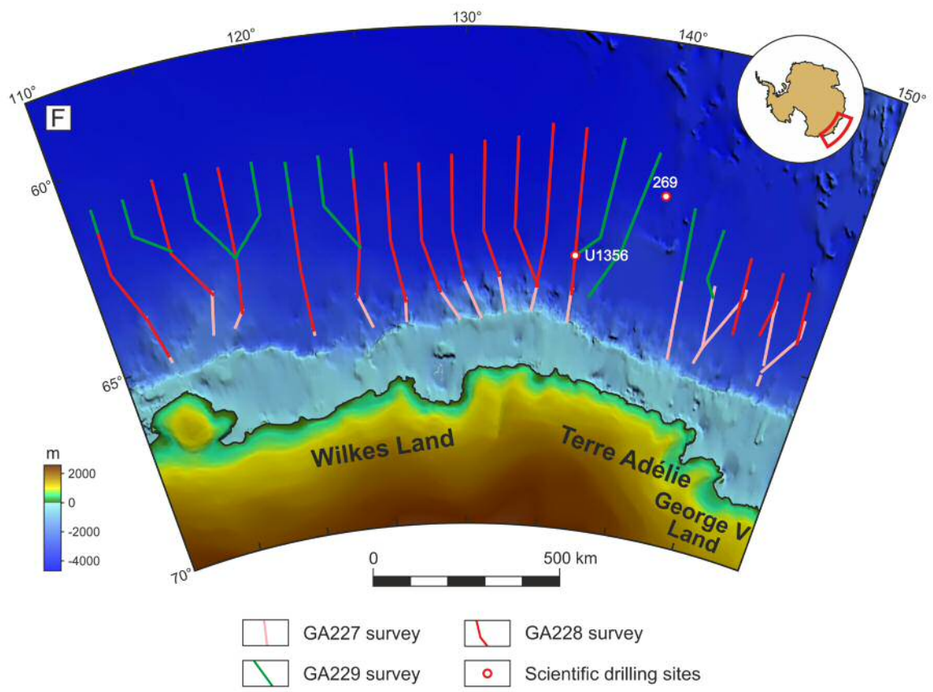
F
269
U1356
Wilkes Land
Terre Adélie
George V Land
m
2000
0
-2000
-4000
0 500 km
GA227 survey
GA228 survey
GA229 survey
Scientific drilling sites

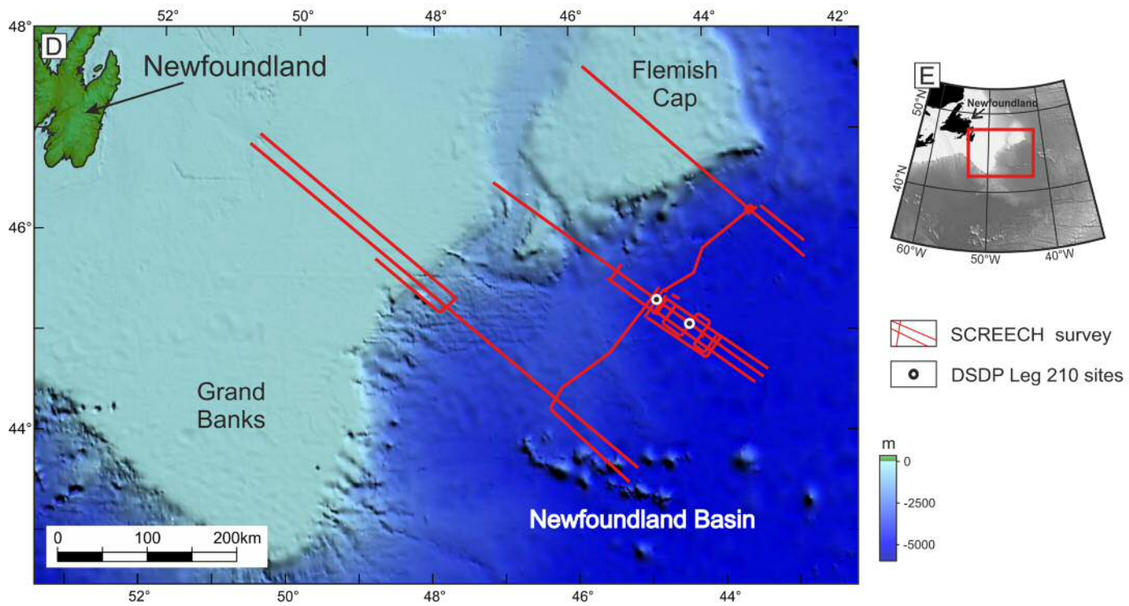
D
Newfoundland
Flemish Cap
Grand Banks
Newfoundland Basin
0 100 200km
E
SCREECH survey
DSDP Leg 210 sites
m
0
-2500
-5000

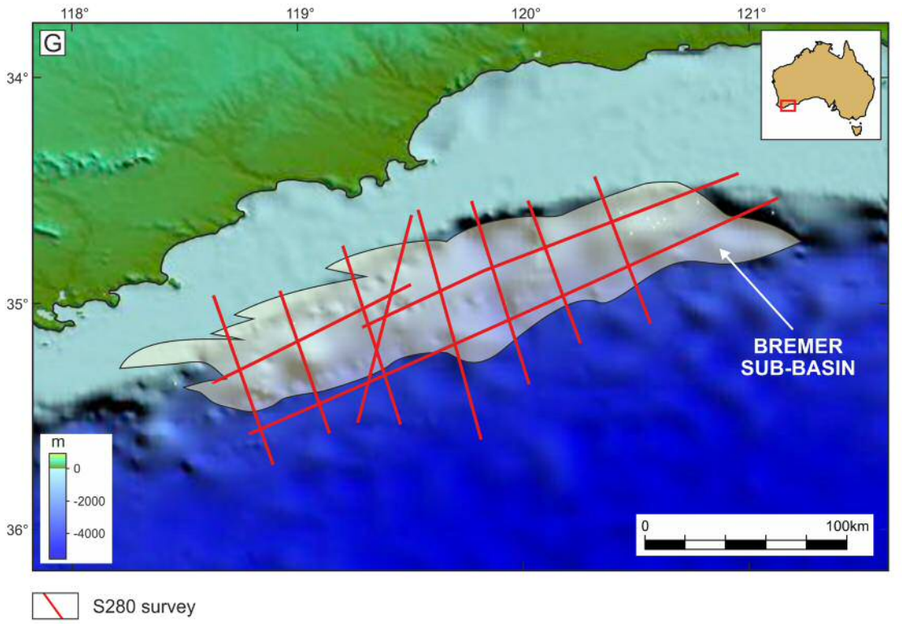
G
BREMER SUB-BASIN
m
0
-2000
-4000
0 100km
S280 survey

**Figure 2.2** (previous page) Seismic surveys and wells used in this study. A—study area in Northwest Iberia. B—position of A in its regional context. C—detail of the dataset used in the Northwest Iberia inner proximal margin. D—study area in Newfoundland. E—position of D in its regional context. F—study area in East Antarctica. G—study area in Bremer Sub-basin (South Australia).

The available seismic data from East Antarctica consists of 2D stacked profiles (unmigrated), which can cause difficulties during its interpretation (Fig. 2.3). In unmigrated data, the presence of diffractions masks the true subsurface structure due to the bow-tie effect (Fig. 2.3A). Time- or depth-migration‡ remove the bow-ties and render the structure more clearly (Fig. 2.3B). Given the use of stacked data alone, in some seismic profiles the interpretation of two specific horizons (the *end of extension surface* and the top of mass transport deposits) was made with less confidence where the bow tie effect was too strong. As a way to find a more correct positioning of these surfaces, on those problematic seismic profiles I had to partially follow the work of Stagg *et al.* (2005) where the same survey is used, but time migrated (Fig. 2.3B).

No digital seismic datasets from Southern Australia were available in SEG Y format. However, in Bradshaw (2005) the seismic survey S280 (covering the Bremer Sub-basin) is depicted in a large format (in large PDF files) and with a quality that allows for its interpretation.

### 2.2.2. Seismic data interpretation

The reader will find a comprehensive description of the specific methods and criteria used in each of the chapters of this thesis. Throughout the data analysis chapters, seismic–stratigraphic interpretations are based on criteria given in Bally, (1987), Payton, (1977), Catuneanu (2006) and Mitchum *et al.* (1977). In this thesis, unless otherwise stated, 'basement' includes the acoustic basement and pre-rift sediments.

‡ For an in-depth explanation of the seismic data migration processes, the reader is directed to (Gadallah & Fisher, 2009)

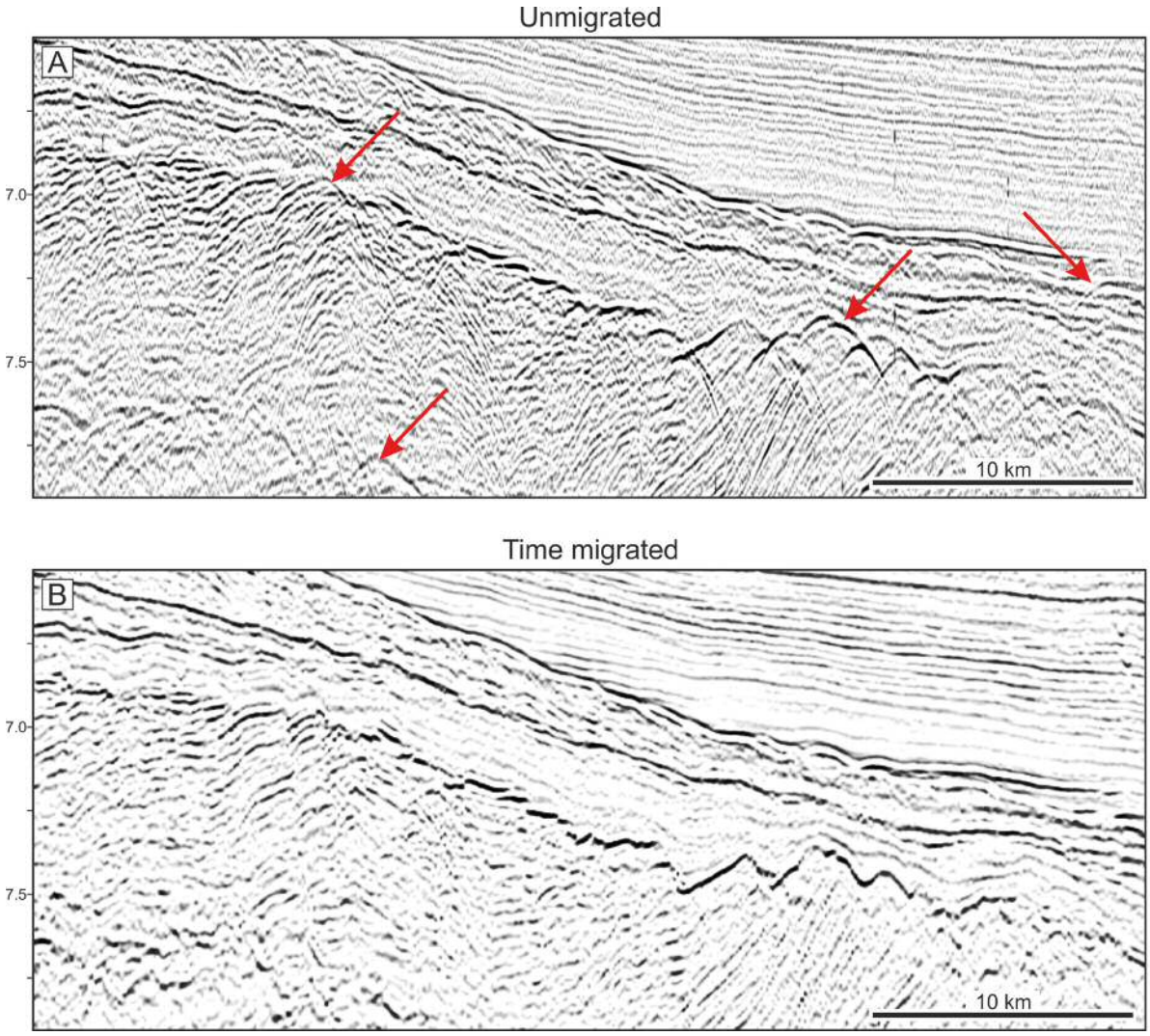


**Figure 2.3** Comparison between unmigrated and migrated data. A—East Antarctica unmigrated data that was available for this study. B—the same section as in A but time migrated, from Stagg *et al.* (2005). Notice the removal of hyperbolic interferences (bow-ties, some marked by red arrows) on the migrated section, especially on the faulted deep reflector. Seismic profile GA228-23.

For the identification of key stratigraphic surfaces, well data were used to identify major unconformities and depositional hiatuses. For example, in Northwest Iberia, the surface contemporaneous with the lithospheric breakup event (the so-called *breakup unconformity*, redefined in this work as lithospheric breakup surface—LBS), was found to be different from the 'classical' breakup unconformity, as no divergent reflectors were to be found below it (see Chapters 1 and 7). This discrepancy was

found after the drilling of IODP Site 398, which crossed this surface allowing its dating (Sibuet *et al.*, 1979). Similarly, on the inner proximal margin the use of well data allowed the dating of key stratigraphic sequences.

In order to accurately define the *breakup sequence*, regional correlations are based on two major seismic–stratigraphic unconformities: (1) the Late Aptian–Albian '*breakup unconformity*', or LBS as redefined in this paper, which is pervasive in both West Iberia (Shipboard Scientific Party, 1979; Alves *et al.*, 2006; Clark *et al.*, 2007) and Newfoundland (Tucholke *et al.*, 1989) and, (2) a latest Cenomanian–Early Turonian unconformity marking a widespread regressive event in the North Atlantic (Sibuet *et al.*, 1979; Alves *et al.*, 2002; Alves *et al.*, 2003b). Importantly, these two unconformities, and correlative stratigraphic surfaces, are systematically recorded in onshore, shallow- and deep-offshore wells drilled in the North Atlantic (Tankard & Welsink, 1987; Hiscott *et al.*, 1990; Williams *et al.*, 1999; Baur *et al.*, 2010; Dickie *et al.*, 2011).

Due to differences in acquisition and processing parameters, the profiles from the five different seismic surveys used in the study of the Northwest Iberia margin have different degrees of seismic resolution and image quality (Table 2.1, Fig. 2.4). Vertical resolution can be defined as how closely two reflections can be positioned vertically, yet be identified as two separate reflections. The distance between these two reflections needs to be a minimum of ¼ of the wavelength of the sound wave used for seismic acquisition. The highest contrast in seismic resolution between the Iberian surveys used in this work was between the CAM and ISE or TGS-NOPEC and NESTE and TGS-NOPEC surveys. Carrying the interpretation from the TGS-NOPEC and ISE to the lower resolution CAM posed some difficulties, which were tackled by a more critical analysis of the later dataset. As a result, whenever possible the interpretation of CAM dataset was always controlled by the higher resolution ISE and TGS-NOPC datasets.

**Figure 2.4** (next page) Resolution comparison between different seismic surveys used in Northwest Iberia. A, B and C—examples from the different seismic surveys sharing the same vertical and horizontal scale (in panel D). E—location of the examples in A, b and C.

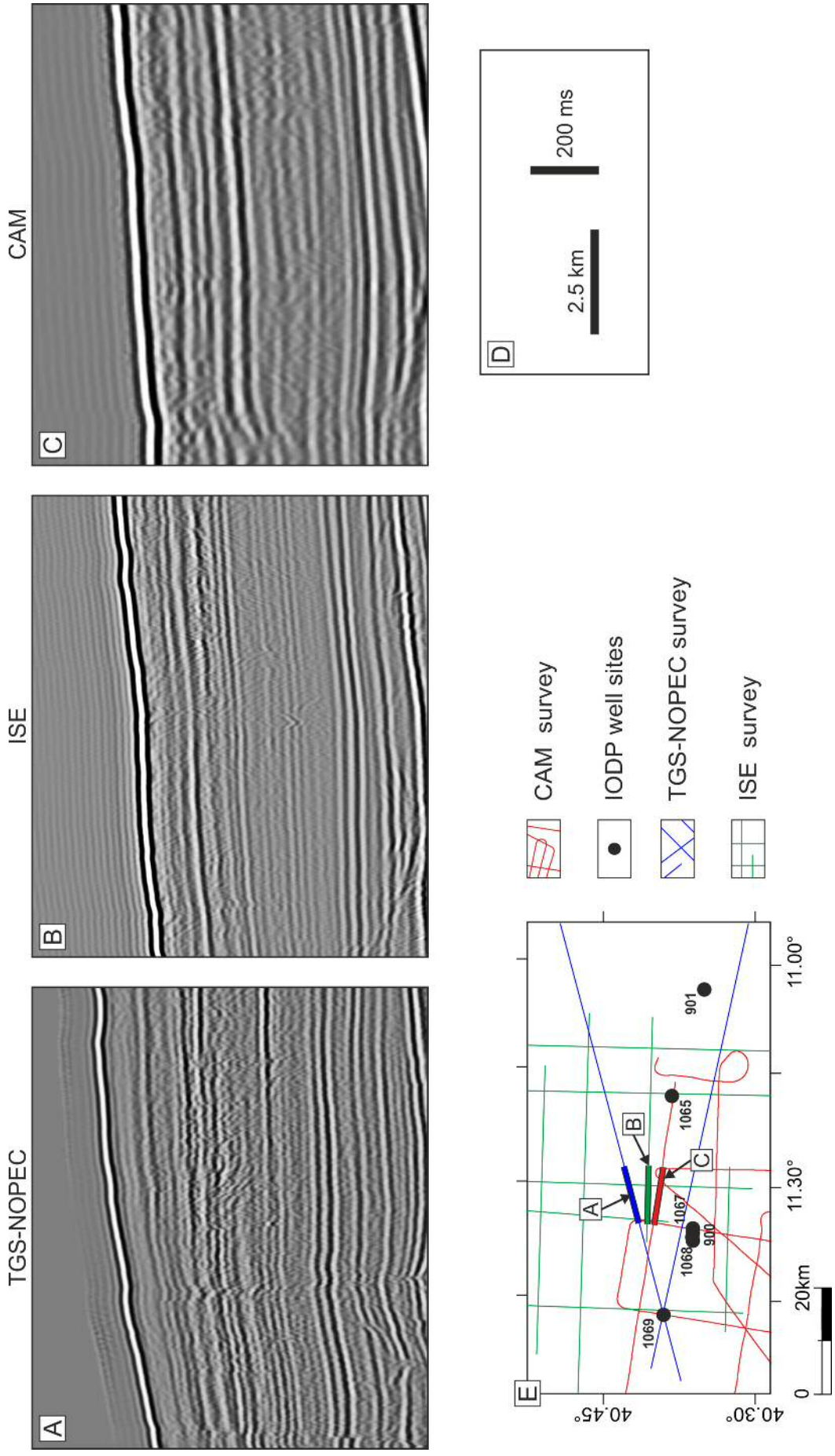
TGS-NOPEC
ISE
CAM
A
B
C
D
200 ms
2.5 km
CAM survey
IODP well sites
TGS-NOPEC survey
ISE survey
E
901
1065
1067
1068
900
1069
40.30°
40.45°
11.00°
11.30°
0
20km

#### *2.2.2.1. Diagnostic criteria for contourite drifts in deep-water margins*

The unexpected observation of contourites within the stratigraphical interval of interest in this study motivated a need for the understanding of their diagnostic features in seismic and core data.

The proposed tripartite methodology of Faugères *et al.* (1999), further developed in Rebesco & Stow (2001) and Nielsen *et al.* (2008), was used in this thesis to characterize the different types of contourite drifts interpreted in Northwest Iberia . The analysis in this thesis is based on the identification of features considered diagnostic of contourite deposits at different scales: (1) the morphology and boundaries of the deposit at the larger scale, (2) the architecture of internal discrete depositional units at medium scales, and (3) its seismic acoustic facies at the smaller scale. These are termed first, second and third-order seismic elements in Nielsen *et al.* (2008).

Apart from the architectural and acoustic criteria in Nielsen *et al.* (2008), the presence of large-scale erosional features with regional expression was one of the diagnostic criteria used in Northwest Iberia to assess the presence of bottom current activity (Faugères *et al.*, 1999; Rebesco & Stow, 2001; Rebesco *et al.*, 2014). They can materialize the boundaries between different units in contourite drifts or occur within the same unit marking discrete sub-units (Maldonado *et al.*, 2005). For the classification of contourite drifts, in terms of their depositional architecture and erosional features and large-scale erosional features, the classification scheme proposed by Rebesco *et al.* (2014) (which build on previous work by Faugères *et al.*, 1999; Rebesco & Stow, 2001; Hernández-Molina *et al.*, 2008; García *et al.*, 2009a) was adopted (Fig. 2.5).

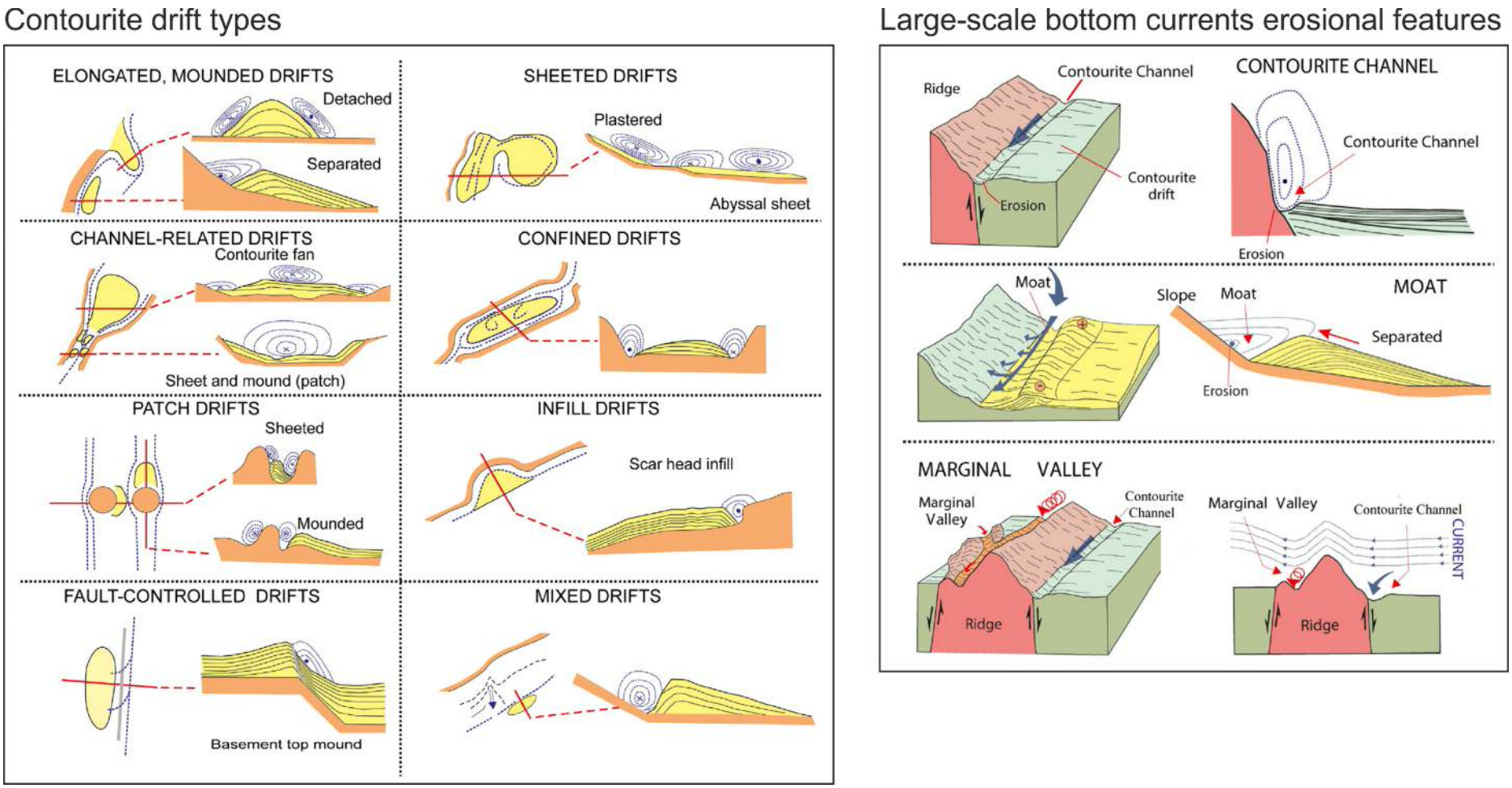


**Figure 2.5** Classification scheme proposed by Rebesco *et al.* 2014 for the main depositional (contourite drifts) and large-scale erosional features produced by bottom current activity. Modified from Rebesco *et al.* (2014).

## 2.3. Well data

The well data used in this work are derived from industry and public sources (DSDP, ODP and IODP). Well data were used to provide 'ground truth' to the interpreted seismic data and to characterise sedimentological changes across studied intervals. Well data from the Porto Basin were provided by DGEG/DPEP (Table 2.3) and include LAS logs, paper logs, and completion reports. Completion reports include data on lithological logs (from cuttings retrieved during drilling), biostratigraphical reports, operations report, side wall core descriptions, dipmeter logs, VSP data (vertical seismic profiles, which provide the best way to correlate the well data with seismic data). None of the completion reports included such a complete array of information, the most complete reports being those relative to the wells LIMA-1 and LULA-1.

**Table 2.3** Industry well used in this study. All of the wells were drilled in the Porto Basin and used in Chapter 4. For their geographical location, see Figure 2.2A-B.

| Well name | Operator | Year drilled |
|---|---|---|
| **TOURO** | Taurus Petroleum | 1995 |
| **LIMA-1** | Neste | 1990 |
| **LULA-1** | Pecten | 1985 |
| **CAVALA-4** | Texaco | 1979 |
| **5-A1** | Shell | 1975 |

Data from scientific drillings were used in all the studied margins with the exception of the South Australian margin (Table 2.4).

**Table 2.4** Scientific drilling legs from which site data was used in this study. For their geographical location, see Figure 2.2.

| Leg | Most relevant site for this study | Year drilled | Used in chapter | Location | Leg references |
|---|---|---|---|---|---|
| **DSDP 47b** | 398 (crosses the LSB) | 1976 | 4 / 5 | Northwest Iberia | Sibuet *et al.* (1979) |
| **ODP 103** | 641 (crosses the LSB) | 1985 | 4 / 5 | Northwest Iberia | Boillot *et al.* (1987b); Boillot *et al.* (1988) |
| **ODP 149** | — | 1993 | 4 / 5 | Northwest Iberia | Sawyer *et al.* (1994); Whitmarsh *et al.* (1996a) |
| **ODP 173** | — | 1997 | 4 / 5 | Northwest Iberia | Whitmarsh *et al.* (1998); Beslier *et al.* (2001a) |
| **ODP 210** | 1276 (crosses the LSB) | 2003 | 4 / 5 | Newfoundland | Tucholke *et al.* (2004); Tucholke *et al.* (2007b) |
| **IODP 318** | 1356 (allowed dating of the LSB) | 2010 | 6 | East Antarctica | Escutia *et al.* (2011) |

Seismic profiles crossing DSDP site 398 (PD0-901 and PD0-902), were tied to borehole data using information provided in DSDP volume XLVII part 2 (Shipboard Scientific Party, 1979). The correct vertical positioning of DSDP Site 398 against the seismic data crossing this site was paramount for this thesis, since it provide the age and identifies in core the stratigraphic boundaries here studied.

To tie seismic and borehole data, a synthetic log was attempted, using density and velocity data taken from point measurements on the cores (von Rad *et al.*, 2004, 2005), instead of continuous, in-hole acquired data. This posed several problems in terms of achieving an accurate time-depth relationship. The achieved synthetics presented several artefacts such as for example very strong reflectors on the unit immediately above the lithospheric breakup surface (the black shales) where its seismic expression is constituted by almost transparent reflections.

The solution found was to use the depths and penetration times of seismic reflectors given on Shipboard Scientific Party (1979) as checkshots to insert in the Petrel project and to do manually the necessary adjustments (Fig. 2.6 and Table 2.1). For the manual adjustments, it was decided to maintain the given depths (acquired

on the cores) and to adjust the two way time depth according to the position of the more prominent reflectors identified on seismic lines PD0-901 and PD0-902 (crossed at site 398) (Table 2.1). This proved to be a good option since the required adjustments were minimal and the time-depth relationship achieved was very satisfactory.

**Table 2.5** Given and adjusted depth values used to tie DSDP Site 398 to the available seismic dataset. The original two way time (TWT) data from Sibuet *et al.* (1979) have as reference datum the sea bottom, which is in contrast with the average sea surface reference datum used on the Petrel project. Therefore, the values here presented for measured depth (MD) were added of 3910 m (the given sea depth for site 398) and TWT values were added 5.200ms (the time position of the sea bottom on seismic lines PD0-901 and PD0-902, crossed by site 398). The reflector names are from Sibuet *et al.* (1979), in parentheses the names used in this work.

| Reflector | MD (m) | | | TWT (s) | | |
|---|---|---|---|---|---|---|
| | Given (original+ 3910 m) | Used | Δ between given and used | Given (original+ 5.2 s) | Used | Δ between given and used |
| Sea bottom | 3910 | 3910 | 0 | 5.200 | 5.200 | 0 |
| Green | 4283 | 4283 | 0 | 5.615 | 5.615 | 0 |
| Purple | 4628 | 4628 | 0 | 5.975 | 5.990 | 0.015 |
| Yellow (top BS) | 4858 | 4858 | 0 | 6.180 | 6.142 | -0.038 |
| 7b (intra-BS2) | 5050 | 5050 | 0 | 6.240 | 6.251 | 0.011 |
| 8 (intra BS1) | 5170 | 5170 | 0 | 6.420 | 6.389 | -0.031 |
| Orange (LBS) | 5311.5 | 5311.5 | 0 | 6.590 | 6.612 | 0.022 |

Observed discrepancies between the original and the adjusted time-depth relationship values can be explained by the higher resolution of the available seismic lines for the present study (compared with the seismic data used in 1976 when Site 398 was drilled), and the positioning of the seismic lines in relation to the exact well location. This last issue is valid both for the original seismic lines (from where the initial time/depth relationship was obtained) as well for the here used seismic lines.

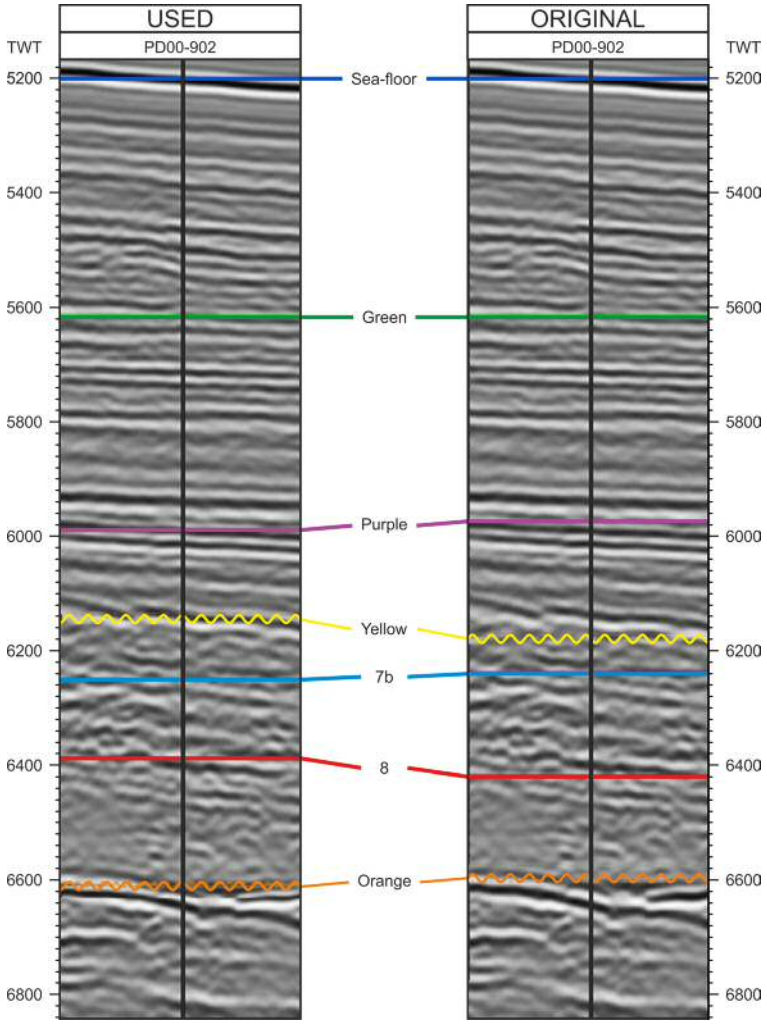


**Figure 2.6** Graphical difference between the original time data and the same horizons adjusted for this study. This adjustment was done have as a base the position of some of the identified reflectors on seismic lines PD0-901 and PD0-902. The seismic line here represented is PD0-902, where penetrated by DSDP site 398D. The reflector names are from Sibuet *et al.* (1979).

## 2.4. Seismic interpretation along the continental slope

Seismic facies was the main tool used to correlate seismic-stratigraphic surfaces between distinct basins due to a lack of better well control (Fig. 2.2). Within the outer proximal margin, the presence of salt diapirs, disconnected small sub-basins and (certainly) several different sediment entry points are impediments for a seismic interpretation completely free of issues and interrogations when using as a work

base a (geographically discontinuous) 2D dataset. Nevertheless, the close spacing of the TGS-NOPEC survey in this area and the use of comprehensive seismic facies associations overcame those issues. Concerning the deeper parts of the outer proximal and distal margins, the location of the available wells crossing and sampling the BS is well dispersed (Sites 398 and 641), covering a large part of the study area (Fig. 2.2). Moreover, the seismic facies displayed by the BS in these areas of the rift basin are quite regular and distinct (Chapters 4 and 5) allowing their recognition and interpretation across sub-basins, which in turn here are not so frequent as in the more proximal regions and with a less intricate morphology and distribution.

### 2.4.1. Interpreting horizons along different margin segments in Northwest Iberia

According to previous authors, the Aveiro Fault constitutes the boundary between two different margin segments with different extensional and breakup histories (Alves *et al.*, 2009). Although the available seismic dataset covering the outer proximal Peniche Basin and part of the inner proximal margin south of the Porto Basin extends southward of the Aveiro fault (Fig. 2.2), the interpretation in this thesis stop at this important tectonic feature. Discerning the LBS and the BS position proved to be increasingly difficult towards the Aveiro Fault and impossible (within the limits of plausibility, given the available data) to correlate across it. Several factors account for this, such as: (1) the prominence of the fault scarp of Aveiro fault which acts as an important rupture point; (2) this fault is the boundary between two margin segments, with different timings in terms of its extensional and rupture history, therefore the position of the LBS is likely to be placed at a different (older) stratigraphic level (and no well data was available in this area) and (3) the presence of important halokinesis in this area masks the sedimentary syn-rift tectonic signature.

## 2.5. Clarification of some terms used in this thesis

Throughout this thesis, three terms are used which due to a lack of general agreement in the literature should be clarified in terms of their definition:

**Continental rifting**—this term refers to the extensional processes that affect the continental lithosphere promoting its thinning at a tectonic plate scale. It may or may not lead to a complete rupture of the lithosphere and oceanic crust accretion.

**Continental crust breakup**—this term refers to the rupture of the continental crust following a period of continental rifting. It may lead to upper mantle exhumation (lower lithosphere) or to oceanic crust accretion. In the latter case, the term 'lithospheric breakup' can be applied.

**Lithospheric breakup**—this term refers to the complete rupture of the continental lithosphere leading to the accretion of oceanic crust. It may or may not have been preceded by upper mantle exhumation. **Continental breakup** is a synonym of lithospheric breakup.

Chapter Three

# WEST IBERIAN MARGIN PHYSIOGRAPHY AND GEOLOGICAL HISTORY

## 3.1. Physiography of the study area

The West Iberia continental shelf, extending for more than 700 km, has a width varying from 10 to 65 km. In terms of its geomorphology, major canyons cut the continental shelf along major faults, dividing the margin in four distinct segments, from south to north: (1) the segment between St. Vincent and Setúbal canyons, (2) the segment between Setúbal and Nazaré canyons (3) the segment between the Nazaré and the Aveiro canyons and (4) the segment between the Aveiro Canyon and the Cape Finisterra (Fig. 3.1). The Aveiro Canyon, located on a Mesozoic first-order transfer zone (Groupe Galice, 1979), started its incision during the Oligocene, forming a major conduit for sediment into the Iberia Abyssal Plain (Vanney & Mougenot, 1981). The continental shelf north of the Aveiro fault is thus characterized by a narrow width, varying between 10 and 40 km, followed by a steep and narrow continental slope, and a wide continental rise where several structural highs are observed: the Vasco da Gama, Vigo and Porto seamounts and the Galicia Bank (Fig. 3.1). Using seismic data, these structural highs were interpreted as NNW-SSE oriented horsts formed during the Mesozoic rifting of the margin (Montadert *et al.*, 1974), They were later reactivated and uplifted during an Eocene compressive event (Boillot *et al.*, 1979). The study area includes the Porto Basin on the inner proximal margin, the Peniche-Galicia Interior Basins on the outer proximal margin, and the Iberia Abyssal Plain on the distal margin (Fig. 3.1). The Porto Basin and the Peniche Basin are controlled by NNE-SSW westward dipping normal faults, which become NNW-SSE northwards towards the Galicia Interior Basin (Murillas *et al.*, 1990). For a review of the main physiographic and geomorphological features of the West Iberia continental margin, the reader is directed to Pinheiro *et al.* (1996) and Alves *et al.* (2006).

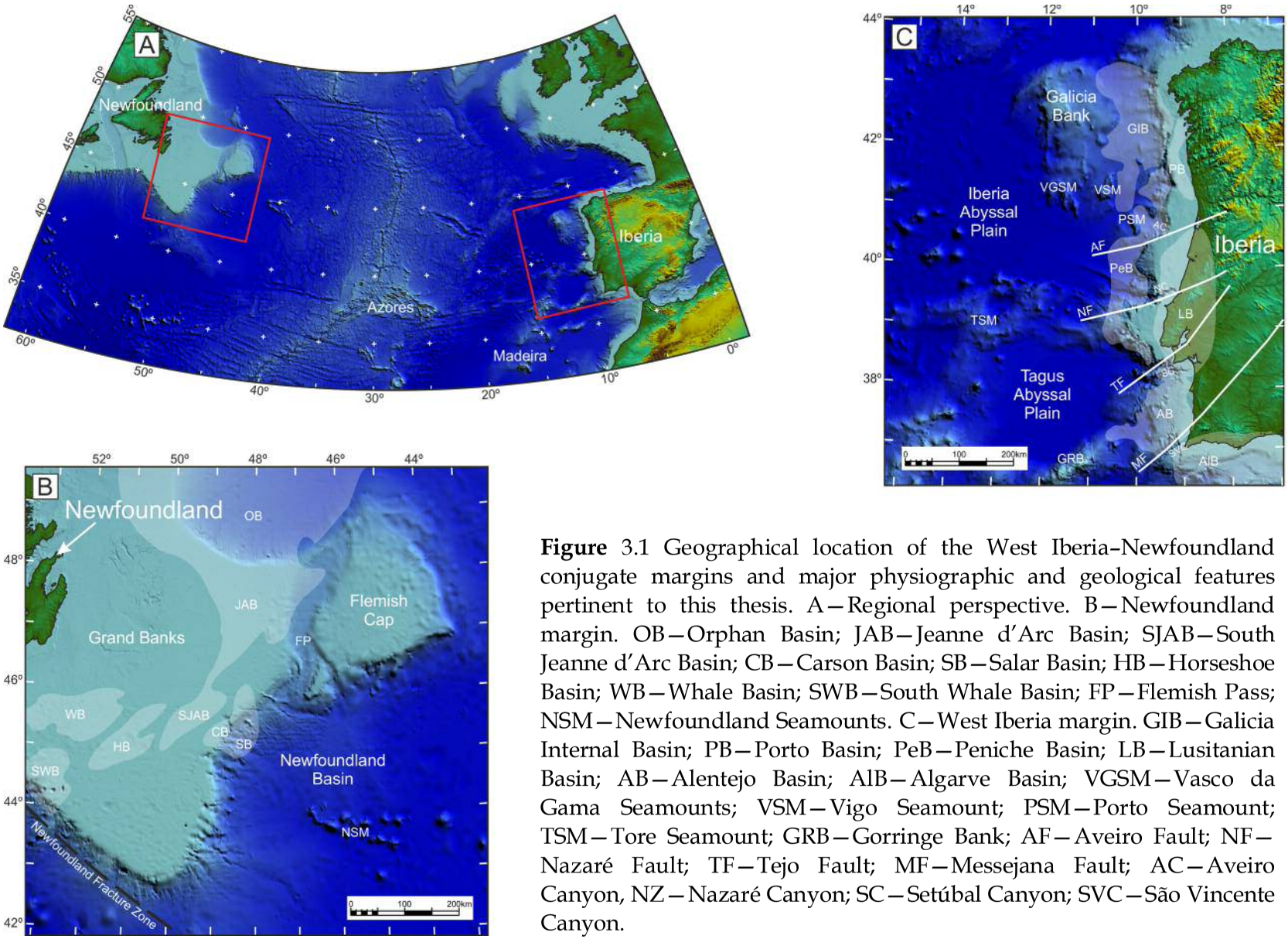


**Figure** 3.1 Geographical location of the West Iberia–Newfoundland conjugate margins and major physiographic and geological features pertinent to this thesis. A—Regional perspective. B—Newfoundland margin. OB—Orphan Basin; JAB—Jeanne d'Arc Basin; SJAB—South Jeanne d'Arc Basin; CB—Carson Basin; SB—Salar Basin; HB—Horseshoe Basin; WB—Whale Basin; SWB—South Whale Basin; FP—Flemish Pass; NSM—Newfoundland Seamounts. C—West Iberia margin. GIB—Galicia Internal Basin; PB—Porto Basin; PeB—Peniche Basin; LB—Lusitanian Basin; AB—Alentejo Basin; AlB—Algarve Basin; VGSM—Vasco da Gama Seamounts; VSM—Vigo Seamount; PSM—Porto Seamount; TSM—Tore Seamount; GRB—Gorringe Bank; AF—Aveiro Fault; NF—Nazaré Fault; TF—Tejo Fault; MF—Messejana Fault; AC—Aveiro Canyon, NZ—Nazaré Canyon; SC—Setúbal Canyon; SVC—São Vincente Canyon.

Located on the Atlantic Margin of East Canada, the Newfoundland margin is characterized by a wide continental shelf, the Grand Banks, which is more than 400 km wide. The Grand Banks are bounded to the southeast by the Newfoundland Fracture Zone, a major tectonic feature separating Newfoundland from the Nova Scotia shelf. Towards the northeast is located a very important bathymetric feature, the Flemish cap, a fragment of continental crust separated from the continental shelf during the Early Cretaceous (Sibuet *et al.*, 2007a). The Grand Banks have several important Mesozoic-Cenozoic sedimentary basins, with a general NE-SW trend, formed during the North Atlantic rifting (Keen & Piper, 1990) (Fig. 3.1). In terms of its sedimentary infill, the Newfoundland margin contains a very thick sedimentary succession, particularly when compared with the conjugate West Iberia margin (Shipboard Scientific Party, 1987b; Tankard & Welsink, 1989). This character shows sediment supply to have been significant throughout the geological history of the Newfoundland Margin.

## 3.2. West Iberia–Newfoundland tectono-stratigraphic rifting evolution

### 3.2.1. Rifting, mantle exhumation and lithospheric breakup

Continental rifting between West Iberia and Newfoundland occurred in two major stages (Boillot *et al.*, 1987a; Whitmarsh & Wallace, 2001; Tucholke *et al.*, 2007a) (Fig. 3.2). The first stage—Lithospheric Rifting Stage 1 (LRS1, Fig. 3.2A), occurring during the Late Triassic–Barremian—records multiple episodes of crustal stretching and an ongoing basinward migration of the extensional locus that, eventually, led to rupture of the continental crust (Murillas *et al.*, 1990; Reston, 2005; Ranero & Pérez-Gussinyé, 2010) (Fig. 3.2A). LRS1 ends with diachronous breakup of the continental crust, starting in the southern part of Iberia and migrating northwards. Continental crust rupture was followed by the second rifting stage (LRS2, Fig. 3.2B), occurring from the Upper Berriasian–Valanginian to the Aptian–Albian transition. The LRS2 is marked

by the exhumation and thinning of serpentinized subcontinental lithospheric mantle, and by localized emplacement of decompression melts (Boillot *et al.*, 1980; Boillot *et al.*, 1988; Sawyer *et al.*, 1994; Boillot *et al.*, 1995; Whitmarsh *et al.*, 1998). The LRS2 is subdivided in two transitional extension periods (TE1—Valanginian/Hauterivian boundary and TE2—Barremian to Aptian/Albian boundary) by Tucholke & Sibuet (2007), occurring respectively to the south and north of Aveiro Fault (Fig. 3.1).

This transitional area, between the continental crust and the true oceanic crust was named the Zone of Exhumed Continental Mantle (ZECM) by Whitmarsh *et al.* (2001). Nevertheless, this then implies that the zone is floored by subcontinental mantle lithosphere (Fig. 3.3). In contrast, the term ocean–continent transition zone (OCTZ) is used without genetic, evolution or compositional connotations for the transition from the distal thinned continental curst margin to the first normal oceanic crust (Pickup *et al.*, 1996; Chian *et al.*, 1999; Dean *et al.*, 2000).

The occurrence of a OCTZ, essentially composed of exhumed mantle, was first recognised between the Galicia Bank and the Iberia Abyssal Plain by dredging, which retrieved serpentinized mantelic rocks (Boillot *et al.*, 1980). Following this discovery, several drilling campaigns retrieved highly serpentinized peridotites and other mantelic rocks from structural highs in Northwest Iberia (Boillot *et al.*, 1987b; Sawyer *et al.*, 1994; Whitmarsh *et al.*, 1998) (Fig. 3.1C).

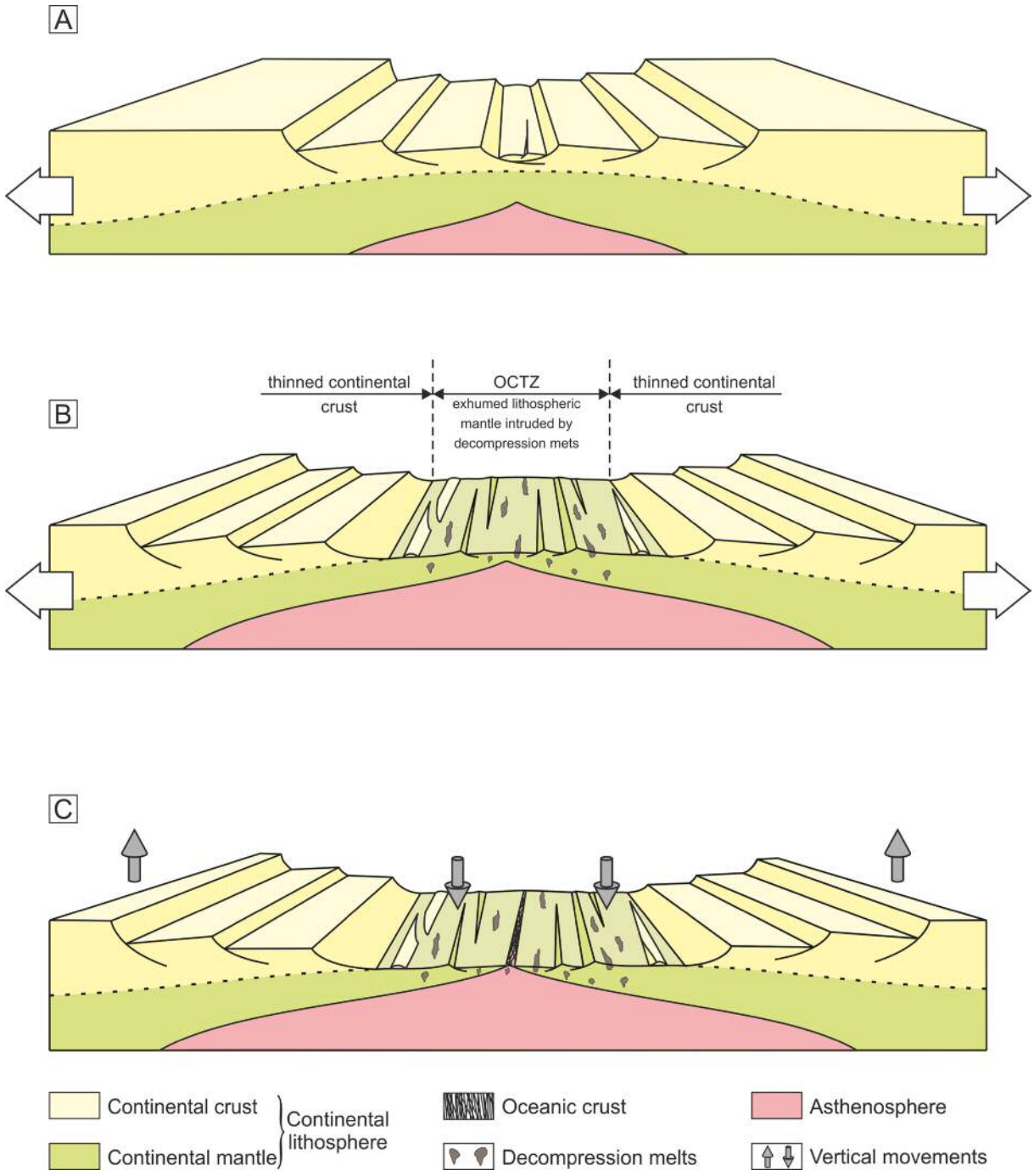


**Figure 3.2** Simplified schematic drawing of the lithospheric rifting stages development and lithospheric breakup. A—lithospheric rifting stage 1 (LRS1): in this stage all lithosphere is thinned until the continental crust suffers rupture and separates—continental crust breakup. B—lithospheric rifting stage 2 (LRS2): after continental crust separation, lithospheric mantle is exhumed and thinned and locally intruded by decompression melts (ocean–continent transition zone—OCTZ). C—LRS2 ends with the complete separation of the continental lithosphere (lithospheric breakup) and the accretion of normal oceanic crust. This dual stage rifting process promotes a strong basinward migration of the extensional locus, particularly after LRS2, in which extensional stresses concentrate on the exhumed lithosphere.

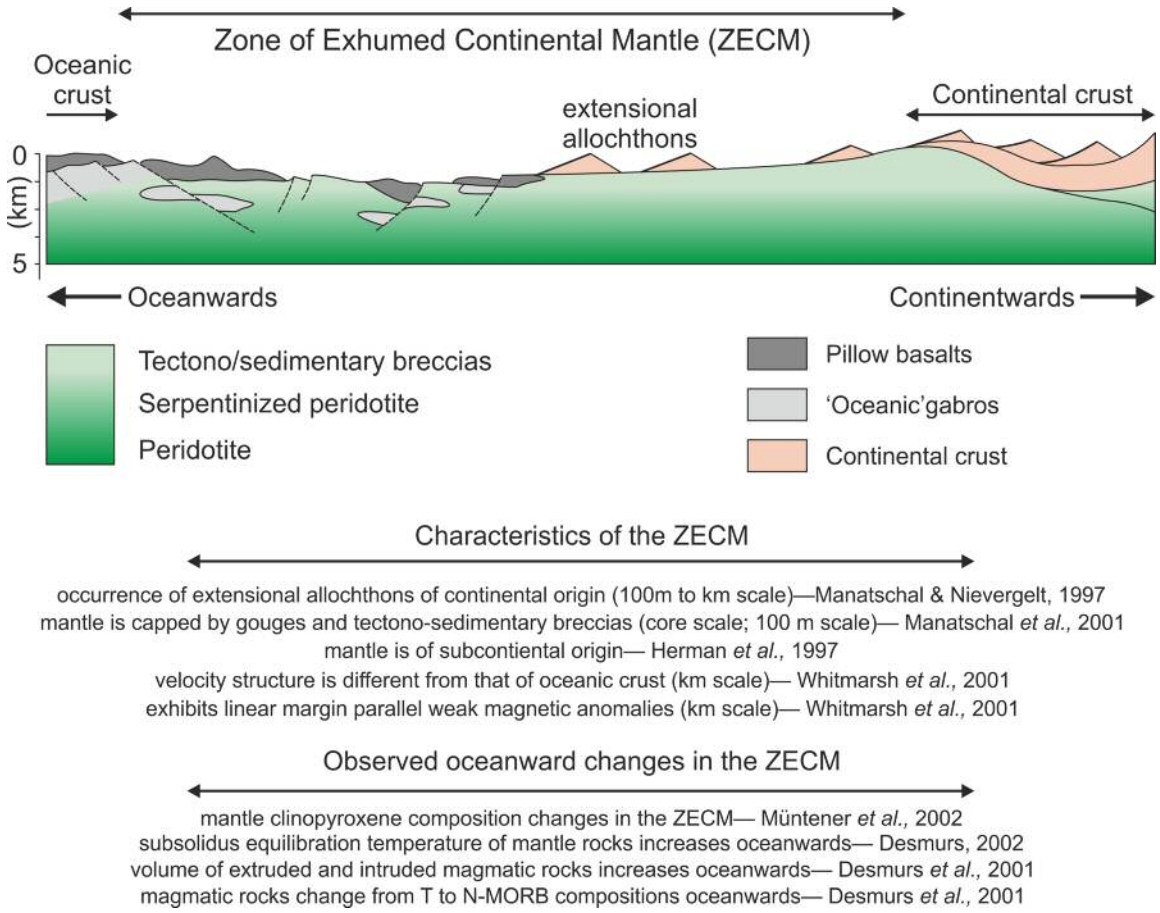


**Figure 3.3** Simplified schematic drawing and characteristics of the zone of exhumed continental mantle (ZECM) in nowadays passive magma-poor rifted margins. Redrafted from Manatschal (2004).

Similarly, on the Newfoundland conjugate margin, ODP Site 1277 drilled through serpentinized mantle on a structural high, showing that both margins underwent similar rifting processes (Shipboard Scientific Party, 2004a) (Fig. 3.1C, Fig. 3.4).

Highly variable in width, the ZECM varies from just a few kilometres west of the Galicia Bank to more than 170 km on the southern Iberia Abyssal Plain (Whitmarsh *et al.*, 1996b; Discovery 215 Working Group, 1998). As of 2014, it is not clear if exhumation of the lower lithosphere occurred along the entire length of West Iberia; debates persist on whether Southwest Iberia went through this process, as no direct evidence (drilling) exist in this region (Pinheiro *et al.*, 1992; Srivastava *et al.*, 2000;

Afilhado *et al.*, 2008; Sibuet & Tucholke, 2012; Sallarès *et al.*, 2013). Nevertheless some authors interpret the ZECM as extending towards the Newfoundland–Gibraltar Fracture Zone (*e.g.* Tucholke & Sibuet, 2007) (Fig. 3.4).

The nature and mode of emplacement of the OCTZ is still debated. Three main schools of thought exist regarding this problem: (1) the OCTZ represents thinned continental crust through which the mantle was exhumed (Tucholke *et al.*, 1989; Dean *et al.*, 2000; Whitmarsh *et al.*, 2001); (2) the OCTZ is composed of mantle rocks exhumed by means of simple or pure shear (Boillot *et al.*, 1989; Brun & Beslier, 1996; Discovery 215 Working Group, 1998; Chian *et al.*, 1999), and (3) the OCTZ comprises a melange of basalt, gabbro and mantle material, considered to be oceanic crust, essentially formed by ultraslow seafloor spreading (Whitmarsh & Sawyer, 1996; Srivastava *et al.*, 2000). In particular, Srivastava *et al.* (2000) presents a very comprehensive review of these three hypotheses.

One of the reasons supporting hypothesis 3 is the presence of magnetic lineations on the OCTZ. These magnetic lineations, following similar trends to those found on normal oceanic crust, are weak and interpreted as evidence for the presence of oceanic crust on the OCTZ (Srivastava *et al.*, 2000). The presence of these magnetic lineations allowed for a more precise understanding of the plate kinematics between West Iberia-Newfoundland and their palaeogeographic reconstruction in its regional context (Srivastava *et al.*, 2000; Vissers & Meijer, 2012) (Fig. 3.4). More recently, other explanations for the presence of weak magnetization on the OCTZ emerged as an alternative for magnetization by cooling of volcanic rocks extruded during the oceanic crust accretion process (Russell & Whitmarsh, 2003; Sibuet *et al.*, 2007b; Bronner *et al.*, 2011). Thus magnetization has also been interpreted as the product of the emplacement of large igneous bodies (dikes or sills) at depths of >3 km (Russell & Whitmarsh, 2003), or due to the serpentinization process of mantle rocks at shallow depths (Sibuet *et al.*, 2007b).

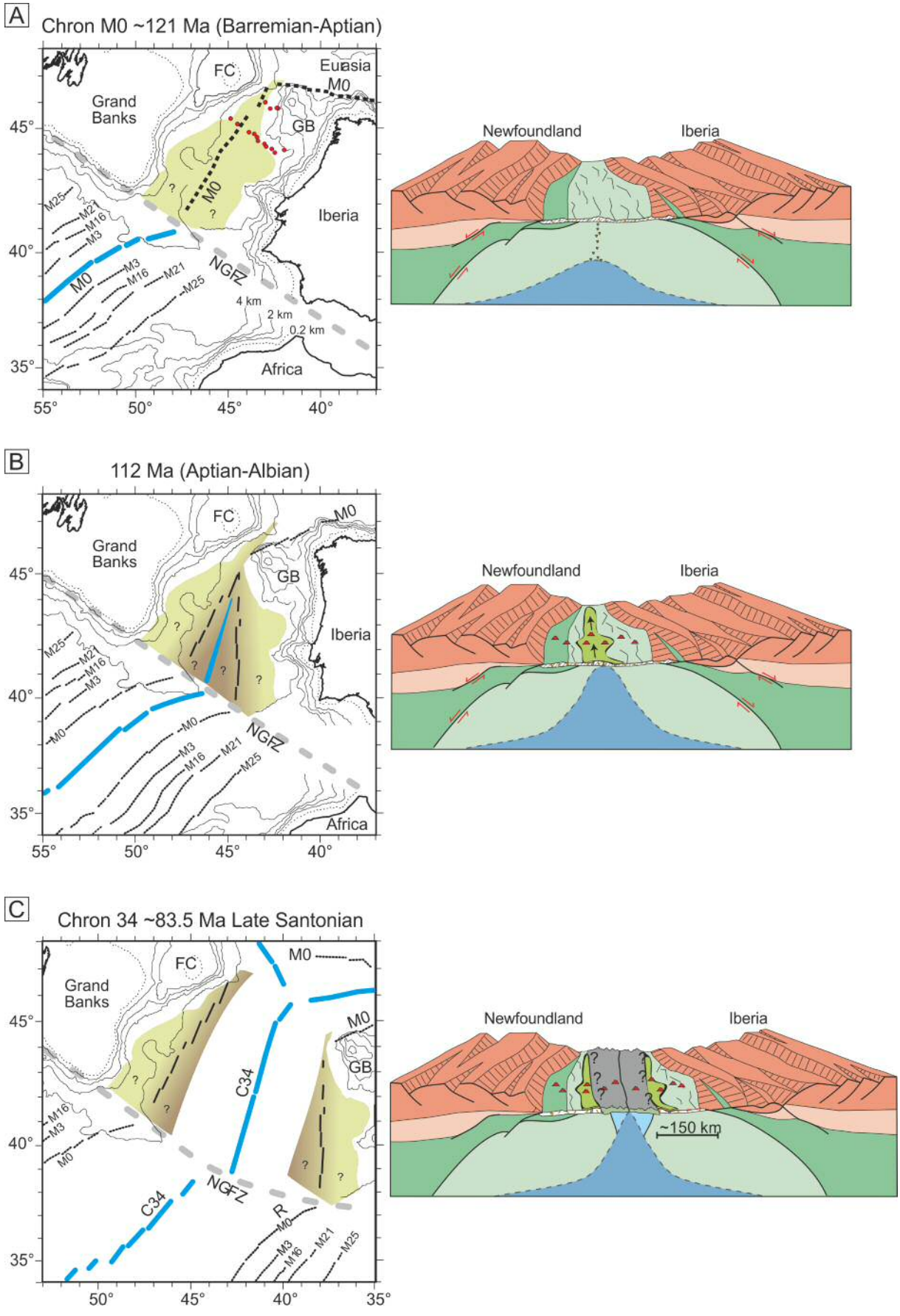


**Figure 3.4** (Key and caption on next page)

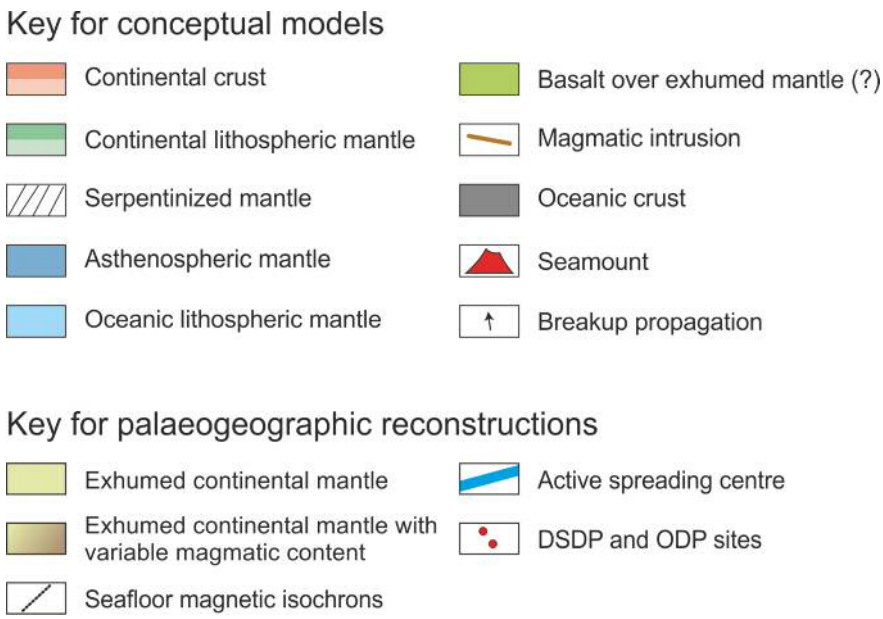


**Figure 3.4** (continuation) Palaeogeographic reconstruction and conceptual models for three stages of the West Iberia–Newfoundland conjugate margins during the Cretaceous. A—reconstruction at Chron M0 showing the lithospheric mantle exhumation occurring in both sides of the conjugate margins. Note that the southward total extensional of the mantelic exhumation is speculative. B—reconstruction at the moment of lithospheric breakup (Aptian Albian transition). Between A and B alongside the mantelic exhumation, localized emplacement of decompression melts becomes more frequent. C—reconstruction at Chron 34, after several million years of oceanic crust spreading. Modified from (Tucholke & Sibuet, 2007; Bronner *et al.*, 2011; Tucholke & Sibuet, 2012).

In detail, four extensional episodes are recorded in West Iberia: (1) Late Triassic to Hettangian; (2) Sinemurian–Early Pliensbachian; (3) Late Oxfordian–Kimmeridgian and (4) Berriasian–latest Aptian (Wilson *et al.*, 1989; Stapel *et al.*, 1996; Leinfelder & Wilson, 1998; Rasmussen *et al.*, 1998; Alves *et al.*, 2009). The last extensional episode was followed by complete separation between Iberia and Newfoundland (Boillot & Malod, 1988; Wilson, 1988; Tucholke *et al.*, 1989; Whitmarsh & Miles, 1995; Srivastava *et al.*, 2000; Sibuet *et al.*, 2007b; Bronner *et al.*, 2011). Diachronous breakup occurred progressively from south to north along the two margins (Tankard & Welsink, 1987; Hiscott *et al.*, 1990; Pinheiro *et al.*, 1992; Pinheiro *et al.*, 1996; Stapel *et al.*, 1996; Alves *et al.*, 2009), with crustal thinning occurring mainly on the outer proximal and distal margins after the end of 'wide-rift mode' extension ('thinning phase' of Lavier & Manatschal, 2006; Welford & Hall, 2007; Afilhado *et al.*, 2008).

Final lithospheric breakup in Northwest Iberia occurred during the Aptian-Albian transition, following complete separation of the lithosphere and the emplacement of true oceanic crust (Boillot *et al.*, 1987b; Sawyer *et al.*, 1994; Whitmarsh *et al.*, 1996a) (Fig. 3.4B). This event is considered to have occurred as a gradual process, in which the exhumation and extension of the lower lithosphere was taking place at the same time 'normal' oceanic crust was being formed—until the later prevailed and complete lithospheric breakup was achieved (Russell & Whitmarsh, 2003; Jagoutz *et al.*, 2007; Sibuet *et al.*, 2007b; Sibuet & Tucholke, 2012). In this thesis, the final breakup is called 'lithospheric breakup' in order to distinguish it from the preceding phase of continental crust rupture, hereon called continental crust breakup (Fig. 3.2).

The lithospheric breakup event releasing in-plane stresses accumulated during continental rifting, promoted flexural rebound of the lithosphere with consequent rift shoulder uplift. This event is recorded by a forced regressive systems tract in the Porto Basin (see Chapter 4, Soares *et al.*, 2012). Flexural uplift occurring at this time has also been suggested by fission-track data from Galicia (Grobe *et al.*, 2014).

During the remaining Cretaceous, the post-rift phase is marked by several pulses of magmatic activity during the Late Cretaceous, which are recorded by the intrusion of large igneous bodies (and extrusion of volcanic rocks) both onshore and offshore (Miranda *et al.*, 2009; Neres *et al.*, 2014).

### 3.2.2. Stratigraphic evolution

The first extensional episode, responsible for the initiation of a wide-rift mode, i.e. the 'stretching phase' of Lavier & Manatschal (2006), resulted in the deposition of extensive fluvial red bed deposits in onshore basin, the Grés de Silves Formation, filling shallow grabens and half-grabens during the Triassic (Palain, 1976; Rasmussen *et al.*, 1998) (Fig. 3.5). A relative deepening is recorded at the transition between the Grés de Silves continental red beds and the evaporitic deposits of the Dagorda formation (latest Triassic–earliest Jurassic) (Fig. 3.5). The second and third extensional episodes record a predominant carbonate deposition up to the start of the Late Jurassic (Fig. 3.5). During the fourth extensional episode, a carbonate-siliciclastic

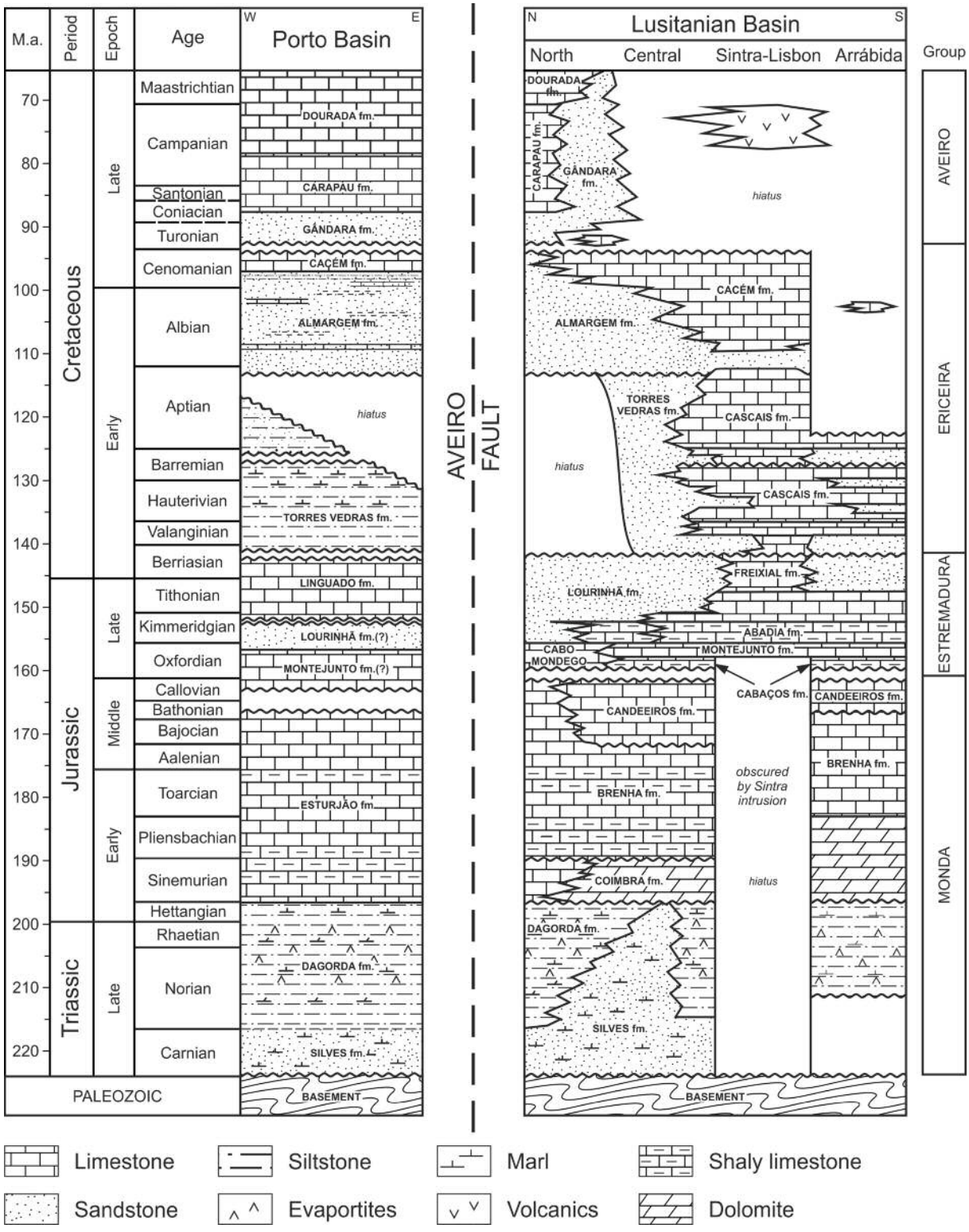


**Figure 3.5** Simplified lithostratigraphic columns for the Mesozoic of the Lusitanian Basin and the Porto Basin (basin location in Figure 3.1). Lusitanian Basin from Pereira & Alves (2011), Porto Basin based on Witt (1977), GPEP (1986), Wilson *et al.* (1989), Salén/Pecten (1985), Texaco (1979).

deposition becomes predominant until lithospheric breakup occurs during the Aptian-Albian transition. After lithospheric breakup, the deposition of a thick siliciclastic sequence (Almargem formation) is recorded onshore and offshore until the middle Cenomanian, when carbonate deposition was again resumed (Witt, 1977; Wilson *et al.*, 1989; Alves *et al.*, 2006) (Fig. 3.5).

In Northwest Iberia, the syn- to post-rift transition occurs within the Ericeira Group, between the Torres Vedras (lower Valanginian-upper Aptian) and the Almargem formations (Uppermost Aptian-lower Cenomanian) (Fig. 3.5). In the Porto Basin, the Torres Vedras formation comprises marly siltstones and claystones grading upwards into fine sandstones and siltstones deposited in neritic environments (Fig. 3.5). The Almargem formation, resting over the eroded Torres Vedras formation, was initially deposited during a forced regression, prograding markedly over the continental shelf. This progradation was accompanied by significant sediment by-pass of the continental shelf, with consequent sediment input occurring directly into deeper parts of the basin (Chapter 4, Soares *et al.*, 2012). This siliciclastic sequence is capped by a regional carbonate unit, the Cacém formation.

In deep-offshore basins of Northwest Iberia, several dredging and drilling campaigns sampled basement rocks, syn-rift and post-rift strata (Dupeuble *et al.*, 1976; Groupe Galice, 1979; Boillot *et al.*, 1987b; Sawyer *et al.*, 1994; Whitmarsh *et al.*, 1998). Lower Cretaceous syn-rift units comprise turbidites intercalated with slump deposits, later capped by strata interpreted to represent the final lithospheric breakup event (Shipboard Scientific Party, 1979, 1987a). These strata, comprising widespread mass-wasting deposits, contrast with the extensive black-shale deposits above, thus generating a regional seismic reflection interpreted as marking the lithospheric breakup [the orange reflector of Sibuet *et al.* (1979) and its conjugate counterpart, the U reflector of Tucholke *et al.* (1989)] (Tucholke *et al.*, 2007a). For a detailed description of the Portuguese West Iberia margin stratigraphy, the reader is directed to the following works: Kullberg *et al.* (2013), Rey *et al.* (2006), GPEP (1986), Witt (1977).

Chapter Four

# THE BREAKUP SEQUENCE AND ASSOCIATED LITHOSPHERIC BREAKUP SURFACE

An abridged version of this chapter has been published as:

Soares, D.M., Alves, T.M., Terrinha, P., 2012. *The breakup sequence and associated lithospheric breakup surface: Their significance in the context of rifted continental margins (West Iberia and Newfoundland margins, North Atlantic)*. Earth and Planetary Science Letters 355–356, p. 311-326.

## 4.1. Abstract

Regional (2D) seismic-reflection profiles and borehole data are used to characterise the syn- to post-rift transition in the shallow offshore Porto Basin, and in deep-offshore regions of West Iberia and Newfoundland (East Canada). The interpreted data highlight the development of a regional stratigraphic surface at the time of complete lithospheric breakup between West Iberia and Newfoundland. This surface, usually called 'breakup unconformity', is renamed in this work as lithospheric breakup surface (LBS), on the basis that: (1) it is not always developed as an unconformity and (2) all lithosphere is involved on the breakup process, not only the continental crust. Depositional changes occur across the LBS in association with Late Aptian lithospheric breakup, which is marked by the deposition of a breakup sequence (BS) rather than a single stratigraphic surface. Stratigraphic correlations between strata in shallow and deeper parts of the two margins led to propose the BS as representing the transitional period between lithospheric breakup and the establishment of thermal relaxation as the main process controlling subsidence on divergent continental margins. The results in this chapter are important for other continental margins as they demonstrate that during lithospheric breakup significant quantities of sediment bypassed the inner proximal margins of West Iberia and Newfoundland on their way to the outer proximal margin. In addition, the interpreted data show that complete lithospheric breakup between conjugate margins is recorded by similar tectono-stratigraphic events. In Iberia and Newfoundland, these events are associated with reservoir successions in sediment overfilled basins and with carbon-rich strata ('*black shales*') in sediment-starved basins.

## 4.2. Introduction

The classic definition of '*breakup unconformity*' (Falvey, 1974) implies the generation of a basin-wide unconformity separating syn-rift from post-rift strata at the time of crustal breakup and onset of oceanic crust accretion (Falvey, 1974;

Ziegler, 1975; Tankard & Welsink, 1987; Wernicke & Tilke, 1989; Embry & Dixon, 1990; Moore, 1992; O'Driscoll *et al.*, 1995; Withjack *et al.*, 1998; Jungslager, 1999; Whitmarsh & Wallace, 2001; Kyrkjebø *et al.*, 2004; Tucholke *et al.*, 2007a). However, this concept has been questioned after the discovery in Iberia-Newfoundland that rifting and final (lithospheric) breakup occurred in two distinct lithospheric rifting stages. Here, where slow and ultraslow rifting rates are recorded (Sibuet *et al.*, 2007b; Cannat *et al.*, 2009), rifting and lithospheric breakup comprised: (1) a first stage of rifting and separation of the continental crust (continental crust breakup), followed by (2) upper mantle exhumation, extension and lithospheric breakup with accretion of normal oceanic crust (Boillot *et al.*, 1987a; Whitmarsh *et al.*, 2001; Tucholke *et al.*, 2007a). The fact that continental breakup is not promptly associated with the generation of normal oceanic crust on the distal margin, resulting instead in the generation of a transitional zone with exhumation and thinning of the lower lithosphere, led several authors to regard the existence of a '*breakup unconformity*' as doubtful (Manatschal, 2004; Péron-Pinvidic *et al.*, 2007; Sibuet *et al.*, 2007b; Tucholke *et al.*, 2007a).

The existence of a transitional phase recording the change from syn-rift to post-rift conditions is, however, acknowledged on several divergent margins (Keen *et al.*, 1987; Tankard & Welsink, 1987; Moore, 1992; Platt, 1995; Cainelli & Mohriak, 1999; Jungslager, 1999; Beglinger *et al.*, 2012). For instance, Moore (1992) interpreted a well defined unconformity-bounded sequence between syn-rift and post-rift units in the Porcupine Basin. Defined on the inner proximal margin and limited to main depocentres, Moore's (1992) '*transition sequence*' is affected by extensional faulting during its early stages, and pre-dates the Aptian–Early Albian lithospheric breakup between Iberia and Newfoundland. This character associates the sequence with Late Jurassic–earliest Cretaceous rifting in the North Atlantic. Such a discrepancy illustrates the difficulties in recognising '*breakup unconformities*' on distinct continental margins, particularly when in the presence of multi-phased rifting and breakup. Thus, the boundaries of '*transitional sequences*' are often diffused and the criteria proposed to identify them are so far only applicable on a regional scale.

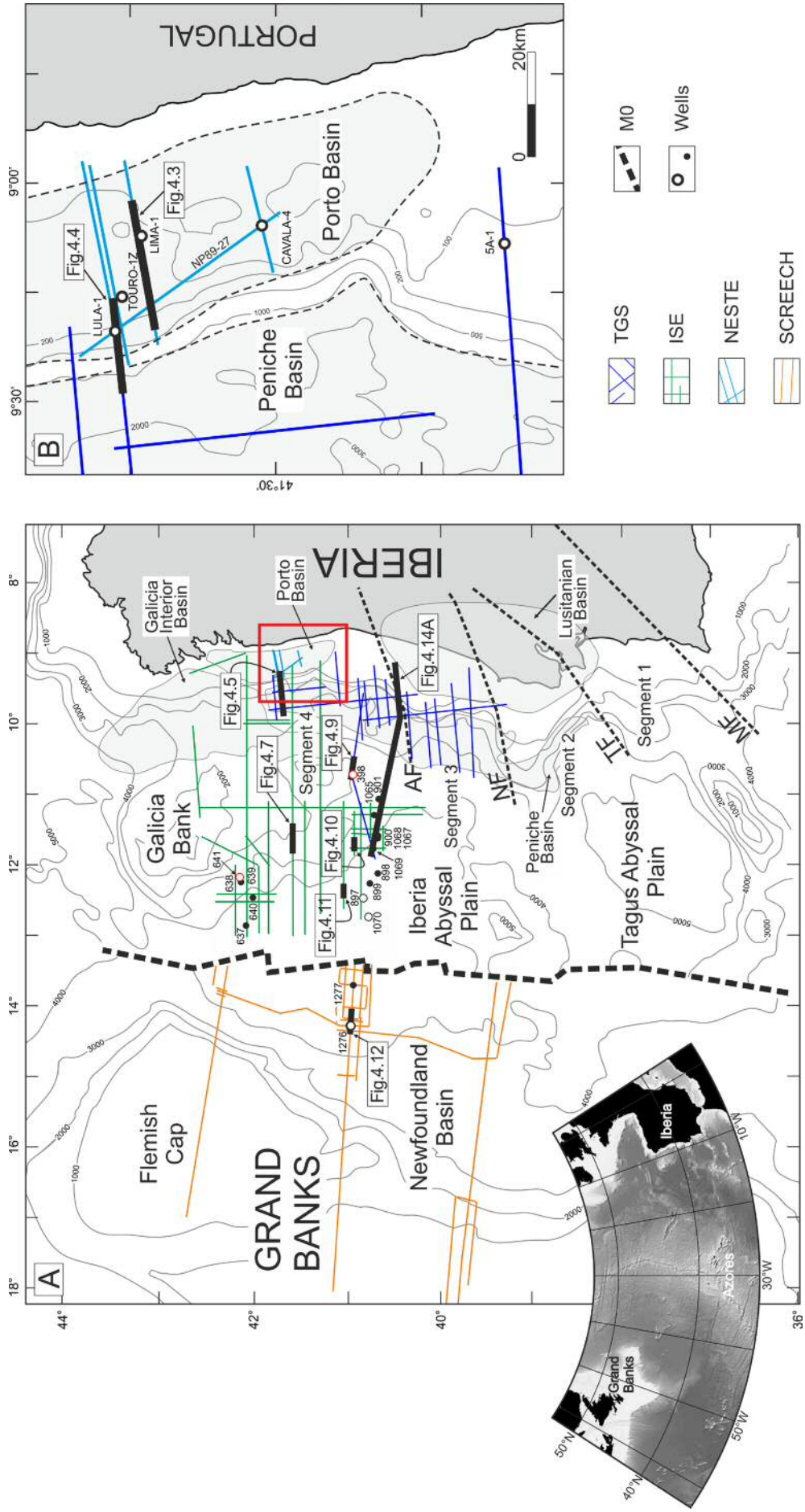


**Figure 4.1** Maps showing the location of the study area and data sets used in this Chapter. A—reconstruction of the Iberia–Newfoundland rift margins at chron M0 (~125Ma, thick dashed line) before lithospheric breakup (after Srivastava *et al.*, 2000), with the Iberian plate fixed relatively to its present geographic coordinates). DSDP/ODP sites are shown in the image. Those with open circles are represented in Figure 4.14. Those with red circles indicate the sites where Lithospheric breakup surface was cored. AF—Aveiro fault; NF—Nazaré fault; TF—Tejo fault. The red box indicates the position of B. Inset shows present day position of the conjugate margins. B—Porto Basin and Peniche Basin detail with the location of key seismic profiles and industry boreholes.

Using regional (2D) seismic and borehole data, this chapter describes the timing and significance of depositional changes occurring across the Late Aptian–Early Albian *'breakup unconformity'* offshore West Iberia and Newfoundland (Fig. 4.1). Results from the inner proximal margin (Porto Basin) are integrated with data from the outer proximal (Peniche Basin, West Galician Margin) and distal margins (Iberia Abyssal Plain and Newfoundland Basin) for the time-period associated with the main, and final (lithospheric), breakup event between the two margins.

When of continental breakup, the Porto and Peniche Basins were located in a marginal position to the distal basins where ODP legs 103, 149 and 173 were drilled (Alves *et al.*, 2006) (Fig. 4.1). In contrast to the work of Kyrkjebø *et al.* (2004) on the '*breakup unconformity*' of a Neocomian aulacogen (North Sea), West Iberia and Newfoundland consist of rifted margins that experienced complete lithospheric breakup.

In this chapter, it is suggested that the Aptian–Albian stratigraphic surface known as '*breakup unconformity*' should continue to be recognised, at a regional scale, as the principal stratigraphic feature related to continental breakup between these conjugate margins. However, as both continental crust and lower lithosphere are involved in the breakup process, the term '*lithospheric breakup surface*' (LBS) is proposed to replace the term '*breakup unconformity*'. It is acknowledged that the stratigraphic surface created by this lithospheric breakup event is not developed as an unconformity in all rift-related basins on the proximal, outer proximal and distal margins. In this chapter it is also proposed the concept of '*breakup sequence*' (BS) as comprising the complete seismic and stratigraphic expression of lithospheric breakup. The BS, recognisable on seismic data, is bounded by stratigraphic unconformities (or their correlative surfaces) from proximal to distal parts of a continental margin, and can be sub-divided in distinct units. The concepts of time- and spatially-changing *'lithospheric breakup surface'*, and overlying '*breakup sequence*', are able to answer questions regarding the validity and significance of regional stratigraphic unconformities generated in the context of the lithospheric breakup of continents.

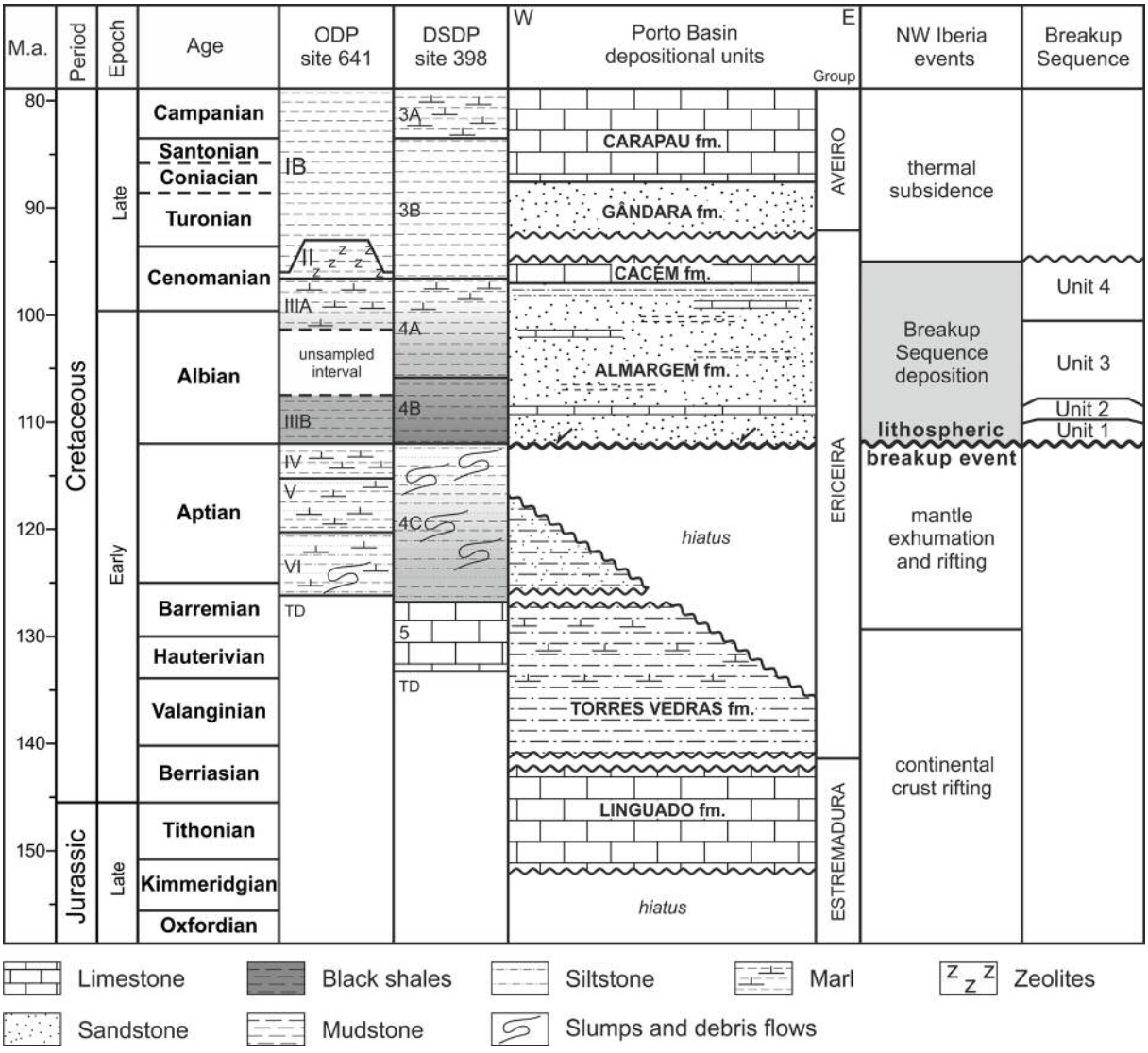


**Figure 4.2** Lithostratigraphic table comparing the Porto Basin with DSDP Site 398 and ODP Site 641 (Witt, 1977; Sibuet *et al.*, 1979; Boillot *et al.*, 1987b; Wilson *et al.*, 1989; GPEP, 1986; Alves *et al.*, 2003b). Note that the lithospheric breakup surface is blanketed by a downlapping, westward prograding unit, and the correspondence between the post-lithospheric breakup event strata, the Almargem formation and units 4b and 4a in DSDP site 398. TD—total depth. LRS—lithospheric rifting stage.

Furthermore, in this chapter it is suggested that although not exerting direct influence in the beginning of the BS deposition, post-breakup thermal subsidence gradually becomes a major control on the stratigraphic architecture of the BS. Nevertheless, in contrast to the *transitional mega-sequence* of Beglinger *et al.* (2012), the BS does not record the complete peneplanation (in a overall 'sag basin' setting) of the syn-rift topography of West Iberia. By naming it '*breakup sequence*' (BS), it is

emphasised the fact that the BS comprises a well-defined stratigraphic sequence on divergent continental margins, deposited under the control of tectono-stratigraphic events triggered by the breakup event *per se*.

This chapter starts with a description of the '*breakup unconformity*' and overlying sequences in West Iberia and Newfoundland, followed by the redefinition of this latter surface as LBS. The tectono-stratigraphic significance of strata deposited above the LBS is then addressed in detail. The chapter finishes with a discussion on the definition of the LSB and BS, and of criteria used for their recognition on continental margins. West Iberia is also reassessed as a sediment-nourished to sediment-balanced margin on its outer proximal margin.

## 4.3. Data used in this chapter

On the inner proximal margin, this chapter uses industry well log data from the Porto Basin (Lula-1, Touro-1Z, Lima-1, Cavala-4 and 5A-1) and regional 2D reflection seismic data from NESTE PORTUGAL (Fig. 4.1B). On the deeper margin was used seismic data from TGS-NOPEC (Iberian Margin), the Iberia Seismic Experiment, ISE 97 (data available for download from Shipley *et al.*, 2005) and from the SCREECH programme (Newfoundland) (data available for download from Shipley *et al.*, 2005) (Fig. 4.1A). In addition, published data from DSDP 47b and ODP legs 103, 149, 173 and 210 (Sibuet *et al.*, 1979; Boillot *et al.*, 1987b; Sawyer *et al.*, 1994; Whitmarsh *et al.*, 1998; Tucholke *et al.*, 2004) are correlated with the available seismic dataset for the deep margin (Fig. 4.1B).

## 4.4. The 'breakup unconformity' offshore West Iberia and Newfoundland

On the outer proximal and distal margins, the '*breakup unconformity*' is marked on seismic data by the '*orange reflector*' offshore West Iberia, and by the '*U reflector*' offshore Newfoundland (Sibuet *et al.*, 1979; Tucholke *et al.*, 1989). These two reflectors

were cored by DSDP leg 49 and ODP legs 103 and 210, and dated as latest Aptian–earliest Albian (Sigal, 1979; Boillot *et al.*, 1987b; Tucholke *et al.*, 2004). They are recognised as prominent high-amplitude seismic reflections of regional extent. However, differences exist between the two reflectors, on both margins.

On the western Iberian margin, the '*breakup* unconformity' is pervasive onshore and on the proximal margin, where it forms an erosional surface over older deposits of the Torres Vedras formation and Upper Jurassic strata, merging inland with older unconformities (Rey *et al.*, 2006) (Fig. 4.2). Thick intervals of coarse-grained siliciclastics were deposited above the '*breakup unconformity*' (Fig. 4.2, Wilson, 1988; Dinis & Trincão, 1995; Alves *et al.*, 2002). On the distal margin, the '*orange reflector*' marks the transition from submarine mass-wasting processes to calmer, lower energy depositional environments. These are represented by hemipelagic sediments with high organic content ('*black shales*') and by thin turbidite intervals occurring towards the top of Albian units (Graciansky & Chenet, 1979; Shipboard Scientific Party, 2004b) (Fig. 4.2).

On the proximal margin of Newfoundland, the '*U reflector*' merges with the Avalon unconformity, a major composite unconformity related to Lower Cretaceous uplift of the Avalon High (Grant *et al.*, 1988; Tucholke *et al.*, 1989). At Site 1276, the '*U reflector*' is coincident with magmatic sills emplaced during the Middle Albian (Tucholke *et al.*, 2004; Hart & Blusztajn, 2006). Although observed in a large portion of the Newfoundland margin, these sills are apparently absent on the western Iberian margin (Péron-Pinvidic *et al.*, 2010).

---

**Figure 4.3** (next page) Section of seismic profile NP89-10 across the Porto Basin showing the lithospheric breakup surface (LBS) (base of unit 1) and the associated breakup sequence (BS) (units 1 to 4). Well log curve is gamma-ray. A—uninterpreted section of seismic profile NP89-10. B—seismic profile NP89-10 interpretation of the stratigraphic architecture of the BS. C—detail of seismic profile NP89-10 showing the distal end of the force regression systems tract (Unit 1), onlaped by transgressive deposits (Unit 2) and these donwlaped by the mainly aggradational Unit 3. D—detail of NP89-10 showing the truncation of syn-rift sediments by the forced regression systems tract, materializing the LBS. E—detail of NP89-10 showing the subaerial erosive surface developed atop of the forced regression systems tract and the resulting topography filled by the transgressive Unit 2. LBS—lithospheric breakup surface; BS—breakup sequence. Location of seismic profile in Figure 4.1.

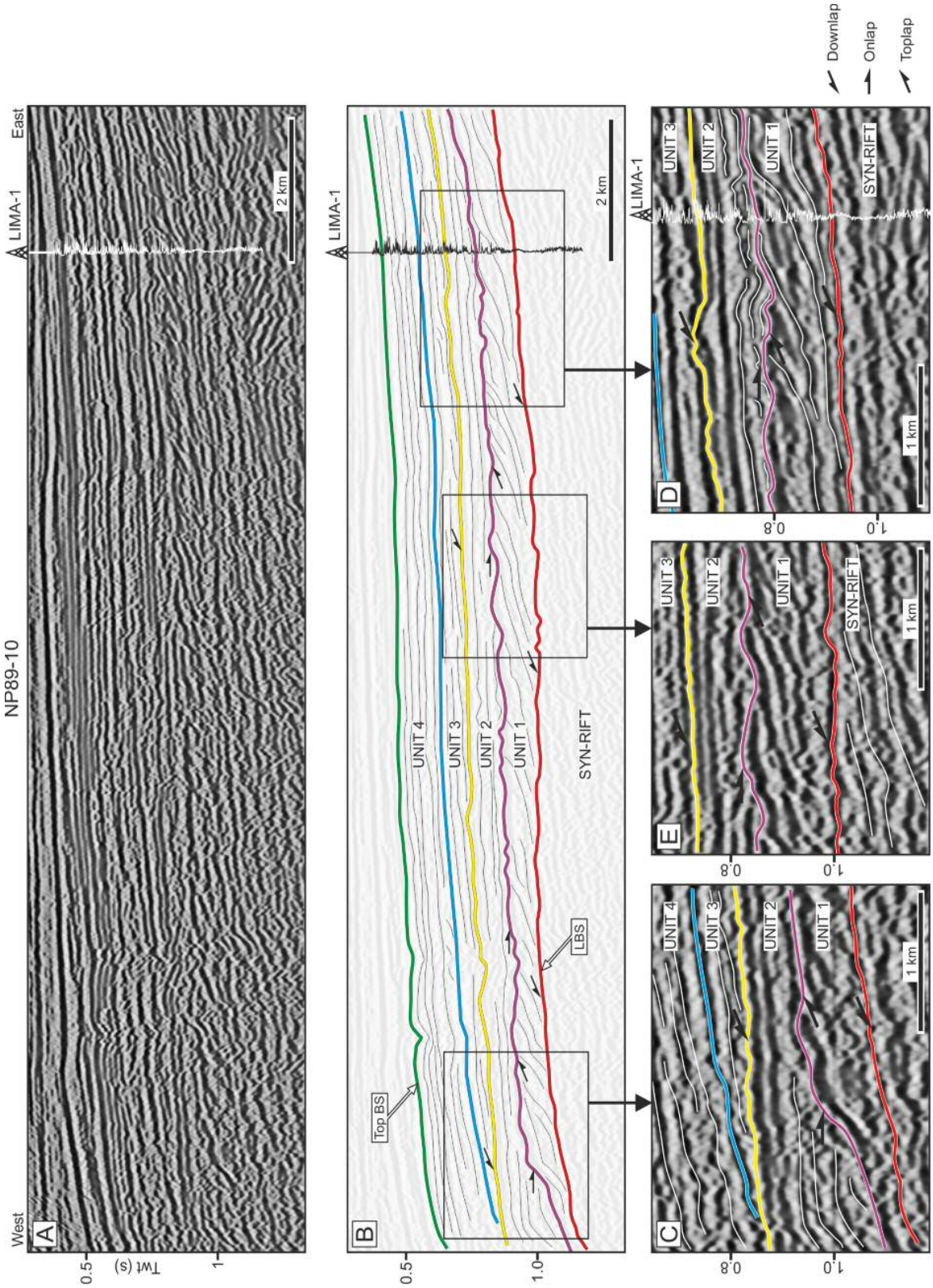
NP89-10
West
East
LIMA-1
2 km
A
Twt (s)
0.5
1
B
Top BS
LBS
UNIT 4
UNIT 3
UNIT 2
UNIT 1
SYN-RIFT
C
D
E
1 km
0.8
1.0
Downlap
Onlap
Toplap

### 4.4.1. Lithospheric vertical movements due to lithospheric breakup

Rather than a rapid tectonic event, lithospheric breakup has recently been proposed as reflecting a gradual process where extension on exhumed upper mantle (LRS2) and normal oceanic crust emplacement occur simultaneously until the latter becomes predominant (Russell & Whitmarsh, 2003; Jagoutz *et al.*, 2007; Sibuet *et al.*, 2007b).

Considering individual crustal segments on a rifted margin, numerical modelling shows that complete separation of exhumed mantle, with resulting cessation of lithospheric thinning, releases accumulated extensional in-plane stresses in an event considered to be instantaneous at a geological scale (Braun & Beaumont, 1989; Bott, 1992b). This release of in-plane stress will generate a flexural rebound of the lithosphere as large wavelength vertical and horizontal movements, thus creating localized uplift, subsidence and minor compression along the thinned lithosphere (Braun & Beaumont, 1989; Cloetingh *et al.*, 1989; Issler *et al.*, 1989; Cathles & Hallam, 1991; Egan, 1992; Kooi & Cloetingh, 1992; van Balen *et al.*, 1998; Cloetingh & Ziegler, 2007) (see Chapter 1). As a result, abrupt changes in sedimentation, stratigraphic architecture and in the loci of erosion/deposition occur in association with the lithospheric breakup event on divergent continental margins, generating a very distinct stratigraphic surface (LBS) of regional significance, and a distinct stratigraphic sequence (BS) topping the LBS, as proposed in this chapter.

## 4.5. The seismic–stratigraphic expression of continental breakup on the inner proximal margin (Porto Basin)

Seismic profiles and borehole data were interpreted and integrated with the available seismic data from the Porto Basin in order to recognise the seismic–stratigraphic character of continental breakup in the inner proximal margin of West Iberia (Figs. 4.3–4.6). The interpreted seismic data shows a Late Aptian–Albian unconformity correlative with the '*breakup unconformity*' of the outer proximal and distal margins (Fig. 4.5). Above this unconformity are interpreted four distinct

stratigraphic units (Unit 1–4) spanning the lower Albian to earliest Turonian (Fig. 4.6). The seismic expression of Units 1–4 comprises high to moderate-amplitude reflections showing significant progradation towards the shelf edge (Figs. 4.3–4.5). This sediment progradation, which is related to a reduction in accommodation space due to a forced base-level fall or an increase in sediment input, does not fit with the overall transgressive trend proposed for the Cretaceous by regional eustatic curves (Haq *et al.*, 1987).

Environmental interpretation is based on the well log data and sediment descriptions from the completion reports of the available wells (Salén/Pecten, 1985; Neste, 1990; Taurus Petroleum AB, 1995)

### 4.5.1. Late Aptian–Albian unconformity and the forced regressive Unit 1

Figures 4.3 to 4.5 shows a series of seismic sections imaging the Late Aptian–Albian unconformity (LBS) in the Porto and Peniche Basins. Three wells, LIMA-1, TOURO-1Z and LULA-1 cross the interpreted seismic sections. On the inner proximal margin, the LBS comprises an erosive surface truncating sub-parallel west-dipping strata of the Lower Cretaceous Torres Vedras formation (Figs. 4.3–4.6).

Based on wireline data, borehole cuttings and palaeontological data, the Torres Vedras formation is interpreted as a neritic unit comprising marly siltstones and claystones grading to fine sandstones and siltstones up in the sequence (*e.g.* LULA-1, Fig. 4.6).

---

**Figure 4.4** (next page) Detail of seismic profile PD00-101A showing the maximum extent of the forced regression deposits. Note the prograding clinoforms accumulating beyond the palaeo shelf break (westwards of LULA-1) and the erosional surface atop of them, suggesting a considerable drop in sea-level. In this seismic line the onlaping character of Unit 2 is difficult to observe. This can be related both with the line position and the presence of several seismic artefacts. Unit 3 apparently is missing landwards, showing that lateral variation/migration of the depositional locus occurred during its deposition. Gamma ray values (in purple) increase towards the right. Sonic velocity (in red) increase towards the right. Several areas in this seismic section are difficult to interpret due to the existence of seismic artefacts. LBS—lithospheric breakup surface; BS—breakup sequence. Location of seismic profile in Figure 4.1. See Figure 4.5 for the location of this section in the seismic line.

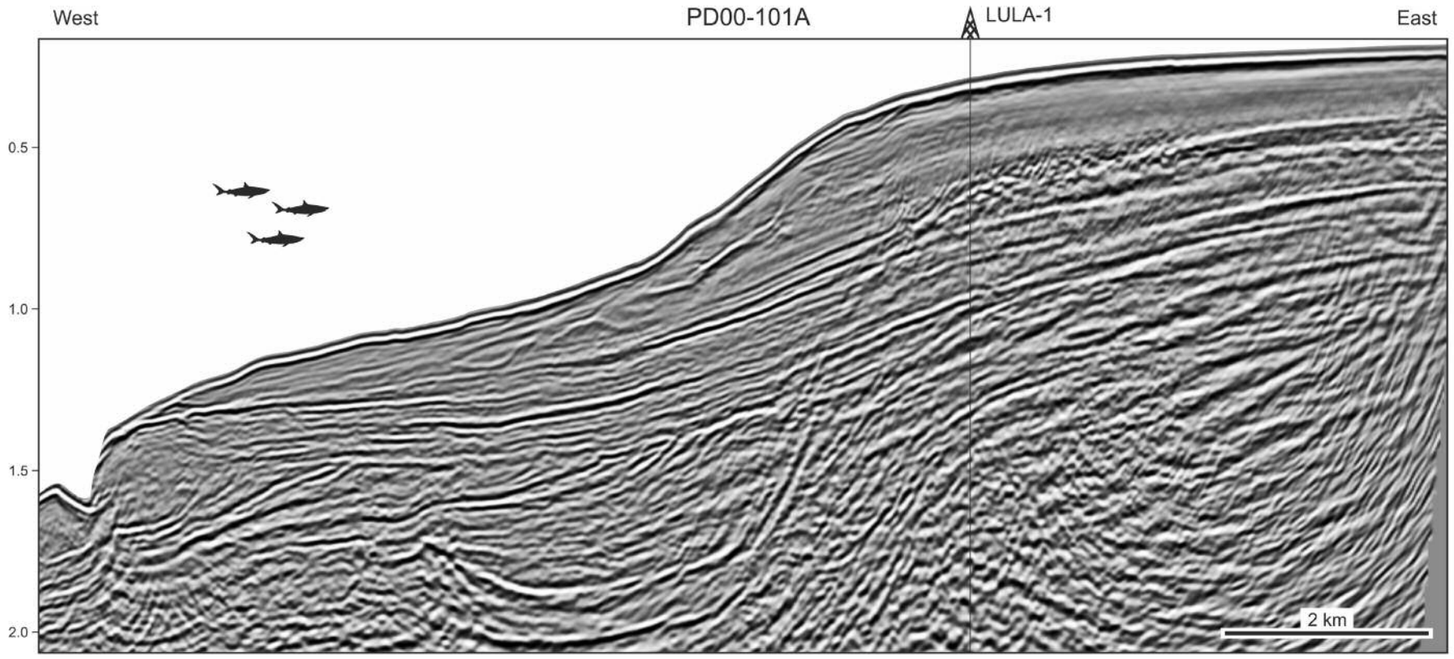
West
PD00-101A
LULA-1
East
0.5
1.0
1.5
2.0
2 km

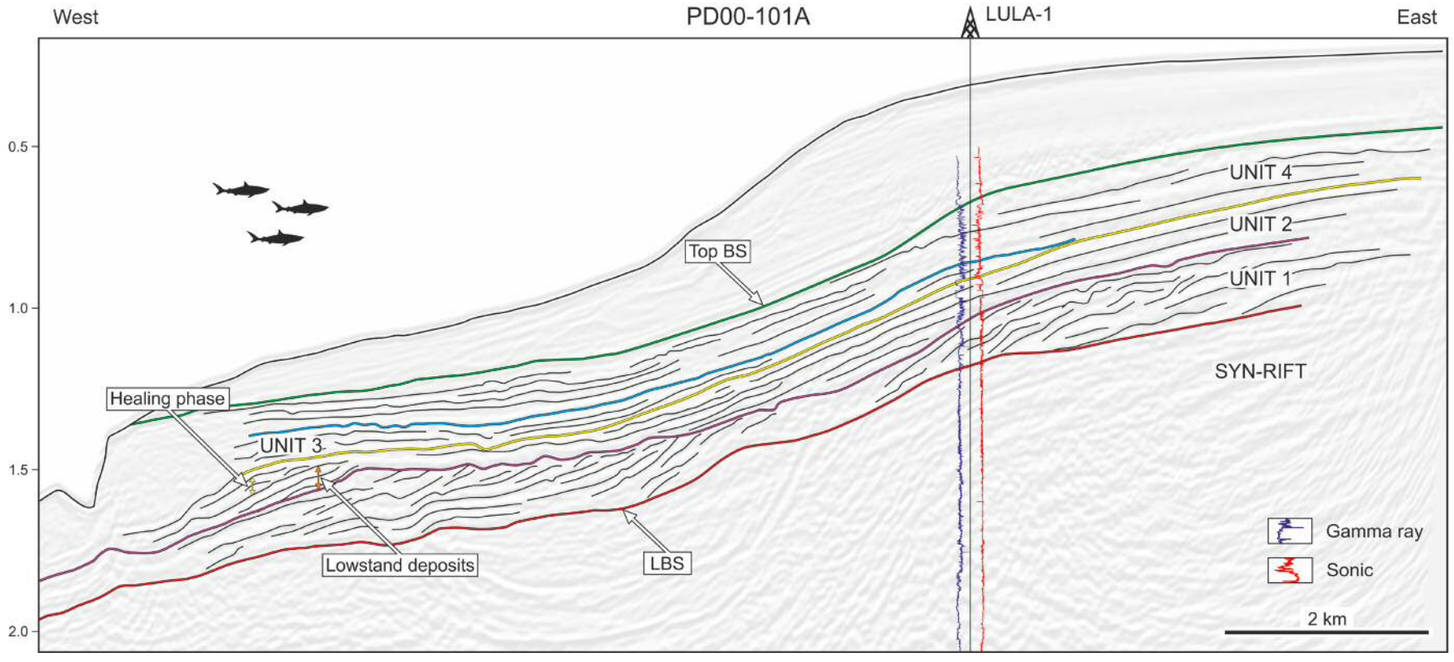
West
PD00-101A
LULA-1
East
0.5
1.0
1.5
2.0
UNIT 4
UNIT 2
UNIT 1
Top BS
SYN-RIFT
Healing phase
UNIT 3
Lowstand deposits
LBS
Gamma ray
Sonic
2 km

Biostratigraphy data show that the time-span of the hiatus materialised by the LBS is reduced oceanwards, spanning the Hauterivian–Aptian to the East and the Aptian *pro parte* towards the shelf edge (Fig. 4.6).

The LBS is overlaid by a low angle progradational forced regressive deltaic system (Unit 1, Figs. 4.3–4.5). In LIMA-1, Unit 1 is dated as lower Albian on the basis of the occurrence of *Complexiopollis sp.* at 1140m (97 m above the LBS) over Valanginian sediments with *Classopolis hammenii* and *Classopolis equinatus* (1230m, 7 m below the LBS) (Neste, 1990). Towards the shelf edge (LULA-1), this same unit overlies the Barremian–Aptian sediments (Fig. 4.6).

Showing the typical stratal architecture of an attached forced regression, i.e. downward trajectory, basinwards foreset increasing angle, offlap and a subaerial erosional surface to the top of the unit (Hunt & Tucker, 1992; Posamentier & Morris, 2000), the progradation observed in Unit 1 marks a period of significant transport of sediment onto the deeper margin (Figs. 4.3–4.4). On Figure 4.4 it is possible to observe the maximum extent of this forced regression, with the presence of prograding clinoforms after the shelf break. The top of these prograding clinoforms is irregularly eroded, suggesting that subaerial exposure of the shelf reached this far (Fig. 4.4).

Well data show the prograding strata as comprising coarsening-upwards parasequences of siltstones to fine–medium and coarse sands (Fig. 4.6). Sandstones have predominantly sub-rounded to angular clasts, abundant mica and feldspar in places, and coal fragments (completion reports: Salén/Pecten, 1985; Neste, 1990; Taurus Petroleum AB, 1995).

In summary, Unit 1 relates to an abrupt phase of important sediment progradation and high sediment supply on the continental margin. Its deposition above westwards tilted strata and depositional architecture along with the degree of sediment immaturity reflects tectonic uplift on the inner proximal margin, rejuvenation of sediment sources and a simultaneous westward tilt of syn-rift units below the LBS.

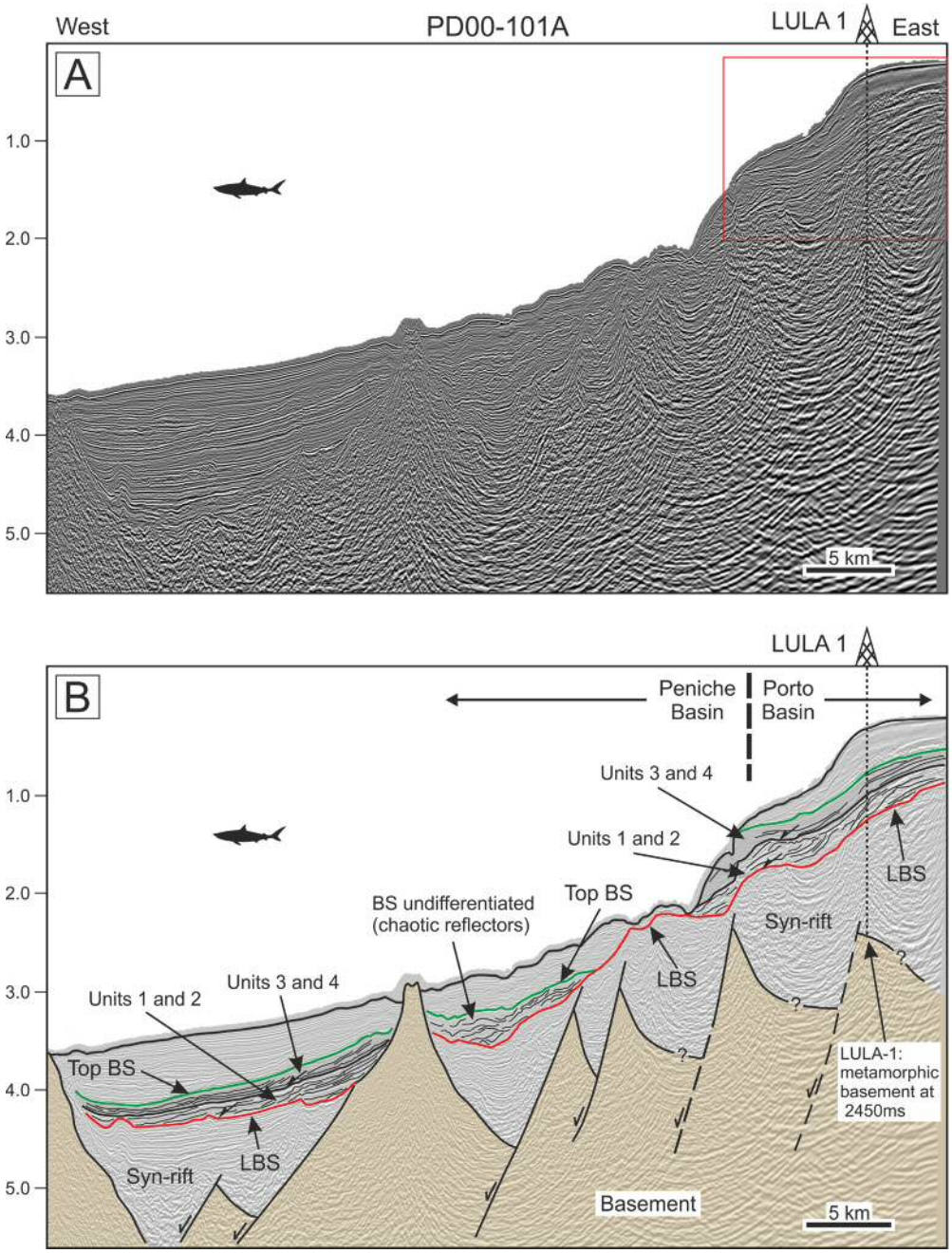


**Figure 4.5** Seismic profile (A) and interpretation (B) showing the lithospheric breakup surface (LBS) and the stratigraphic architecture of the breakup sequence (BS) across the transition between the outer proximal (Peniche Basin) and inner proximal (Porto Basin) margins. Strong progradation characterizes the BS, although chaotic reflectors are observed. LBS—lithospheric breakup surface; BS—breakup sequence. Area within the red box in A is zoomed in Figure 4.4. Location of profile in Figure 4.1A.

### 4.5.2. Transgression and progradation (Units 2 and 3)

Sediment in Units 2 and 3 shows the same immature character of Unit 1. Unit 2 contrasts with Unit 1 and Unit 3 mainly by the presence of interbedded fine sediments and occasional thin carbonate beds towards the top of the unit, deposits interpreted to have accumulated during the Albian in coastal to lagoonal environments (Fig. 4.6).

Unit 2 comprises distally lowstand sediments, apparently deposited as a very thin layer immediately above the distal end of Unit 1 in Figure 4.4. These can be observed as few reflections above the top of the forced regression package. Thus, transgressive deposits cover the majority of Unit 1 (Figs. 4.3–4.6). Onlapping the lowstand sediment package, transgressive healing-phase deposits (*sensu* Posamentier & Allen, 1993) can be observed on the distal end of Unit 2 (Fig. 4.4). Eastward, Unit 2 comprises estuarine and fluvial-deltaic sediments, filling the erosional relief formed at the end of the previous forced regressive stage (Figs. 4.3, 4.6 at TOURO-1Z; LIMA-1).

A maximum transgressive surface, shown as a landward-thinning dolomitic interval, marks the top of Unit 2. This surface is downlaped by Unit 3, prograding over the shelf at a very low angle trajectory. This low angle (but ascending) trajectory reflects the abundance of sediment supply, rapidly filling any accommodation space available in the basin and showing a predominantly aggradational staking pattern. Unit 3 is formed by ~200 m of interbedded fluvial, lagoonal and shallow marine sediments (Figs. 4.3 and 4.6).

### 4.5.3. Transgression and the end of nearshore sedimentation (Unit 4)

The boundary between Units 3 and 4 is subtle both on seismic and well log data (Figs. 4.3–4.6). It corresponds to a conformable surface marking the transition from the aggradational top of Unit 3 to the essentially transgressive Unit 4, a change recorded in the Late Albian–Early Cenomanian throughout West Iberia (Rey, 1979; Floquet, 1998; Dinis *et al.*, 2008). On seismic and borehole data the sequence records an increasingly larger marine influence towards the top of Unit 4, as shown by

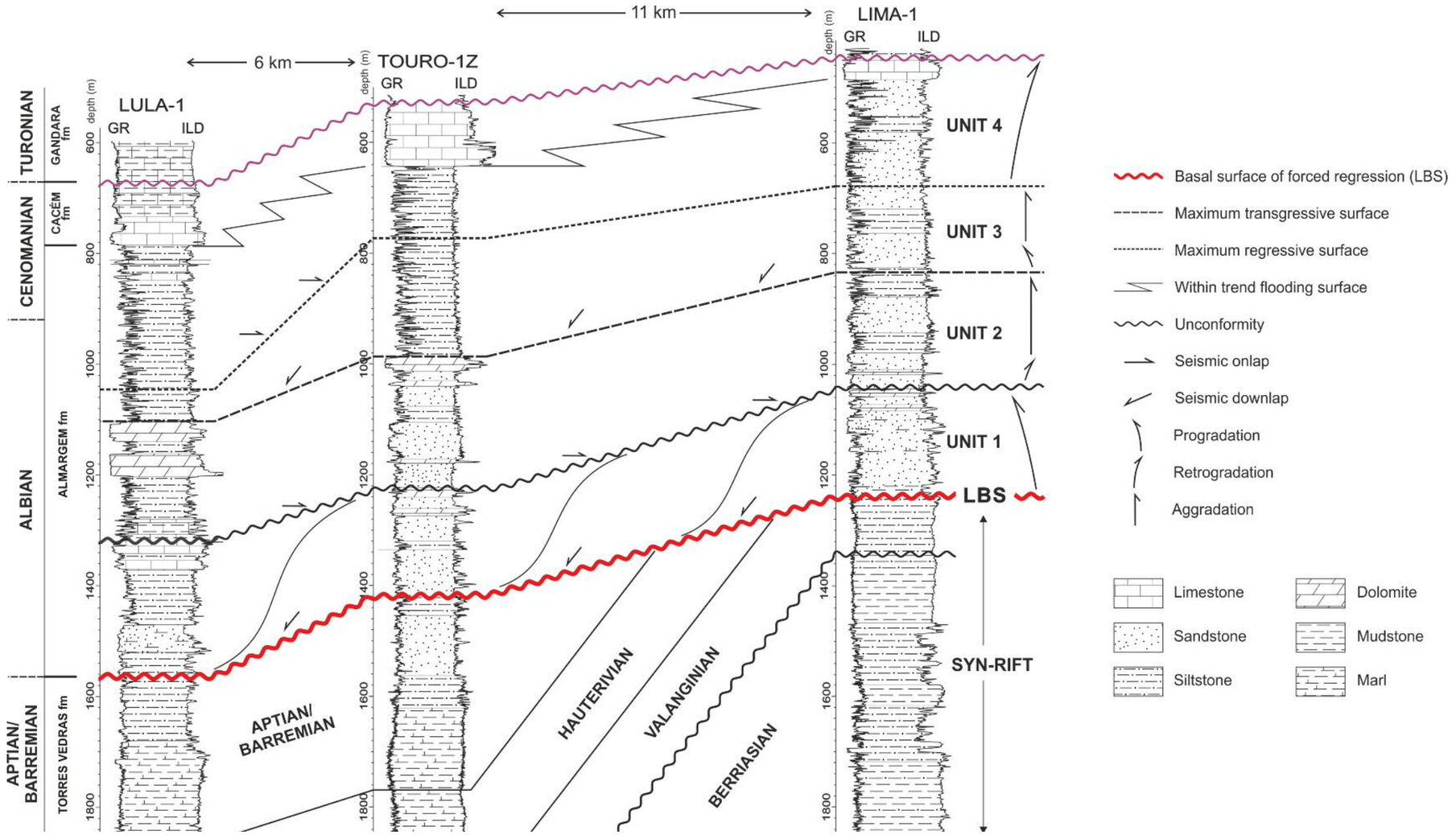


**Figure 4.6** Gamma-ray (GR) and deep resistivity (ILD) cross section from Porto Basin, showing the stratigraphic architecture of the lithospheric breakup surface (LBS) and the overlying breakup sequence (BS). Unit 1 is a forced regressive systems tract prograding over the lithospheric breakup surface. Note the massive character in the GR, representing fluvial deposition in a basin with very little accommodation space available. Unit 2 is here a transgressive systems tract, nevertheless, lowstand deposits can be observed on seismic data (Fig. 4.4). Unit 3 is a highstand systems tract with a very low downward angle trajectory on seismic data, indicative of a very large sediment supply being deposited rapidly or under a low pace of accommodation space creation. This unit shows an aggradational trend towards its top, interpreted here as due to a balance between the sediment supply and the increasing accommodation space. Unit 4 is a transgressive systems tract showing a more aggradational pattern at its base, until the complete transgression and the beginning of the deposition of carbonates (Cacém formation). The BS comprises fluvial, lagoonal and shallow marine sediments, with Units 2 and 4 showing an increasing marine influence toward their tops. LBS—lithospheric breakup surface; BS—breakup sequence. Location of wells in Figure 4.1.

the increasing occurrence of thin carbonate beds towards its top and by an overall decrease in grain size in more proximal parts of the Porto Basin (Fig. 4.6). Unit 4 is capped by a marine carbonate unit, part of the Cacém formation.

## 4.6. The LBS and BS on the outer proximal and distal margins

Seismic profiles and borehole data from the Peniche Basin, Iberia Abyssal plain and Newfoundland margin reveal a similar Late Aptian–Albian unconformity to the Porto Basin (Figs. 4.5, 4.7–4.12). In West Iberia above this unconformity also occurs a well-defined seismic package spanning the latest Aptian to middle Cenomanian (Fig. 4.2). Seismic Units 1 to 4 show distinct geometries in deeper parts of the two margins. However, similar prograding reflections to those in the Porto Basin are visible above the LBS in proximal parts of the outer proximal margin (Fig. 4.5). These prograding reflections change into transparent to moderate amplitude sub-parallel reflections in main depocentres basinwards (Figs. 4.7–4.12).

### 4.6.1. Iberian margin

On the outer proximal margin, seismic data shows the LBS developing over chaotic, strong reflectors. The presence of divergent reflectors close to the LBS is uncommon, instead parallel reflectors are observed below the LBS (Figs. 4.7–4.9). On the easternmost part of this margin, close to the continental shelf is observed the presence of prograding reflectors at the base of the BS (Fig. 4.5). Basinwards, still on the outer proximal margin, these reflectors become sub-parallel although their continuity is not very extensive (Figs. 4.5, 4.7–4.9). In fact, the base of the BS is commonly developed as transparent reflectors, which become stronger and more reflective upwards (Figs. 4.7–4.9).

On the distal margin, the LBS character is very similar to the one found on the outer proximal margin. Nevertheless, its character as a strong reflector resting on top

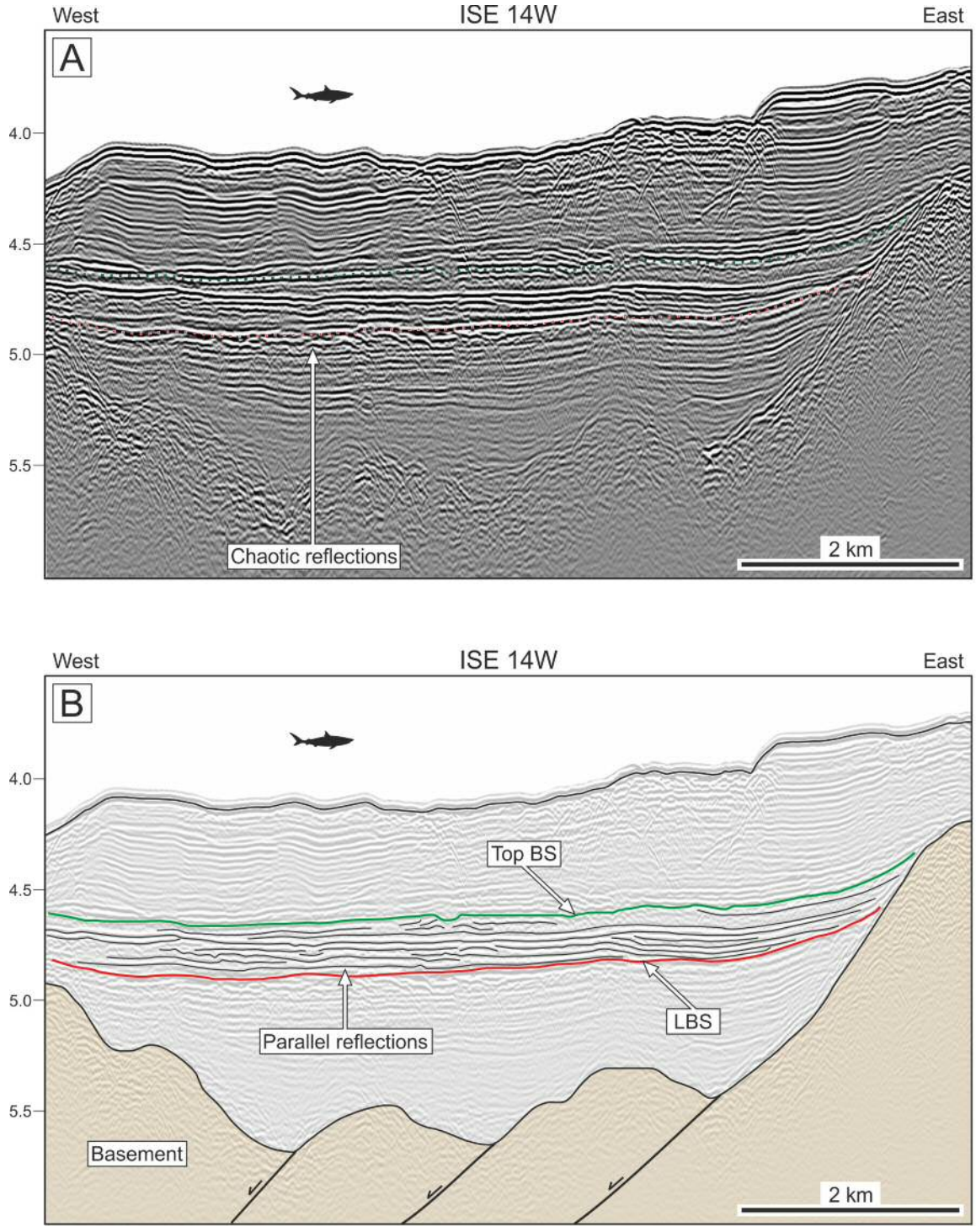


**Figure 4.7** Seismic profile across the West Iberia westernmost outer proximal margin. showing the LBS and the BS, here constituted by the deposition of black shales. A—partially uninterpreted line, where the chaotic character of the syn-rift reflectors immediately below the LBS (thin red dotted line) is well observed, along with the unconformity on top of the BS (thin green dotted line), better observed towards the east of the profile. In this line, the typical transparent character of the lower part of the BS is not observed, except towards the west of the line. B—Interpretation of reflections within the BS, showing the presence of partially discontinuous parallel reflections. LBS—lithospheric breakup surface; BS—breakup sequence. Location of profiles in Figure 4.1.

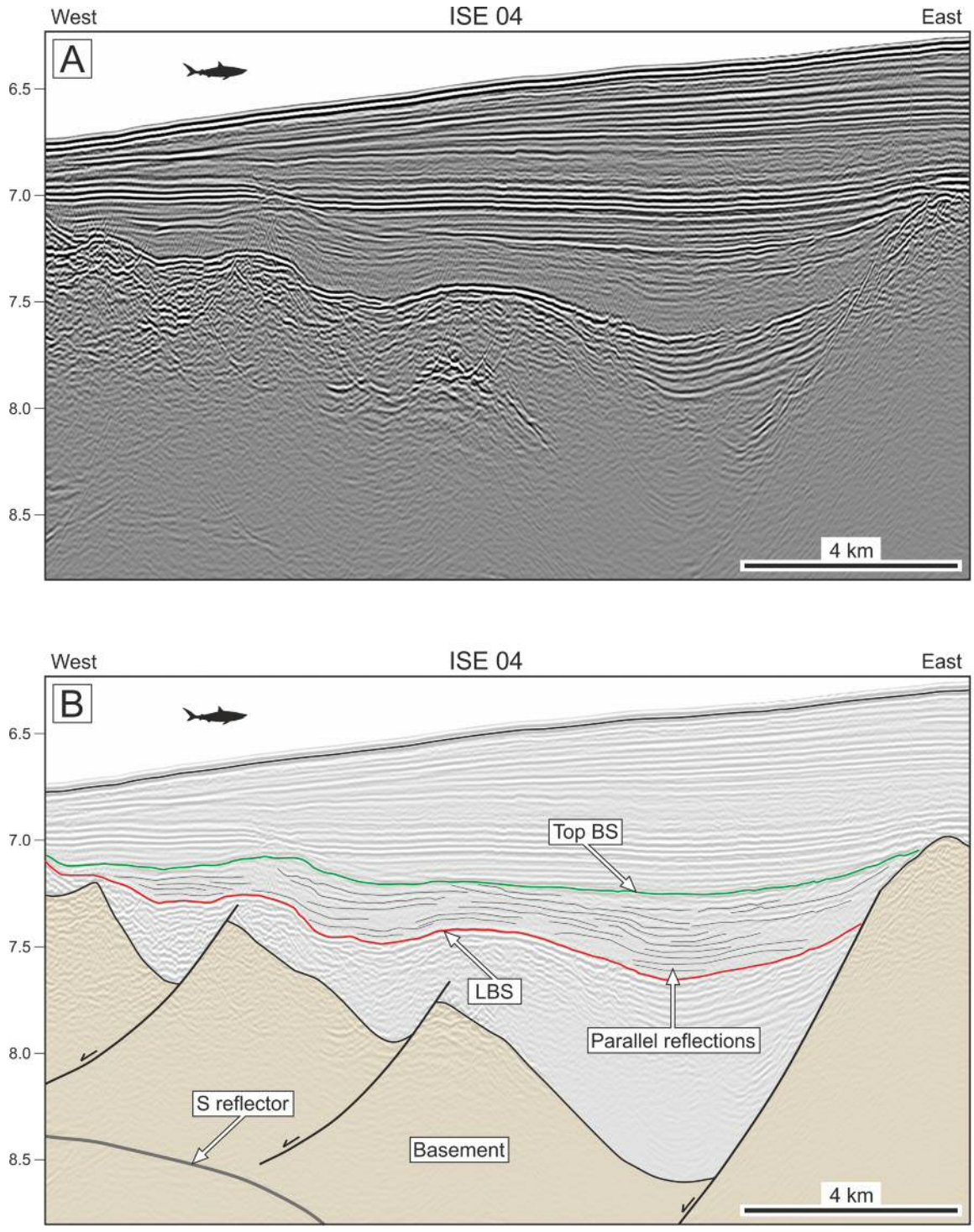


**Figure 4.8** Seismic profile across the West Iberia westernmost outer proximal margin. showing the LBS and the BS, here constituted by the deposition of black shales. A—uninterpreted line. Here the LBS is marked by a strong reflection separating well layered, and chaotic reflections below from the BS above. The BS here shows its typical transparent character grading to better layered reflections upwards. B—interpretation of reflections within the BS, showing the presence of partially discontinuous parallel reflections. LBS—lithospheric breakup surface; BS—breakup sequence. Location of profiles in Figure 4.1.

of chaotic reflections is more frequently found on the distal margin (Figs 4.10 and 4.11). As well in common with the outer proximal margin is the BS aspect. On the distal margin, the same transparent reflections occur within the BS, frequently without discernible individual reflectors. Once again, these transparent reflections become stronger towards the top of the sequence (Figs. 4.10 and 4.11). In this part of the margin, the BS can show the presence of extensive erosional features (Figs. 4.10 and 4.11). These erosional features suggest the presence of bottom currents activity controlling different depositional episodes within the BS, strikingly observed in Figure 4.11.

The LBS was drilled and cored on the outer proximal margin at DSDP site 398 (Leg 49B) and ODP site 641 (Leg 103) (Figs. 4.1, 4.2 and 4.9, Sibuet *et al.*, 1979; Boillot *et al.*, 1987b). Rhythmic successions of turbidites and slump deposits characterize the Barremian–Aptian syn-rift interval at DSDP Site 398. Strata in this interval are interpreted to derive either from fault scarps or deposited in the distal part of submarine fan systems (Graciansky *et al.*, 1978; Chamley *et al.*, 1979). At this same Site 398, the LBS is dated as uppermost Aptian to earliest Albian, being associated with a diastem or condensed interval (Chamley *et al.*, 1979; Graciansky & Chenet, 1979; Berthou *et al.*, 1982).

The unit immediately above the LBS (Unit 4B in Sibuet *et al.*, 1979) marks the end of mass-wasting and slumping and the beginning of the deposition of organic-rich black shales with abundant plant debris, kaolinite and interstratified clays derived from the continent, in a setting marked by high sedimentation rates (Habib, 1979; Shipboard Scientific Party, 1979; Taugourdeau-Lantz *et al.*, 1982) (Figs. 4.2 and 4.13). The end of black shale deposition is marked at DSDP Site 398 by an abrupt change in sedimentation, marked by the deposition of barren red-brown shales and the development of a probable unconformity ranging from mid-Cenomanian to Santonian–Campanian (Sigal, 1979) (Figs. 4.2 and 4.13).

Hole 641C, drilled on the West Galician Margin (Figs. 4.1 and 4.2), was the only in ODP leg 103 to recover sediment across the LBS (R2 reflector). Here, the syn- to post-

rift transition is very similar to that recorded at ODP Site 398. An upper Barremian to uppermost Aptian syn-rift succession of turbidites and debris flows was followed by the deposition of claystones with a high organic content (black shales) across the LBS (Boillot *et al.*, 1987b) (Fig. 4.13).

ODP Legs 173 and 149 in the Iberian distal margin had all their sites drilled over basement highs and no post-rift sedimentation older than mid-Campanian was recovered (Kuhnt & Collins, 1996; Whitmarsh *et al.*, 1998). Nevertheless, seismic profiles show that pre-Campanian strata occur between important structural highs. Syn-rift strata dated as upper Aptian were drilled (Sites 1070, 897, 899), and comprise mass flow deposits, olistostromes and breccias of serpentinite and peridotite clasts mixed with pelagic sediments (Fig. 4.13). They were formed by the erosion of exhumed lithospheric mantle during the late episodes of crustal extension (LRS2) affecting the distal margin (Sawyer *et al.*, 1994; Whitmarsh *et al.*, 1998; Beslier *et al.*, 2001a).

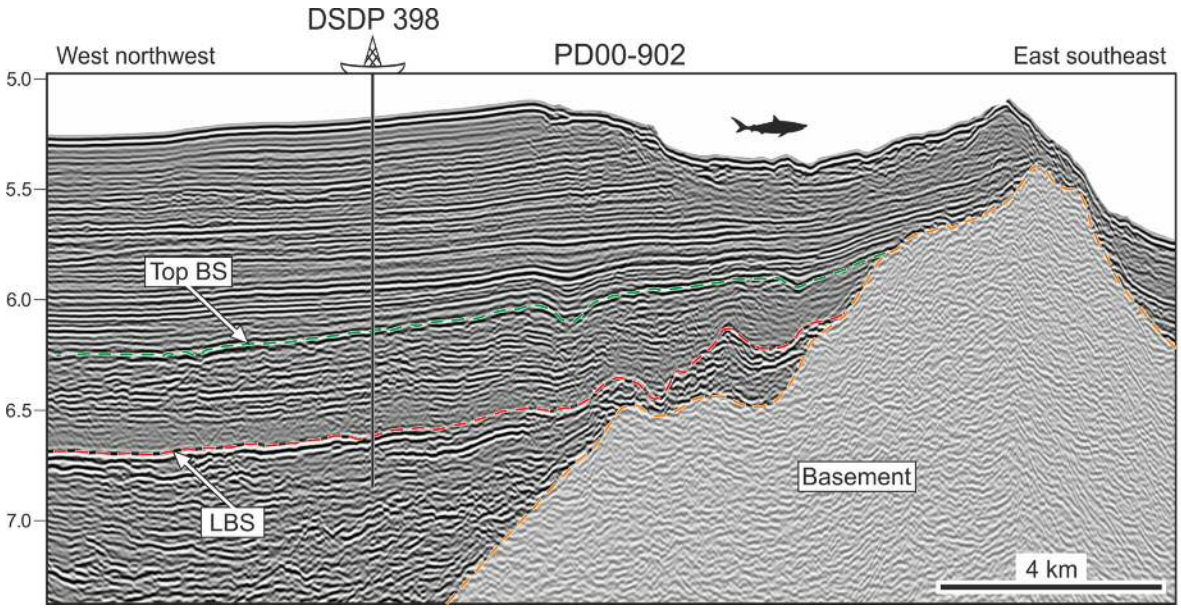


**Figure 4.9** Seismic profile across the DSDP Site 398 on the West Iberia westernmost outer proximal margin. The chaotic character of the syn-rift reflectors immediately below the LBS is observed (although not very developed in this seismic line), along with the unconformity on top of the BS. Note the transparent reflections on the lower part of the BS, increasing in amplitude upwards. LBS—lithospheric breakup surface; BS—breakup sequence. Location of profiles in Figure 4.1.

### 4.6.2. Newfoundland margin

At Site 1276 (Figs. 4.1 and 4.12), the LBS coincides with earliest post-breakup magmatic sills emplaced during the Albian–Cenomanian (Hart & Blusztajn, 2006) within uppermost Aptian and lower Albian strata. The sills occur at a relatively uniform depth and are widespread throughout the Newfoundland Basin, which explains the stronger character of the '*U reflector*' compared with the '*orange reflector*' (Péron-Pinvidic *et al.*, 2010). Nevertheless, ODP Site 1276 also penetrated and recovered sediment across the LBS on the Newfoundland margin. Here, the oldest recovered sediments date from uppermost Aptian to the lowermost Albian (Shipboard Scientific Party, 2004b; Trabucho Alexandre *et al.*, 2011). In detail, seismic reflection profiles show a similar sequence to the one drilled in West Iberia across the '*orange reflector*' (Shipboard Scientific Party, 2004a). At Site 1276 the LBS is not characterized by an abrupt sedimentological change as it is in West Iberia (Fig. 4.13).

Instead, it occurs within a unit (unit 5C in Shipboard Scientific Party, 2004b) dated as Late Aptian to Early/mid-Albian comprising the Aptian/Albian oceanic anoxic event (OAE1b, Arnaboldi & Meyers, 2006; Trabucho Alexandre *et al.*, 2011). At Site 1276, strata above the LBS comprise turbidites and debris flows with rare interbedded black shales, which occur more frequently towards the top of the unit. The unit above it (5B, Albian–Cenomanian) are mainly composed of burrowed hemipelagites alternating with 'black shales' (Shipboard Scientific Party, 2004b). Significantly, there is a strong input of sediment from the continent immediately above the LBS, shown by an relative increase in terrigenous organic matter (plant debris, palynoclasts and sporomorphs), further decreasing in volume towards the top (Urquhart *et al.*, 2007). As in West Iberia, here the end of the black shales is marked by the deposition of a mostly barren red-brown shale, representing a Turonian–Maastrichtian condensed sequence (Urquhart *et al.*, 2007).

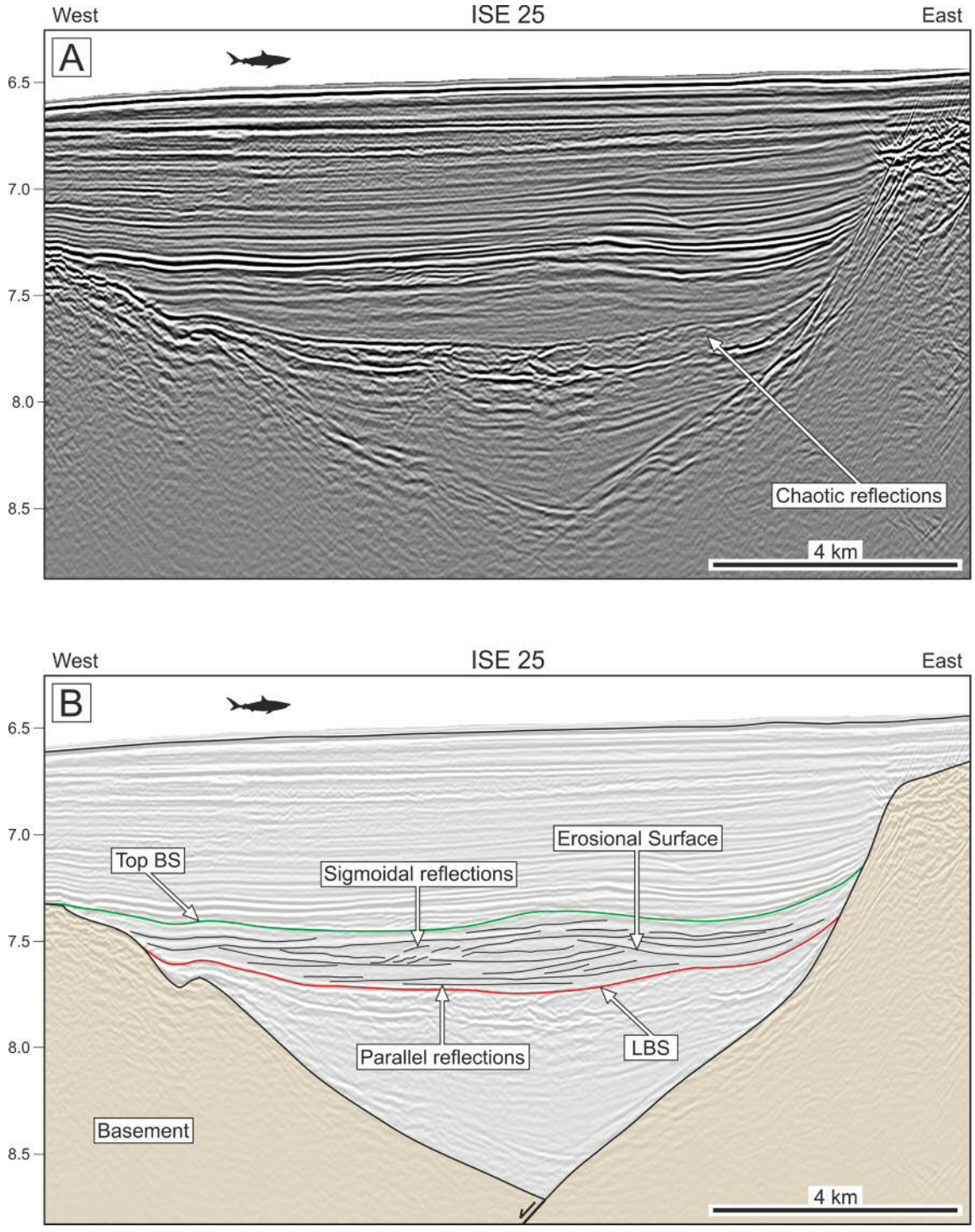


**Figure 4.10** Seismic profile across the West Iberia distal margin showing the LBS and the BS. A—uninterpreted line. The chaotic character of the syn-rift reflectors immediately below the LBS is observed (labelled on the figure). B—interpretation of reflections within the BS, showing at least two erosional surfaces and sigmoidal reflections. These structures suggest the action of bottom currents during the deposition of the BS in this area. Parallel reflections occur on the lower part of the BS, onlaping the LBS. LBS—lithospheric breakup surface; BS—breakup sequence. Location of profiles in Figure 4.1.

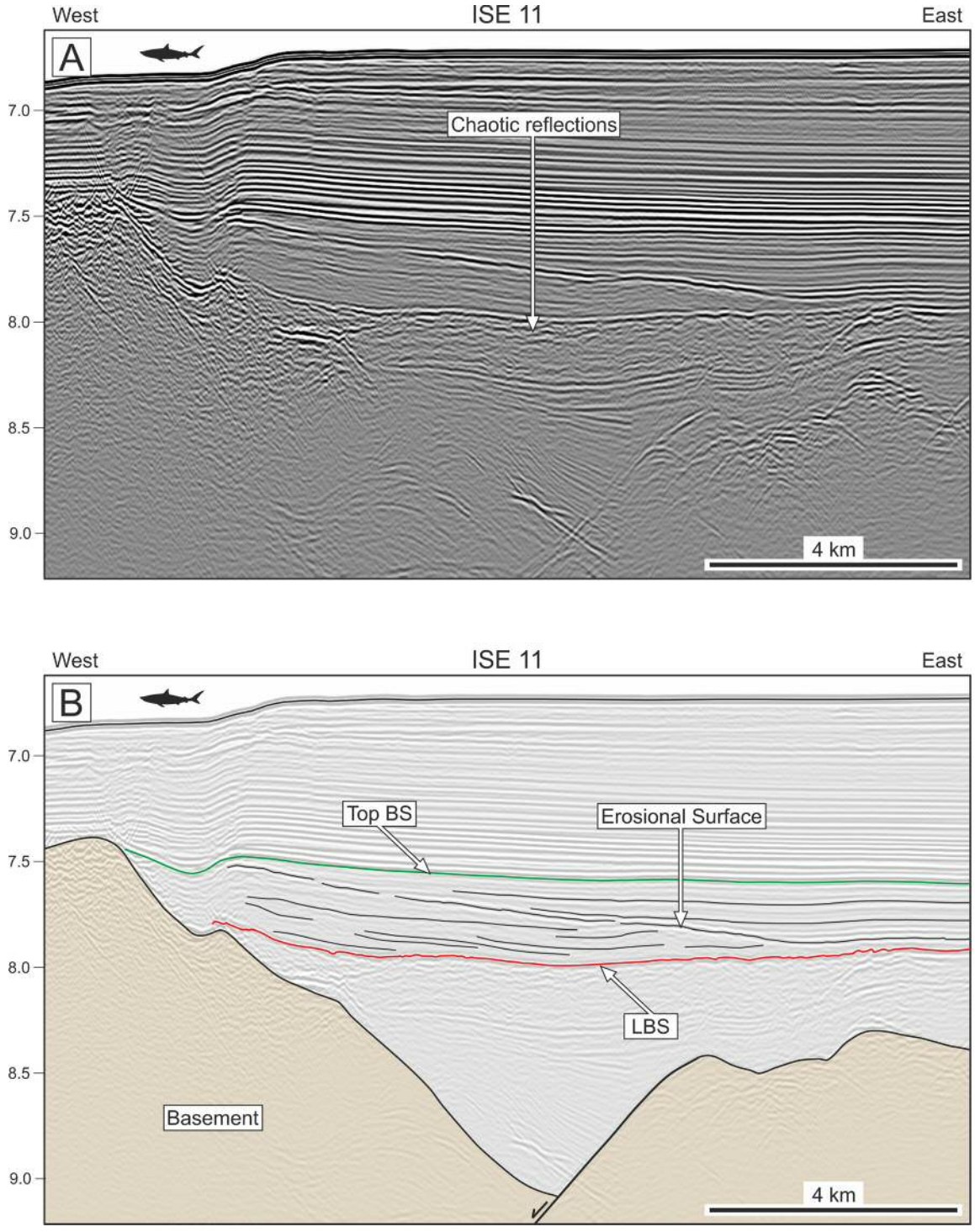


**Figure 4.11** Seismic profile across the West Iberia distal margin showing the LBS and the BS. A—uninterpreted line. The chaotic character of the syn-rift reflectors immediately below the LBS is observed (labelled on the figure). B—interpretation of reflections within the BS. A striking erosional surface can be observed within the BS separating two depositional episodes. Remarkably, the first depositional episode displays the typical transparent character found on the lower BS, while the second depositional episode (onlaping the first) shows the reflectors increasing in amplitude upwards. This erosional surface suggests the action of bottom currents during the deposition of the BS in this area. LBS—lithospheric breakup surface; BS—breakup sequence. Location of profiles in Figure 4.1. The westward folding is Miocene (Masson *et al.*, 1994).

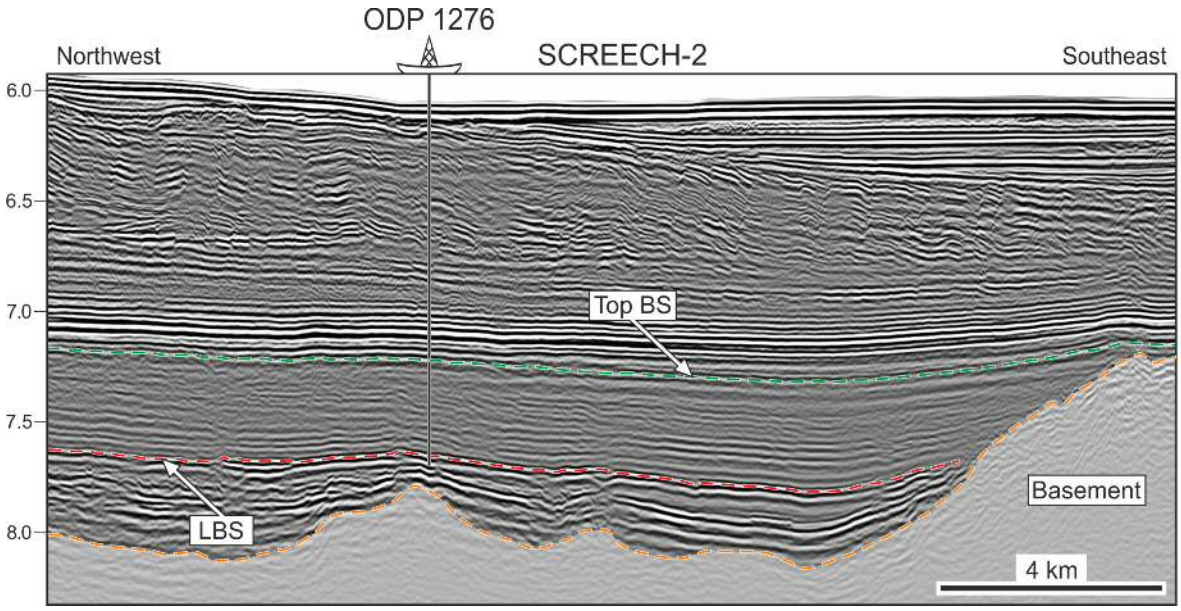


**Figure 4.12** Seismic profile across the ODP Site 1276 on the Newfoundland distal margin. In this margin, the transition from syn- to post-rift is very well marked, partially due to the presence of magmatic sills along it (see text for references). The unconformity on top of the BS is well observed. The same transparent character of the BS found in the West Iberia margin is observed in this margin as well. LBS—lithospheric breakup surface; BS—breakup sequence. Location of profiles in Figure 4.1.

## 4.7. Discussion

### 4.7.1. Seismic–stratigraphic architecture of lithospheric breakup

In West Iberia, the LBS and the BS show different seismic and stratigraphic character from proximal to distal regions of the margin (Fig. 4.14). Differences in character naturally relate to changes in the way that depositional systems responded to factors such as palaeodepth, distance from sediment sources, palaeotopography, and the position of depocentres relatively to the extensional locus (see Kyrkjebø et al, 2004).

The seismic data interpreted in this paper shows that Late Aptian flexural rebound of the lithosphere created an angular unconformity (the LBS) on the inner proximal margin (Porto Basin), followed by the deposition of a forced regression systems tract up to the shelf edge (Unit 1). In fact, the development of a forced regression due to breakup was predicted by numerical models (Cloetingh *et al.*, 1989; Kooi &

Cloetingh, 1989, 1992). This resulted in bypass of sediment from the continental shelf to the deeper parts of the margin (Figs. 4.3–4.5). Significantly, well data shows that the hiatus associated with this unconformity decreases in magnitude towards the west, with progressively younger sediments subcropping oceanwards below the LBS (Fig. 4.6). Such an observation suggests that tectonic uplift was more pronounced eastwards, resulting from uplift of a significant portion of the proximal margin, a character agreeing with the large wavelength deformation expected to uplift the rift margins at the time of complete lithospheric breakup (Cloetingh *et al.*, 1989; Kooi & Cloetingh, 1989, 1992).

In the Porto Basin, the LBS is thus a basal surface of forced regression, becoming a correlative paraconformity in the areas where a forced regressive wedge was not deposited or where subaerial exposure is not recorded across the LBS (Fig. 4.14). Landward, the LSB becomes a composite subaerial erosional surface since it merges with older unconformities generated on the basin shoulder, which was likely to form a region of predominant erosion from early syn-rift times (see Alves *et al.*, 2002; Alves *et al.*, 2003a).

Strata below the LBS were drilled at several DSDP/ODP Sites (398, 641 and 1276), comprising slumps, turbidites and debris flow deposits derived from continental sources and from eroded footwall crests, deposited above or at the transition to the calcite compensation depth (CCD). These strata are subsequently blanketed by post-LBS black shales in sites 398 and 641 (Sibuet *et al.*, 1979; Boillot *et al.*, 1987b) deposited above or near the transition to the CCD. The black shales are imaged in seismic reflection as transparent and sub-parallel reflectors interpreted as deposited during a period of tectonic quiescence (Fig. 4.9). Elsewhere on the continental slope, prograding post-LBS strata fill discrete syn-rift depocenters (Alves *et al.*, 2006) (Fig. 4.4).

These data led here to the redefinition of the term 'breakup unconformity' (Falvey, 1974), which has been associated with the separation of continental crust and subsequent onset of seafloor spreading (Embry & Dixon, 1990; Falvey, 1974;

Jungslager, 1999; Kyrkjebø *et al.*, 2004; Moore, 1992; O'Driscoll *et al.*, 1995; Tucholke *et al.*, 2007; Ziegler, 1975) as a lithospheric breakup surface (LBS). In discrete depocenters on the outer proximal and distal margins, the LBS represents the principal stratigraphic feature related to lithospheric breakup between divergent continental margins, preceding the deposition of a breakup sequence (BS) accumulated during the lithospheric breakup event.

On the distal and on the westernmost part of the outer proximal margin (DSDP site 398 and ODP site 641) of West Iberia, the sudden cessation in mass-wasting events across the LBS was caused by the tectonic quiescence that followed the breakup event, with hemipelagites and distal-fan turbidites predominating thereafter. It should be noted, however, that by comparison with Newfoundland margin the distal margin of West Iberia was sediment starved at this time (Shipboard Scientific Party, 1987b), therefore less prone than the Newfoundland margin to turbidite deposition without significant tectonism. Widespread triggering of turbidite and mass-wasting events is expected to happen during lithospheric breakup in a sediment rich margin such as Newfoundland simply due to stability loss of sediment accumulated in the shelf edge and upper slope regions (Mulder, 2011).

The definition of *breakup unconformity* is extended towards a 'breakup sequence' (BS). Offshore West Iberia and Newfoundland, the complete establishment of a setting dominated by widespread thermal subsidence and relative tectonic quiescence occurs gradually towards the top of the BS (Figs. 4.3 and 4.6). This BS comprises an unconformity-bounded, seismically-resolved unit that can be interpreted in other divergent continental margins (*e.g.* Beglinger *et al.*, 2012). Examples of margins where the LBS can be potentially recognised include Norway–Greenland (Reemst & Cloetingh, 2000), Morocco–Nova Scotia (Withjack *et al.*, 1998), SE Brazil–SW Africa (Macdonald *et al.*, 2003) and Australia–Antarctica (Direen *et al.*, 2007).

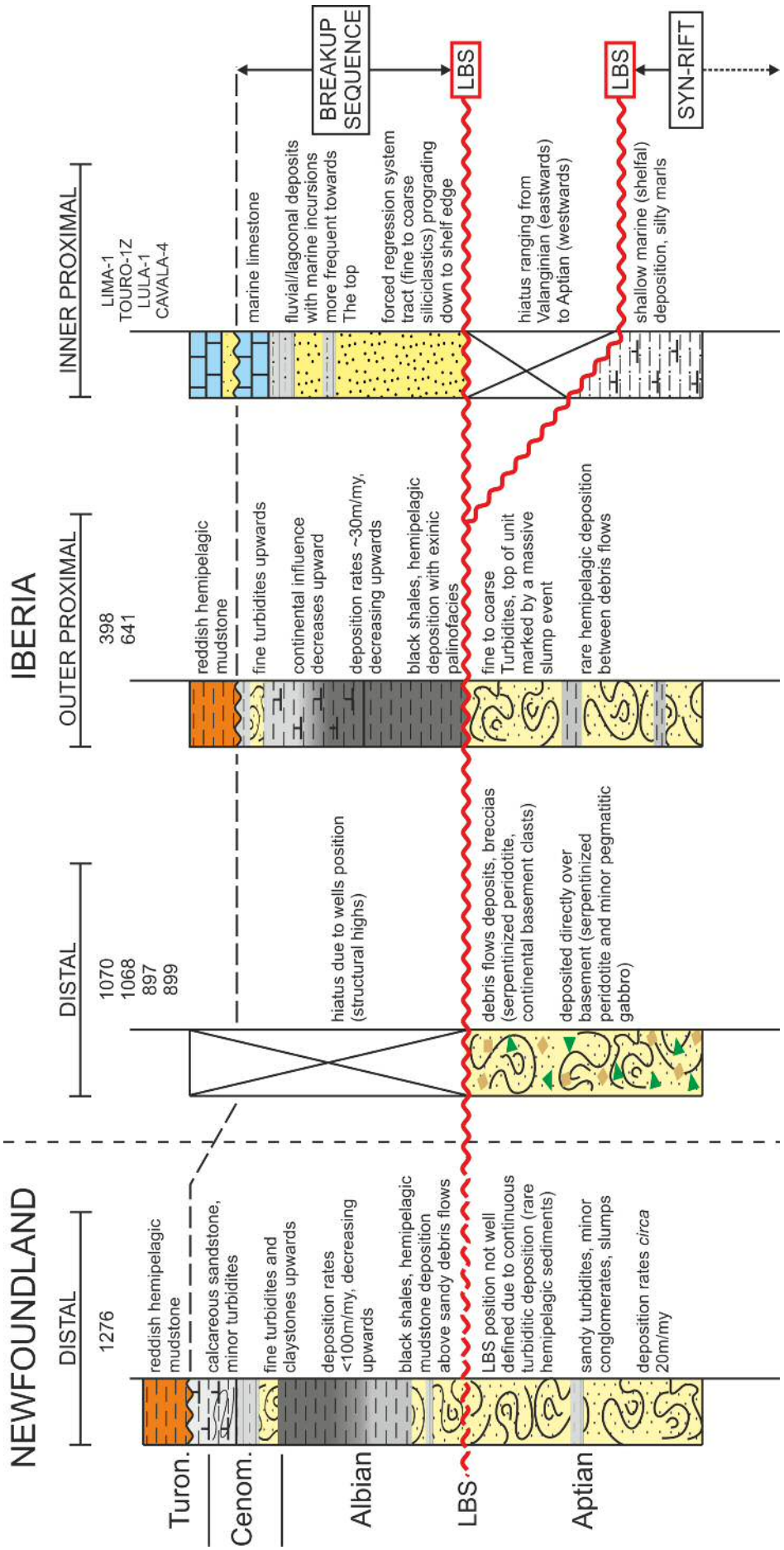


**Figure 4.13** Schematic lithological and stratigraphic correlation between wells drilled across the LBS in the different zones of the margin and relative position of the Lithospheric breakup surface (LBS) and breakup sequence (see text for discussion). Data from inner proximal margin taken from this work; data from the outer proximal margin taken from Sibuet *et al.* (1979), and Boillot *et al.* (1987b); distal margin Sawyer *et al.* (1994), Whitmarsh *et al.* (1998), Tucholke *et al.* (2004). No scale implied. Location of wells in Figure 4.1

On divergent margins, the relative timing in which thermal subsidence dominates over the uplift generated by the lithospheric breakup probably depends on several points: (1) how fast complete breakup is achieved (a probable function of the rheological, thermal and structural characteristics of the lithosphere close to the breakup locus), (2) the extent to which lithospheric uplift triggers changes in density in the upper mantle (a decrease in density promotes the lithospheric buoyancy and consequently generate more uplift) and (3) the influence exerted by the erosional unloading of the uplifted proximal areas. This last point is discussed in detail below.

Consequently, the way sedimentary sequences record the lithospheric breakup event depends on relative sediment supply, subsidence, climate and the balance between tectonic movement and eustasy across and along a continental margin. These parameters are thus responsible for the diachronicity observed in the LBS, and within the distinct units forming the BS.

### 4.7.2. Recognising the LBS and BS on deep-water continental margins

A way to overcome the difficulties of recognising the BS is to integrate information from the proximal margin with seismic–stratigraphic information from more distal regions. On proximal margins, the BS will mark a sudden progradational event (Unit 1) regardless of the formation, or not, of a basal unconformity (Figs. 4.3, 4.4 and 4.6). On the inner proximal margin, this progradational event can be well imaged in seismic data given the abrupt changes in sediment architecture that occur across it (Fig. 4.3–4.5). Yet, evidence for this forced regression can be absent or easily misidentified when interpreting seismic data from the outer proximal margin alone, particularly in regions where sediment supply was relatively high during the syn-rift phase. Depending on the available sediment supply or on relative accommodation space, the forced regressive systems tract (Unit 1) can be deposited as a detached forced regression systems tract (Posamentier & Morris, 2000), making its identification difficult, particularly when obliterated by erosion on an evolving continental slope. In fact, rift shoulder erosion, enhanced by the uplift due to the

breakup event will promote even further uplift this time due to flexural rebound as response to erosional unloading (van Balen *et al.*, 1995; Burov & Cloetingh, 1997; Burov & Poliakov, 2003). This prolonged erosional period can then erase the evidence of the BS on the inner proximal margin. In addition, in West Iberia the preservation of the BS on the inner proximal margin can be due to this erosional unloading effect, since at the time of deposition of the BS, a globally recognized transgression was taking place (Haq *et al.*, 1987; Hardenbol *et al.*, 1998). The competing uplift due to the erosional unloading and the eustatic sea-level rise could have prolonged the deposition of the BS, contributing to its preservation and the somewhat aggradational stacking pattern displayed in Unit 3 and the beginning of Unit 4.

In individual depocenters where lithospheric extension is no longer active—due to extensional locus migration or a mere local abandonment of previously active faults—strata deposited after the main episodes of syn-rift extension, but prior to lithospheric breakup, can be blanketed by sediments showing a 'post-rift' architecture, i.e. parallel reflectors with no growth sequences (*e.g.* Péron-Pinvidic *et al.* 2007). This 'post-rift' geometry is not related to the end of the rifting process on a continental margin but to the exhumation of the upper mantle at the end of LRS1, an event preceding full lithospheric breakup. This promoted the migration of the main locus of extension to more distal regions, focusing on the newly exhumed upper mantle. In this way, the already separated continental crust experience a phase of (partial) tectonic quiescence. Despite the fact that the depositional architecture of

---

**Figure 4.14** (next page) Summary of the lithostratigraphic character of the Breakup Sequence (i.e. earliest post-rift) and latest syn-rift sequences along the Iberian margin. Data from inner proximal margin taken from this work; outer proximal margin data from Sibuet *et al.* (1979), Boillot *et al.* (1987); distal margin data from Sawyer *et al.* (1994), Whitmarsh *et al.* (1998). Simplified margin architecture from interpreted seismic reflection profiles (TGS-NOPEC PD00-903 and PDT00-103) from West Iberia Margin (location on Figure 4.1), showing the margin zonation adopted in this paper and the location of ODP sites (site numbers in parentheses are projected). LBS—lithospheric breakup surface; ZECM—zone of exhumed continental mantle.

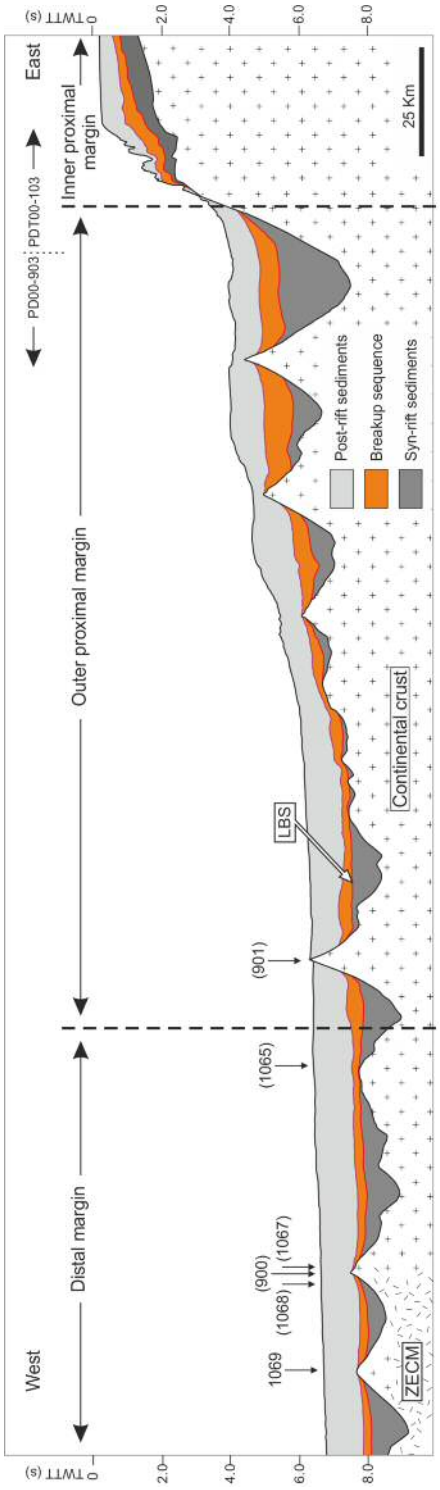


| | | DISTAL | OUTER PROXIMAL | INNER PROXIMAL |
|---|---|---|---|---|
| Seismic Character | Earliest syn-rift | Transparent reflectors onlapping structural highs and LBS | Transparent reflectors onlapping structural highs and LBS | donwlapping (with toplap) reflectors on the LBS |
| | Latest post-rift | Chaotic, divergent, strong reflectors | Chaotic, parallel and divergent reflectors | Parallel reflectors |
| Depositional environment | Earliest syn-rift | Pelagic deposition below CCD | Pelagic deposition below CCD | Deltaic to fluvial deposition |
| | Latest post-rift | Pelagic deposition below CCD | Pelagic deposition below (distally) and above CCD (proximally) | Neritic |
| Lithology | Earliest syn-rift | Black shales (in starved depocentres) | Black shales (in balanced depocentres) | Fine to coarse siliciclastics (overfilled depocentres) |
| | Latest post-rift | Mass flow deposits (hemipelagic background.) | Mass flow deposits (hemipelagic background) | Marls to fine siliciclastics |
| Stratigraphic contact | | Diastem? | Diastem/conformable (probable short hiatus or condensed level) | Unconformity (hiatus less expressive basinwards) / Composite subaerial unconformity |
| Sequence stratigraphic surface | | Correlative conformity | Correlative conformity | Erosive basal surface of forced regression / Subaerial unconformity |
| | | | | OFFSHORE / ONSHORE |

sediments deposited in these now tectonically quiescent regions of the rift can resemble post-rift strata, they are still part of the syn-rift depositional package since mantelic exhumation and thinning are still part of the rifting process (see also Nøttvedt *et al.*, 1995; Reston, 2005).

Other factors that can affect the BS deposition are inherent to the structure of the lithosphere. Given its heterogeneities and discontinuities (*e.g.* transfer faults such as the Nazaré fault, Fig. 4.1), uplift of the lithosphere during lithospheric breakup will vary spatially when due to in-plane stress release. This can pose problems for the generation and preservation of the BS on the inner proximal margin. The prograding BS can be more or less complete depending on the relative position of sediment discharge points.

If on the inner proximal margin the BS is characterized by its basal erosional surface (the LBS), distinct stratigraphic architecture, and distinct degrees of sediment immaturity, on the outer proximal and distal margins its character will markedly differ. Here the base LBS can be a diastem or a correlative conformity (depending on sediment availability), followed by hemipelagic deposition of black shales with significant amounts of continental organic matter within the BS (Fig. 4.14).

Despite these differences, a direct correlation exists between the deposition of Units 1 to 4 on the inner proximal margin, and the strata immediately above the LBS at DSDP Site 398. Organic matter is more easily transported over long distances compared with heavier components of the sediment load which promotes its deposition and accumulation in deeper parts of the rift basin. In fact, at DSDP Site 398, the relative percentage of continental plant remains is high throughout the Albian, with a marked peak that is reached shortly after the lithospheric breakup, during the Early Albian (Deroo *et al.*, 1978; Deroo *et al.*, 1979; Taugourdeau-Lantz *et al.*, 1982). This sudden increase in organic matter may be linked to the Aptian–Albian OAE1b. The existing sluggish bottom ocean currents during the Albian (Robinson *et al.*, 2010) would not be able to quickly replenish the oxygen consumed by the degradation of this sudden influx in organic matter, leading to anoxia. The

lithospheric breakup event can therefore be related to the onset of oceanic anoxic events, though not necessarily triggering it, the breakup is at least one of the probable contributing mechanisms responsible for the existence of OAE1b in the Central Atlantic.

This variable character of the BS is observed on seismic and borehole data from West Iberia, suggesting its reassessment as a sediment-starved margin.

### 4.7.3. Reassessing the concept of a sediment-starved western Iberian margin

Given the abrupt relative sea-level fall triggering the forced regression at the start of the BS, abundant turbidites would be expected to accumulate after lithospheric breakup is achieved, as large quantities of sediment bypass the continental shelf. In contrast, the immediate expression of this relative sea-level fall on the outer proximal and distal margins is the deposition of black shales with abundant continental carbon-rich material that otherwise are expected to occur closer to shore [exinitic palynofacies found in site 398 (Habib, 1979)].

The discrepancy in the amount of turbidite material expected to be transported onto the distal margin is interpreted to result from important sediment capture in syn-rift basins located on the outer proximal margin during the deposition of the BS. Therefore, the reassessment of West Iberia is proposed as comprising a sediment starved margin only in its distal part, towards the Iberia Abyssal Plain. After the syn-rift stage, sediment starved (underfilled) basins distally located preserving significant accommodation space formed anoxic sub-basins with low sedimentation rates (Figs. 4.7–4.12). In contrast, the outer proximal margin shows overfilled depocenters where the locus of sediment progradation from the shelf and upper slope areas was located during the syn-rift phases and after lithospheric breakup. This character is revealed on seismic data by the vertical stacking of chaotic and westward-prograding strata in some parts of the outer proximal margin (Fig. 4.5). These strata should comprise intercalations of hemipelagites, coarse-grained turbidites, channel-fill and mass-transport deposits, accumulated above syn-rift units of similar seismic–stratigraphic

character (Fig. 4.14). Between sediment-starved and overfilled basins, sediment-balanced depocenters, as that at DSDP site 398, will show a sharp lithological contrast across the LBS but a simpler sub-horizontal geometry in strata above and below this same surface.

The presence of a forced regression and the subsequent BS units shedding sediment directly or close to the shelf edge implies an important quantity of siliciclastic material being transported to the slope and basin floor fans. These siliciclastic units are also proximally equivalent to 'black shales' deposits found throughout the North Atlantic. Therefore, it is proposed that Aptian–Cenomanian depocenters on the outer proximal margin comprise mainly siliciclastic strata, whilst distal margin depocenters and structural highs will preferentially form regions of 'black shale' deposition offshore West Iberia.

## 4.8. Conclusions

The data in this chapter provide evidence that the lithospheric breakup event triggers important changes in the depositional architecture of divergent margins, but that these changes can be correlated across and along a divergent continental margin. Lithospheric breakup generates crustal uplift due to a large wavelength flexural rebound of the lithosphere, triggering a forced regression observed in Porto Basin and allowing the development of a recognisable basin-wide surface, the LBS and the deposition of a subsequent stratigraphic unit across rifted margins, the BS (Fig. 4.14).

Ranging from the uppermost Aptian to Late Albian–Early Cenomanian, the BS includes in the Porto Basin: (1) a basal forced regressive Unit 1 (Albian), prograding to the shelf edge and generating a hiatus landwards; (2) a transgressive Unit 2 topping the forced regressive package, with carbonates materialising a maximum transgressive surface; (3) an Albian Unit 3 showing predominant aggradation. Unit 4 (Albian–Cenomanian) reflects a transgressive event related to the complete establishment of a passive margin in the Late Aptian–Early Cenomanian.

Accompanying lithospheric breakup, significant portions of the studied margins were uplifted and eroded.

Different regions of newly-formed divergent margins will show distinct expressions in both the LBS and BS. While onshore the LBS is a composite unconformity, in proximal basins it is an unconformity with a hiatus of decreasing magnitude towards the shelf edge, becoming a diastem or a correlative surface on the distal margin (and outer proximal margin pro parte). The onset of the BS is marked by the deposition of a forced regressive prograding wedge (Unit 1), which distally on the margin can be correlated with carbon-rich hemipelagites. Above this first progradational package occur episodical events of transgression and further progradation (Units 2 and 3). The top of the BS coincides with the stage in which regional thermal subsidence predominates over intra-plate tectonism, and a deepening-upwards trend becomes reflected on the sedimentation (Unit 4). On the inner proximal margin, this later phase culminates in the deposition of a transgressive carbonate unit (Cacém formation). On the distal margin (and outer proximal margin pro parte), the upper boundary of the BS is recognised by a shift from black shale deposition to barren red mudstones. Several factors contribute to the deposition, preservation and timing of the different units that constitute the BS, such as palaeodepth, distance from sediment sources, relative position of sediment discharge points, palaeotopography, position of depocentres relatively to the extensional locus and the unloading effect due to erosion of the rift shoulder.

Based on this analysis a new name is proposed, the lithospheric breakup surface (LBS), for the stratigraphic surface previously known as '*breakup unconformity*', on the basis that: (1) all lithosphere is involved on the breakup process and not only the continental crust, and (2) although an unconformity is not always present, a distinct surface marking the lithospheric breakup event is observed throughout the rift basin. In this work, a more comprehensive definition of continental breakup concept is proposed—a prolonged event that marks the end of brittle extensional deformation, instead of mere continental breakup, with the gradual emplacement of normal oceanic crust separating fully rifted margins. Furthermore, instead of a single

'*breakup unconformity*', the lithospheric breakup event is considered to be associated with a distinguishable sedimentary sequence (BS), of regional extent, showing a distinct architecture to strata deposited prior to the lithospheric breakup event. The BS records the lithospheric adjustments caused by lithospheric breakup. It marks the transitional period spanning from the onset of the lithospheric breakup event to the establishment of thermal relaxation as the main control on subsidence on a divergent margin. Therefore, the BS presents time- and spatial-variable architectures that reflect the equilibrium between the tectonic phenomena associated with lithospheric breakup and the progressive establishment of thermal subsidence along and across divergent continental margins.

Chapter Five

# CONTOURITE DRIFTS AS AN INDICATOR OF ESTABLISHED LITHOSPHERIC BREAKUP

An abridged version of this chapter has been published as:

Soares, D., Alves T., Terrinha, P. (2014): *Contourite drifts on early passive margins as indicators of established lithospheric breakup*, Earth and Planetary Science Letters, 401, p. 116-131.

## 5.1. Abstract

The Albian–Cenomanian breakup sequence (BS) offshore Northwest Iberia is mapped, described and characterised in terms of its seismic and depositional facies. The interpreted dataset used in this chapter comprises a large grid of regional (2D) seismic-reflection profiles, complemented by industry and ODP/DSDP borehole data. Within the BS are observed distinct seismic facies that reflect the presence of: a) black shales and fine-grained turbidites, b) mass-transport deposits (MTDs) and coarse-grained turbidites, and c) contourite drifts. Borehole data show that these depositional systems developed as mixed carbonate-siliciclastic sediments proximally, and as organic-carbon-rich mudstones (black shales) distally on the Northwest Iberia margin. MTDs and turbidites tend to occur on the continental slope, frequently in association with large-scale olistostromes. Distally, these change into interbedded fine-grained turbidites and black shales showing widespread evidence of deep-water current activity towards the top of the BS. Current activity is expressed by intra-BS erosional surfaces and sediment drifts. The results in this chapter are important as they demonstrate that contourite drifts are ubiquitous features in the study area after Aptian–Albian lithospheric breakup. Therefore, the recognition of contourite drifts in Northwest Iberia is interpreted as having significant palaeogeographic implications. Contourite drifts materialise the onset of important deep-water circulation marking the establishment of oceanic gateways between two fully separated continental margins. As a corollary, the generation of deep-water geostrophic currents is postulated to have had significant impact on North Atlantic climate and ocean circulation during the Albian–Cenomanian, with the record of such impacts being preserved in the contourite drifts analysed in this work.

## 5.2. Introduction

As showed previously, lithospheric breakup has been the focus of significant research work addressing the triggering mechanisms, kinematical models and

structural evolution of divergent continental margins (*e.g.* Braun & Beaumont, 1989; Bott, 1992b; Healy & Kusznir, 2007; Manatschal *et al.*, 2007; Reston & Pérez-Gussinyé, 2007).

However, few research papers thoroughly document the seismic-stratigraphic changes occurring on continental margins undergoing lithospheric breakup (*e.g.* Péron-Pinvidic *et al.*, 2007; Soares *et al.*, 2012, see as well Chapter 4). When documented, such changes have led to the recognition of the *breakup unconformity* (*sensu* Falvey, 1974), the surface defining the exact moment of lithospheric breakup, as an oversimplified model (Manatschal, 2004; Péron-Pinvidic *et al.*, 2007; Soares *et al.*, 2012, see as well Chapter 4).

In fact, in the previous chapter we saw that the *breakup unconformity* per se can merely represent the end of activity in local syn-rift faults, rather than the true end of crustal stretching and the initiation of the drifting phase on newly formed divergent margins (Reston, 2005; Péron-Pinvidic *et al.*, 2007). Recognising this latter caveat, data on the conjugate margins of West Iberia and Newfoundland was used in Chapter 4 to propose new criteria to characterise the transition between syn-rift and post-rift settings on continental margins.

This chapter uses 2D seismic data from five different surveys, together with well data from deep sea drilling and industry campaigns, to describe the BS along Northwest Iberian in terms of its stratigraphic architecture and sedimentology (Fig. 5.1). Additionally, seismic and deep-sea borehole data were used on the conjugate margin of Newfoundland and compared with data from Northwest Iberia. The focus of this chapter is on the outer proximal and distal margins (see Chapter 4 for a detailed description of the BS on the proximal margin of Northwest Iberia).

Lithospheric breakup is documented in this chapter as marking the onset of increased, widespread bottom current activity in West Iberia. Importantly, mass-wasting and turbidite deposits are concentrated in the lower half of the BS, with contourite drifts predominating towards the top of the sequence. This character suggests that the BS comprises a mixed contourite-turbidite system in Northwest

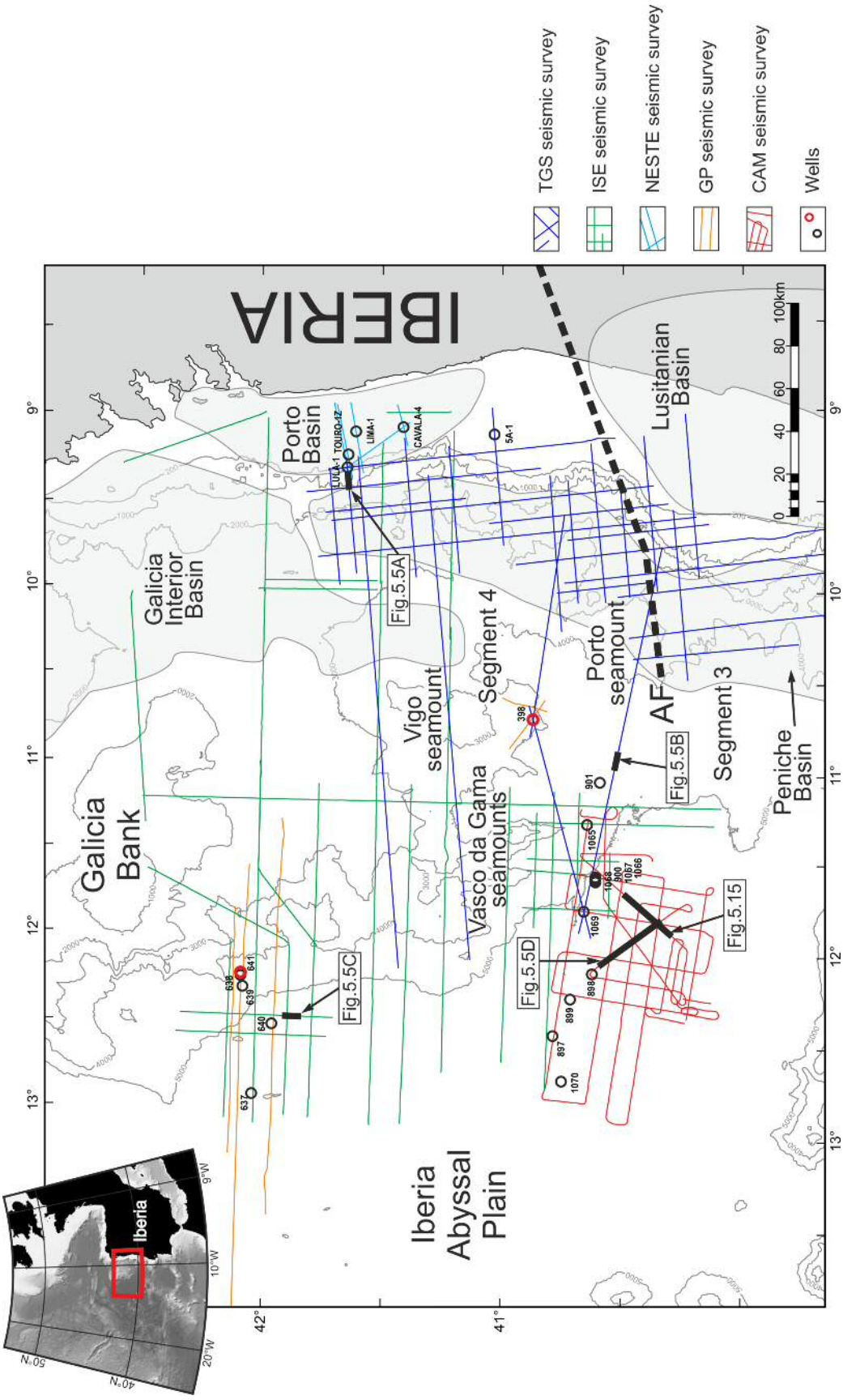


**Figure 5.1** Location of the datasets used and several figures showed in this chapter. DSDP/ODP sites are located West of 10°W, with the red circles in the figure indicating the sites where the breakup sequence was recovered. Industry wells are located East of 10°W. AF – Aveiro Fault.

Iberia, with contourite drifts (*sensu* Rebesco *et al.*, 2008) becoming more prominent as Northwest Iberia and Newfoundland evolved as separate continental margins.

In summary, this chapter aims to address the following questions:

1) What is the seismic-stratigraphic character of the BS from the proximal to distal margins of Northwest Iberia?

2) Which depositional processes encompassing a rift basin, from proximal to distal environments, are associated with the syn-rift to a post-rift transition on continental margins?

3) What is the significance of contourite drifts within the BS?

## 5.3. Data used in this chapter

A comprehensive dataset comprising time-migrated 2D reflection seismic and borehole data is used in this chapter (Fig. 5.1). The seismic dataset (with a much wider coverage than the one used in the previous chapter), includes multiple 2D seismic surveys covering different parts of Northwest Iberia, from the inner proximal margin to the Iberia Abyssal Plain (Fig. 5.1). Seismic data from NESTE PORTUGAL were interpreted on the inner proximal margin. Data from a regional TGS-NOPEC speculative survey acquired in Northwest Iberia were interpreted on the outer proximal margin (Fig. 5.1). Seismic profiles from the Iberian Seismic Experiment (Shipley *et al.*, 2005), GP (Groupe Galice, 1979) and CAM surveys (Discovery 215 Working Group, 1998) were interpreted on the distal margin (Fig. 5.1). The SCREECH survey was used in Newfoundland, the conjugate margin of West Iberia (Shipley *et al.*, 2005). See Chapter 2 for details on the different seismic surveys.

The borehole dataset comprise the same wells used in the previous chapter. From the inner proximal margin (Porto Basin) industry wells Lula-1, Touro-1Z, Lima-1, Cavala-4 and 5A-1, were used tied to seismic data in order to date and characterise the breakup sequence and its stratigraphic boundaries, as defined in Chapter 4. For the outer proximal and distal margins, published data from ODP Legs 47b, 103, 149, 173 (Sibuet *et al.*, 1979; Boillot *et al.*, 1987b, 1988; Sawyer *et al.*, 1994; Whitmarsh *et al.*,

1996a; Whitmarsh *et al.*, 1998; Beslier *et al.*, 2001a) were used and compared with ODP data from Leg 210 on the Newfoundland distal margin (Fig. 5.1). See Chapter 2 for details related to the boreholes.

## 5.4. Breakup Sequence characterization

The BS is pervasive across Northwest Iberia, developing along and above thinned continental crust and exhumed upper mantle. Significantly, the BS drapes remnant syn-rift topography, burying several of the structural highs observed on seismic data—this way setting the stage for the post-rift sedimentation. Distinctive from the units below (syn-rift sediments, roughly characterized by divergent reflections occurring mainly at the base of this unit and chaotic reflections atop) and above (post-rift sediments, observed as parallel, strong reflections), the BS is easily perceived by its characteristic seismic facies as well as by its distinctive basal reflection that constitutes the LBS, the 'orange reflector' of Sibuet *et al.* (1979) (Figs. 5.3, 5.4, 5.7, 5.8, 5.10–5.13).

### 5.4.1. Sub-units in cored sections of the Breakup Sequence (BS)

The integration of seismic data from lines PD00-901 and PD00-902 with data obtained from DSDP Site 398D allowed the identification of three units within the BS (Units A, B and C) that are separated by erosional surfaces; the intra BS-1 and intra BS-2 surfaces (Fig. 5.2). These surfaces were found to be equivalent to the boundaries separating velocity groups 7a-7b and 7b-8 of DSDP Site 398D (Shipboard Scientific Party, 1979) (Figs. 5.2, 5.3). The base of group 8 coincides with the base of the BS [orange reflector in Shipboard Scientific Party (1979)] and the top of group 7a with the top of the BS [yellow reflector in Shipboard Scientific Party (1979)] (Fig 5.2).

#### *5.4.1.1. Unit A*

Bounded at its base by the LBS and at is top by the intra BS-1 surface, Unit A corresponds to velocity group 8 in Shipboard Scientific Party (1979) and is the oldest unit (earliest Albian to early middle Albian) in the BS. Unit A shows transparent

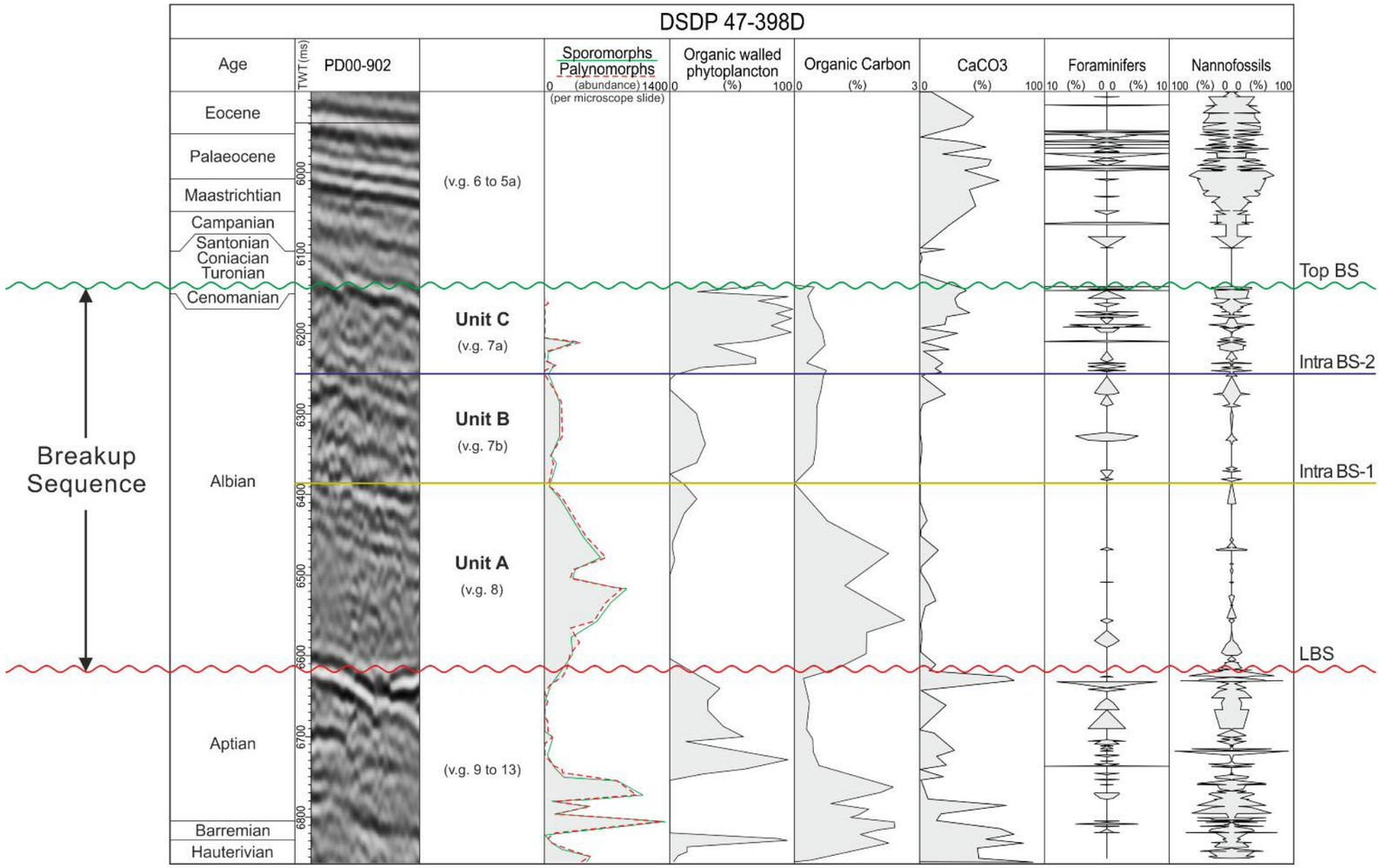


**Figure 5.2** (next page) Correlation between data from DSDP Site 398 and seismic line PD00-902. Here one can see the the units that contitute the the BS, their bounding surfaces and expression in data from DSDP Site 398 and in seismic data. Note the correlation between the intra BS surfaces and changes within the parameters presented. As well of note is that after mid-Unit A, a decrease of continentally derived organic matter (sporomorphs and palynomorphs) is observed, coinciding with an increase in marine phytoplankton. Palynological and organic carbon data is from Habib (1979); CaCo3 data from von Rad *et al.* (2004) (from smear slides); foraminifera and nannofossils data from von Rad *et al.* (2005) (from smear slides). 'v.g.' stands for 'velocity group'. Velocity groups and their boundaries were defined by Shipboard Scientific Party (1979). Depth in two-way time (ms). Location of DSDP Site 398 in Fig. 5.1 (regional context) and in Fig. 5.4 (in detail). Depth in two-way time (ms). LBS—lithospheric breakup surface; BS—breakup sequence.

reflections of low amplitude, changing to parallel reflections with stronger intensity towards its top (Figs. 5.2, 5.3). Its base onlaps and drapes the LBS, whereas the top of the unit corresponds to an erosional surface (intra BS-1; Figs. 5.2, 5.3). The erosive character of the intra BS-1 surface is better observed in line PD00-902 than in PD00-901, where it appears to form a paraconformity (Fig. 5.3).

At DSDP Site 398, Unit A is recorded at cores 398D-87 to 398D-103, coinciding with unit IIIa of Sigal (1979) and unit 3a of Basov *et al.* (1979) (Fig. 5.2). Sedimentologically, this unit is characterised by a very low to almost absent content in $CaCO_3$. Unit A also shows the highest content in organic matter, mainly derived from terrigenous plant debris, and the lowest content in agglutinated benthic foraminifera in strata drilled at DSDP Site 398 (Sibuet *et al.*, 1979) (Fig. 5.2). This character reflects the abundance of terrigenous plant material transported from the continent to deep-offshore depocenters at this time (see as well Chapter 4). It should also be stressed that the transition from the basal transparent seismic facies to the parallel reflections on top of Unit A is marked by a decrease in the abundance of palynomorphs and sporomorphs (Habib, 1979). Strikingly, the amount of phytoplankton in cored strata starts to increase at this same boundary, denoting an increasing importance in terms of marine organic contribution to the BS (Fig. 5.2).

#### *5.4.1.2. Unit B*

Unit B is bounded at its base by intra BS-1 and at its top by intra BS-2 erosional surfaces (Figs. 5.2, 5.3). It corresponds to velocity group 7b in DSDP Site 398D (Shipboard Scientific Party, 1979). The intra BS-2 surface is likely to correspond to the upper boundary of unit IVa of Sigal (1979). Seismically, Unit B comprises a base with chaotic and transparent to parallel reflections that can downlap the intra BS-1 (better observed in Figure 5.3B). The intra BS-1 and intra BS-2 surfaces are erosional in places, a characteristic that is observable on seismic data from the TGS-NOPEC survey (Fig. 5.3). Seismic data show that intra BS-2 surface marks an important change in depositional conditions within the BS, marked by a change in seismic character accompanied by channel incision (Fig. 5.3).

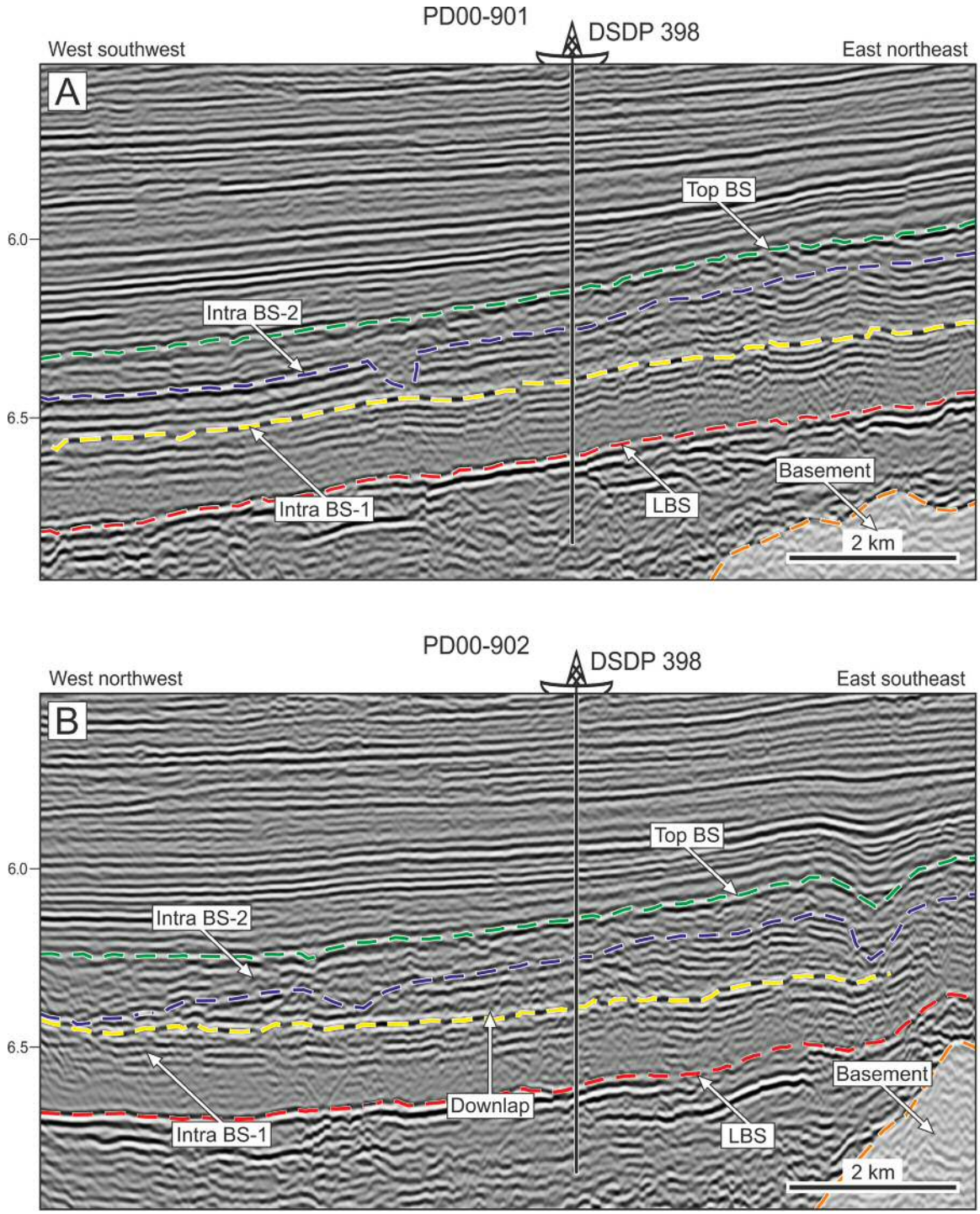


**Figure 5.3** Seismic sections crossing DSDP Site 398. Note how the orientation of the seismic profiles is important for the recognition of the intra-BS erosional surfaces: despite the low angle between them, the erosive character of intra BS-1 and intra BS-2 is not displayed uniformly in both seismic sections. In fact, the surface intra BS-1 is more clearly observed as an erosional surface at B than at A, where it appears to be a paraconformity. In the same way, in B downlap over Intra BS-1 surface is clearer. LBS—lithospheric breakup surface; BS—breakup sequence. Location of seismic profiles in Fig. 5.1 (regional context) and in Fig. 5.4 (in detail).

In palynological terms, the base of Unit B marks a transition from the progressive decrease of palynomorphs and sporomorphs observed in Unit A to relatively constant values (Habib, 1979) (Fig. 5.2). According to Sigal (1979), in Unit B occurs the initial stage of 'dilution' of black shales by turbidite sands and silts. Reworked foraminifera are also found in the unit (Sigal, 1979). In sediment cores, an increase in parallel and wavy laminations is observed when comparing Unit B with Unit A, together with an increase in bioturbation, especially at the bottom and top of Unit B (Shipboard Scientific Party, 1987a). Chamley *et al.* (1979) report the presence of intercalations of reworked sediment in core 398D-78.

#### *5.4.1.3. Unit C*

Unit C correlates with velocity group 7a from Shipboard Scientific Party (1979). Its age ranges from the Middle Albian to early Cenomanian. Unit C is bounded at its base by the intra BS-2 surface, and its top corresponds to the unconformity marking the top of the BS (Fig. 5.2). Seismically, Unit C shows chaotic to parallel reflections of lower amplitude than in Unit B (Figs. 5.2, 5.3). The top of this unit is the yellow reflector defined by Shipboard Scientific Party (1979). Roughly corresponding to units IVb and V of Sigal (1979), Unit C shows a marked increase in carbonate content and bioturbation within the BS (Fig. 5.2). At the base of the unit occur several sandy laminae displaying reverse grading and erosional basal contacts. Parallel and wavy laminations, erosional surfaces, sandy and graded beds increase in frequency towards the top of Unit C (Shipboard Scientific Party, 1979). Along this unit, the terrigenous supply decreases in significance and the progressive development of a more dominant pelagic sedimentary regime applies (Sigal, 1979). This change to more pelagic conditions is also evidenced by a sharp increase in phytoplankton and nannofossils content (Graciansky & Chenet, 1979; Habib, 1979) (Fig. 5.2). The boundary between Unit C and Unit B is marked by the lowest smectite (and highest attapulgite) content in all the pre-Danian succession of DSDP Site 398 (Chamley *et al.*, 1979).

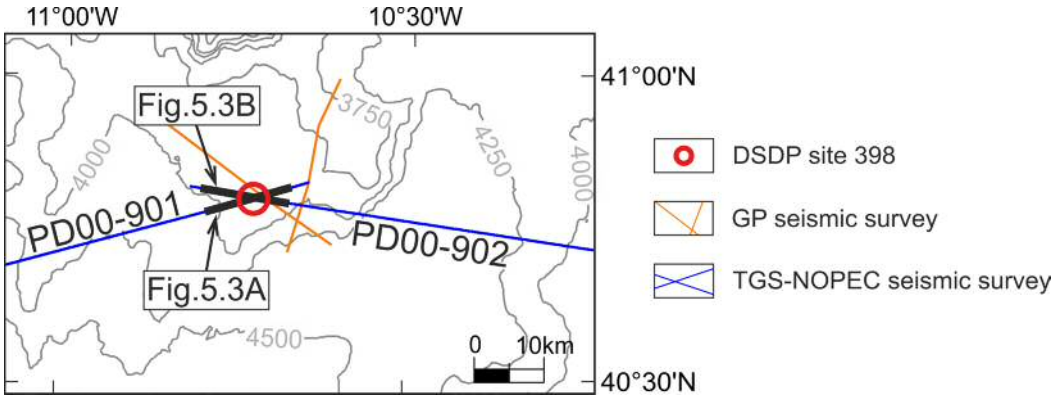


**Figure 5.4** Detail of the location of DSDP Site 398 and the seismic lines that cross it.

## 5.4.2. Internal seismic facies and associated deposits

The seismic character of the BS is not uniform in the study area. However, characteristic seismic facies within the BS can assist its recognition on seismic data. The base of the BS coincides with the LBS. Seismically, the LBS usually comprise a strong reflector separating two well distinct seismic packages (*e.g.* Fig. 5.5). Below the LBS, the reflections are usually moderately strong and can be chaotic, divergent or parallel (Figs. 5.3, 5.4, 5.7, 5.8, 5.10-5.13).

The lower part of the BS is often composed of low amplitude, transparent reflections. Towards the top of the unit occurs a transition, which can be gradual or abrupt to higher amplitude, continuous reflections (*e.g.* Figs. 5.5 and 5.3). This pattern can change across the basin with the presence of depositional features such as contourite drifts or erosional surfaces (Figs. 5.5D, 5.10 to 5.13). In fact, besides contourite drifts, one of the main characteristics of the BS that can be observed on seismic data is the widespread presence of erosional surfaces within it (Figs. 5.5D 5.13). The top of the BS is itself an erosional surface, which in places controls its thickness (Fig. 5.5B). Truncation of reflections below the BS, and onlaping onto its upper surface, are common characteristics observed in Northwest Iberia.

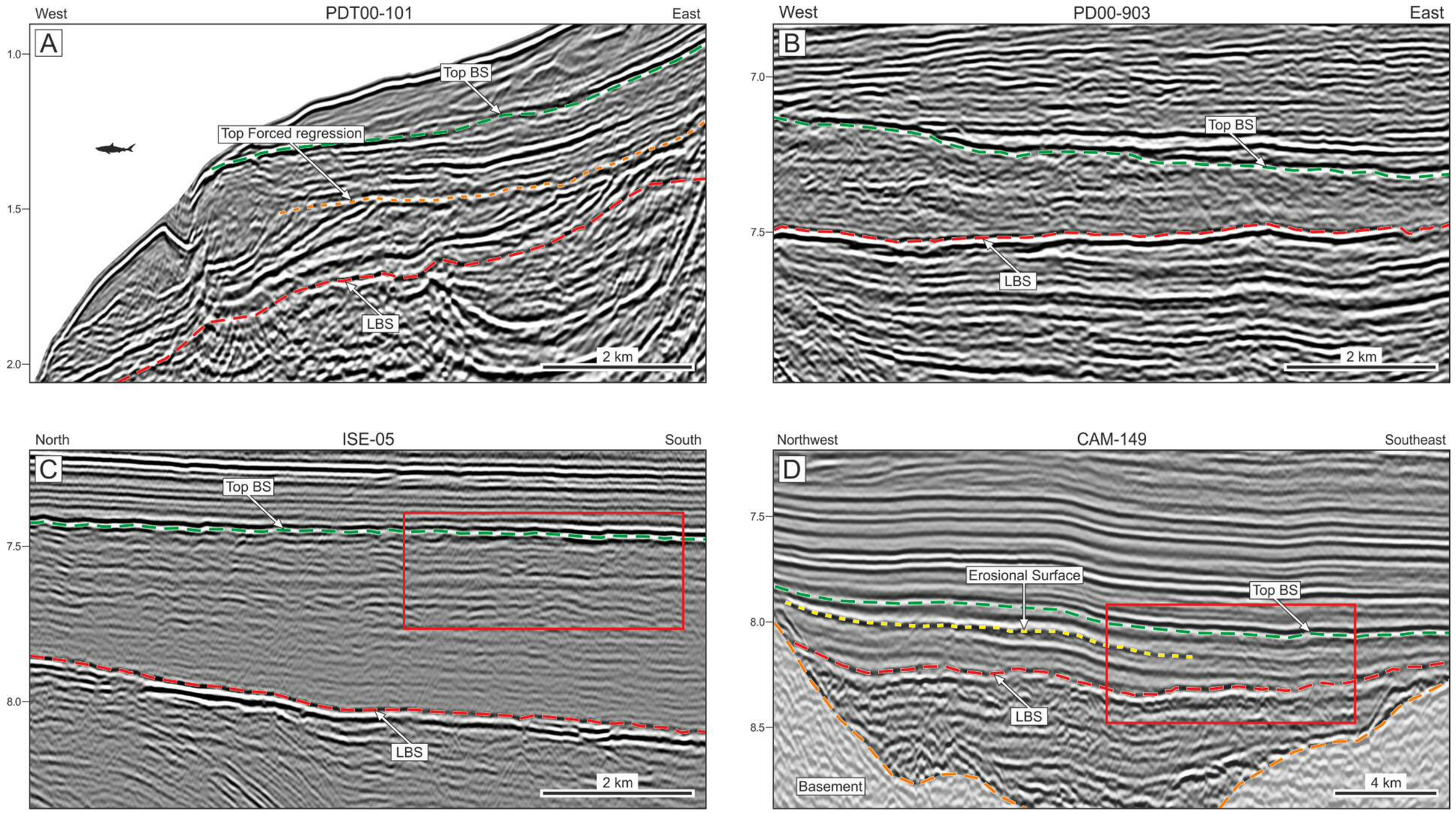


**Figure 5.5** Variability in seismic character of the BS and the LBS present in the study area. The following descriptions are relative to structures within the BS. A—seismic profile located at the transition between the inner and outer proximal margins, displaying the basinward edge of the prograding forced regressive deposits identified at the base of the BS. These deposits are capped by a succession of transgressive-regressive events in which the regressive phases never became as extreme as during the initial forced regression interpreted at the base of the BS. B—seismic profile showing the erosive character of the LBS and top BS. C—seismic profile showing seismic reflections of higher amplitude and more continuous towards the top of the BS. D—internal erosional surface with downlaping reflections above it. Note the different scale of D (both vertical and horizontal). LBS—lithospheric breakup surface; BS—breakup sequence. Location of seismic profiles in Fig. 5.1. The boxes in C and D are zoomed in Figure 5.15.

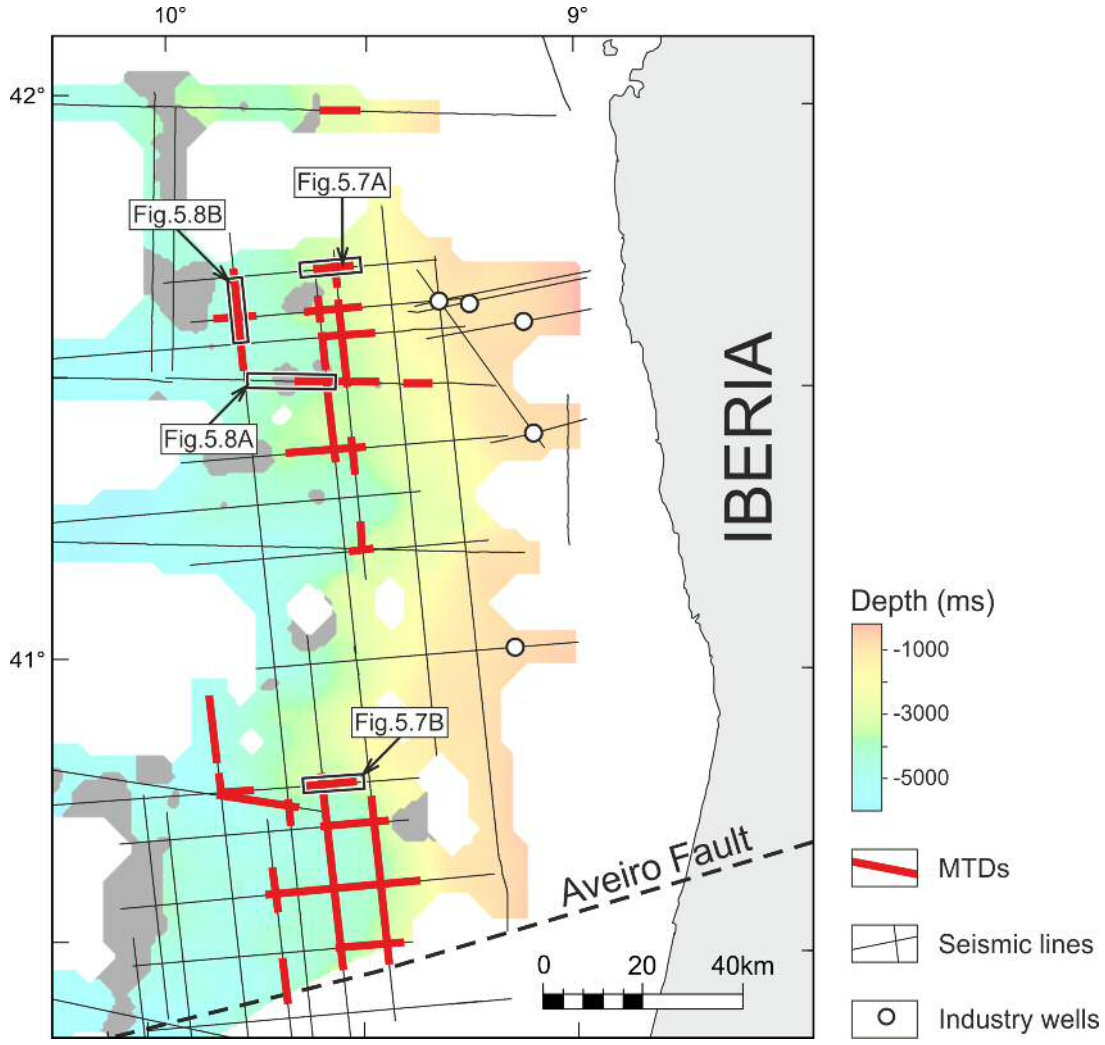


**Figure 5.6** Distribution map of MTDs identified within the BS, and location of MTDs seismic examples. The surface over which the MTD distribution is shown is the LBS. Note the existence of two main clusters of MTDs, one towards the north of the figure and a second cluster immediately northwards of the Aveiro Fault.

#### *5.4.2.1. Transparent and chaotic facies (interbedded black shales and turbidites)*

The presence of sediment rich in organic matter (black shales) in the Early–Late Cretaceous of Northwest Iberia was first identified during the drilling of DSDP Site 398, and suggested to have occurred by means of turbiditic deposition (Shipboard Scientific Party, 1979) (Figs. 5.1, and 5.2). Very distinctive on seismic data, interbedded black shales and turbidites are imaged as transparent reflections, with

chaotic reflections predominating on the distal margin and in parts of the outer proximal margin. An important observation is that this seismic facies occurs chiefly at the base of the BS where the amount of organic matter is interpreted to be higher (Figs. 5.2, 5.3 and 5.5B–D). In Figure 5.11, a very extensive turbidite fan can also be seen at the base of the BS, partially blanketing the LBS.

#### *5.4.2.2. High-amplitude convolute facies and megablocks (mass-transport deposits and proximal turbidites)*

Mass-transport deposits (MTDs) and proximal turbidites occur on the outer proximal margin, along the continental slope and close to the shelf break (Fig. 5.6). In these areas, convolute seismic facies characteristic of MTDs are observed in the form of contorted, chaotic, and structureless internal architecture; erosional nature of their base and lateral margins; presence of blocks within MTDs complexes; and abrupt terminations of contorted reflectors against continuous reflections.

The interpreted 2D seismic data does not allow an extensive analysis of the geomorphological features and internal structures in MTDs accumulated in the study area. Nevertheless, some important features characteristic of this kind of deposits (*e.g.* Posamentier & Walker, 2006; Bull *et al.*, 2009) can still be recognized. Distributed around two main regions below the shelf break, several MTDs comprise large rotated blocks, bounded by low-angle faults, and often following a step-wise distribution (Fig. 5.7). On their translational domain (*sensu* Martinsen, 1994), the MTDs are characterized by chaotic reflections with deep down-cutting bases (Fig. 5.8A). Distally, isolated MTDs are observed within continuous and undisturbed reflections (Fig. 5.8B). Towards the south of the study area, active halokinesis prior to the lithospheric breakup disrupted syn-rift sediments, complicating the recognition of MTDs.

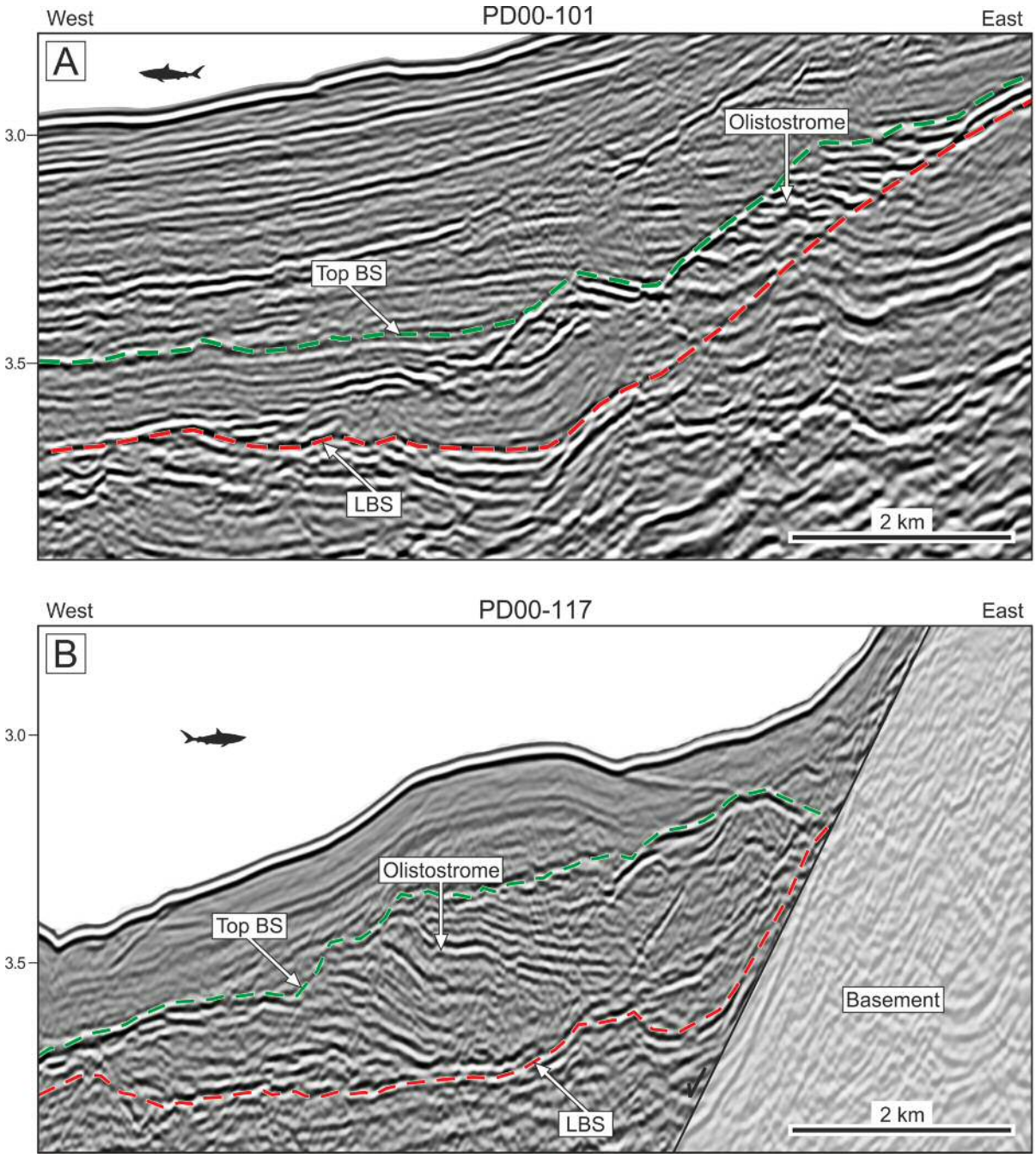


**Figure 5.7** Seismic profiles showing examples of MTDs identified within the BS. The following descriptions are relative to structures within the BS. A and B—Olistostromes embedded in and onlaped by the BS, suggesting concomitant deposition. LBS—lithospheric breakup surface; BS—breakup sequence. Location of seismic profiles in Figure 5.6.

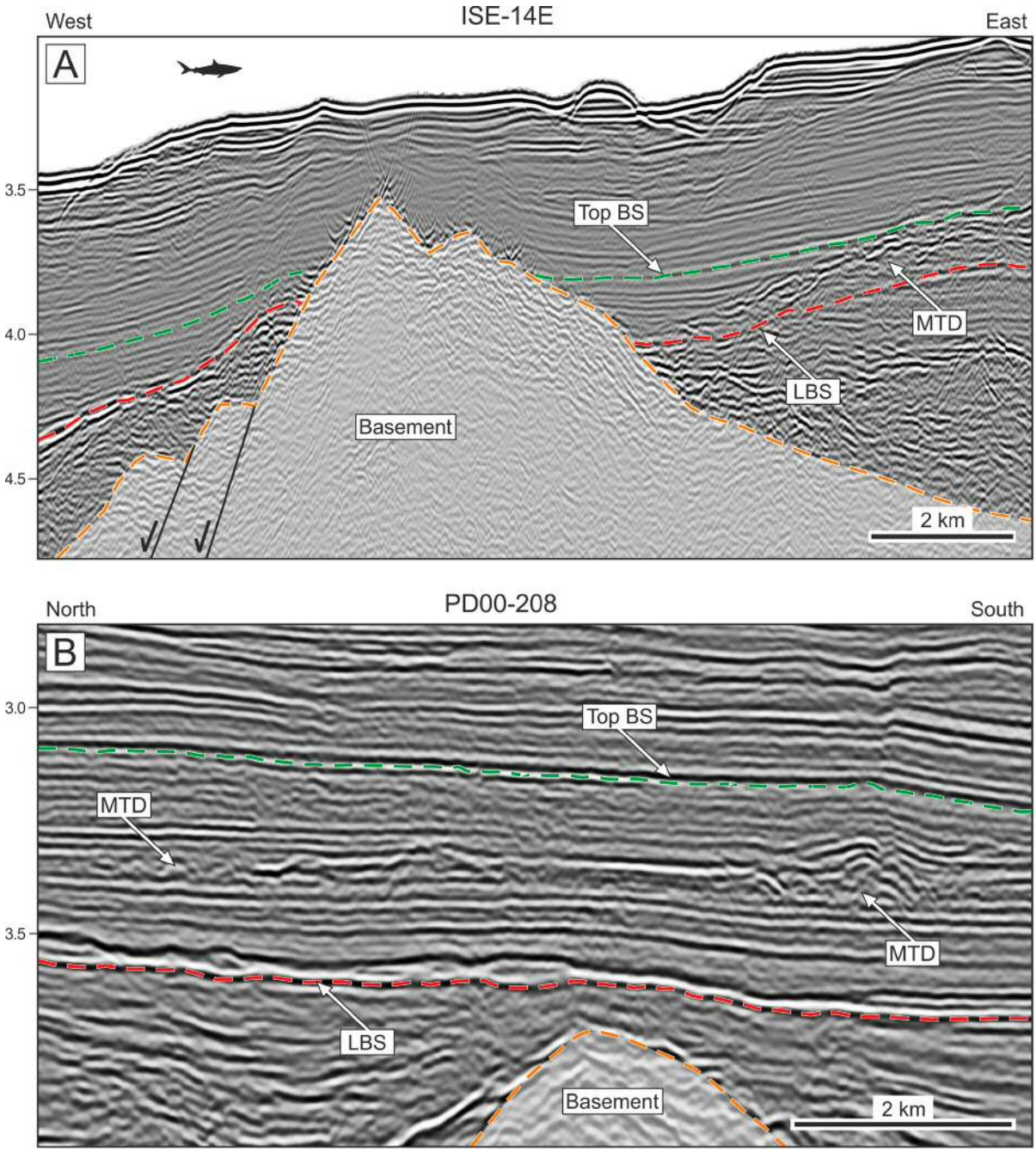


**Figure 5.8** Seismic profiles showing examples of MTDs identified within the BS. The following descriptions are relative to structures within the BS. A—MTD within the BS showing contorted and discontinuous reflections. B—MTD within the BS (in the same sub-basin shown westwards of the basement high in Figure 5.6), where several blocks can be observed, possibly deposited during different episodes. LBS—lithospheric breakup surface; BS—breakup sequence. Location of seismic profiles in Figure 5.6.

#### *5.4.2.3. Mounded high amplitude sub-parallel facies (contourite drifts)*

This facies is composed of variable thickness sub-parallel reflections with strong to moderate amplitude, showing the characteristic geometry of contourite drifts (Faugères *et al.*, 1999; Rebesco *et al.*, 2014), and displaying internal erosional surfaces.

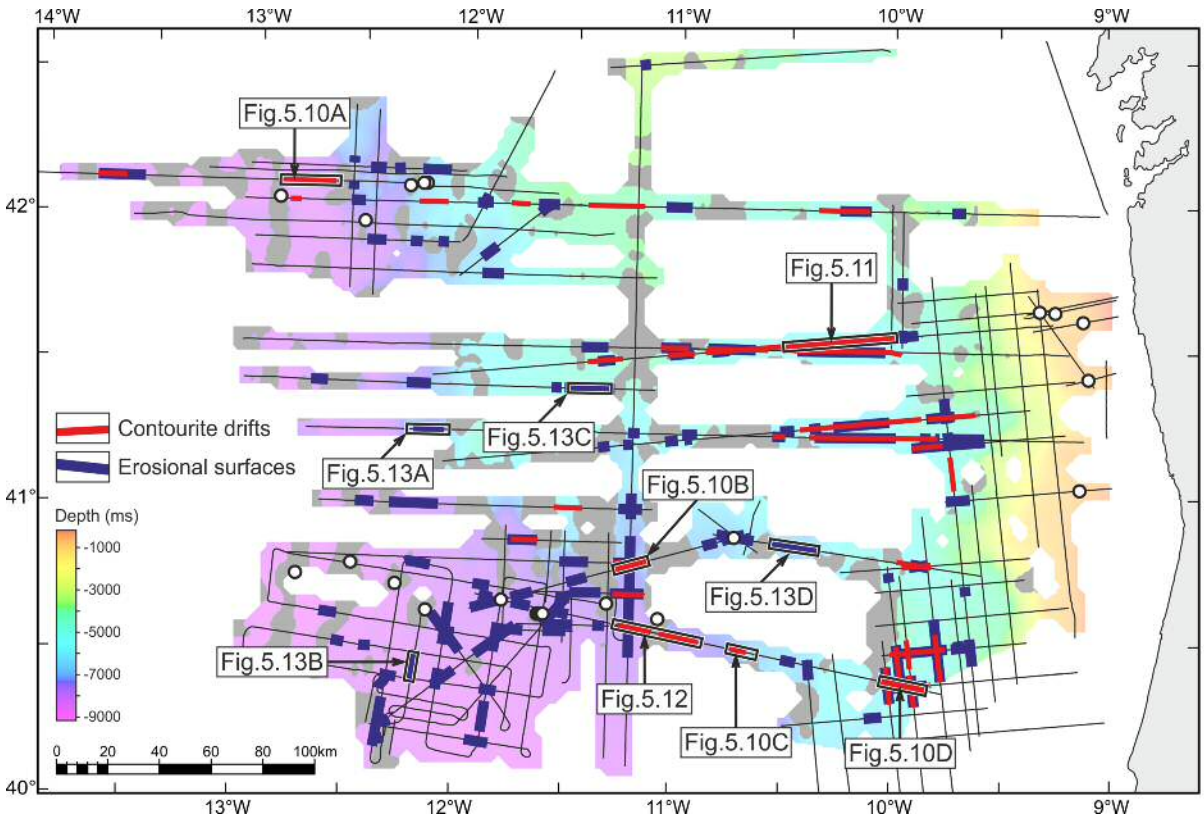


**Figure 5.9** Distribution map of contourite drifts and erosional surfaces identified within the BS. Contourite drifts represented by red yellow lines; erosional surfaces represented by thicker purple lines). The surface over which the contourites and erosional surfaces distribution is shown is the LBS.

The identification of contourite drifts was made mainly based on their large and medium-scale characteristics (the first and second order seismic elements of Nielsen *et al.* [2008]). In the study area, several types of contourite drifts can be distinguished (Fig. 5.9). These tend to occur not at the base of the BS but mainly towards the top of it (Figs. 5.10A-B and 5.11). Elongated mounded drifts (both detached and separated) and channel related drifts are the most common identified (Figs. 5.10C and 5.12). The

elongated mounded drifts present in the area do not always show an evident lower boundary. For example, in Figure 5.12 is difficult to ascertain where the lower boundary of both contourite drifts is located (this considering that the LBS is not that boundary).

Multiple seismic units can be observed within elongated mounded drifts and confined drifts. These units are separated by erosional surfaces, demonstrating the occurrence of episodic variations in the intensity of the currents, with episodes of strong currents promoting non-deposition and erosion alternating with periods of weaker currents that allowed the deposition of the drifts (Fig. 5.10B, D and 5.12). Current migration can be observed in some elongated mounded drifts in the form of migrating sigmoidal reflections with variable degrees of aggradation (Figs. 5.10A and 5.11). In fact, the elongated mounded and detached drift shown in Figure 5.11 does not display aggradation, suggesting the presence of a current rapidly migrating westward. On top of these sigmoidal reflections, what appear to be several generations of sediment waves can be observed, developing for almost 15 km (Fig. 5.11).

In detail, the seismic facies internally displayed by the contourite drifts can vary, with some internal units presenting almost transparent reflections while others show predominant moderate to strong amplitudes (*e.g.* Fig. 5.10C and D). In terms of lateral reflection continuity, although generally continuous and sub-parallel, some chaotic character can be observed (*e.g.* east drift at Figure 5.12).

The occurrence of large-scale erosional features in the BS was mapped across the study area (Fig. 5.9). They are observed on the distal and outer proximal margins below present-day depths of circa 4000 ms two-way time (TWT). Large, km-scale linear erosional features frequently occur near structural highs as moats (Fig. 5.12 and 5.13D) and less frequently as contourite channels (Fig. 5.11). Abraded surfaces are the most common large-scale erosional feature found in the study area (Fig. 5.13).

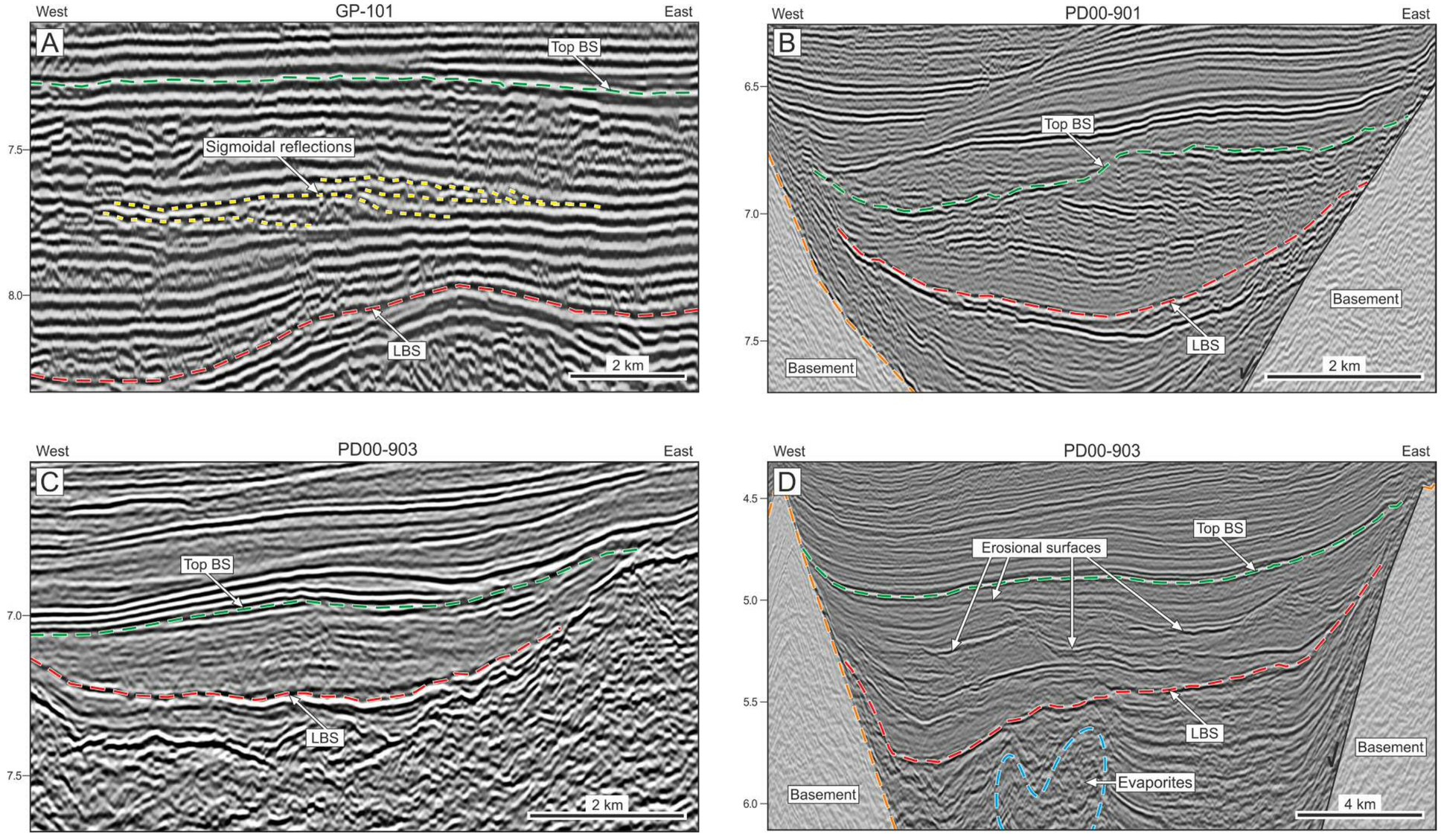


**Figure 5.10** Examples of contourite drifts identified within the BS. The following descriptions are relative to contourite drifts observed within the BS. A—elongated mounded drift displaying eastward lateral migration as revealed by the aggrading sigmoidal reflections (yellow dashed lines). B—confined drift with several depositional episodes. This drift evolves southwards into a separated drift, the same one that is observed on the west side Figure 5.12. C—separated drift with an upslope migrating character towards East. D—confined drift with several stacked depositional episodes marked by multiple strong basal erosive surfaces (not all erosional surfaces are signalled on the panel). The presence of deeply incised channels and the fact that they are located closer to the shelf break (towards SW) suggests that there was some degree of interaction with turbidites during drift deposition in this panel. Note the scale variations among the seismic profiles. Location of seismic profiles in Figure 5.9.

### 5.4.3. Depositional surfaces and isopach maps

When compared, isopach maps computed for the syn-rift and BS packages show a sharp change in sediment paths and depocenters (Figs. 5.14A and 5.14B)[‡‡]. During the syn-rift event, strata were preferentially deposited close to the inner proximal margin, particularly on the hanging wall of the Aveiro Fault (SE of the area in Figs. 5.14A) and in fault-bounded sub-basins parallel to the continental slope (ENE of the area in Figs. 5.14A). In contrast, isopach data for the BS show a different pattern of sediment distribution. Deposition to the SE of the study area lost the significance it had during the syn-rift (Figs. 5.14B). To the NE, deposition becomes more widespread, i.e. not confined to local depocenters. In addition, an important path for sediment sourced from the inner proximal margin can be interpreted in the NE corner of the study area by the presence of a significantly thicker BS (Figs. 5.14B). Another important change in the location of main depocenters is observed on the west flank of the Galicia Bank, where the largest thickness of BS strata on the distal margin is observed (Figs. 5.14B). The BS becomes considerably less developed towards the Iberian Abyssal plain, to the south of the Galicia Bank (Figs. 5.14B).

After the BS, the depositional setting changes considerably once again. The most important depocenter for post-BS strata becomes the area west of the Galicia Bank and the Iberia Abyssal Plain, where sediment can reach around 850 ms TWT in thickness (Fig. 5.14C).

During its deposition, the filling of the inherited syn-rift topography, and the observed re-routing of sediment paths caused by the lithospheric breakup event per se, resulted in the deposition of a BS of variable thickness. A relative uniform thickness of strata is only observed above the BS, when the majority of syn-rift structural highs was finally draped (Fig. 5.14C).

[‡‡] Larger images of the surfaces and thickness maps figured as Figures 5.14, 5.15, 5.16 and 5.17, along with other surfaces not figured in this chapter but computed in order to produce the thickness maps can be found in Appendix 1.

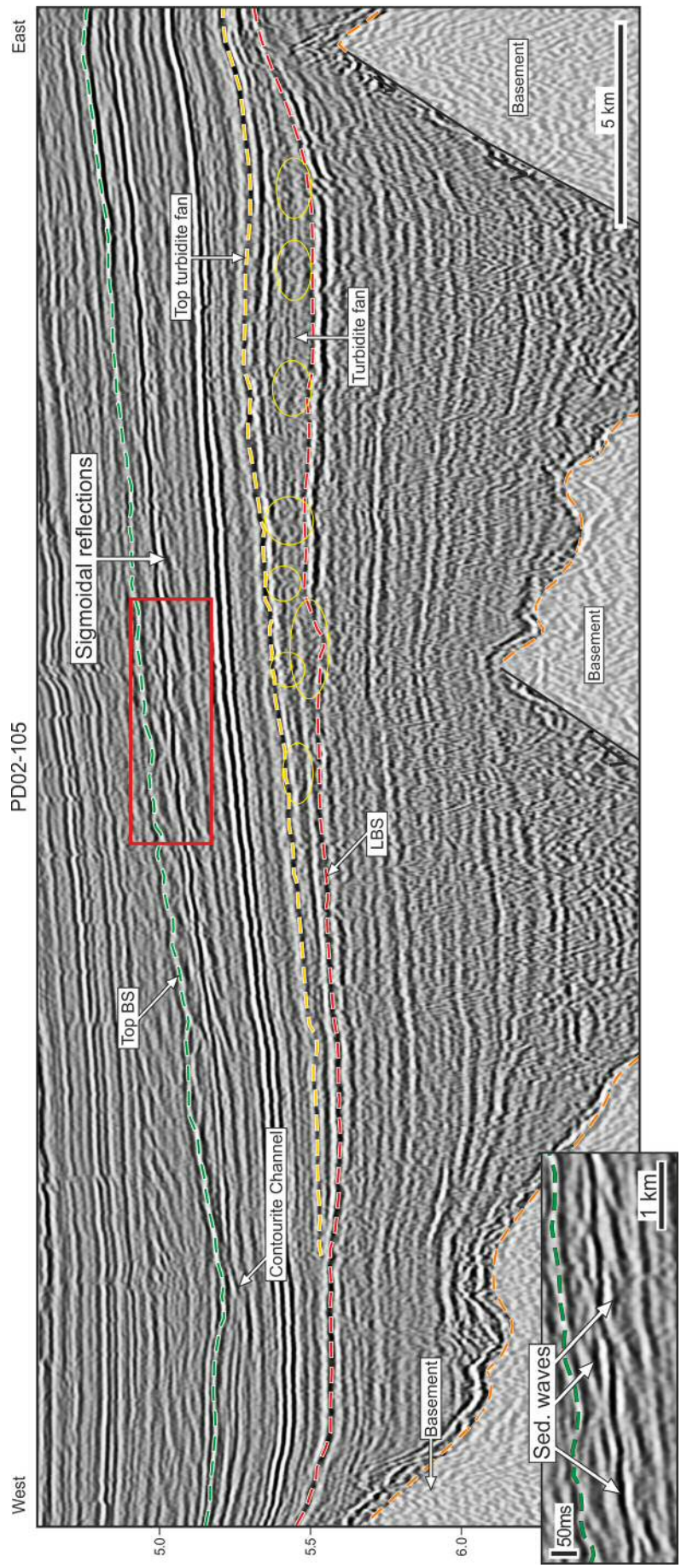


**Figure 5.11** Giant elongated mounded and detached drift. This contourite drif display an impressive lateral migration and channel development towards the west. The absence of aggradation suggests rapid downslope current migration (towards west). The inset box shows several generations of sediment waves developed above the sigmoidal reflections. In this seismic profile, a turbidite fan can be observed, deposited immediately above the LBS. Yellow circles on the turbidite fan signal the position of channels structures. Location of seismic profile in Figure 5.9.

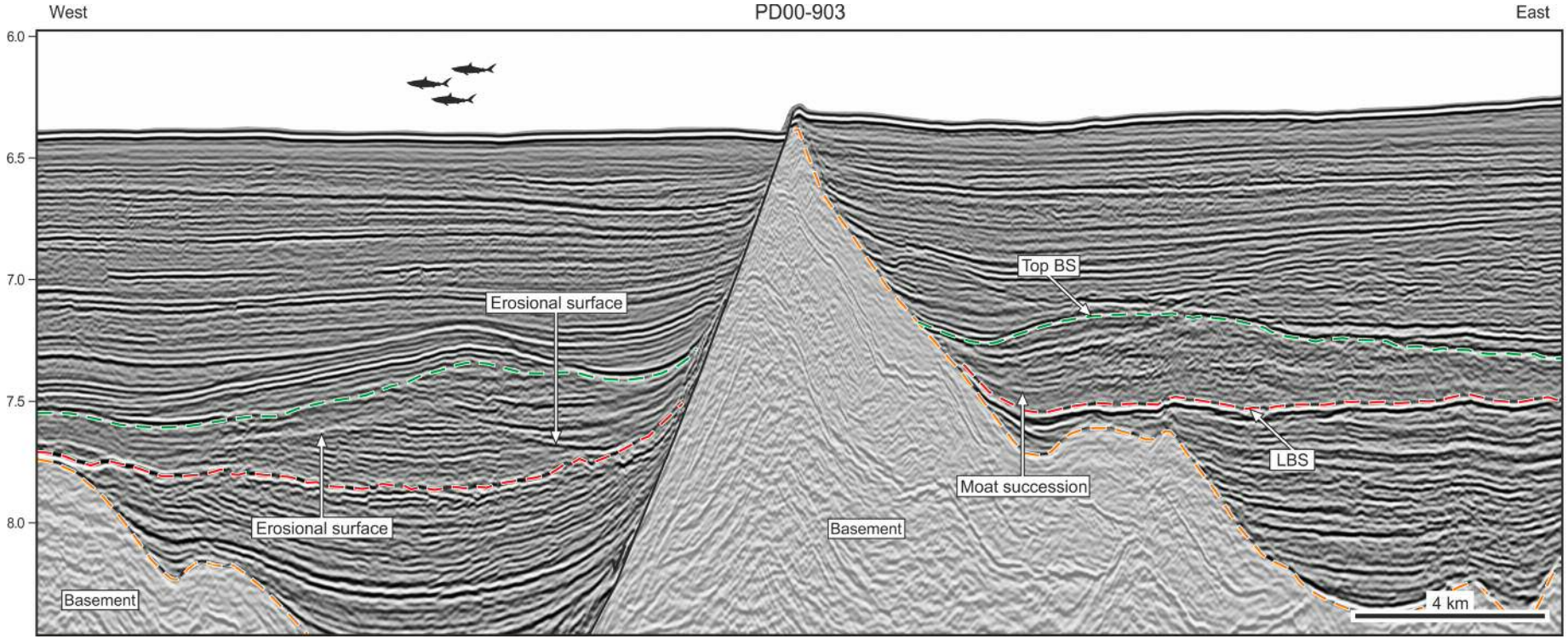


**Figure 5.12** Two elongated mounded and separated drifts along a common structural high. Two elongated mounded and separated drifts showing upslope migration onto the structural high where ODP site 901 was drilled. Separated by erosional surfaces, several depositional episodes can be observed, particularly on the west side drift. The drift on the east is not so well layered, but palaeo-moats are clearly observed. Location of seismic profile in Figure 5.9.

## 5.5. Discussion

### 5.5.1. MTDs and turbidites

MTDs are mainly observed in two regions of the outer proximal margin (Fig. 5.6). The northern MTD cluster was accumulated basinward of a known sediment input zone (see Chapter 4) where sediment bypassed the shelf and was transported directly into the outer proximal margin. This direct shelf to slope sediment delivery contributed to the accumulation of large quantities of sediment on the shelf edge and upper slope, creating unstable conditions in those areas. The consequent instability of this accumulation, coupled with the lowering of the wave base level due to the forced regression, allowed this area to become a MTD prone area (Catuneanu, 2006; Posamentier & Walker, 2006). The southern MTD cluster is located immediately north of the Aveiro Fault, where the thickest syn-rift units are found (Fig. 5.14A). Although the available dataset does not cover the continental shelf in this area, and no sediment progradation associated with the BS is observed on the upper slope, it can nonetheless be inferred that this was an important sediment input zone during the deposition of the BS. Some of the MTDs observed in the area can be attributed to halokinesis, especially those on the vicinity or on the flanks of diapirs.

Turbidite deposition within the BS seems to be more important during its early depositional stages, as suggested by the transparent reflections at the lower part of the BS. In fact, the lack of traction structures and bioturbation plus the important quantities of continental plant material present in Unit A, suggest a strong turbidite influx into the rift basin. Proof of that is the extensive turbidite fan deposited immediately above the LBS (Fig. 5.11), indicative of the importance of turbidite activity during the initial stages of the BS deposition. Nevertheless, during the BS deposition, this trend is inverted, with turbidites losing their depositional prevalence while contour currents become more frequent, possibly along with hemipelagic/pelagic deposition.

### 5.5.2. Significance of contourite drifts within the *breakup sequence*

Of special importance for the recognition of the BS is its characteristic seismic character. The seismic facies observed at DSDP Site 398, comprising transparent reflections at the base, grading to stronger, parallel reflections above (Fig. 5.3, see section 4.1), can also be interpreted on the outer proximal margin and in parts of the distal margin where the BS is well developed (*e.g.* Fig. 5.5B, C). This similarity in seismic facies, associated with its post-extensional architecture, denotes a common genetic process on the entire continental margin of Northwest Iberia immediately after lithospheric breakup.

A significant result in this work is that the units here defined as composing the BS match important events recorded by palaeontological changes in DSDP Site 398 cores, corresponding at the same time to specific velocity groups defined by Shipboard Scientific Party (1979) (Fig. 5.2). At the time of publication of Leg 47B results (Sibuet *et al.*, 1979) the surfaces corresponding to the boundaries between these velocity groups were not observed on seismic data given the lower resolution of the seismic data available at the time, nor correlated with palaeontological data. This work, using recently acquired data, identified those surfaces as higher rank surfaces (*sensu* Catuneanu *et al.*, 2009)—the LBS and the top of Unit C bounding the BS, and lower rank surfaces—the Intra-BS1 and Intra BS2 (Fig. 5.2 and 5.3).

The recognition of contourite drifts based solely on 2D seismic data is difficult without the aid of core data, or 3D seismic data (Rebesco & Camerlenghi, 2008). Nevertheless, in certain cases bottom current activity can produce a particular geometrical signature that is unmistakable even on 2D seismic data.

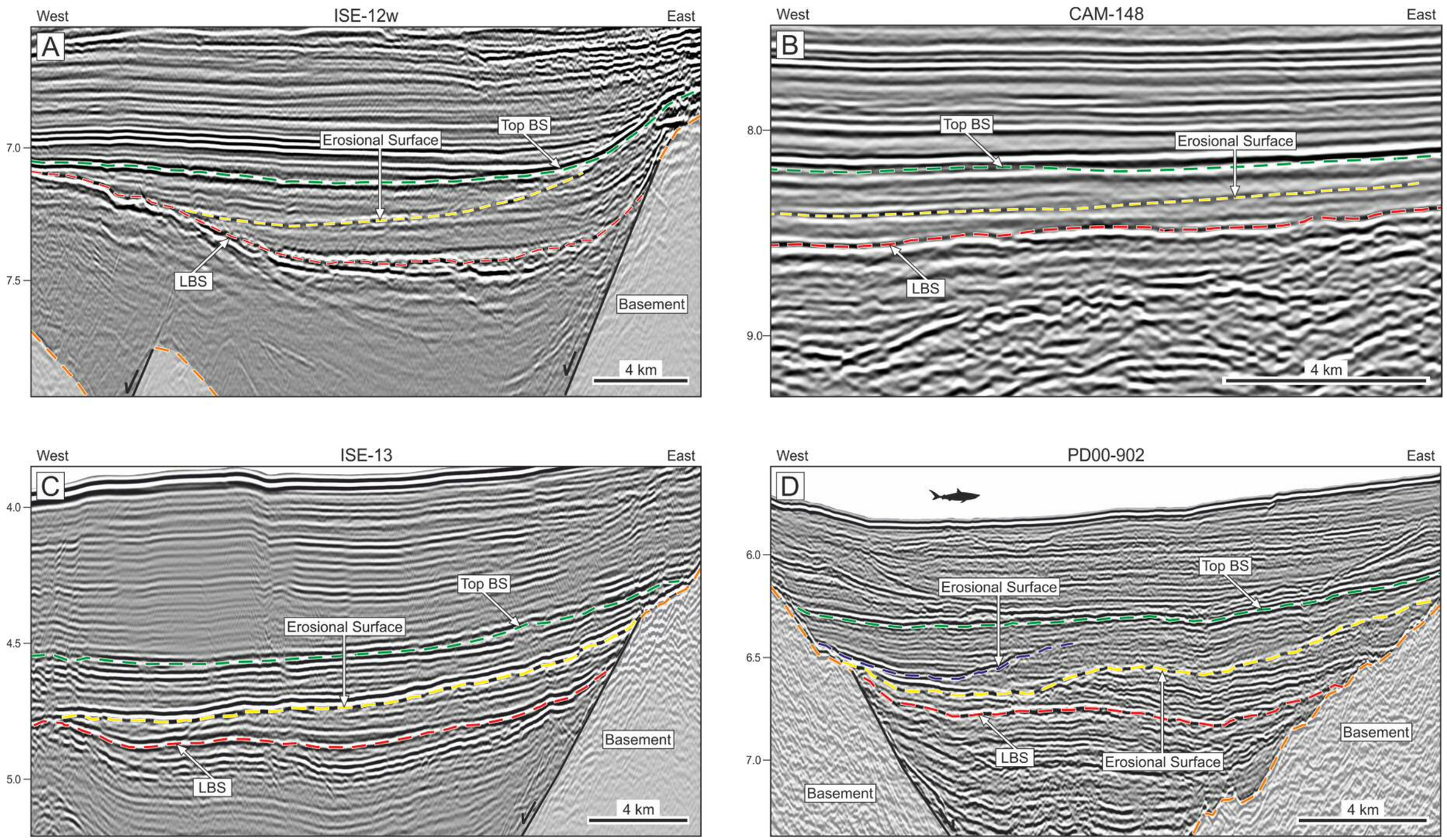


**Figure 5.13** Examples of large scale abraded surfaces identified within the BS. A to D—seismic sections with representative examples of erosional surfaces identified within the BS (yellow and purple dashed lines). Note the horizontal scale, these abraded surfaces extend for several kilometres. The vertical resolution of the seismic line in B (CAM survey) is smaller than on the other panels. Note the development of several erosional surfaces in panel D. Seismic profiles in two-way time (ms). Location of seismic profiles in Figure 5.9.

This is particularly true in deep-sea environments where depositional processes are limited to and controlled by the action of the continuous pelagic/hemipelagic rain, occasional distal turbidites and mass wasting deposits and bottom currents. From these three processes, bottom current activity is the one that has wider geographic influence, generating extensive deposits and erosional surfaces that can reach thousands of square kilometres in a single deposit (Rebesco & Camerlenghi, 2008). Some of these deposits have particular geometries which, when associated with a geographically extensive occurrence, are reliable indications of bottom current activity, even on 2D seismic data (Nielsen *et al.*, 2008).

The seismic data used in this work allowed the recognition of sedimentary bodies with an architecture typical of contourite drifts (Figs. 5.10, 5.11 and 5.12). The types of contourite drifts found within the BS reflect a marked control of palaeo-seafloor topography on their geometry and depositional architecture. At the time of lithospheric breakup, the underfilled (sediment starved) sub-basins within the outer and distal margins of West Iberia maintained a topography akin to the syn-rift stage (Shipboard Scientific Party, 1987b) (Fig. 5.14D). This topographic control restricted the geometry of the majority of the drifts to types typical of narrow seaways, which were essentially located in underfilled sub-basins inherited from the syn-rift stage (*e.g.* Figs. 5.10D and 5.13A, D).

**Figure 5.14** (next page) Maps interpolated from the seismic datasets interpretation.
A—Thickness map between the LBS and the surface defined as acoustic basement. It shows the thickness of the syn-rift package. B—Thickness map of the BS (the stratigraphic succession between top BS and the LBS). C—Thickness map between the sea bottom and the top BS. D—Surface map of the LBS, over which the BS was deposited. The black areas in the maps show the position of basement structural highs not covered by the sedimentary packages interpreted in this paper. Circles show borehole locations. Grey lines over the surfaces show the position of the seismic data used (for the position of individual seismic surveys see Figure 1). Depth and thickness are represented in two-way travel time (ms). For larger images of these panels and the other surfaces not figured in this chapter but computed in order to produce the thickness maps see Appendix.

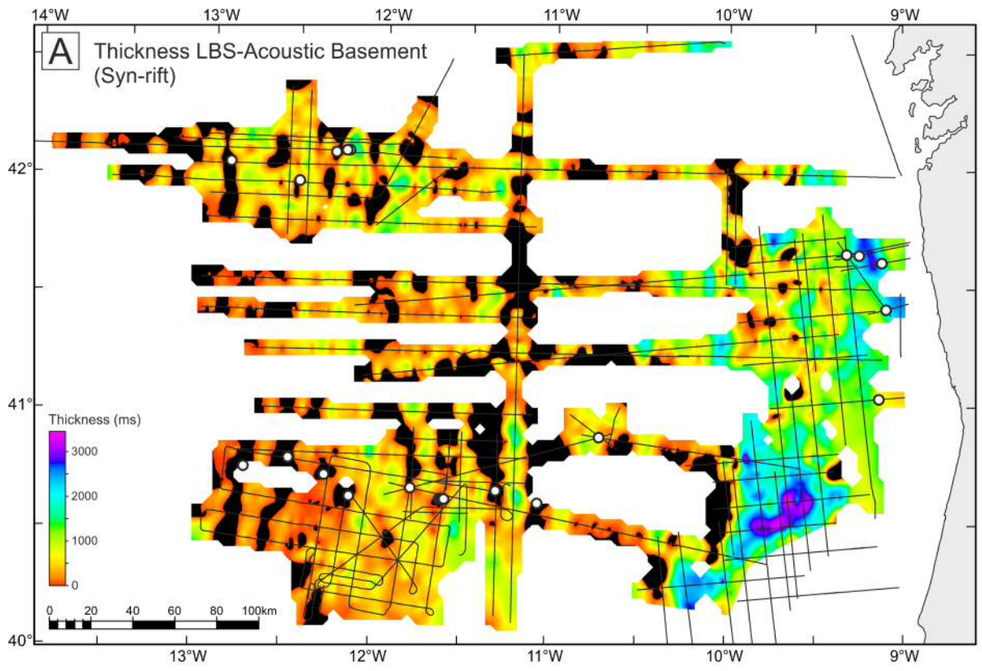
A
Thickness LBS-Acoustic Basement
(Syn-rift)
Thickness (ms)
3000
2000
1000
0
0 20 40 60 80 100km
14°W
13°W
12°W
11°W
10°W
9°W
42°
41°
40°

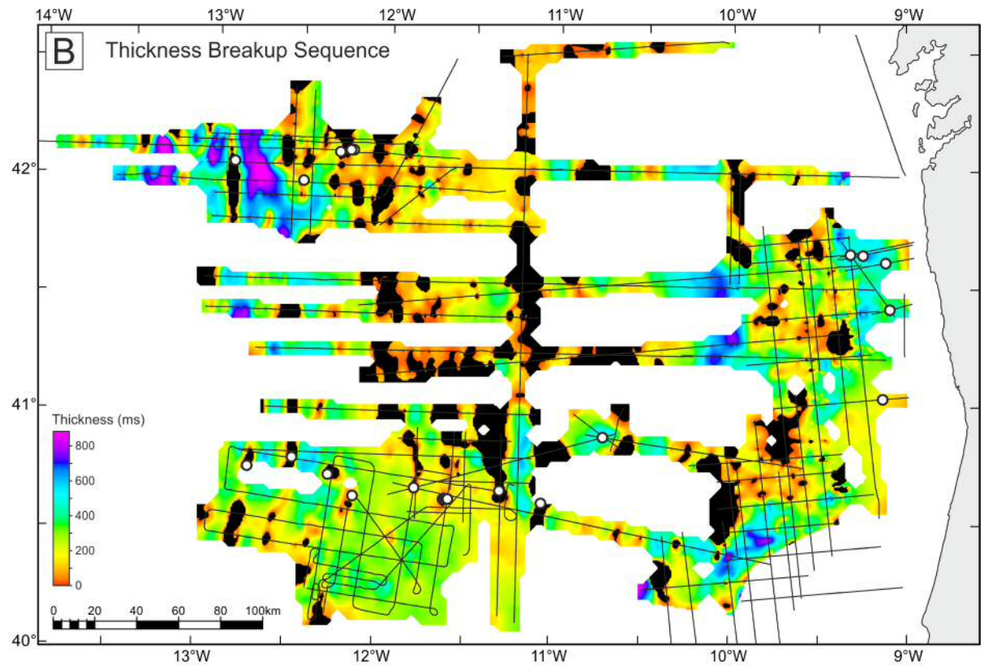
B
Thickness Breakup Sequence
Thickness (ms)
800
600
400
200
0
0 20 40 60 80 100km
14°W
13°W
12°W
11°W
10°W
9°W
42°
41°
40°

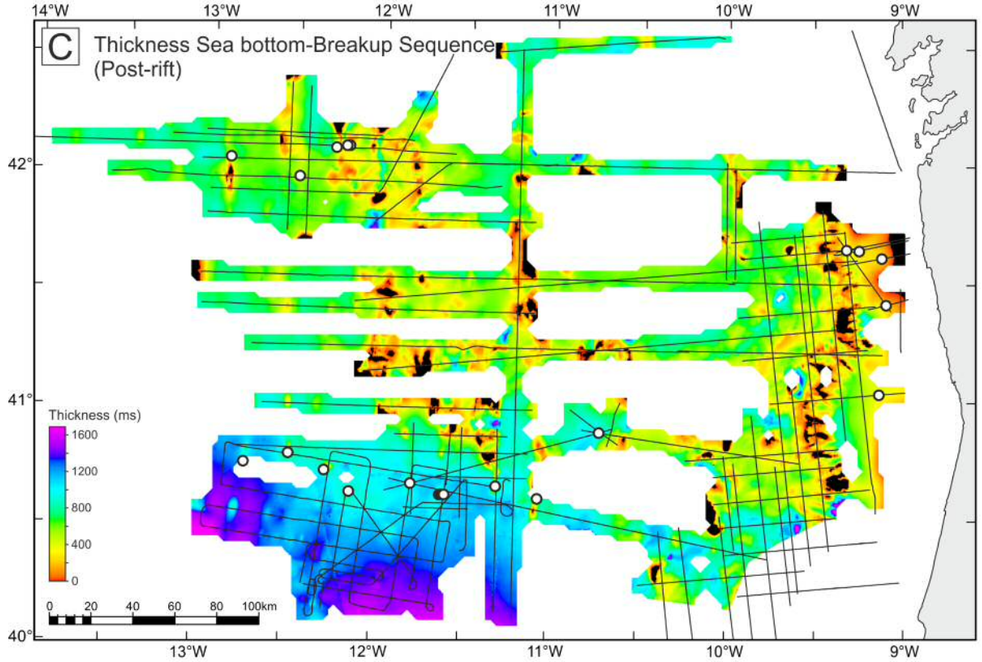
C
Thickness Sea bottom-Breakup Sequence
(Post-rift)
Thickness (ms)
1600
1200
800
400
0
0 20 40 60 80 100km
14°W
13°W
12°W
11°W
10°W
9°W
42°
41°
40°

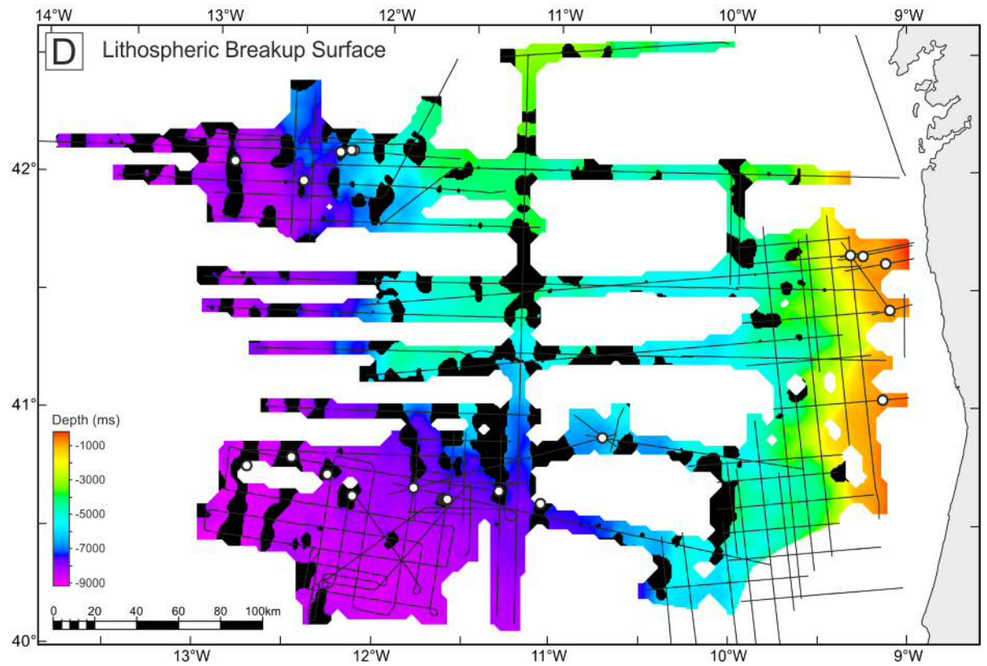
D
Lithospheric Breakup Surface
Depth (ms)
-1000
-3000
-5000
-7000
-9000
0 20 40 60 80 100km
14°W
13°W
12°W
11°W
10°W
9°W
42°
41°
40°

However, a contrasting setting can be interpreted in Figure 5.9, where the absence of contourite drifts is noted in the Southwestern part of the study area. At the time of lithospheric breakup, this area contained few topographic obstacles to bottom currents due to its subdued relief when compared with the rest of the study area (Fig. 5.9). This probably resulted in the deposition of sheeted drifts, which are difficult to identify using 2D seismic data. Nevertheless, several erosional surfaces with regional significance were identified in this area (Figs. 5.5D, 5.9 and 5.13B). Unequivocal contourite drifts displaying remarkable inclined reflections showing lateral current migration are observed above the BS in this area (Wilson *et al.*, 1996) (observed in Fig. 5.15, on the northeast side of the contourite above the BS). Once the inclined reflections of these contourite drifts become flat, their acoustic facies is very similar to that found within the BS across most of the distal part of the study area (Fig. 5.15).

In Northwest Iberia, the development of regionally extensive erosional surfaces within the BS is better explained by bottom current activity, as turbidites do not possess enough erosive power in more distal parts of the margin to generate the prominent erosional surfaces observed in Figures 5.5D and 5.13, and are somewhat limited to geographically less extensive areas (Faugères *et al.*, 1999). These widespread erosional surfaces, occurring in deep-sea successions, reflect episodes of increased bottom current flow strength with consequent removal of material from the seafloor (Hernández-Molina *et al.*, 2008).

The observation on seismic data of the intra-BS erosional surfaces is conditioned by several factors, both intrinsic and extrinsic to the BS itself. Intrinsic to the BS are (1) the extent of erosion created, (2) the angle that the erosional surface makes with the previously deposited sediments, (3) the angle that the subsequent sediments make with the erosive surface and the truncated sediments and (4) the lithological contrast between the sediments below and above the erosive surface. Extrinsic factors are related with (1) the resolution and processing of the available seismic data and (2) the angle that the seismic profiles make with the BS sedimentary body (Fig. 5.3).

The same type of conditioning factors can be accounted for the observation of these surfaces in cores: intrinsic to the cored material are (1) the type of stratigraphic contact of the erosional surfaces [a paraconformity (*sensu* Bates & Jackson, 1987) is difficult to be recognized in cores], (2) the presence or not of biostratigraphical indicators with enough resolution that permit the pinpoint of short (with a duration of few thousands of years or less) gaps in deposition due to erosion, (2) the superimposition or not of a different lithology or a coarser sediment enriched layer over an erosional surface. Extrinsic to the cores are (1) continuous core recovery (discontinuities are preferential zones for core disruption and consequent loss of material during the core recovery process) and (2) the (fortuitous) penetration of a zone where the surfaces themselves are present and are observable as angular disconformities.

Sedimentological data from DSDP Site 398D show several characteristics that can be attributed to bottom current activity during the BS deposition. The BS displays increasing amount of bioturbation towards its top, particularly after the Intra BS-1 surface (i.e. in Units B and C, Fig. 5.2). A similar increase in traction structures upwards in the succession is observed in the form of wavy and parallel lamination, especially where silty and sandier beds were deposited. Coarser beds, which can display reverse grading, occur at the base of Unit C. Towards its top, the BS is marked by thin, fining-upwards radiolarian sands, thin mudchip sandstone layers, fining-upwards quartzose sandstone and siltstone laminae displaying cross-bedding and erosional basal contacts (Shipboard Scientific Party, 1979).

---

**Figure 5.15** (next page) Seismic facies comparison between an unequivocal contourite drift and the BS. A Middle Eocene to Early Miocene sheeted drift in Iberia Abyssal Plain where it loses its inclined reflector character due to lateral current migration, acquire an acoustic facies remarkably similar to that commonly found within the BS along the distal margin. A—sheeted drift delimited by the blue dashed lines. Note that the inclined reflections become horizontal eastwards. B—detail of the BS in CAM-159. C—detail of the sheeted drift in CAM-159. D—detail of the BS in ISE-05 from Figure 5.5C. E—detail of the BS in CAM-149 from Figure 5.5D. Note the similarity of contourite drift acoustic facies between panels B, C D and E. Location of seismic profiles in Figure 5.1.

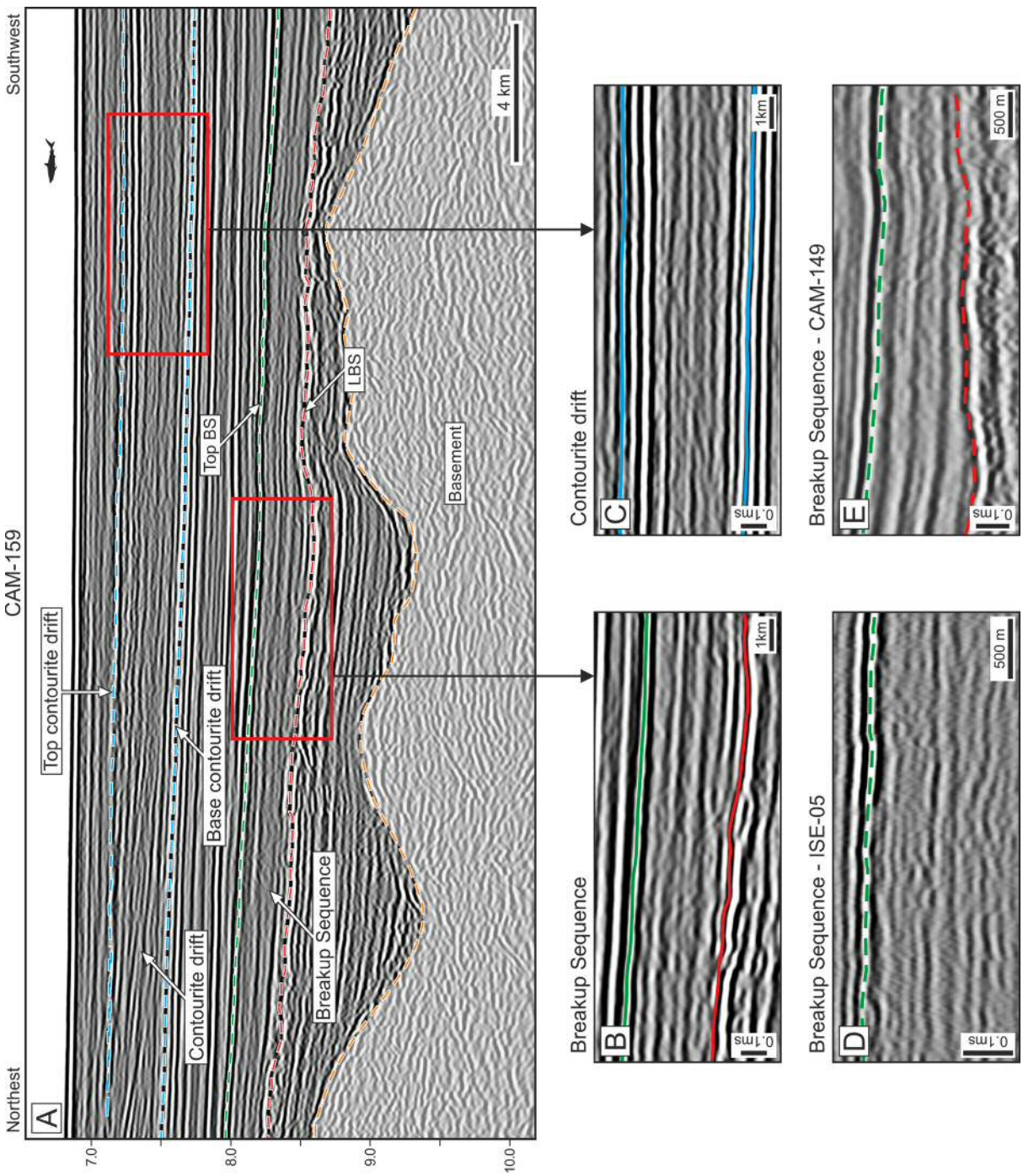
Southwest
Northest
CAM-159
A
Top contourite drift
Base contourite drift
Contourite drift
Breakup Sequence
Top BS
LBS
Basement
4 km
7.0
8.0
9.0
10.0
Contourite drift
C
1km
0.1ms
Breakup Sequence
B
1km
0.1ms
Breakup Sequence - CAM-149
E
500 m
0.1ms
Breakup Sequence - ISE-05
D
500 m
0.1ms

At the BS, the scarcity of sedimentary structures in interpreted contourite drifts is in agreement with the presence of muddy contourites, which are less likely to be preserved than in coarser grained contourites and predominance of bioturbation is expected (Martín-Chivelet *et al.*, 2008; Faugères & Mulder, 2011).

In terms of bioturbation, *Chondrites*, *Zoophycos* and other unidentified ichnofossils are relatively frequent towards the top on Unit B, increasing further in frequency within Unit C. This character is interpreted to reflect an increase in oxygenation from the base to the top of the BS, which is also suggested by the decrease in preserved organic matter (Shipboard Scientific Party, 1979) (Fig. 5.2). This change is interpreted as related to the presence of bottom currents in Northwest Iberia, replenishing oxygen levels and allowing benthonic organisms to thrive (Stow & Piper, 1984).

Although some of the cored sedimentary structures can also be associated with turbidite deposits, the degree of erosion and extension of erosional surfaces observed on seismic data indicates the action of deep currents activity, rather than then more localised turbidity flows sourced from proximal areas of the margin (Faugères *et al.*, 1999).

Published data from DSDP Site 398 points out that deep oceanic circulation in this area started after the Cenomanian (Chamley *et al.*, 1979; Graciansky & Chenet, 1979; Groupe Galice, 1979; Maldonado, 1979; Shipboard Scientific Party, 1979). Yet, some authors briefly mention the presence of bottom currents during the Albian–Cenomanian interval (Arthur, 1979; Graciansky & Chenet, 1979; Groupe Galice, 1979; Réhault & Mauffret, 1979).

Even though the presence of unequivocal bottom current indicators within the BS is limited to some areas, the data in this paper shows a degree of current activity concomitant with widespread contourite drift deposition, at least during part of the BS deposition.

Regarding the syn-rift package, Sibuet *et al.* (1979) made two brief mentions to bottom currents activity during the Hauterivian (Arthur, 1979; Shipboard Scientific Party, 1979). Nevertheless, no signs of bottom current activity were found on seismic data. This absence can be related with the resolution of the available seismic data in

combination with the fact that in the study area during syn-rift deposition bottom currents were rare/slow. It should also be noted that the observation of bottom current activity below the LBS can be conditioned by the active syn-rift tectonism present in the area, which being prone for turbidite generation, can mask eventual bottom currents activity (Mulder *et al.*, 2008).

### 5.5.3. Lithospheric breakup as a trigger for deep current intensification

The relationship between tectonics and major oceanographic events, such as the onset of bottom currents, is well known (Frank & Arthur, 1999; Poulsen *et al.*, 2003; Meijer *et al.*, 2004; Maldonado *et al.*, 2006; Hernández-Molina *et al.*, 2008; Knies *et al.*, 2014). As lithospheric breakup evolves in Northwest Iberia, the lithospheric rebound expected to occur in association with this event was able to generate vertical tectonic movements large enough to promote subsidence in deep-offshore depocenters (Braun & Beaumont, 1989; Cloetingh *et al.*, 1989; Kooi & Cloetingh, 1992; van Balen *et al.*, 1998) (Fig. 5.16A). This lithospheric subsidence, altering the pressure gradient of the water masses around the ruptured lithospheric segment could potentially trigger the installation of a more permanent and stronger geostrophic current regime, in contrast with the previous sluggish bottom waters present on the Central Atlantic and its intermittent, presumably rare bottom currents (Tucholke & McCoy, 1986; Robinson *et al.*, 2010) (Fig. 5.16B).

---

**Figure 5.16** (next page) Schematic depiction of the evolution of the BS deposition in Northwest Iberia. A—Shows the movements originated by lithospheric breakup with uplift of the rift shoulder and subsidence of deep-offshore basins. The seafloor between structural highs becomes the LBS (horizon in red in B and C). B—Shows the instalment of shelf edge deltas due to the forced regression caused by the rift shoulder uplift, shelfal by-pass of sediment and the initiation of bottom current activity during the deposition of Unit A. Nonetheless, this same unit seems to be dominated by turbidites due to weak/incipient bottom currents, or due to large amounts of turbidite deposition masking the evidences of bottom currents activity. C—Shows the full establishment of bottom currents towards the top of the BS with the deposition of extensive contourite drifts and the end of predominant turbidite deposition. Along the upper continental slope, mass-transport deposits occur due to slope instability promoted by sediment accumulation on the shelf edge/continental slope, with mass-transport deposits becoming included in the BS (see text for more details). LBS—lithospheric breakup surface; BS—breakup sequence.

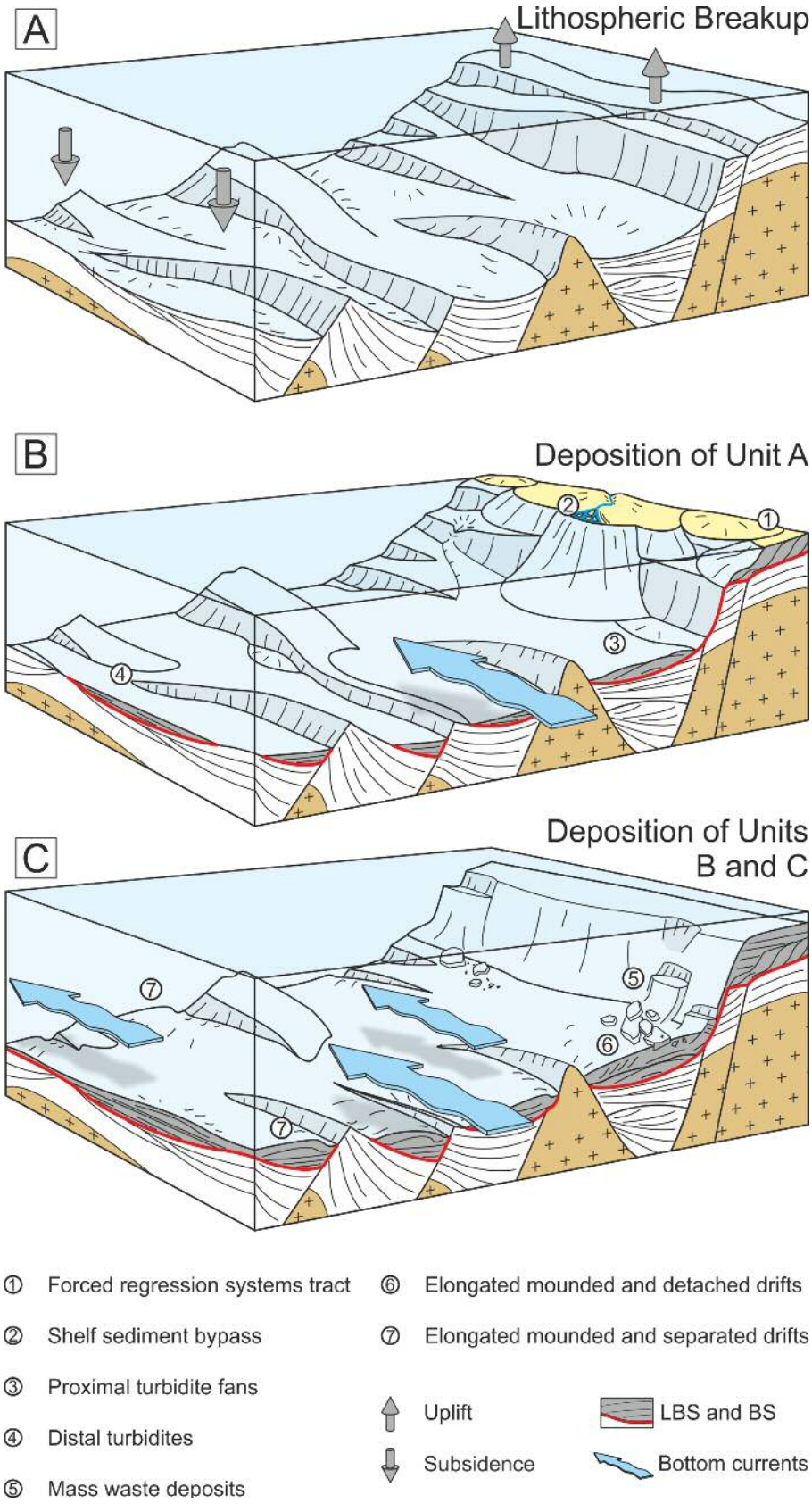
A
Lithospheric Breakup
B
Deposition of Unit A
C
Deposition of Units B and C
① Forced regression systems tract
② Shelf sediment bypass
③ Proximal turbidite fans
④ Distal turbidites
⑤ Mass waste deposits
⑥ Elongated mounded and detached drifts
⑦ Elongated mounded and separated drifts
Uplift
Subsidence
LBS and BS
Bottom currents

Landward, the lithospheric vertical movements promoted widespread rift-shoulder uplift recorded as a widespread forced regression on the proximal margin (Tucholke *et al.*, 2007a, see as well Chapter 4; Soares *et al.*, 2012; Grobe *et al.*, 2014) (Fig. 5.16A). This had as consequence the erosion of important volumes of sediment, which bypassing the continental margin, were delivered directly onto the continental slope (Fig. 5.16B). This suggests that this period of important sediment influx, transported to deep-offshore depocenters by turbidity currents, to have masked ongoing bottom current activity during the early stages of the lithospheric breakup (Fig. 5.16B).

Later in the BS, with the shutdown of the continental shelf sediment bypass (see Chapter 4), the amount of turbidite deposition was reduced, reducing the input of terrestrially derived organic matter to deep-offshore basins, and allowing bottom current activity to develop the stratigraphic architecture characteristic of drift deposits, without the 'masking effects' of mixed turbidite-contourite deposits (Fig. 5.16C). In fact, this gradual transition explains the absence of more pronounced lower boundaries on the majority of the observed contourite drifts (*e.g.* Fig. 5.12) and the vertical change in seismic facies commonly observed in the BS, from a transparent, less structured lower part to sub-parallel reflections in sediment drifts accumulated to the top of the BS (*e.g.* Figs. 5.3C, 5.5C).

Another plausible reason for this vertical change in seismic facies is, as proposed by Stow *et al.* (2002), an increase in bottom current velocity. In fact, an increase on the velocity of these bottom currents can be inferred towards the upper part of the BS (*e.g.* more frequent erosional surfaces and traction structures at DSDP Site 398), which cannot be merely related with declining turbiditic activity. It should also be noted that the top of the BS is marked by a regional unconformity resulting from erosion exerted by strong bottom currents (Shipboard Scientific Party, 1979). Most likely both hypotheses had a part on the formation of the BS in Northwest Iberia.

### 5.5.4. Origin of deep-water currents

Thermohaline currents, the main driver of ocean circulation, occur due to differences in density between water masses, promoted by variations in temperature and/or salinity (Shanmugam, 2008). In contrast with modern thermohaline ocean circulation, which is driven by the strong temperature gradient between the poles and the equator, during the Cretaceous more homogeneous and higher global temperatures meant that ocean circulation was mainly driven by differences in salinity in a 'Greenhouse World' (Brass *et al.*, 1982; Roth, 1986; Hay, 2008).

At the time of lithospheric breakup in Northwest Iberia, water depth between the Iberian margin and its conjugate in Newfoundland was already significant. Where sediments contemporaneous to the lithospheric breakup event were drilled, inferred water depths were in the order of >2000 m for DSDP Site 398 (Sibuet & Ryan, 1979) and near or below the carbonate compensation depth (CCD) at ODP Sites 641, 1070 and 1276 (Moullade & Boillot, 1988; Shipboard Scientific Party, 1998, 2004b) (Fig. 5.1). At that time, the CCD was located between water depths of 2500 m and 3000 m (Tucholke & Vogt, 1979).

Limited by shallow gateways from the surrounding oceanic basins, palaeogeographic reconstructions show that at the time of lithospheric breakup between West Iberia and Newfoundland the Central Atlantic formed an isolated oceanic basin in terms of deep-water circulation (Tucholke & McCoy, 1986; Summerhayes, 1987; Ziegler, 1988; Handoh *et al.*, 1999).

The origin of mobile water masses in the study area can be suggested as coming from three sources: 1) from the epeiric seas that covered West Europe to the north of the Iberian plate; 2) from the SE Central Atlantic, and 3) from the Tethys via the Proto-Gibraltar Strait (Fig. 5.17). For the reasons explained below, hypotheses 3 tend to be the favoured one.

Deep-water circulation between the Central Atlantic and the northern Boreal regions occurred only through an epicontinental sea developed across Northwest Europe, and via incipient rift basins developed between Europe and East Greenland

(Doré, 1992; Doré *et al.*, 1999) (Fig. 5.17). These waters probably did not contribute significantly to the presence of bottom currents in the Central Atlantic Ocean, as the higher rainfall recorded in Northwest Europe meant that northern water masses had low salinity surface waters (Roth, 1986). Although contourite drifts were described in the Danish Basin (Surlyk & Lykke-Andersen, 2007), these occur in post Cenomanian sediments and are due to currents flowing north-westwards from the Tethys. Nevertheless, several authors advocate the NW European area as a source for deep-water currents in the Upper Cretaceous Central Atlantic (Voigt *et al.*, 2004; Voigt *et al.*, 2013).

During the Early–Middle Albian, final lithospheric breakup between Africa and Brazil promoted the opening of the Central Atlantic Gateway (Eagles, 2007; Moulin *et al.*, 2010). However, it was not until after the Cenomanian–Turonian that a deep water gateway was established (Tucholke & Vogt, 1979). In the Middle Albian, mixtures of Tethyan and South Atlantic faunas in this area denote active southwards shallow currents coming from the Tethys (Moullade & Guérin, 1982; Azevedo, 2004). On the Atlantic Moroccan margin, Dunlap *et al.* (2013) report Late Aptian–Early Albian and Late Albian–Cenomanian sediment waves derived from northward flowing bottom currents. Data from DSDP sites 415 and 416 suggest that these sediment waves were formed at a water depth between 2000 to 3000 m (Vincent *et al.*, 1979).

At the time of lithospheric breakup in Northwest Iberia, the connection between the Central Atlantic and the Tethys in the Pyrenean region was closing due to the opening of the Bay of Biscay, reducing the depth of what was in the past a deep oceanic gateway (Sibuet *et al.*, 2004; Vissers & Meijer, 2012). Probably the deepest connection between the Central Atlantic and external water masses was, at this time, in the western part of the Tethys through the Iberia–Africa passage (Thurow & Kuhnt, 1986; Ziegler, 1988) (Fig. 5.17).

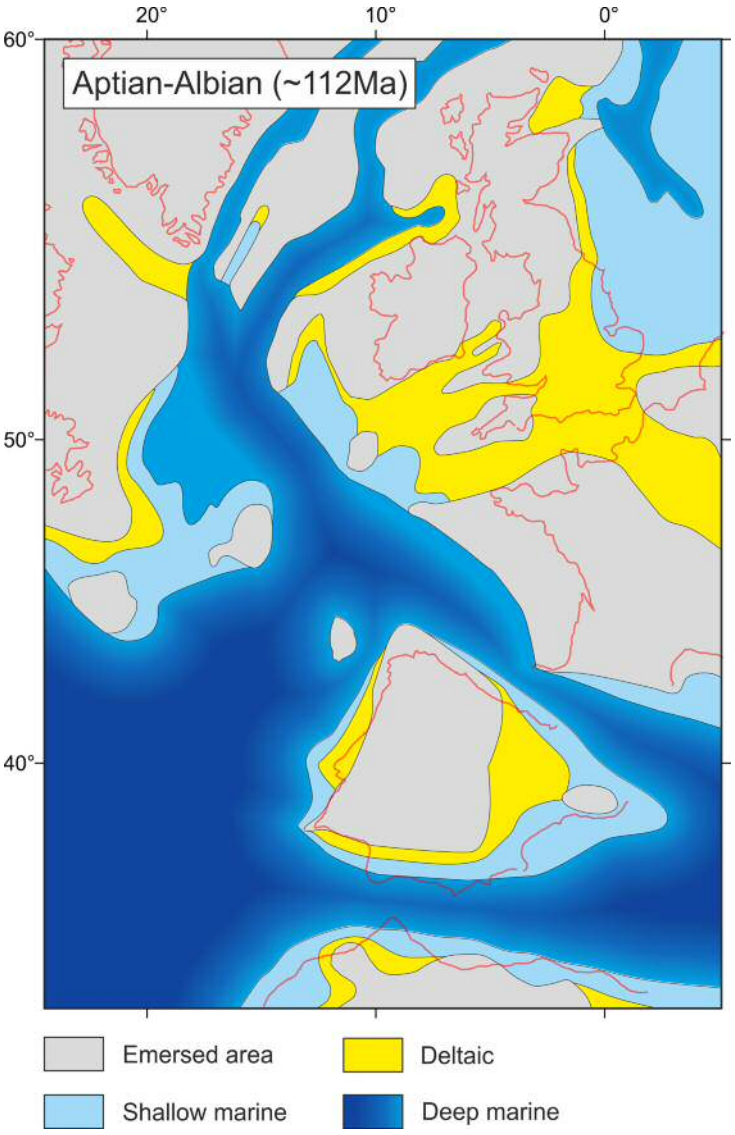


**Figure 5.17** Aptian–Albian palaeogeography at the time of lithospheric breakup and BS deposition. Simplified palaeogeographic reconstruction of the Central–North Atlantic at the Aptian–Albian transition (112 Ma). In red are present-day coastlines. Based on Hay *et al.* (1999), Sibuet et al (2007), Vissers & Meijer (2012), Ziegler (1988).

The presence of evaporitic basins in north Africa epeiric seas at this time (Parrish *et al.*, 1982), and the westward surface currents entering the Central Atlantic via the Gibraltar passage (Roth, 1986; Stille *et al.*, 1996) suggest that the Tethys was a source for highly saline bottom water masses, similarly to today's Mediterranean Outflow Water, flowing northwards due to the effect of the Coriolis force (García *et al.*, 2009b).

As in Northwest Iberia, such an important oceanographic event should have left a significant sedimentary record observable along the current paths. As inter-basin homogenization due to the instalment of a widespread bottom current regime is expected to occur in the study area [see Maldonado *et al.* (2006) for the Scotia and Weddell Seas], contourite drift units and related bounding surfaces should be correlatable across different basins in West Iberia. Therefore, the presence of similar age contourite drifts, both south and north of the study area, should be expected. Despite the evidence of bottom current activity found on the Moroccan margin, their (at least vertical) weak expression do not seem to be compatible with the source of the bottom currents that motivated the widespread and diverse character of the contourite drifts observed in Northwest Iberia. Given this, it seems to us more plausible to consider the Tethys as the source of the bottom currents described in this paper.

On the Newfoundland conjugate margin, using the SCREECH seismic dataset (Shipley *et al.*, 2005), no contourite drifts where found within the BS. This can be due to three main reasons: (1) the Coriolis effect would have deflected the bottom currents towards the eastern margin of the conjugate pair, (2) one of the source areas for deep currents (source 3) was too far from the Newfoundland margin, and (3) the coverage of the SCREECH dataset is not as extensive as the data that was available on the Iberian margin. This drift absence on Newfoundland reinforces the idea of a deep water current origin as coming from the Tethys or the SE Central Atlantic.

## 5.6. Conclusions

In Northwest Iberia, the role played by bottom currents after the lithospheric breakup event is more important than previously thought. Seismic data interpreted in this work reveal the presence of developed contourite drifts within the BS, and confirms the presence of strong deep-water currents at the time of deposition of this sequence (Figs. 5.9 to 5.13). The distribution and morphology of contourite drifts was controlled by the inherited syn-rift topography with an observed prevalence of

elongated mounded drifts on the outer proximal margin and (inferred) sheeted drifts in the distal margin where it was topographically smoother.

In Northwest Iberia, the main results can be summarised as follows:

1) Seismic data reveal the presence of three main seismic facies within the BS, which can be associated with the deposition of (1) black shales and distal turbidites, (2) mass-transport deposits and proximal turbidites, and (3) contourite drifts.

2) Distally, thick mass-transport deposits change laterally into black-shales and distal turbidites, which show widespread evidence of deep-water current activity towards the top of the BS.

3) Deep-water current activity is expressed by intra-BS erosional surfaces and characteristic contourite drifts.

Our interpretation brings forward a new depositional model for strata in the BS, previously interpreted as reflecting pelagic and hemipelagic deposition with occasional turbidite flows. This new model takes into account the tectonic and sedimentological changes induced by the lithospheric breakup, explaining in a comprehensive way variations in seismic facies observed within the BS itself.

The main result from this interpretation is that the presence of contourite drifts probably can act as a reliable marker for the establishment of complete breakup between two continental margins.

The results in this chapter are therefore key to demonstrate that after the Aptian–Albian lithospheric breakup the presence of contourite drifts is a ubiquitous feature in Northwest Iberia. The widespread bottom current activity recorded during the deposition of the BS suggests that important changes in terms of oceanic circulation occurred after the lithospheric breakup event.

The recognition of contourite drifts within the BS in Northwest Iberia is postulated as representing the onset of important deep-water circulation between two rifted continents (contrasting with the previous slow/rare bottom current regime), marking

the establishment of fully separate continental margins. In addition, is suggested that important changes in the climatic and oceanic conditions of the North Atlantic occurred in association with established lithospheric breakup between Northwest Iberia and Newfoundland, and that the record of such changes is preserved in the contourite drifts interpreted in this work.

Chapter Six

# REVIEW OF THE TECTONO-STRATIGRAPHIC CHARACTER OF LITHOSPHERIC BREAKUP AT SOUTH AUSTRALIA–EAST ANTARCTICA

## 6.1. Abstract

In this Chapter, the South Australia-East Antarctica conjugate margins are studied in order to assess the validity of results from Chapters 4 and 5 on a different pair of conjugate margins. Given the variability found among different large-scale geological settings, some degree of variation was expected on different continental margins. Therefore, for a first tentative extrapolation of the Iberia-Newfoundland findings, the choice of a study ground with somewhat similar characteristics of the initial study area was very important. Similarly to West Iberia-Newfoundland, the South Australia-East Antarctica conjugate margins underwent magma-poor rifting with upper mantle exhumation occurring before lithospheric breakup. Similarly to West Iberia and Newfoundland, lithospheric breakup was diachronous across the different lithospheric segments which compose South Australia and East Antarctica margins. Several regional 2D seismic surveys from East Antarctica were used along with data from IODP Leg 318 to unveil the stratigraphic syn- to post-rift transition history of these margins. Comparison of east Antarctica data was made with published data from South Australia, resulting in novel interpretations in both margins. Two recognizable LBSs were found in the East Antarctic margin. The oldest LBS (of probable Early Campanian age), appears eroded and is limited in its geographical expression due to the action of bottom currents which deposited extensive contourite drifts above it. The youngest LBS (a regionally important horizon, recognizable in all East Antarctic margin) was found to be formed around the Maastrichtian-Palaeocene transition, with a calculated age of ~65.2 Ma using data from IODP Site 1356. Its age and characteristics led to the interpretation of this surface being the LBS corresponding to lithospheric breakup at the west Otway Basin, in a zone where is observed the cessation of orthogonal/oblique rifting and the transition to transtension along a transform margin, located between two important fracture zones, the Spencer Fracture Zone and the Tasman Fracture Zone. This thesis thus postulates that lithospheric breakup in this area led to a major plate rearrangement, originating the LBS and the onset of important bottom current activity, with the deposition of a regionally extensive contourite drift field along the East Antarctic

margin. Although a BS with a well defined upper boundary was not found, the occurrence of prograding reflectors downlapping the LBS (in South Australia), MTDs and widespread contourite drifts denotes strong similarity with the BS in West Iberia. Of particular importance is the regionally extensive contourite drifts deposited above the Maastrichtian-Palaeocene LBS. This bottom current activity should have eroded or deterred the deposition of a seismically resolvable upper boundary in the BS. The same argument is used to explain the partially eroded Early Campanian LBS and respective BS absent upper boundary offshore East Antarctica.

## 6.2. Introduction

The results in Chapters 4 and 5 concerning NW Iberia and Newfoundland raise questions on how unique are they to these two margins. Does the lithospheric breakup surface (LBS) show the same variability elsewhere on divergent margins, from shallow to deep offshore environments? Can the breakup sequence be identified on other margins using the same criteria used in West Iberia and Newfoundland? If so, does the breakup sequence share the same stacking patterns recognised in Chapters 4 and 5? Is the presence of a proximal forced-regressive sequence, together with the widespread occurrence of contourite drifts, a common feature observed above the LBS on all continental margins? Concerning the deposition of black shales, can the same depositional trends be observed elsewhere in the world? These questions are important as the application of the *lithospheric breakup surface* and the *breakup sequence* concepts on other passive margins than the NW Iberia–Newfoundland conjugate depends on how easily one can identify them on seismic and borehole data. Knowing this latter caveat, the South Australia–East Antarctica margin is analysed in detail in this Chapter in order to verify the applicability of the results presented in Chapters 4 and 5.

Differences in the initial thermal, structural and regional settings of the lithosphere were shown, in the previous chapters, to influence how rifting develops on different divergent margins. In fact, variations in rifting mode and breakup (*e.g.* continental

crust breakup and lithospheric breakup) account for the bulk of sedimentological and stratigraphic changes experienced by each conjugate pair of margins (and for each margin of the same pair) across the lithospheric breakup surface (see Chapter 4). Given this variability, one should not expect the model presented in Chapters 4 and 5 to be applicable to other divergent margins without certain methodological changes, reflecting the unique particularities of each study area. In order to test the robustness of the model presented in the previous chapters, choosing a conjugate pair similar to the NW Iberia–Newfoundland margins was an important step to carry out this kind of analysis.

The Australia–Antarctica conjugate margins present many similarities with NW Iberia–Newfoundland. For example, both endured a long and complex rifting history in which are included several diachronous rifting episodes along distinct lithospheric segments. Both are magma poor rifted margins and, crucially, underwent upper-mantle exhumation followed by lithospheric breakup (*e.g.* Whittaker *et al.*, 2008; Tucholke & Whitmarsh, 2012; White *et al.*, 2013). Another important similarity is that the two conjugate pairs of margins constitute at present, and constituted in the past, important ocean gateways allowing communication between distinct water masses.

This chapter uses a comprehensive regional 2D seismic dataset covering the East Antarctic margin, where the syn- to post-rift transition is investigated in detail and compared with the Australian conjugate margin. For South Australia, the dataset utilised derives from high quality seismic data from published works.

Using well data from IODP Leg 318 Site 1356 drilled in East Antarctica an important regional onlap surface, previously regarded as Middle Eocene to Early Oligocene by comparison with the Australian margin, was dated in this Chapter as being Maastrichtian-Palaeocene. This date has important implications for both conjugate margins, and allows for a complete re-evaluation of the significance of this surface. This surface is, in fact, a LBS with margin wide expression, not confined to the local lithospheric segment but observed along East Antarctica. This Chapter postulates this LBS to be the product of the lithospheric breakup event marking the

end of orthogonal/oblique rifting (recorded along the Bight and NW Otway Basin) and the transition to transtension along a transform margin (west of Sorrel Basin).

As in West Iberia, the East Antarctica dataset allowed the recognition of previously non-documented bottom current activity starting shortly after lithospheric breakup events. In fact, despite the several lithospheric breakup events, the recognition of LBSs was difficult on sediments deposited prior to the Maastrichtian-Palaeocene lithospheric breakup event. A tentatively identified LBS is, in the interpreted dataset, partially to completely eroded by bottom currents showing that these can completely obliterate the LBS. Furthermore, persistent bottom current activity can inhibit (or erase) the formation of the top of the BS, rendering its presence unrecognizable on the post-rift package.

## 6.3. Datasets and methodology

On the Australian side, a great deal of published work was conducted by Geoscience Australia and its predecessor organizations (references below), focusing on the sedimentological, tectonic and geodynamic aspects of the Southern Rift System with the main purpose of understanding the evolution of hydrocarbon systems.

On the Antarctic side, the existing body of work has a more diversified authorship. Nevertheless, Geoscience Australia carried out important studies on this margin and acquired several seismic surveys, some of them used in the present study.

Covering the inner proximal, outer proximal and distal margins, several publicly available 2D seismic surveys from East Antarctica were used in this chapter (GA227, GA228 and GA229; see Figure 6.1). The seismic data from the Antarctic margin available for this study is unmigrated, which causes difficulties to its interpretation. Given this, as an aid to find a more correct positioning of this surface, I had to partially follow the work of Stagg *et al.* (2005) where the same survey is used, but time migrated (see Figure 2.3).

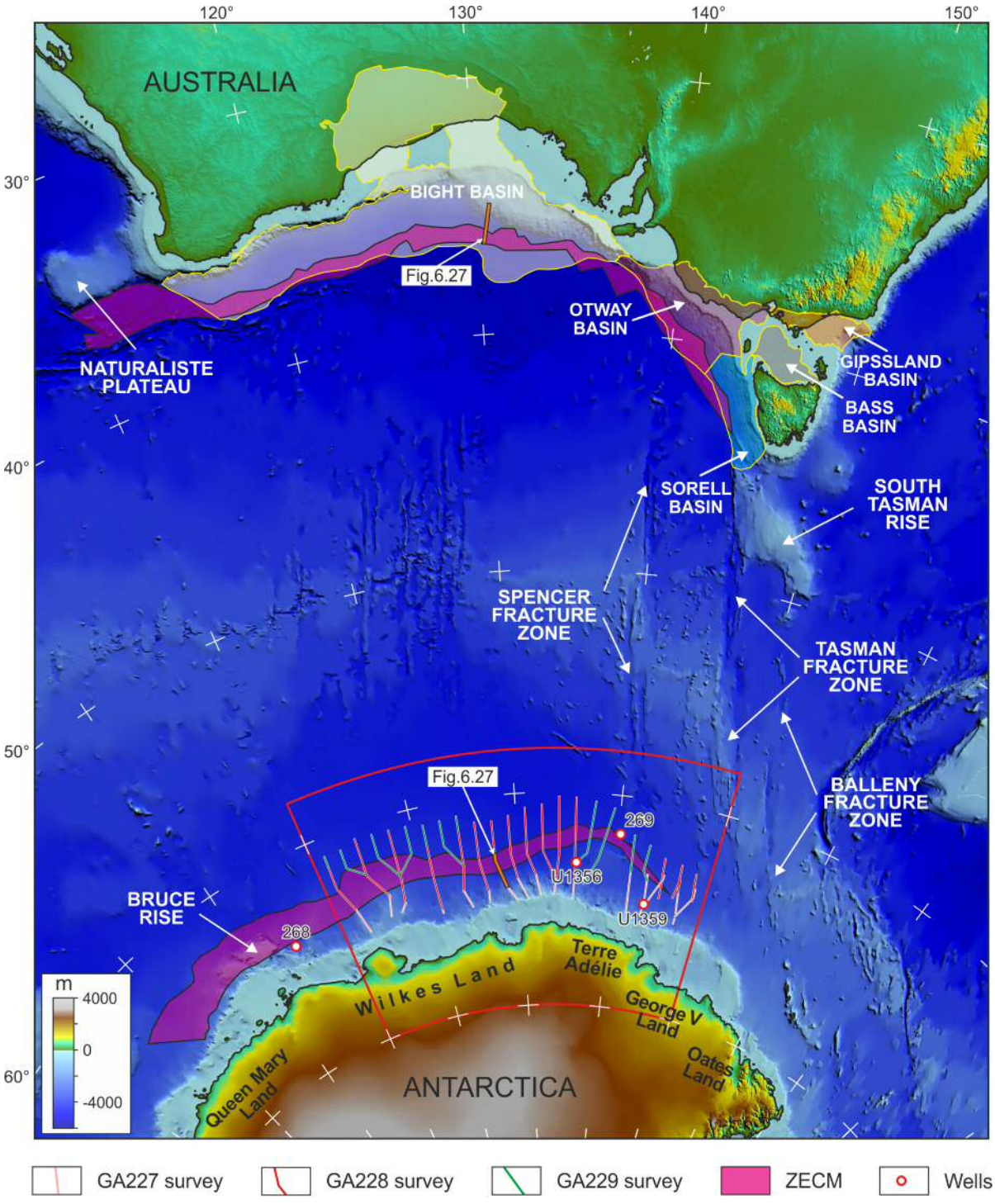


**Figure 6.1.** Geographical location and present day configuration of the Southern Rift System. The location of exhumed continental mantle is taken from Direen *et al.* (2012). Wells shown in this figure are those referred in the text. Wells are from DSDP (sites 268 and 269) and IODP (sites U1356 and U1359) expeditions. ZECM—zone of exhumed continental mantle.

From Southern Australia, although no digital seismic dataset was available (in SEG Y format), in Bradshaw (2005) the seismic survey S280 (covering the Bremer Sub-basin) is depicted in a large format and with a quality that allows for their interpretation. See Chapter 2 for details on the different seismic surveys used.

Data from IODP Expedition 318, Site 1356 (Expedition 318 Science Party, 2011b) was used in order to calculate the age of reflector Maastrichtian-Palaeogene (Maas/Pal).

## 6.4. Physiography and geological context

The Australia-Antarctica conjugate margins are commonly referred to as the Southern Rift System (SRS) based on the work of Stagg *et al.* (1990). Initially referring to the South Australian margin only, the SRS was later expanded to include the Antarctic conjugate margin (Stagg *et al.*, 2005). On the Australian margin, the SRS extends for more than 3500 km between the Naturaliste Plateau in the west, to the South Tasman Rise in the east. On the Antarctic margin, it extends from the Bruce Rise on the west, to the Balleny Fracture Zone on the east (Fig. 6.1).

Separated nowadays by more than 3000 km of oceanic crust, the margins of the SRS present significant geomorphologic variability. The Australian southern margin, from its western tip to approximately longitude 125°E, has a narrow shelf with a steep (up to 8°) terraced continental slope. This morphology changes quickly into a wide continental rise that continues onto ridged ocean floor with a depth of 5.5 km (Fig. 6.1). Eastward of 125°E until approximately 135°E, the continental shelf widens considerably becoming very narrow eastward of this area, then widening again off the Otway Basin (Fig. 6.1). Conversely, on the Antarctic margin the continental shelf has an approximate length of 1400 km and is much more regular in terms of its morphology than Southern Australia. In general terms, the shelf is broader, around 100 to 200 km in width, with a slope around 2° to 4° in gradient, decreasing to less than 1° on the abyssal plain (Hayes, 1972; Stagg *et al.*, 2005) (Fig. 6.1).

The southern margin of Australia is the largest segment of the Australian subcontinent considered amagmatic in respect to its rifting mode (Symonds *et al.*, 1998). In this region, rifting between Australia and Antarctica occurred chiefly in the form of orthogonal rifting, with main extensional faults oriented parallel to the two margins, and oceanic crust transform faults developing almost perpendicularly to these latter (Brown *et al.*, 2003; Stagg *et al.*, 2005; White *et al.*, 2013) (Fig. 6.1). Eastwards of the Spencer Fracture Zone, rifting becomes oblique in the Otway Basin (creating basin axis aligned at high angles to the predominant E-W rift axis), and changes to a transform continental margin eastwards of the Tasman Fracture Zone (Willcox & Stagg, 1990; Miller *et al.*, 2002; Colwell *et al.*, 2006; Gibson *et al.*, 2012) (Fig. 6.1). Similarly, the east Antarctica conjugate margin of southern Australia (~100–155°E) can be divided in two broad zones, a first zone ranging from the Western Wilkes Land to Terre Adélie where extension was predominantly orthogonal with the southern Australian margin, and a second zone, the George V Land, where rifting occurred by means of oblique to strike-slip extension (Fig. 6.1).

The stratigraphic record of the two margins reveals a rifting history with several episodes of extension followed by established thermal subsidence before lithospheric breakup was achieved (Veevers 1984; Krassay *et al.*, 2004; Blevin & Cathro, 2008). The first rifting phase, spanning the Callovian–Early Berriasian (~165-145 Ma), records ~300 km of NW–SE extension that formed en-echelon half-graben systems. It created the Bight Basin and its sub-basins in a west to east diachronic rifting. Extension ceased in this area during the early Berriasian, and a subsequent phase of slow thermal subsidence ensued until the Middle Albian (Bein & Taylor, 1981; Willcox & Stagg, 1990; Norvick & Smith, 2001; Totterdell *et al.*, 2003; Blevin & Cathro, 2008). A second phase of extension started on the eastern side of the SRS during the early Berriasian, and lasted until Late Barremian creating the Otway, Bass and Gippsland basins (Willcox & Stagg, 1990; Totterdell *et al.*, 2003; Krassay *et al.*, 2004; Blevin & Cathro, 2008).

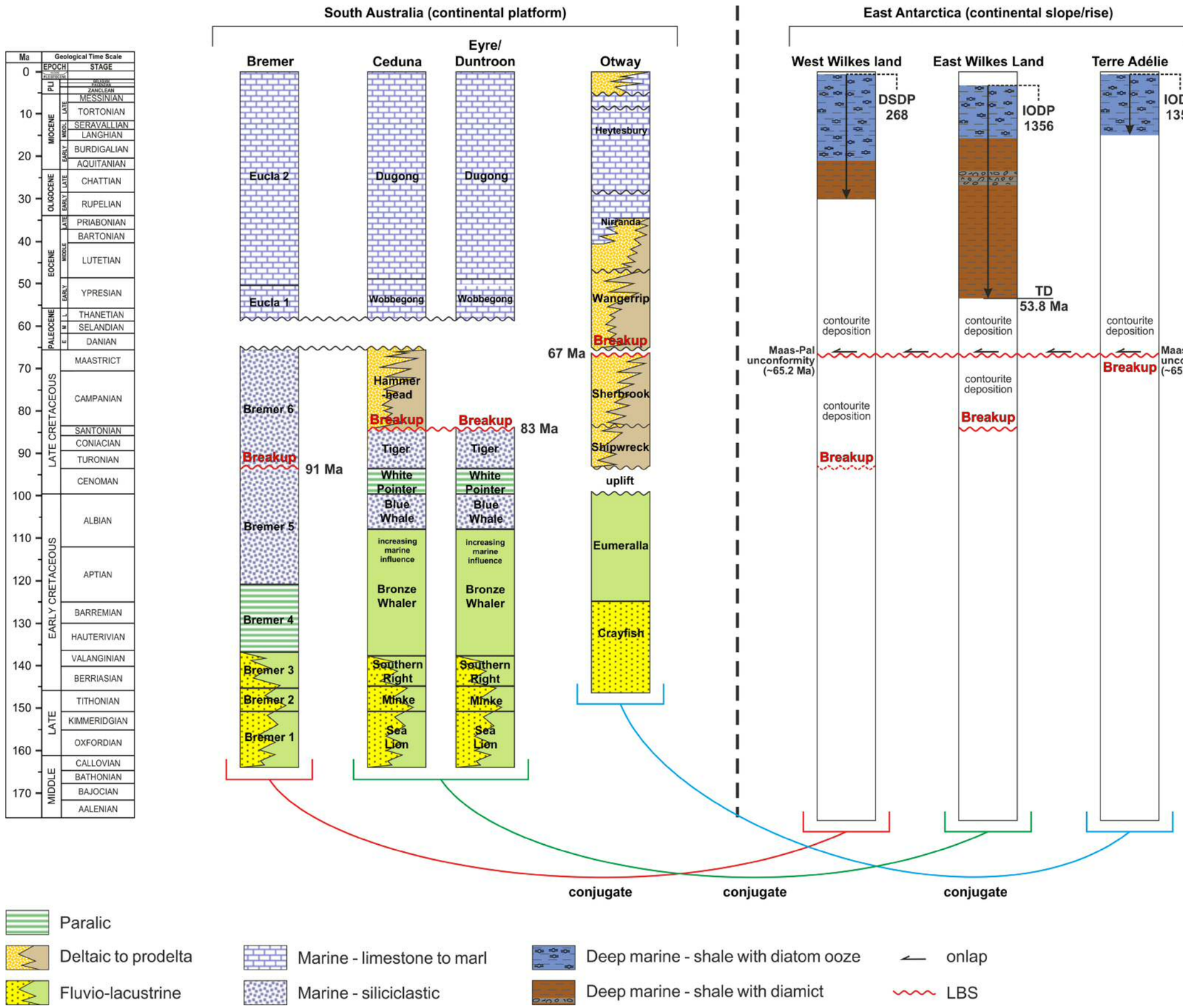


**Figure 6.2.** Chronostratigraphy of the SRS. Data from Blevin *et al.* (2008), Shipboard Scientific Party (1975), Expedition 318 Science Party (2011b, a). Note that the Cenozoic sediments deposited above the Bight Basin are considered to be part of the Eucla Basin (Bradshaw *et al.*, 2003). Lithological information on the east Antarctica margin only cover the LBS—lithospheric breakup surface. For the location of DSDP and IODP sites, see Figure 6.1.

The SRS underwent a significant amount of lithospheric stretching before final breakup, having as a result the exhumation of lithospheric mantle and the emplacement of mafic intrusions derived from decompression melting of the lower lithosphere (Chatin *et al.*, 1998; Sayers *et al.*, 2001; Colwell *et al.*, 2006). These phenomena resulted in the creation of a 60 to 90 km wide continent-ocean transition zone (COTZ, *sensu* Colwell *et al.*, 2006) showing highly complex structuring on both margins (Fig. 6.1). As in Iberia-Newfoundland (*e.g.* Sibuet *et al.*, 2007b; see Chapter 3; Bronner *et al.*, 2011), the outcome of mantelic exhumation in the SRS is that the oldest magnetic anomalies were found to occur not in oceanic crust but in exhumed lithospheric mantle (Sayers *et al.*, 2001; Whittaker *et al.*, 2008). In fact, the COTZ is interpreted to consist primarily of highly thinned continental crust with exhumed serpentinized peridotites and mafic intrusions/extrusions. It is the presence of these igneous and metamorphic bodies that account for the magnetic anomalies interpreted in the COTZ (Sayers *et al.*, 2001; Beslier *et al.*, 2004b; Colwell *et al.*, 2006; Direen *et al.*, 2011). Prior to the work of Sayers *et al.* (2001), other hypotheses regarding the nature of the COTZ were proposed; for example that it represented an end-member of a relatively amagmatic, very slow spreading oceanic crust (Tikku & Cande, 1999).

Similarly to the Iberia-Newfoundland margins, the existence of a COTZ obscuring a clear boundary between continental crust and oceanic crust is the major reason for the controversy surrounding the timing of lithospheric breakup and the manner in which it proceeded along the SRS (*e.g.* Beslier *et al.*, 2004b; Tikku & Direen, 2008; Williams *et al.*, 2011; Veevers, 2012; White *et al.*, 2013; Whittaker *et al.*, 2013).

The first attempts to date and identify palaeomagnetic anomalies (Weissel & Hayes, 1972) were successively reinterpreted and refined in more recent publications (Cande & Mutter, 1982; Veevers, 1986; Tikku & Cande, 1999). Initially, Weissel & Hayes (1972) identified C22 (~49 Ma) as the oldest magnetic anomaly in oceanic crust, leading these authors to attribute this age (Lower Eocene) to the initiation of breakup between Australia and Antarctica. In contrast, Cande & Mutter (1982) stated that the magnetic chron previously identified as C22 was in fact C34, meaning that

sea-floor spreading between Australia and Antarctica must have started by ~83.5 Ma (Coniacian–Santonian) or, by extrapolation of spreading rates, around 110–90 Ma (Albian–Turonian). More recent analyses in Veevers (1986) propose that the C34 anomaly of Weissel & Hayes (1972) coincides with the edge of the continent-ocean boundary, estimating an age of continental breakup around 99 ± 5 Ma (Albian–Cenomanian), i.e. correlating it to the unconformity observed in the Otway Basin between the Early Cretaceous Otway Group and the overlying Sherbrook Group (Figs. 6.1 and 6.2). It was in this same basin where Falvey (1974) coined the term *breakup unconformity*, although at a higher stratigraphic level, between the Sherbrook Group and the Wangerrip Group (Figs. 6.1 and 6.2).

Sayers *et al.* (2001), using seismic reflection and refraction data from the central Great Australian Bight (GAB), recently proposed the existence of serpentinized exhumed mantle at the C34 isochron (83.5 Ma). For these authors, lithospheric breakup started during C33o (~84 Ma, Late Santonian), an age considered previously by other authors to represent the lithospheric breakup event on these margins (*e.g.* Tikku & Cande, 2000).

Occurring at different times in different segments of conjugate margins, lithospheric breakup developed from west to east in the SRS, as demonstrated by several authors (Mutter *et al.*, 1985; Tikku & Direen, 2008; Direen *et al.*, 2011; Whittaker *et al.*, 2013). Contrasting points of view arguing for a more synchronous lithospheric breakup rely on isochron picks which can be generated within the serpentinized exhumed mantle during LRS2 (*e.g.* Whittaker *et al.*, 2007; Müller *et al.*, 2008) and are not representative of true oceanic mantle accretion (see Chapter 1). Direen *et al.* (2012) defends the point of view that isochrons picks from magnetic data alone are not a reliable way to access lithospheric breakup age. Instead, they advocate the use of all possible datasets to define the timing of breakup. Direen (2012) produces a comprehensive account of the lithospheric breakup diachronicity as recorded on the Australia–Antarctica conjugate margins:

'*Off the southern Naturaliste Plateau, breakup with Bruce Rise or Queen Mary Land can be deduced to have occurred at around 90–87 Ma (Turonian-Coniacian) (…), from dating of exhumation fabrics in dredge samples from the continent–ocean transition zone (Beslier et al., 2001b; 2004a; Halpin et al., 2008). In the Bremer Basin, conjugate to western Wilkes Land, dating of breakup volcanics reported in Blevin & Cathro (2008) suggests breakup at around 91 Ma (Turonian) (…), whereas in the Great Australian Bight, conjugate to eastern Wilkes Land (Colwell et al., 2006), magnetic anomalies and seismic data (Sayers et al., 2001) indicate breakup at chron 33o (~83 Ma) to as young as chron 32y (71 Ma) (Santonian–Campanian), consistent with seismic stratigraphy (Totterdell et al., 2000). In the Otway Basin, conjugate to Terre Adélie (Colwell et al., 2006), breakup appears to be at anomaly A20 (~68-63 Ma Maastrichtian) (Veevers & Li, 1991), agreeing with seismic stratigraphy (Krassay et al., 2004). Breakup between the Sorell Basin and the George V Land, eastward to the George V fracture zone, was by ridge jumps, and is separable into at least two compartments of ~58 Ma (Late Paleocene) and ~49 Ma (Early Eocene) age, based on magnetic anomalies (Müller et al., 2000).*' Direen (2012, p. 303). See Figures 6.1 and 6.2.

Concerning the time of lithospheric breakup on the easternmost Australian margin (Sorrel and Bass basins), Eocene (~34 Ma) is the date preferred by several authors for the end of extension and complete separation between the Australian and Antarctic margins (Norvick & Smith, 2001; Whittaker *et al.*, 2013).

## 6.5. Southern Australia tectono-stratigraphy

In tectono-sedimentary terms, the Australian side of the SRS can be divided in two main sectors: (1) a western sector comprising the Bight Basin and (2) an eastern sector, comprising the Otway, Sorrel, Bass and Gippsland basins (Figs. 6.1 and 6.3). This division results from the distinct extension modes experienced during continental rifting: in the western part extension was predominantly orthogonal, while in the eastern part rifting occurred by means of oblique extension grading to strike-slip on the most eastern side of the rift axis.

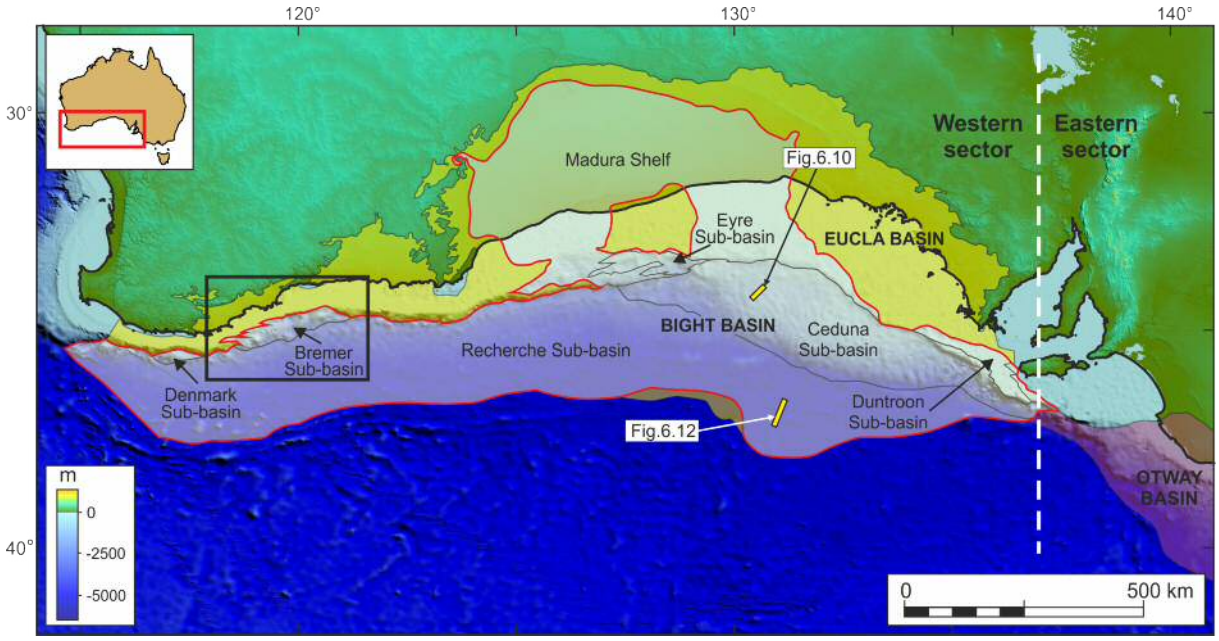


**Figure 6.3.** Location of the Mesozoic Bight Basin and its sub-basins, and the Cenozoic Eucla Basin. Line in red shows the boundaries of the Bight Basin. Black box shows the position of Figure 6.4. Basin and sub-basin limits from Bradshaw (2005).

### 6.5.1. West sector: Bight Basin

The Bight Basin comprises the Mesozoic cover of the western region of the Southern Australia margin**. It develops mainly offshore, comprising a large basin with an east-west elongated shape extending for more than 2,000 km, and an area of around 804,000 km² (Figs. 6.1 and 6.3). Yet, it is a poorly explored area with only ten exploration wells drilled (nine offshore, one onshore), all of them on the eastern side of the basin.

The Bight Basin is sub-divided into several sub-basins from the continental shelf (and onshore), to the abyssal plain (Fig. 6.3). Within a total of seven sub-basins, six are located along the coast: the Madura Shelf (with a broad onshore component); the Denmark, Bremer, Eyre, Ceduna and Duntroon sub-basins (comprising perched half-grabens) and the Recherche Sub-basin, one single deep-water depocentre in water

** In Southern Australia, the Cenozoic cover is considered a different basin, the Eucla Basin (see Hill, 1995).

depths of more than 5,000 m that extends through the basinward side of the Bight Basin (Bradshaw *et al.*, 2003; Totterdell *et al.*, 2003) (Fig. 6.3).

The following description of the Bight Basin divides the basin in two distinct sectors: west and east. The west sector is where the Bremer and Denmark sub-basins are located, whereas the east sector accommodates the Eyre, Ceduna and Duntroon sub-basins (Fig. 6.3). Each sector shares a different stratigraphic framework. In fact, the west sector lacks a formal, detailed stratigraphic framework, partly due to the absence of exploration wells in this area. Since the Recherche Sub-basin represents the deep offshore areas of the Bight Basin (i.e. its southern margin), this sub-basin occur in both sectors (Fig. 6.3). As a result, in this work the Recherche Sub-basin is dealt not as a separate sub-basin but as the distal counterpart of the proximal sub-basins of Southern Australia. For a detailed description of the structural elements of the Bight Basin, the reader is directed to Bradshaw (2003).

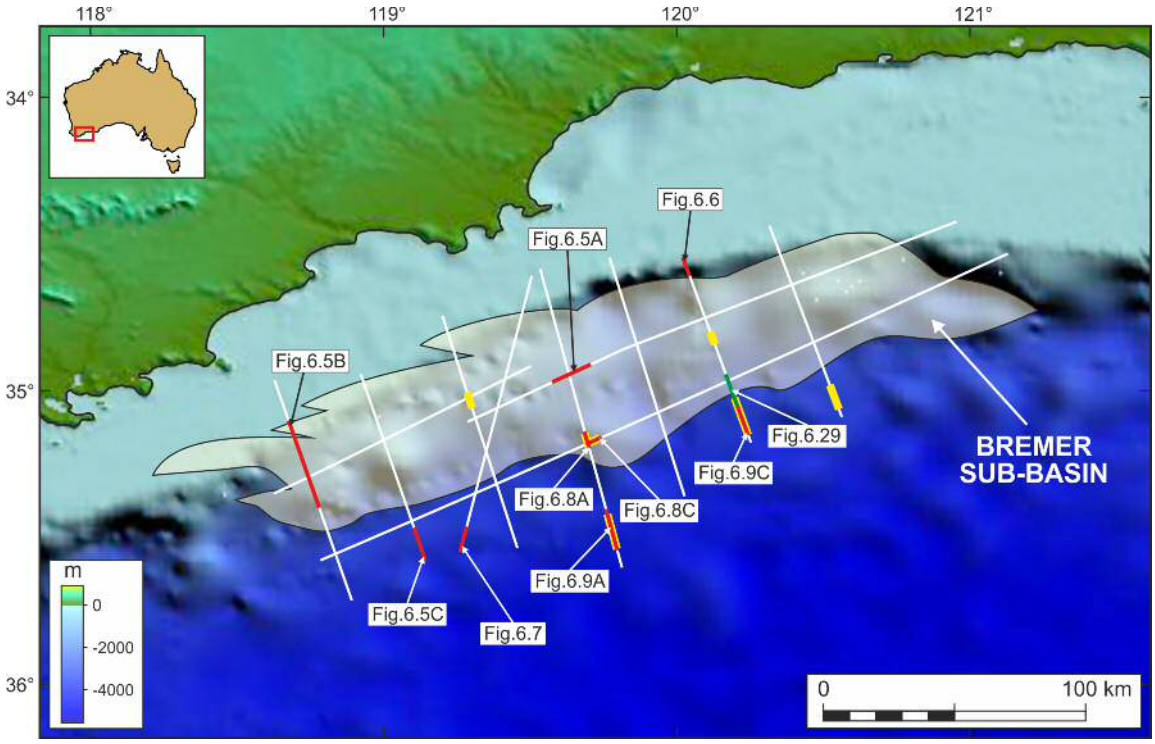


**Figure 6.4.** Bremer Sub-basin location and contourite distribution map. Solid white lines show location of the S280 seismic survey. Thick yellow lines are contourite drifts. For the location of this figure within the Bight Basin see Figure 6.3. Sub-basin limits taken from Blevin (2005).

#### *6.5.1.1. Bremer Sub-basin*

Located in the western Bight basin, the Bremer and Denmark sub-basins comprise perched half-grabens that cover an approximate area of 11,500 km$^2$ and 2,300 km$^2$, respectively (Stagg & Willcox, 1991). Given that no wells have been drilled in these sub-basins, the development of a stratigraphic framework tied to seismic profiles was achieved by means of an extensive dredging campaign in the Bremer Sub-basin, also taking advantage of the many submarine canyons that incise this sub-basin (Blevin, 2005; Bradshaw, 2005) (Fig. 6.4).

Latest syn-rift strata in the Bremer Sub-basin include marine sediments (seismic stratigraphic unit Bremer 5 of O'Leary *et al.*, 2005; Fig. 6.2), with a seismic architecture consisting mainly of sub-parallel reflectors with an aggradational character, themselves concordant with the underlying Bremer 4 unit (Fig. 6.5A). Generally deposited as a thin layer (less than 0.5 s TWT) in proximal parts of the margin, basinwards this unit can reach a maximum thickness of 1 s TWT. Ranging from Late Aptian to Late Cenomanian (Blevin & Cathro, 2008), Bremer 5 comprises marine inner-shelf sediments—mainly micaceous claystones and siltstones and minor fine-medium grained sandstones (O'Leary *et al.*, 2005). These sediments represent the onset of marine sedimentation in the region. The top of unit Bremer 5 is eroded by the LBS due to important rift-flank uplift associated with lithospheric breakup in this segment of the SRS (Nicholson & Ryan, 2005) (Fig. 6.5A and B). This event promoted the reactivation of older faults and significant uplift occurred in the western part of the sub-basin, producing proximally an angular unconformity that truncates a considerable portion of older sediments (Fig. 6.5B). Basinwards towards the Recherche Sub-basin, this unconformity becomes a correlative conformity (Fig. 6.5C).

After lithospheric breakup and subsequent generation of the LBS (the 'Turonian' horizon represented in orange colour in Bradshaw, 2005, and in Figs. 6.5 to 6.9), unit Bremer 6 was deposited during Early Turonian to Late Maastrichtian (O'Leary *et al.*, 2005) (Fig. 6.2). At places absent, especially on the proximal western area of this sub-basin (see Figure 6.5B), Bremer 6 shows a thickness between 0.3 and 0.6 s TWT across

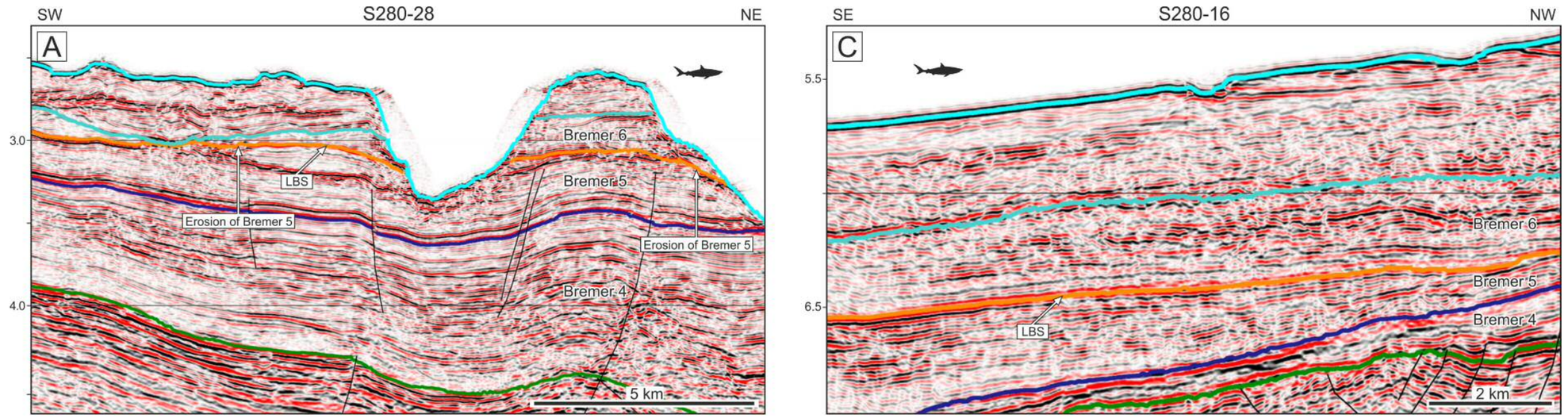


**Figure 6.5**. Variability in seismic facies in sedimentary units present in the Bremer Sub-basin. A—detail of line S280-28, note that the LBS (the base of unit Bremer 6) truncates Bremer 5 in some areas. B—line S280-15. Aspect of the westward, proximal Bremer Sub-basin pronounced erosional surface that constitutes the LBS in this area. Note the patchy continuity of Bremer 6. C—detail of line S280-16, showing the distal correlative conformity between units Bremer 5 and Bremer 6. Panel C is located on the Recherche Sub-basin. All panels modified from Bradshaw (2005). Unit boundaries interpretation from Bradshaw (2005). LBS—lithospheric breakup surface. Location of seismic profiles in Figure 6.4. Notice the changes in scale among the different panels.

the Bremer Sub-basin and the distally adjacent Recherche Sub-basin. Seismically, Bremer 6 comprises low to high amplitude parallel reflectors, at places with low continuity (Fig. 6.5). Basinwards the base of this unit become increasingly transparent, in places grading to stronger reflectors towards its top (Fig. 6.5C). On the continental shelf, prograding reflectors with a downward trajectory and toplap can be observed in some areas, an indication of the presence of a forced regression (Fig. 6.6).

The depositional environment of Bremer 6 is described as the continuation of the marine environments observed in Bremer 5 (O'Leary *et al.*, 2005). However, dredge data suggest that deposition occurred in a shallower sea than the Bremer 5 unit. The dredge samples closest to the continental shelf edge retrieving strata from both Bremer 5 and Bremer 6 (265_23DR23, in Bradshaw, 2005) suggest a much shallower depositional environment for Bremer 6. Sampled lithologies from Bremer 5 are described as '*Carbonaceous claystone (2 samples), dark silty claystone to green sand*', while Bremer 6 lithologies are '*Medium–coarse grained quartz sandstone*' (Bradshaw, 2005 at Appendix F, page F9). In addition, the erosive nature of the base of Bremer 6 in proximal settings, plus the presence of a forced regression on the continental shelf edge, strongly suggest that the depositional environment of Bremer 6 is more proximal than that of the (latest syn-rift) Bremer 5.

Turbidites are observed above the LBS on the distal western side of the Bremer and Recherche sub-basins (Fig 6.7). These turbidites are imaged as continuous strong to moderate amplitude reflections carved by channels at places. The turbidites are followed by a MTD interval that pinches out towards its distal part (toe domain, Fig. 6.7A, B).

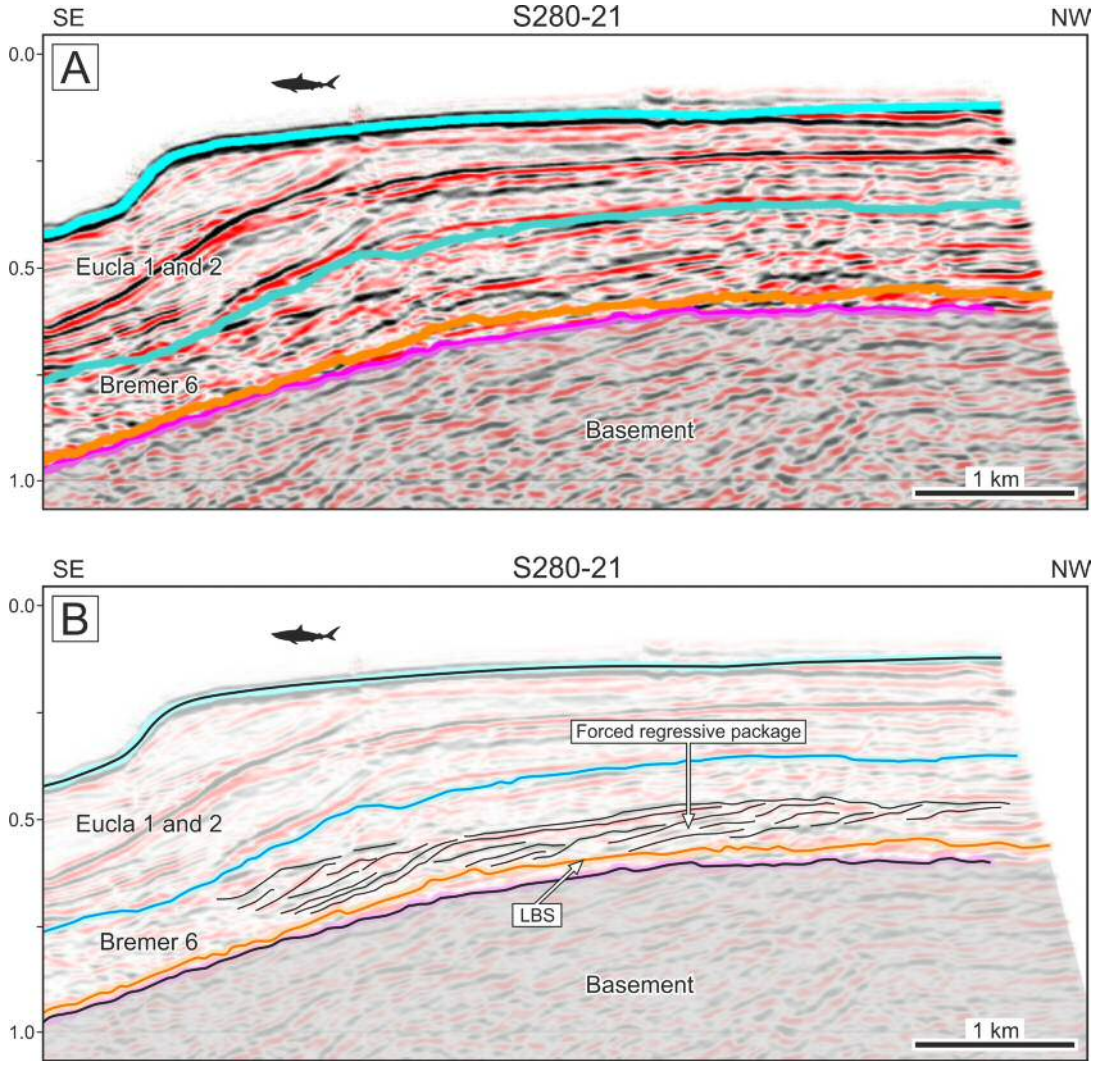


**Figure 6.6.** Forced regression systems tract deposited above the LBS. Unit boundaries interpretation from Bradshaw (2005). Interpretation of the forced regression package from this work. LBS—lithospheric breakup surface. Location of seismic profile in Figure 6.4.

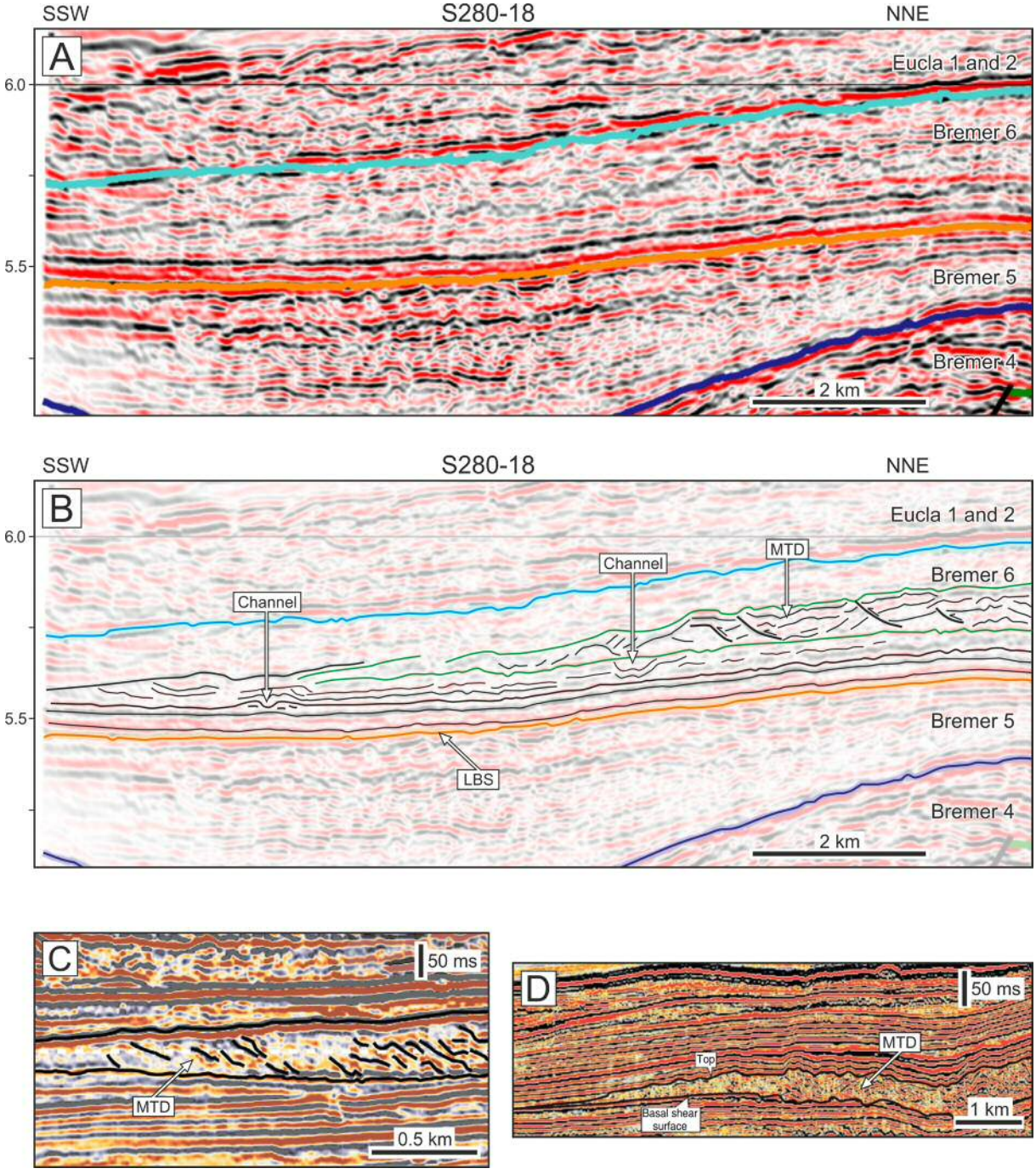


**Figure 6.7** Turbidites and MTD above the LBS at the western side of the Recherche Sub-basin (A and B). No signs of bottom current activity were interpreted here. Nevertheless, turbidite channels can be observed. Above the turbidites, the development of a MTD (between the green horizons) is observed, with internal thrusts visible on the landward side of the figure. Both the turbidites and the MTDs were likely to be fed by the important rift shoulder uplift occurred on the western side of the Bremer Sub-basin (see Figure 6.5B). C and D—modified figures from Alfaro & Holz (2014) (C) and Frey-Martínez *et al.* (2006) showing MTDs for comparison with the MTD in A and B. Unit boundaries interpretation from Bradshaw (2005), other reflections interpretation from this work. LBS—lithospheric breakup surface. Location of seismic profile in Figure 6.4.

Bottom current activity within the unit Bremer 6 in the Bremer Sub-basin and the southwards contiguous Recherche Sub-basin is acknowledged in seismic survey S280 (Fig. 6.4). In fact, several examples of contourite drifts occurring at different depths are observed in sediments immediately above the LBS (Figs. 6.8 and 6.9) but are not found below this same horizon.

Two types of contourite drifts were recognized within unit Bremer 6. The first type comprise elongated mounded and separated drifts showing overall prograding upslope geometry, with continuous reflectors of weak to moderate amplitude (Fig. 6.8). These contourite drifts are found in the Bremer sub-basin. The second type comprises basinward-prograding sigmoidal reflections filling the distal Recherche Sub-basin (Fig. 6.9). The contourites are probably elongated mounded and detached drifts deposited by the action of a rapidly downslope migrating bottom current. They are very similar to a type of contourite drift found in the outer proximal margin of northwest Iberia (*cf.* Fig. 5.11).

No erosive surfaces were identified in Bremer 6, nevertheless this is probably due to the low vertical resolution of the data in survey S280.

The position of the distal LBS as interpreted by Bradshaw (2005) in lines S280-21 and S280-22, considers this latter horizon above extensive contourite drifts. This contradicts interpretations undertaken several lines westwards, where the contourites appear consistently above the LBS. In this thesis it is suggested that the Bradshaw (2005) interpretation of lines S280-21 and S280-22 is not exact (*e.g.* Fig. 6.9) due to the positioning of certain reflectors and the seismic aspect of the acoustic units, which can be traced across this set of lines. It should be noted that, in survey S280, seismic profiles perpendicular to the strike of the Recherche Basin are more than 30 km apart and that no transverse profiles were acquired. This complicates the control of horizon interpretation from line to line on the distal parts of the survey (Fig. 6.4).

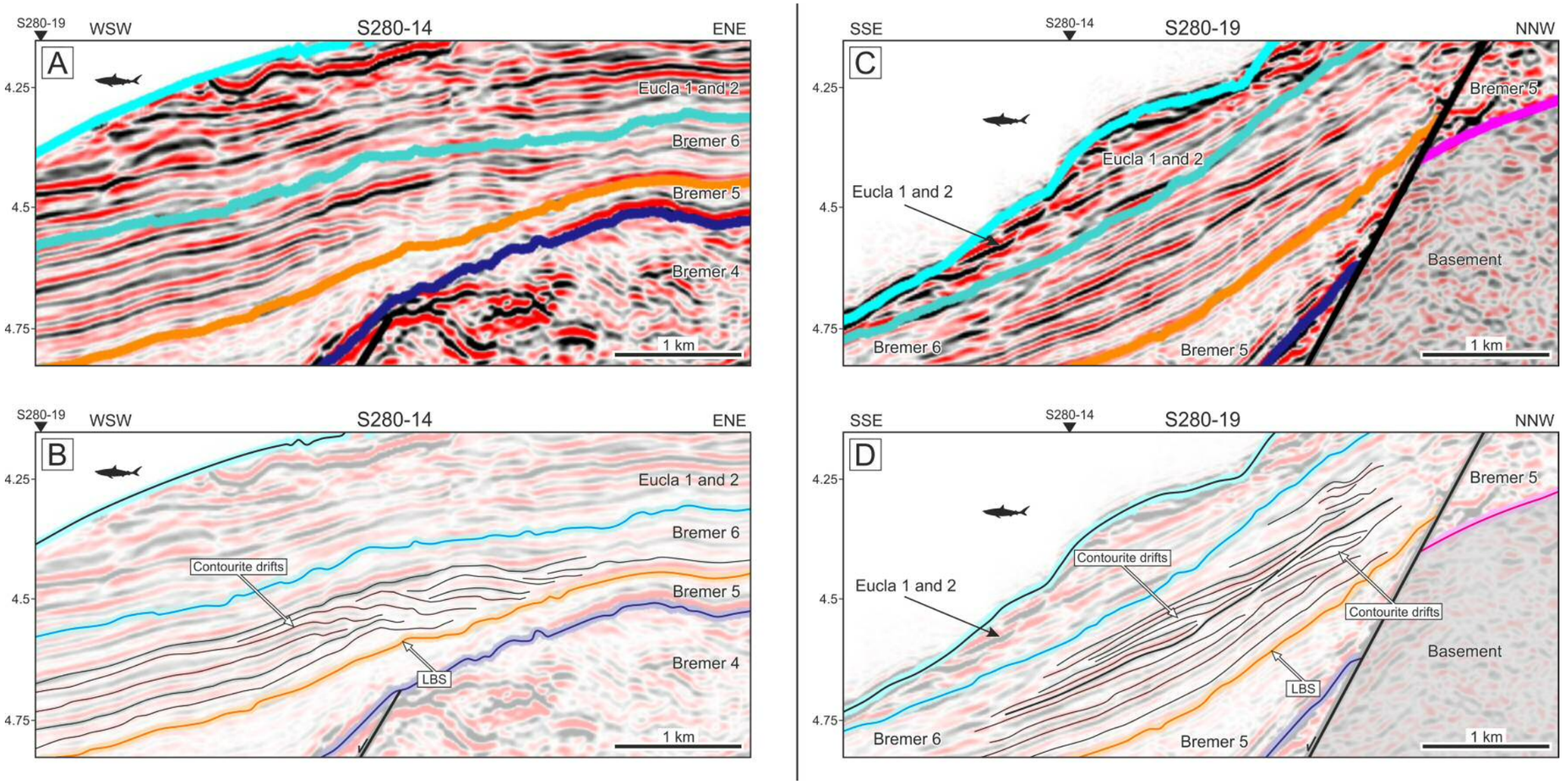


**Figure 6.8** Elongated, mounded and separated drift from Bremer Sub-basin. The same contourite drift is here observed in two different seismic lines, crossing each other almost perpendicularly. A—contourite drift observed in line S280-14. B—the same contourite drift observed in A, now observed in line S280-19. Note the different facies of the contourite deposits in the two seismic sections. Although in A the base of the contourite is almost above the LBS, due to the position of the seismic section relatively to the contourite in B, its base appear to be at a higher stratigraphic level. Unit boundaries interpretation from Bradshaw (2005). Contourite interpretation from this work. LBS—lithospheric breakup surface. Location of seismic profile in Figure 6.4.

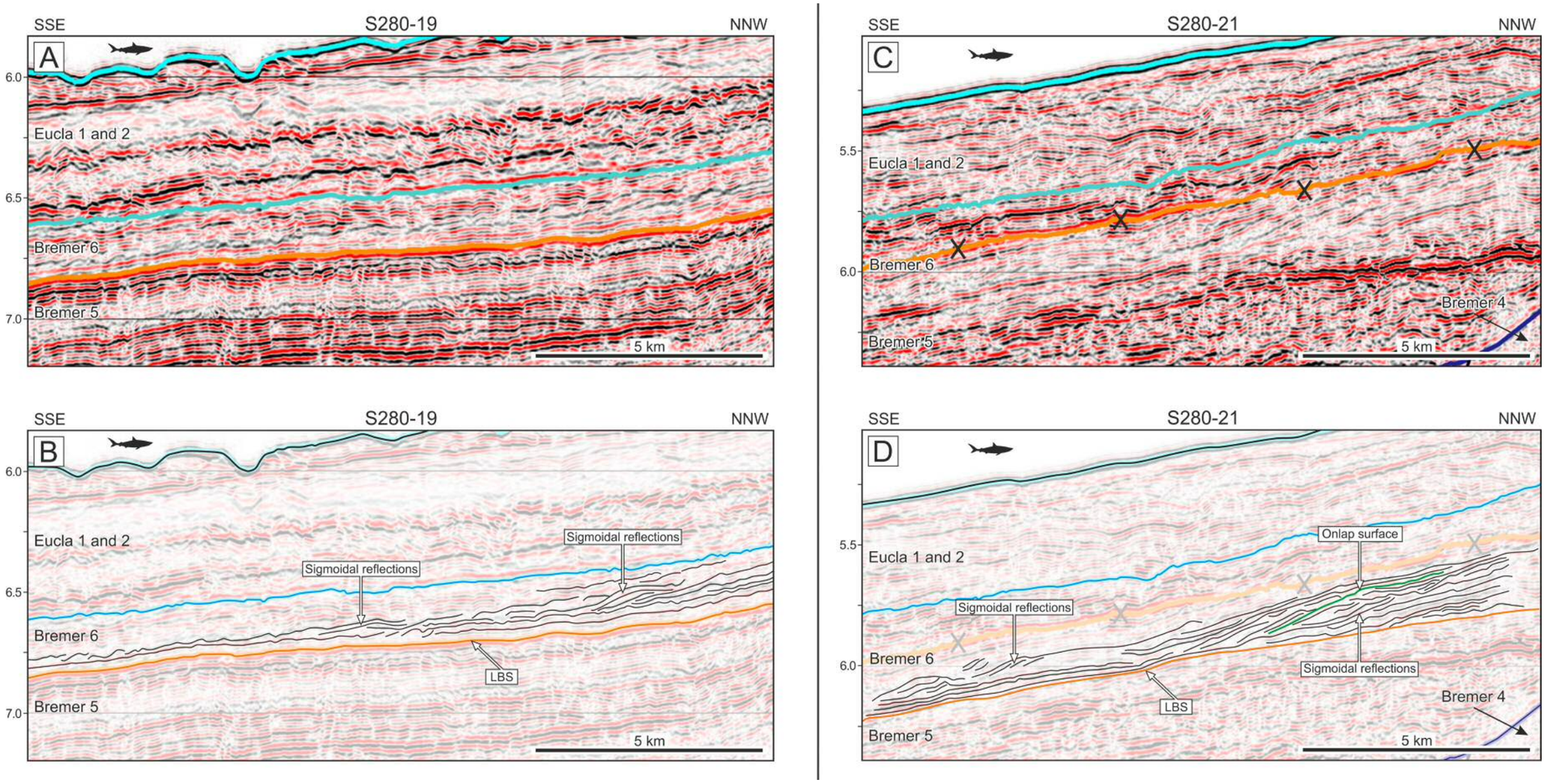


**Figure 6.9** Prograding sigmoidal reflections in the distal Recherche Sub-basin. These prograding reflections suggest downdip current migration. Note that in both lines the sigmoidal reflections truncate the horizons at their base in some places. In C (interpretation in D) an onlap surface is observed landwards (green horizon), above the prograding reflectors, showing the end of progradation in this area. These two lines are 65 km apart. Unit boundaries interpretation from Bradshaw (2005) except in C where top Bremer 5 (the LBS) was reinterpreted (orange horizon with black X is Bradshaw (2005) original interpretation). Contourite interpretation from this work. LBS—lithospheric breakup surface. Location of seismic profile in Figure 6.4.

#### *6.5.1.2. Eyre, Ceduna and Duntroon sub-basins*

The east side of the Bight Basin comprises the Eyre, Ceduna and Duntroon sub-basins, and the eastern part of the (distal) Recherche Sub-basin (Fig. 6.3). These sub-basins share the same stratigraphic framework, proposed by Totterdell *et al.* (2000), in which Mesozoic strata are divided in eight supersequences. These eight supersequences are, in turn, organized in four megasequences relating to several phases of basin development. This stratigraphic framework was created with the purpose of unifying previous different frameworks (*e.g.* Cockbain & Hocking, 1989; Hocking, 1990; Hill, 1995) and is, at present, the most accepted by industry and academia (*e.g.* Bradshaw *et al.*, 2003; Direen *et al.*, 2011; Espurt *et al.*, 2012). Interpreted supersequences and their broad depositional environments are summarised in Figure 6.2. Lithospheric breakup was achieved during Late Santonian-Early Campanian in this sector of the Bight Basin (Sayers *et al.* 2001; Tikku & Direen 2008). Consequently, the LBS separate two different megasequences, the *Basin Phases* 3 and 4 of Totterdell *et al.* (2000). The supersequences involved in this transition are the Tiger Supersequence below the LBS and the Hammerhead Supersequence above (Krassay & Totterdell, 2003) (Fig. 6.2).

The Tiger Supersequence (Turonian-Santonian; Figs. 6.2 and 6.10) is dominated by mudstones and a few thick sandstone units deposited in marginal marine to open marine environments. The Tiger Supersequence is divided into two sequence sets: the strongly faulted, lower Tiger sequence set 1, and the uniformly thin upper Tiger Supersequence set 2 (Totterdell *et al.*, 2000). Offshore, the Tiger Supersequence appears to be absent in part of the Eyre Sub-basin and in the northern border of the Ceduna Sub-basin (Totterdell & Krassay, 2003b). The supersequence is always observed basinward of the continental shelf, but its presence landwards is limited due to pronounced erosion recorded during lithospheric breakup. Nevertheless, this supersequence is found onshore in one single well on the Madura Shelf (Madura-1), north of Eyre Sub-basin, revealing its true extension prior to erosion. Acoustically, the Tiger Supersequence comprises continuous, weak to strong reflectors, with an overall aggradational character (Fig. 6.10).

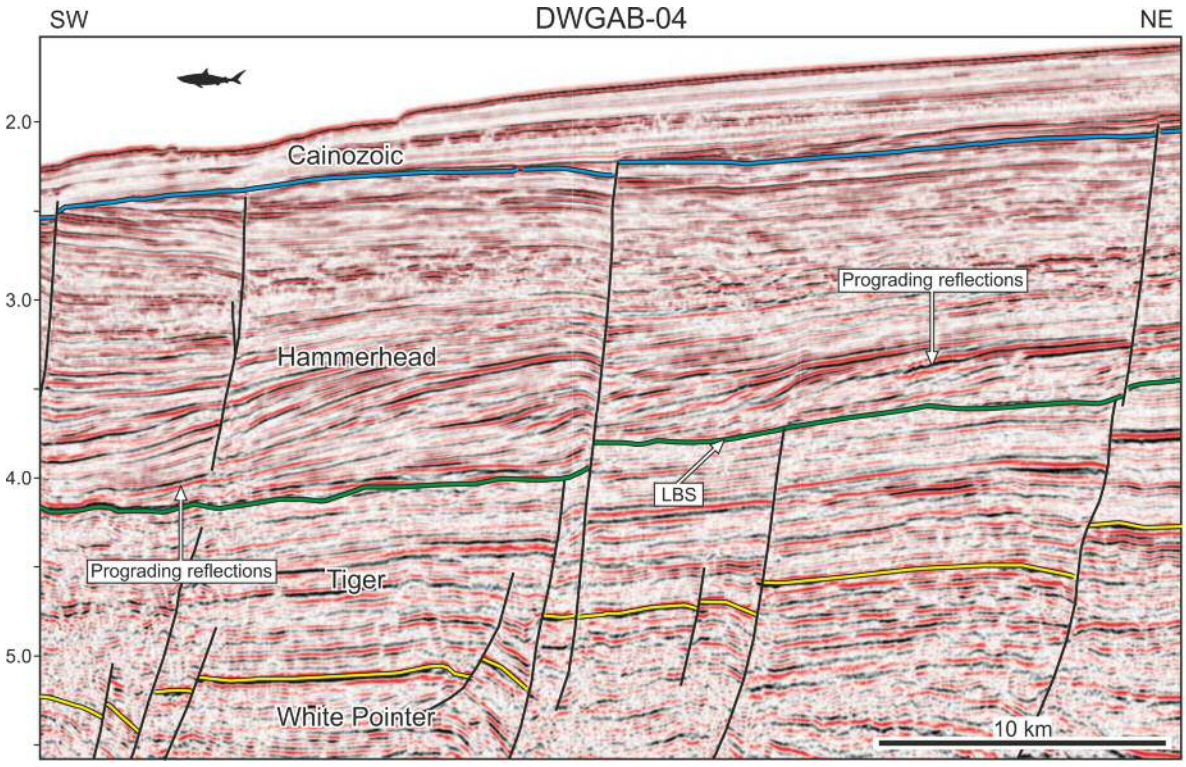


**Figure 6.10** Proximal seismic character of the Tiger and Hammerhead Supersequences. Note the low angle strong progradation immediately above the LBS. The LBS is here an erosional surface, as observed by the truncation of reflections below it. The top of the Hammerhead Supersequence is truncated by a Maastrichtian unconformity, well observed on the SW side of this figure. Modified from (Totterdell *et al.*, 2009). LBS—lithospheric breakup surface. Location of seismic profile in Figures 6.3 and 6.11.

A drop in relative sea level during lithospheric breakup promoted the deposition of the Hammerhead Supersequence, a sandstone dominated shelf-margin deltaic succession dated as Late Santonian-Maastrichtian, and part of the Ceduna Delta (Totterdell *et al.*, 2000; Krassay & Totterdell, 2003) (Fig. 6.11). Comparable to the modern Niger Delta, the Ceduna Delta comprises a very large delta complex (fed by the Ceduna River of Norvick and Smith, 2001) whose bathymetric expression extends for around 600 km across the continental shelf and slope, reaching a maximum thickness of 5 km (Krassay & Totterdell, 2003) (Fig. 6.11).

Absent in the Eyre and Duntroon Sub-basins, the Hammerhead Supersequence of the Ceduna Sub-basin is divided in three stratigraphic sequences, with the lowermost

and the middle sequence showing a strong progradational character (Totterdell *et al.*, 2000). Its top is markedly aggradational. In the continental shelf of the Ceduna Sub-basin, the Hammerhead Supersequence consists of amalgamated sandstones, interbedded sandstones and mudstones, and massive mudstones, representative of delta plain to prodelta environments (Totterdell *et al.*, 2000; Krassay & Totterdell, 2003; Espurt *et al.*, 2009). Its seismic character is variable due to the delta architecture itself, with amalgamated and interconnected channels crossing a delta plain environment (Lane *et al.*, 2012). Basinwards, within the Recherche Sub-basin, its acoustic character changes to flat-lying, continuous reflectors (Fig. 6.12). Once more in similarity with the Niger Delta, it is possible to record the presence of proximal gravity-driven extensional faults and distal compressive structures in the Ceduna Delta, which detach within basinal shales of Albian age (Krassay & Totterdell, 2003; Totterdell & Krassay, 2003a; MacDonald *et al.*, 2012b).

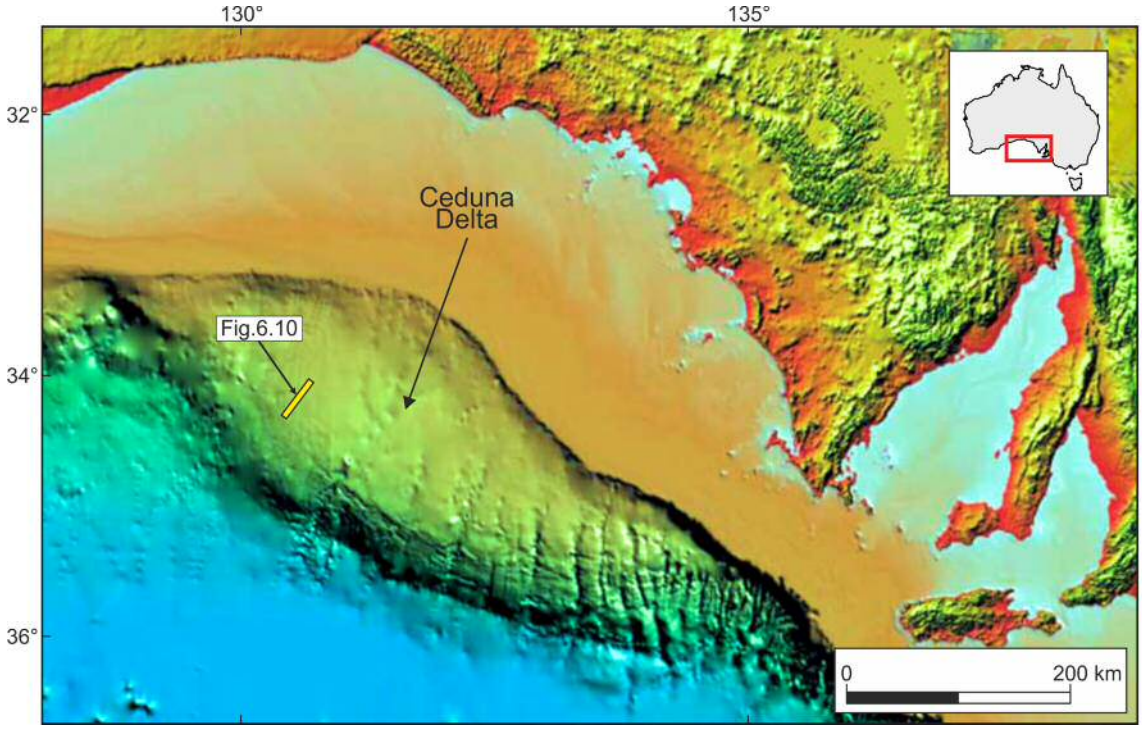


**Figure 6.11** Present day aspect of the Mesozoic Ceduna Delta. Despite its age (deposited during the Late Cretaceous), the Ceduna Delta is an important bathymetric feature at present. Digital elevation model image from Macdonald *et al.* (2012a).

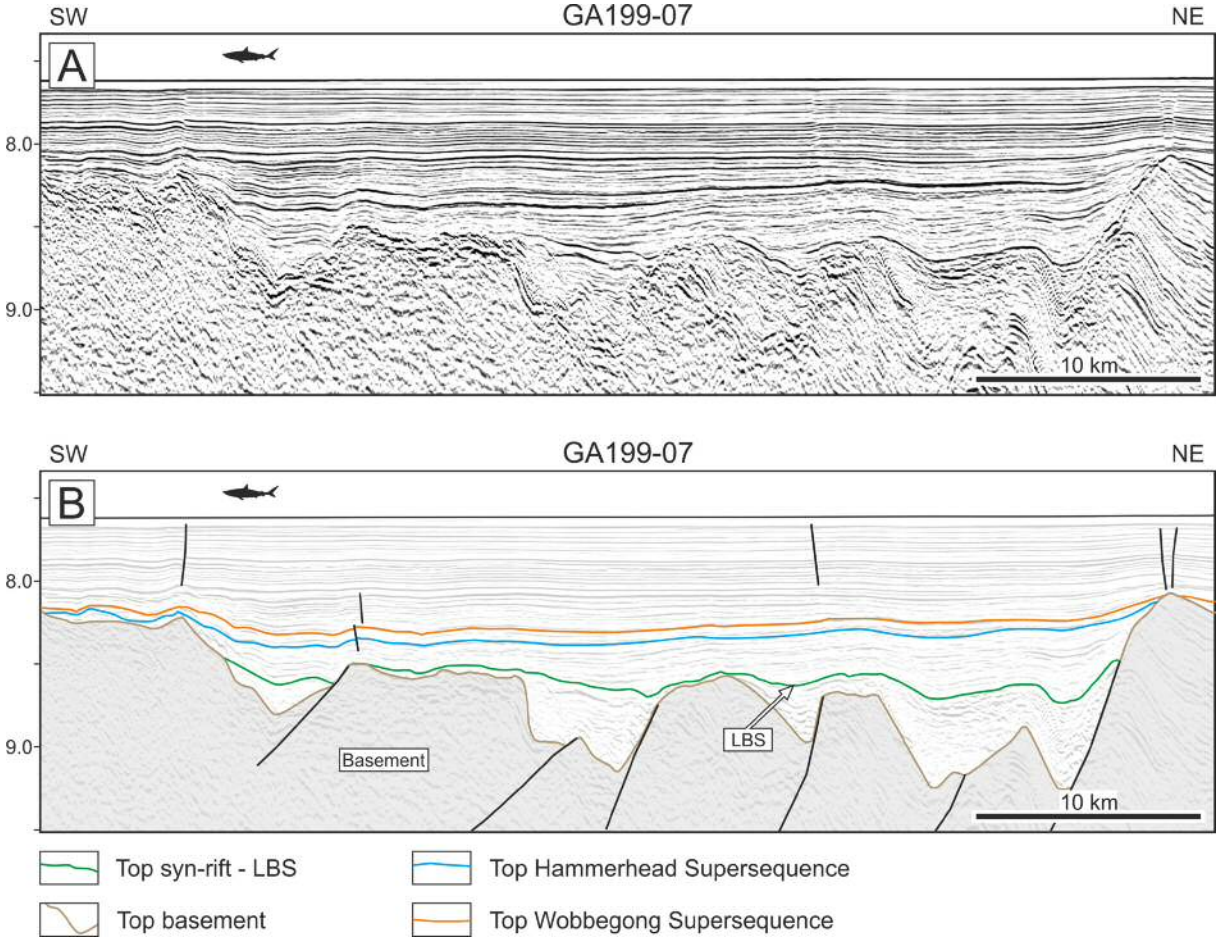


**Figure 6.12** Distal seismic character of the Hammerhead Supersequence (Recherche Sub-basin south of Ceduma Sub-Basin). Note the contrast between the flat lying, LBS onlaping (but with an overall prograding character) sediments of the Hammerhead Supersequence deposited after Lithospheric breakup. Seismic image from Ball *et al.* (2013) with re-interpreted horizons. LBS—lithospheric breakup surface. Location of seismic profile in Figure 6.3.

The east side of the distal Recherche Sub-basin is similar to its western part in terms of seismic facies. Its lithology is, however unknown as the only drilling campaign on this sub-basin was ODP Site 182, and none of its boreholes crossed Mesozoic strata (Feary *et al.*, 2000).

Bremer 6 and the Hammerhead Supersequence show an erosive surface at their top, developed during the Late Maastrichtian across the Bight Basin (Figs. 6.2, 6.10).

In Southern Australia, the Cenozoic cover is regarded as a different basin, the Eucla Basin (Fig. 6.3). Similarly to the Mesozoic Bight Basin, the overlying Cenozoic basin was divided in Supersequences by Totterdell *et al.* (2000) (Fig. 6.2). Following a hiatus of 5 to 6 m.y., the Palaeocene-Early Eocene Wobbegong Supersequence drapes the Hammerhead Supersequence with a series of prograding marginal marine sandstones and siltstones. The acoustic character of this sequence is very constant, with prograding low amplitude reflections in proximal parts, and parallel reflectors, onlaping the top of the Hammerhead Supersequence basinwards (Fig. 6. 10).

### 6.5.2. East sector: Otway Basin

Located between the Bight Basin and the Sorell Basin, the Otway Basin is the Australian conjugate of Terre Adélie in Antarctica (Figs. 6.1 and 6.13). Whereas rift propagation progressed west to east on the western basins (see Krassay *et al.*, 2004 and references within), the history of extension in the Otway Basin was markedly different. In the Bight Basin extension was orthogonal, but in Otway Basin rifting occurred by means of a left lateral oblique extension at approximately 55°, oriented NW-SE. This extension originated basin axes that were aligned at high angles with the predominant E-W trend of the southern coast of Australia (Willcox & Stagg, 1990). Such a rift architecture is even more accentuated in the Sorell Basin, east of the Tasman Fracture Zone, where extension occurred at an angle of ~15° with the Antarctic margin (Colwell *et al.*, 2006; Direen *et al.*, 2011). In fact, the Otway Basin is a transitional zone from an orthogonal to oblique rifted margin to the fully transform margin of the western Tasmania and South Tasmanian Rise (Gibson *et al.*, 2012) (Fig. 6.1). This transition occurs along the lithospheric segment where the west Otway basin is located, between the Spencer Fracture Zone and the Tasman Fracture Zone. These pre-existing basement structures influenced profoundly rift basin architecture (Miller *et al.*, 2002). Similarly, they were an important control on the development of the ocean crust fabric, with the development of volcanic mounds on the ocean floor delineating these structures (Fig. 6.1).

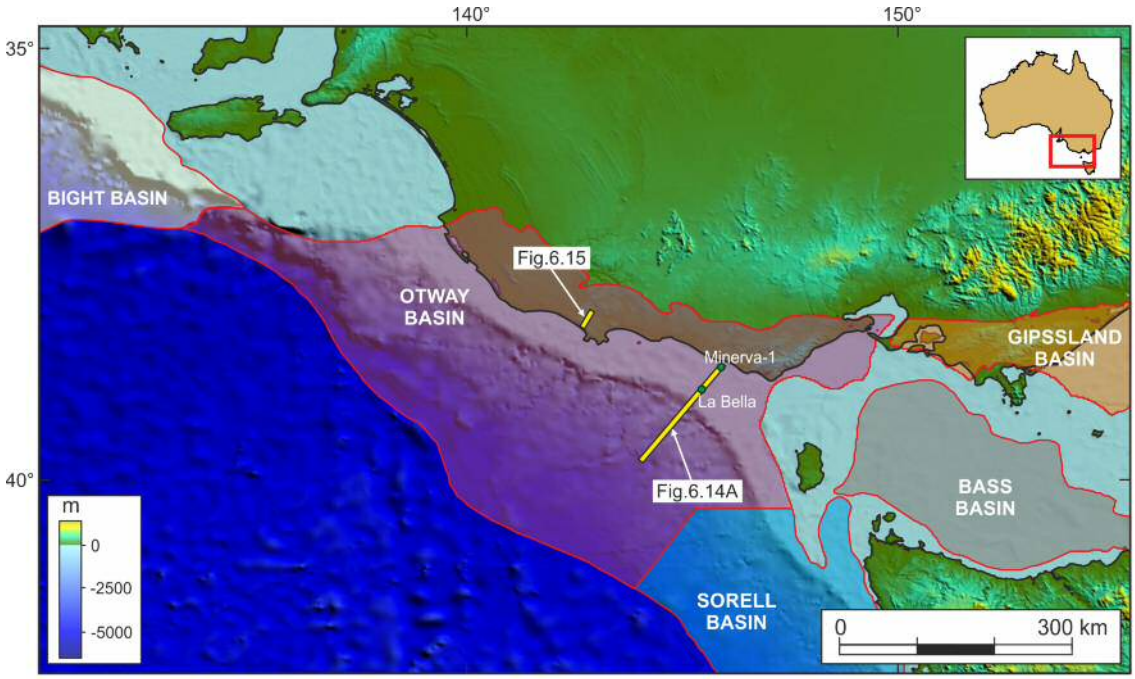


**Figure 6.13** Detailed location of the Otway Basin.

The Sorel Basin was not studied in this chapter, since rifting here (via a transform margin) is markedly different from rifting in Northwest Iberia, where rifting was orthogonal.

Similarly to the Bight Basin, two main rifting episodes occurring prior to lithospheric breakup have been identified in the Otway Basin. Progressing from west to east, the first extensional episode started during the Late Jurassic and continued until the Late Barremian (Williamson *et al.*, 1990; Perincek & Cockshell, 1995). A period of thermal subsidence lasting until the early Late Cretaceous followed this extensional phase without achieving lithospheric breakup or continental crust separation (Krassay *et al.*, 2004; Direen *et al.*, 2012).

A second rifting episode is recorded from the early Late Cretaceous until the Late Maastrichtian, when lithospheric breakup finally occurred (Lavin, 1997; Krassay *et al.*, 2004; Stacey *et al.*, 2013). This second extensional episode is characterized by the deposition of the Shipwreck and Sherbrook supersequences in the Otway Basin (Fig.

6.2), with the top of Sherbrook Supersequence being associated with the end of rifting (Lavin, 1997; Krassay *et al.*, 2004) (Fig. 6.2). In fact, structural controls on the Sherbrook Supersequence are less marked than in the Shipwreck Supersequence, with extensional faults gradually decreasing and ceasing its activity (Krassay *et al.*, 2004). Importantly, lithospheric breakup is marked in the Otway Basin by an episode of regional compression, margin uplift and truncation of pre-breakup sequences (Lavin, 1997; Krassay *et al.*, 2004; Stacey *et al.*, 2013).

The Sherbrook Supersequence is composed of strongly prograding deltaic-marine successions that include delta fans at the bottom of the supersequence to non-marine upper delta plain environments towards its top (Krassay *et al.*, 2004). Large scale prograding clinoforms occur well within the basin, as observed in Figure 6.14 (Stacey *et al.*, 2013). Due to loading and compaction, the Sherbrook Supersequence presents many closely spaced faults concentrated around the main depocentre for deltaic sediments (Fig. 6.14 and 6.15). Its composition ranges from progradational siltstones and prodelta shales, abundant at the base, to mainly aggradational sand-dominated sequences on the top of the Supersequence (Lavin, 1997; Boult *et al.*, 2002).

A widespread Late Maastrichtian unconformity (the LBS in this margin segment), caused by moderate structuring and regional uplift at the time of lithospheric breakup, marks the top of the Sherbrook Supersequence, and separates syn-rift from post-rift strata (Morton *et al.*, 1994; Lavin, 1997; Krassay *et al.*, 2004; Blevin & Cathro, 2008; Stacey *et al.*, 2013). Remarkably, the LBS is associated with an episode of regional compression and formation of antiforms in the Otway Basin, which were subsequently truncated by the erosion caused by tectonic uplift associated with the lithospheric breakup event (Hill *et al.*, 1995; Lavin, 1997; Stacey *et al.*, 2013). In the La Bella-1 well, tectonic uplift related to the lithospheric breakup approaches 300 m, truncating Campanian and Maastrichtian sediments (Krassay *et al.*, 2004). With significant landward erosion of older units, this unconformity decreases in importance basinwards, becoming a conformable surface beyond the continental slope (Falvey, 1974).

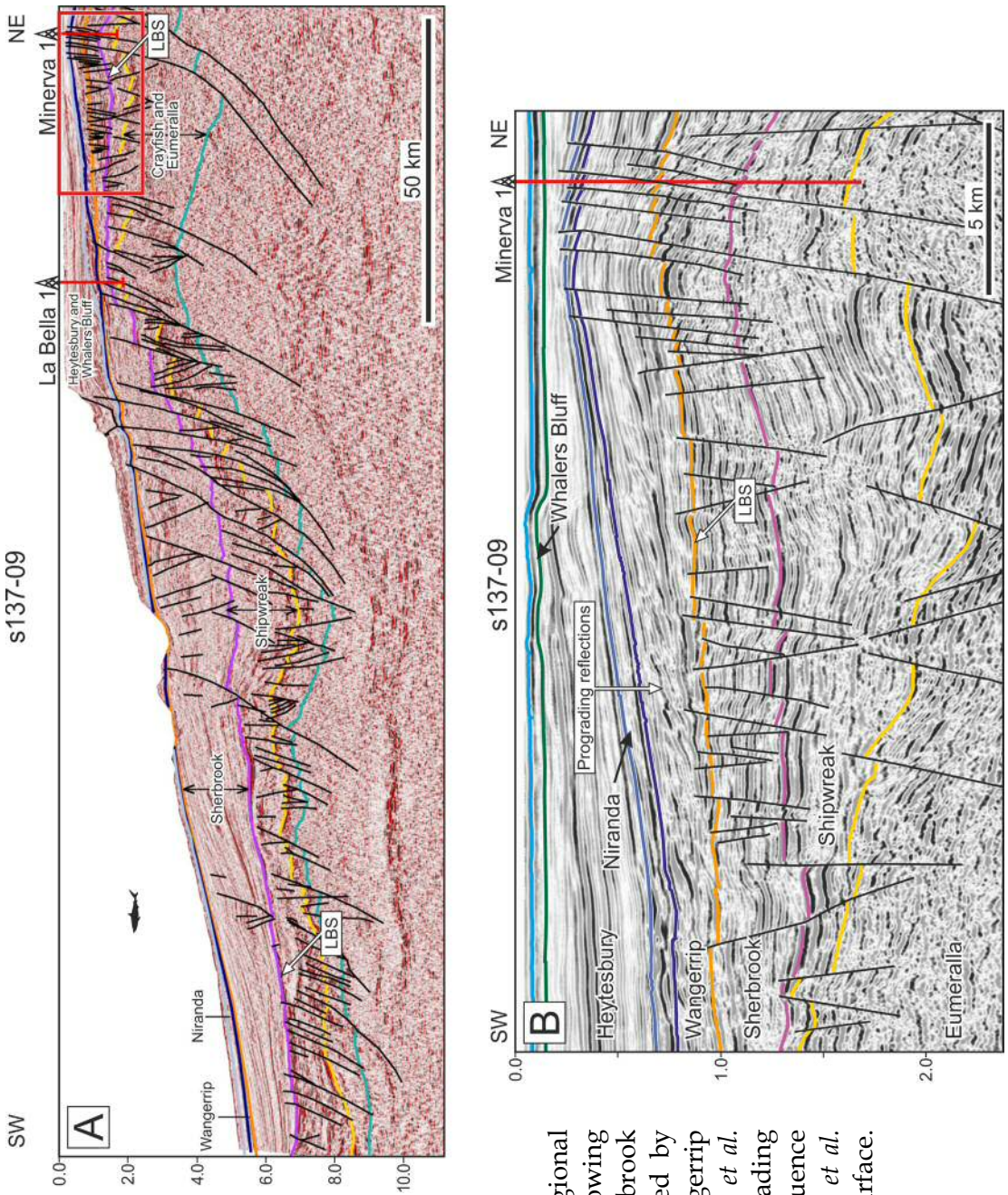


**Figure 6.14** Otway Basin. A—regional seismic profile of the Otway Basin showing the faulted LBS and underlying Sherbrook Supersequence due to loading exerted by the prograding deltaic Wangerrip supersequence. Modified from Stacey *et al.* (2013). B—detail of the basal prograding character of the Wangerrip Supersequence over the LBS. Modified from Krassay *et al.* (2004). LBS—lithospheric breakup surface. Location of A in Figure 6.13.

Sedimentation resumed on the continental shelf with the deposition of the Wangerrip Supersequence above the LBS (Fig. 6.3 and 6.14). Comprising once again deltaic, coastal plain and inner shelf environments, this supersequence is dominated by progradational sequence sets deposited during a highstand period. Basal strata in the Wangerrip Supersequence accumulated as a lowstand systems tract (LST) and an overlying thin transgressive systems tract (TST) (Krassay *et al.*, 2004) (Figs. 6.14 and 6.15). Distally, the Wangerrip Supersequence truncates the underlying Sherbrook Supersequence, with prominent incised valleys being observed along the margin (Stacey *et al.*, 2013). The supersequence is constituted mainly by low to high amplitude reflectors displaying basal flat-lying reflectors, eroded in places, with progradational strata atop—generally thinning basinwards (Holdgate & Gallagher, 2003) (Figs. 6.14 and 6.15). In the most distal areas parallel, continuous reflectors onlap the Sherbrook Supersequence (Stacey *et al.*, 2013). Minor syn-depositional faulting can be observed, restricted to some proximal areas (Fig. 6.15). The basal LST and TST deposits are represented by thin shales (except in its main depocentre, the Portland Trough) with abundant glauconite that is downlaped by the strongly progradational highstand systems tract (HST) deposits (Lavin, 1997; Krassay *et al.*, 2004). This upper HST chiefly consists of amalgamated sandstone with interbedded sandstone, siltstone and mudstone, coal and massive mudstone units (Krassay *et al.*, 2004). Southwest of the Otway Basin, in the centre of Sorrel Basin, growth wedges can be observed on the Wangerrip Supersequence due to ongoing extension in this area (Stacey *et al.*, 2013).

An unconformity separates the Wangerrip Supersequence from the Nirranda Supersequence (Fig. 6.2). This younger supersequence comprises a basal siliciclastic succession deposited during a TST in deltaic to paralic environments, grading to a calcareous HST deposited in open marine environments, with an aggradational to progradational character (Stacey *et al.*, 2013).

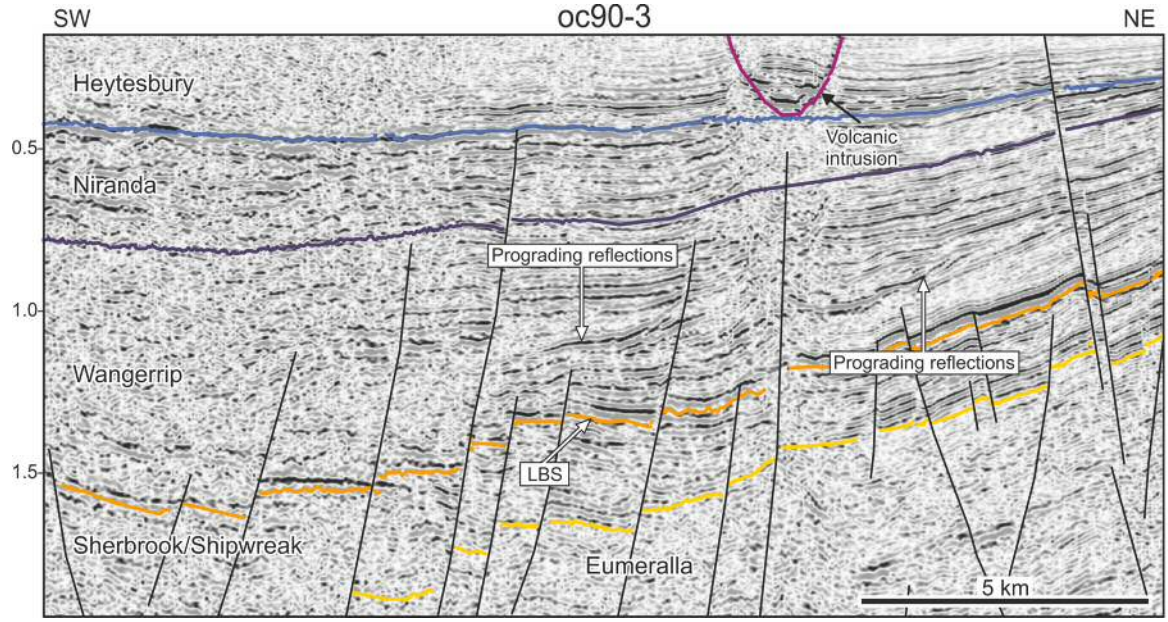


**Figure 6.15** Aspect of the Wangerrip Supersequence. Note that the here observed syn-sedimentary growth within the Wangerrip Supersequence is localized and not widespread. Note the prograding reflections in the Wangerrip Supersequence onlaping the LBS. Modified from Krassay *et al.* (2004) LBS—lithospheric breakup surface. Location of seismic profile in Figure 6.13.

## 6.6. East Antarctica tectono-stratigraphy

Basin nomenclature on the East Antarctic margin is based on the geographical nomenclature of onshore locations. From west to east, East Antarctica is divided in Wilkes Land; Terre Adélie; George V Land and Oates Land (Figs. 6.1 and 6.16). Despite the existence of several seismic surveys acquired on the Antarctic side of the SRS (*e.g.* Fig. 6.16), no industry or scientific wells were drilled down to syn-rift sediments. The deepest well (in terms of geological time) on this margin is IODP Site U1356 (Leg 318), reaching Early Eocene sediments offshore Terre Adélie (Escutia *et al.*, 2011) (Figs. 6.2 and 6.16).

Despite the lack of biostratigraphic or isotopic data available, correlations between the Antarctic and Australian margins have been made by several authors by comparing their seismic stratigraphy, seismic facies and unconformities of regional

expression (Eittreim *et al.*, 1985; Wannesson, 1991; Tanahashi *et al.*, 1994; Eittreim *et al.*, 1995; De Santis *et al.*, 2003; Stagg *et al.*, 2005; Colwell *et al.*, 2006; Close *et al.*, 2007; Lane *et al.*, 2012). In particular, the pronounced rift symmetry observed between the GAB and Wilkes Land (Colwell *et al.*, 2006; Close *et al.*, 2009; Direen *et al.*, 2011) facilitated these correlations. Although this symmetry is not observed eastwards of GAB and Wilkes Land (Espurt *et al.*, 2012), similar seismic facies comparisons were used by several authors to construct workable stratigraphic frameworks for the region (*e.g.* Stagg *et al.*, 2005; Close *et al.*, 2007; Lane *et al.*, 2012) (Fig. 6.2). However, this kind of correlation is prone to errors and its results should be used cautiously. A good example of how problematic long distance correlation without ground truth (well data) can be is found on the Antarctic margin of the SRS.

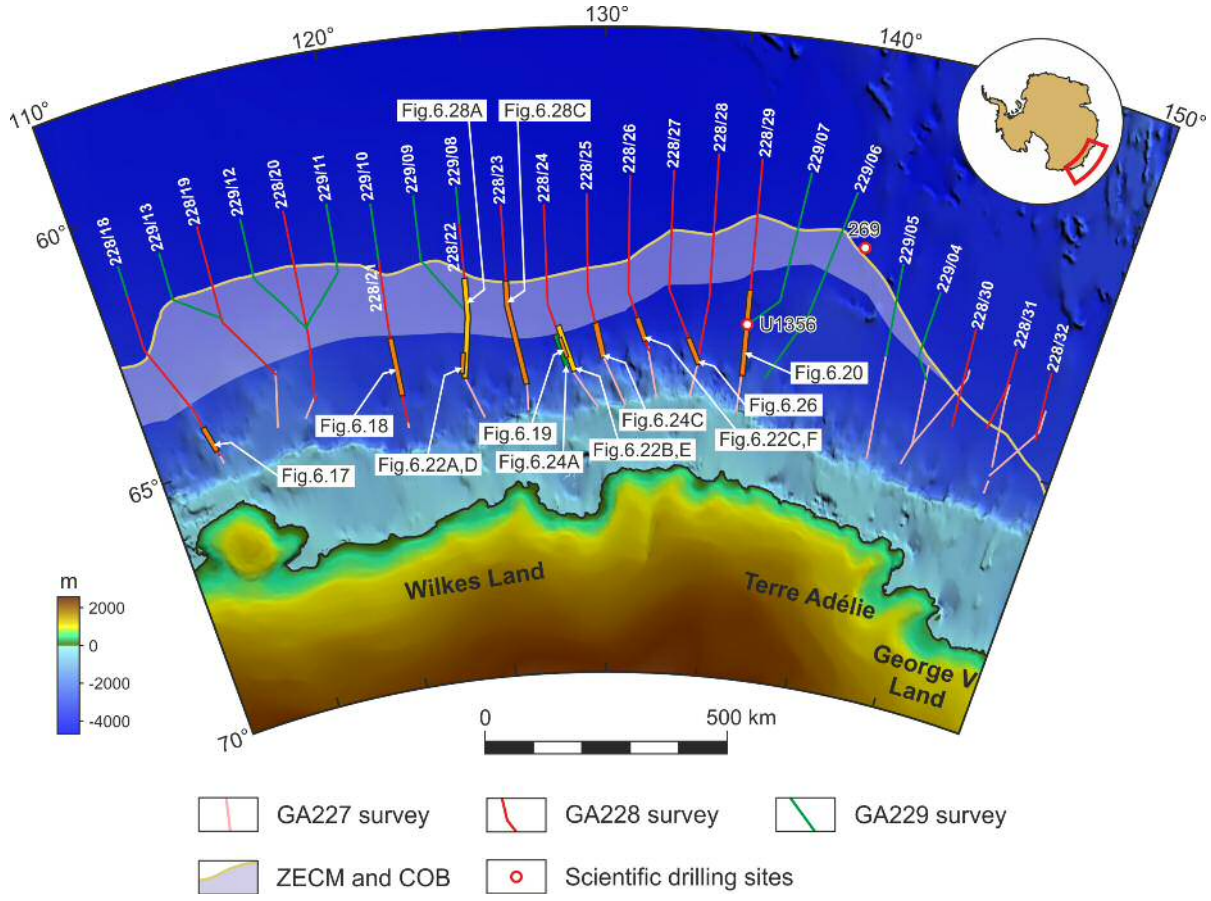


**Figure 6.16.** Antarctic margin of the SRS study area and location of the seismic dataset used in this study. ZECM—zone of extended continental mantle (taken from . COB—continent-ocean transition.

Due to lack of borehole data, the lithology of deep sediments on the Antarctic margin of the SRS is unknown. Yet, some authors proposed a lithological framework for the region. Colwell *et al.* (2006) working with the same seismic surveys used in this study, for purposes of potential field modelling considers the top part of the syn-rift as '*Siliciclastic (…) intruded by sills/dikes*' in the Wilkes Land, and '*Terrigenous (…) with interlayered volcanics*' on Terre Adélie. Without distinguishing between the different observed post-rift packages, the authors give a general depositional/lithological interpretation, '*Post-rift oozes, turbidites and contourites*' for both Wilkes Land and Terre Adélie, adding for the later are the presence of '*Marginal marine chalks, coals*'. Although brief and without much detail, other authors acknowledge the presence of bottom currents during the deposition of post-rift sediments below the so called *Middle Eocene unconformity*, or Maas/Pal unconformity as it is called in this chapter (e.g. Escutia *et al.*, 1997; De Santis *et al.*, 2003; Close, 2004) (Table 6.1).

## 6.6.1. Main unconformities in East Antarctica

Two main unconformities ubiquitous on Wilkes Land and Terre Adélie can be observed on the interpreted seismic datasets (*e.g.* Figs. 6.17-6.19). The oldest of these unconformities marks the end of fault activity in the two regions, while the youngest unconformity is developed as an important onlapping surface.

### *6.6.1.1. End of Extension unconformity (EEU)*

The unconformity marking the cessation of fault activity (Fig. 6.17), was coined as the *breakup unconformity* by several authors (*e.g.* Wannesson *et al.*, 1985; see De Santis *et al.*, 2003 for more references; Eittreim & Smith, 1987; Lane *et al.*, 2012). However, as suggested in Chapter 4, this kind of surface can be merely local, diachronic along the same lithospheric segment, and may not represent the end of continental rifting. Therefore, since this surface effectively represents the end of extension in the areas where it is observed it will be called in this work as *end of extension unconformity* (EEU).

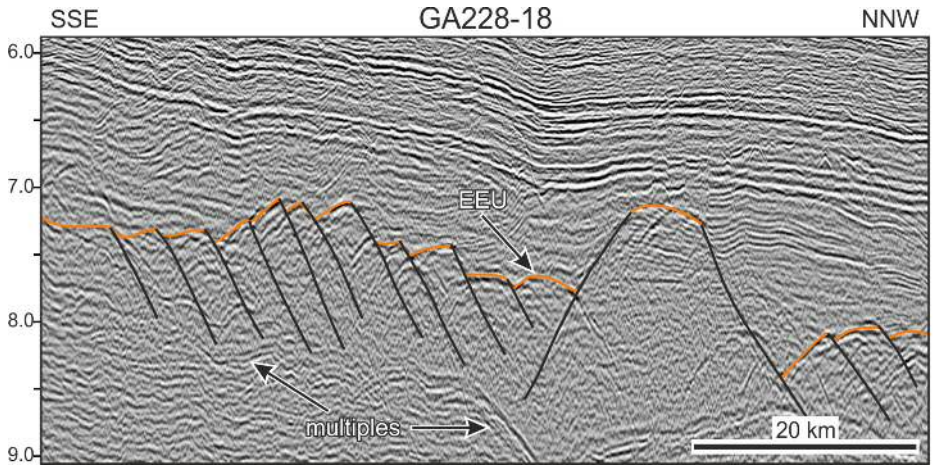


**Figure 6.17** Detail of the *end of extension unconformity* (EEU) on the Wilkes Land. This unconformity is blanketed by sediments deposited during a period of tectonic quiescence, which can be merely local and not representing the end of the SRS extension (see text for more details). Note the downlap on the EEU, well developed on the left of the figure. Location of seismic profile in Figure 6.16.

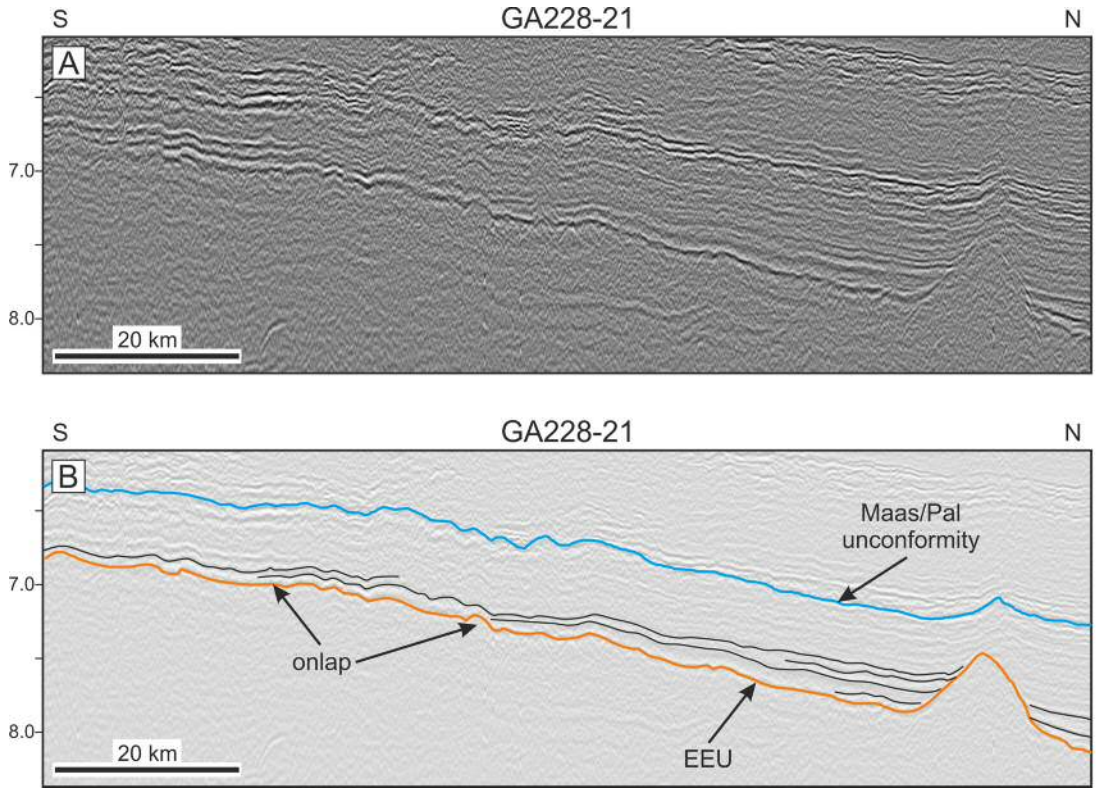


**Figure 6.18**. Onlap of sediments blanketing the end of extension unconformity (EEU). Location of seismic profile in Figure 6.16.

As mentioned above in section 6.3, the age of this unconformity is diachronic along the study area, ranging from Late Turonian in the west to Late Maastrichtian in the east (Blevin & Cathro, 2008; Direen *et al.*, 2012).

Seismic data from the Antarctic margin available for this study are unmigrated, resulting in difficulties in positioning of this surface given its stepped, irregular character (see Chapter 2). In order to find a more correct positioning of this surface it was necessary to partially follow the work of Stagg *et al.* (2005) (*e.g.* Fig 6.18), where the same survey is used, but time migrated (Fig. 2.3). In Stagg *et al.* (2005), due to its inferred diachronic nature, the EEU is called *tur* on the west and *maas* on the east of the area (Table 6.1).

The unconformity develops as a bright reflection, separating faulted sediments due to rifting extension from sediments deposited during a period when tectonic quiescence was achieved at that location, not necessarily implying end of rifting.

Despite the sediments immediately above the EEU being described by some authors as downlaping onto this surface (*e.g.* De Santis *et al.*, 2003; Close *et al.*, 2007), in lines GA228-21 to GA228-26 onlapping is also observed (*e.g.* Figs. 6.18 and 6.19, see Figure 6.16).

Colwell *et al.* (2006) date this same unconformity as base Turonian on the Wilkes Land (Table 6.1), correlating it with the base of the Tiger Supersequence on the conjugate GAB, while on Terre Adélie this unconformity is dated as Maastrichtian, i.e. being equivalent with the Sherbrook Supersequence at Otway Basin (Table 6.1, Fig. 6.2). However, given the lithospheric breakup diachronism found to occur along the GAB (Blevin & Cathro, 2008), it is expected a similar degree of diachronicity at Wilkes Land. In fact, only in the Bremer Sub-basin the LBS can be considered as Turonian in age. Eastwards, on the Ceduna Sub-basin, the LBS is dated as Campanian, whereas on the Otway Basin it is dated as Late Maastrichtian (Blevin & Cathro, 2008) (see section 6.5 above). In addition, Direen *et al.* (2011) assign an Early Turonian to latest Santonian to the unconformity marking the end of rifting on the Antarctic side of the SRS. This was followed by Lane *et al.* (2012), which studying the central part of the Wilkes Land assign an age to this unconformity as latest Santonian-Campanian.

**Table 6.1** Comparative summary of terminology and dates assigned by previous authors for interpreted horizons above the acoustic basement and with relevance for this work. Except for De Santis *et al.* (2003), cited in this table are authors working with the same data sets of the present work (see text for details). Escutia *et al.* (2011) table entry refers only to IODP site 1356 and seismic line GA228-29, crossed by this site. The entries in red [in Donda *et al.* (2001) and Escutia *et al.* (2011)] refer to misinterpreted seismic horizons. All ages were inferred by comparison with the Australian conjugate margin except for Escutia *et al.* (2011) (used dates from strata drilled at IODP site 1356), and the date suggested in this work for horizon Maas/Pal, also calculated using data from IODP site 1356. Maps at the bottom of the columns show the location of the datasets used for each study. For a summary of interpretations older than 2003 the reader is referred to De Santis *et al.* (2003).

| **This work** | | **Stagg *et al.* (2005); Colwell *et al.* (2006); Close *et al.* (2007)** | | **De Santis *et al.* (2003)** | | **Donda *et al.* (2007)** | | **Escutia *et al.* (2011) IODP site 1356, line GA228-29** | |
|---|---|---|---|---|---|---|---|---|---|
| **Name** | **Age** | **Name** | **Age** | **Name** | **Age** | **Name** | **Age** | **Name** | **Age** |
| Olig | Early Oligocene | — | — | — | — | *WL-U3* (only in their Figure 5) | Top of the Eocene sequence | *WL-U3* | Early Oligocene |
| Maas/Pal | Transition Maastrichtian-Palaeocene | *eoc* | early Middle Eocene | *WL-U3* | Top of the Eocene sequence | *WL-U3* | Top of the Eocene sequence | — | — |
| — | — | — | — | WL-U2 (above the LBS) | Top of Palaeocene seq. | — | — | — | — |
| EEU (end of extension unconf.) Terre Adélie-George V Land | Maastrichtian | maas | Maastrichtian | WL-U1 | Top of Cretaceous seq. | WL-U1 | Late Cretaceous | — | — |
| EEU (end of extension unconf.) (Wilkes Land) | Turonian (west) to Campanian (east) | tur | base Turonian | — | — | — | — | — | — |
| 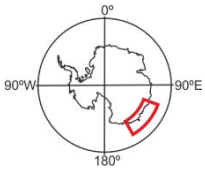 | | 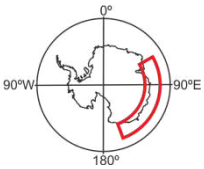 | | 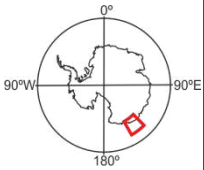 | | 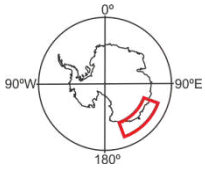 | | 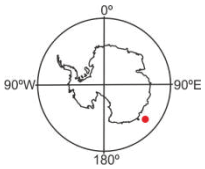 | |

### 6.6.2. The transition Maastrichtian–Palaeocene unconformity

By comparison with the conjugate southern Australian Margin, the youngest unconformity in the studied seismic dataset from Antarctica (called *Maas/Pal* in this work, see below) is dated as Eocene or early Middle Eocene by previous authors (Hampton *et al.*, 1987; Wannesson, 1991; De Santis *et al.*, 2003; *e.g.* Colwell *et al.*, 2006) (Table 6.1). This unconformity is marked by the strong onlap observed on its top surface, with very characteristic upslope climbing reflectors denoting the action of deep bottom currents (Donda *et al.*, 2003; O'Brien *et al.*, 2006) (Fig. 6.19). Observed across the study area, this characteristic is especially developed between 123°E and 132°E (Figs. 6.16). The acoustic expression of contourite drifts is somewhat reduced on the western part of the Antarctic study area. Comprising an erosional unconformity, this surface incises sediments below with variable magnitude (Figs. 6.19). It is usually shown as a basinwards inclined strong reflector, especially where onlap is visible on its top, decreasing in intensity basinwards where it becomes a sub-horizontal, concordant surface. The role played by bottom currents, suggest that the basinwards observable conformity can in fact be a diastem. Given the striking characteristics of this horizon, it is easy to interpret it from line to line on the seismic surveys GA227, GA228 and GA229, even with the wide spacing between the lines of these surveys (*e.g.* Figs. 6.20C and 6.21; see Figure 6.16).

The main objective of IODP Site 1356 was to drill this latter surface and accurately date it (Expedition 318 Science Party, 2011b). As demonstrated in the following paragraphs, at this site the horizon interpreted by Expedition 318 Science Party as *WL-U3* (corresponding to the Maas/Pal unconformity in this work, see Table 6.1) was mistakenly positioned above the actual horizon. This can be inferred by comparing the Expedition 318 Science Party (2011) interpretation of *WL-U3* on the seismic profile crossing Site 1356 (GA228-29, see Figures 6.16 and 6.20B) with the interpretation proposed by Stagg *et al.* (2005) of this horizon (their *eoc* horizon) on the same seismic profile (Fig. 6. 20C, see Table 6.1).

In terms of the continuity of this horizon across the surveys GA227, GA228 and GA229, other authors (*e.g.* Ball *et al.*, 2013; Close *et al.*, 2009; Colwell *et al.*, 2006;

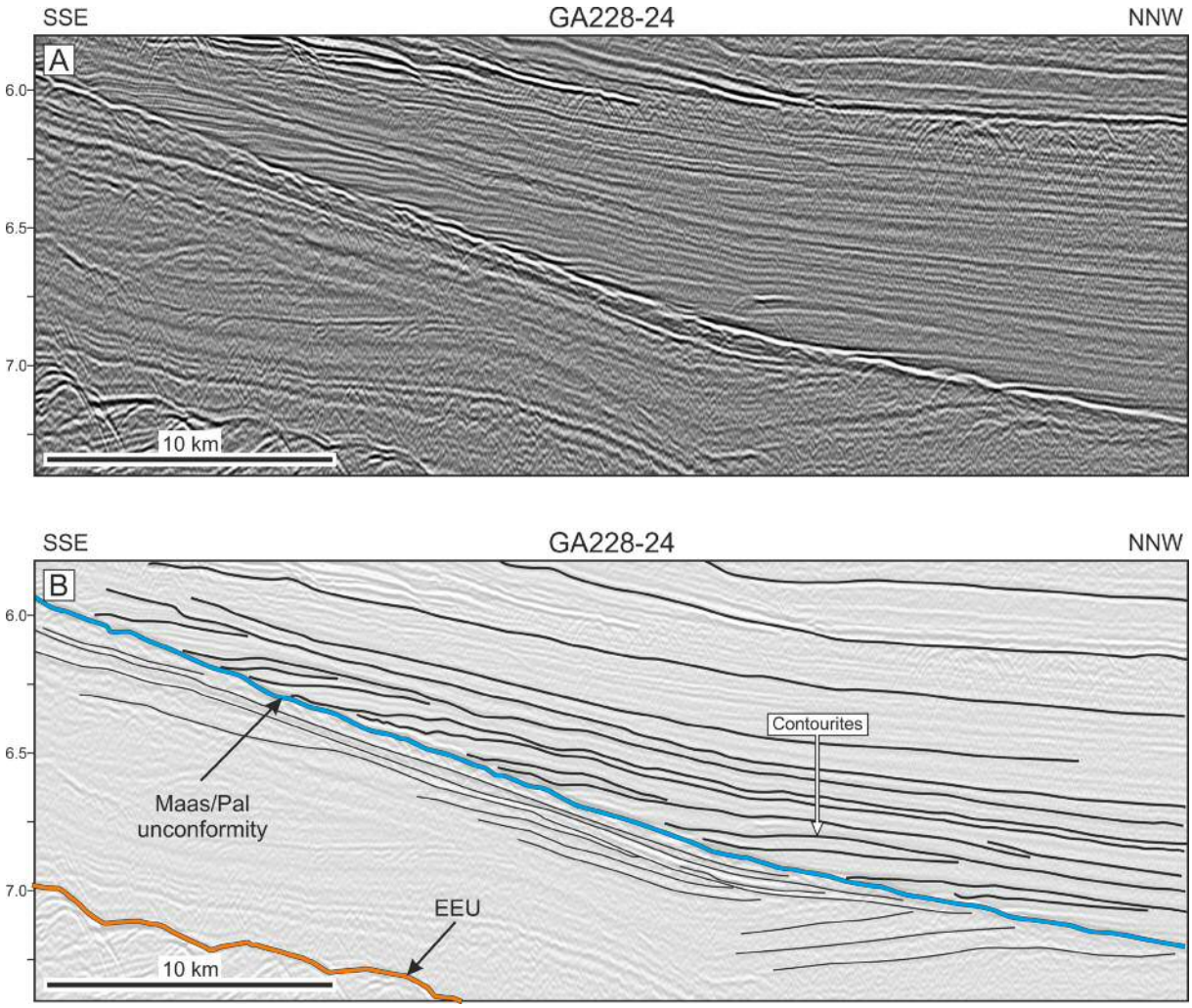


**Figure 6.19.** Detail of the post-rift Maas/Pal unconformity in the Wilkes Land (A) and line drawing of the sedimentary package above it (B). This erosional surface is onlaped by well developed contourites (elongated and separated mounded drifts), which extend for more than 1000 km along the lower slope of this margin. Notice the erosion under this surface, especially on the right side of the figure. For a more regional interpretation of the sedimentary package below the Maas/Pal unconformity in this line, the reader is referred to Figure 6.24 A, B. EEU—end of extension surface. Location of seismic profile in Figure 6.16.

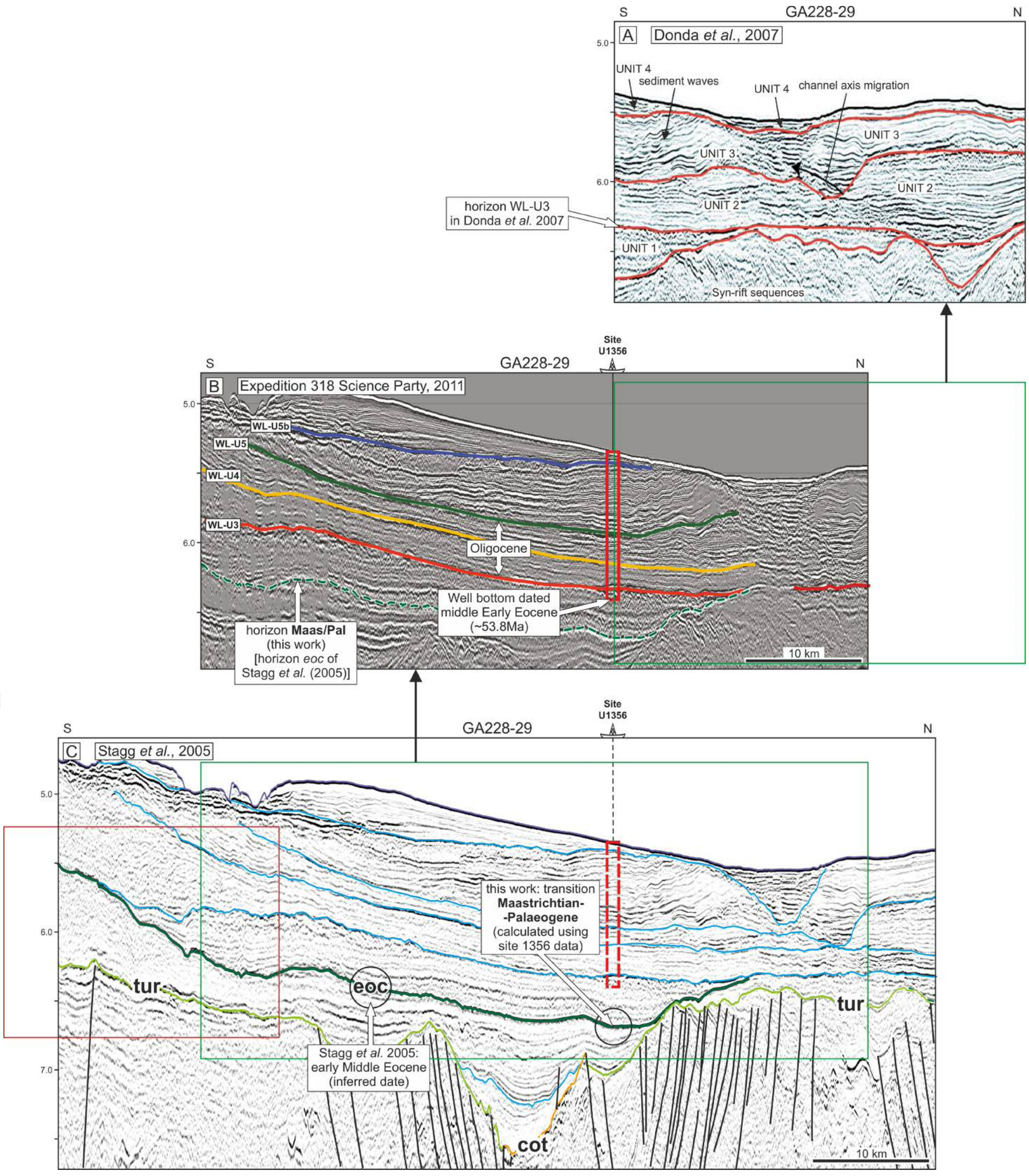


**Figure 6.20** Comparison between Donda *et al.* 2007 interpretation of the Maas/Pal horizon in seismic profile GA228-29. Expedition 318 Science Party, 2011 and Stagg *et al.* 2005 interpretation. A—modified Figure 5 in Donda *et al.* 2007 (major change: scale alteration). The base of Unit 2 is the surface referred by the authors as *WL-U3* (see Table 6.1). B—modified Figure F2 from Expedition 318 Science Party (2011) (major modifications: labels and horizon Maas/Pal added). In their Figure F2 can be seen the location and penetration of IODP 318 Site 1365, together with Expedition 318 Science Party (2011) interpretation of regional unconformities *WL-U3* to WL-U5b. Note that Site 1365 does not cross the horizon 'Maas/Pal' (the green dashed line below the red horizon), named *eoc* in Stagg *et al.* (2005). Green box shows the location of panel A. C—modified section of Plate 17 in Stagg *et al.* 2005 (major modifications: labels and Site 1356 location insertion). In this panel, the *eoc* horizon is equivalent to the Maas/Pal unconformity described in this work (see text). Green box shows the location of panel B, red box shows the location of Figure 6.21. In the southernmost half of seismic profile GA228-29 in panel C are observed the characteristic onlapping of the Maas/Pal unconformity (*eoc* in this panel as in Stagg *et al.* 2005) by contourite drifts, which occurs below the surface labelled as *WL-U3* in panels A and B (compare as well with Figures 6.19 and 6.21). Therefore, Site 1356 did not reach the expected *WL-U3* horizon. All figures share the same vertical and horizontal scale. Location of seismic profiles in Figure 6.16.

Direen *et al.*, 2011; Lane *et al.*, 2012) agree with the interpretation proposed by Stagg *et al.* (2005) independently of the age or formation process they interpret. Similarly, in this work the interpretation of the horizon Maas/Pal is broadly in agreement with what Stagg *et al.* (2005) named horizon *eoc* (Fig. 6.21).

The mispositioning of horizon *WL-U3* by Expedition 318 Science Party is interpreted here to result from the interpretation of seismic profile GA228-29 as shown in Figure 5 of Donda *et al.* (2007) (Fig. 6.20A). Apparently, it was the interpretation of this line by Donda *et al.* (2007) that was adopted by the Expedition 318 Science Party prior to the completion of Site 1356. Unfortunately, although Site 1356 is referred as 'proposed Site WLRIS-07A' in Escutia *et al.* (2011), the available Scientific Prospectus for IODP Expedition 318 does not mention this proposed site (Escutia *et al.*, 2008). Furthermore, the original Integrated Ocean Drilling Program (IODP) drilling Proposal 482 from which Expedition 318 is derived cannot be found online where it should be deposited††.

It should be noted that in Donda *et al.* (2007) the interpretation of horizon *WL-U3* in other seismic profiles from seismic survey GA228 is in agreement with the interpretation proposed by Stagg *et al.* (2005) for their equivalent *eoc* horizon (Fig. 6.22).

Site 1356 crosses the *WL-U3* horizon of Escutia *et al.* (2011) and penetrates 107 m of sediment below it until it reaches a total depth of 1006.4 meters below sea-floor (mbsf). Thus, it does not reach the Maas/Pal horizon (*eoc* horizon in Stagg *et al.*, 2005 and *WL-U3* horizon in De Santis *et al.* 2003; see Table 6.1) (Fig. 6.20B).

Although Site 1356 did not reach the expected target, with the data acquired during the perforation and the seismic data crossing this site (line GA228-29), it is possible to calculate an approximate date for the horizon Maas/Pal. The calculation results are indicated in Figure 6.23A.

†† http://iodp.tamu.edu/scienceops/expeditions/wilkes_land.html; last time accessed: 04-07-2014

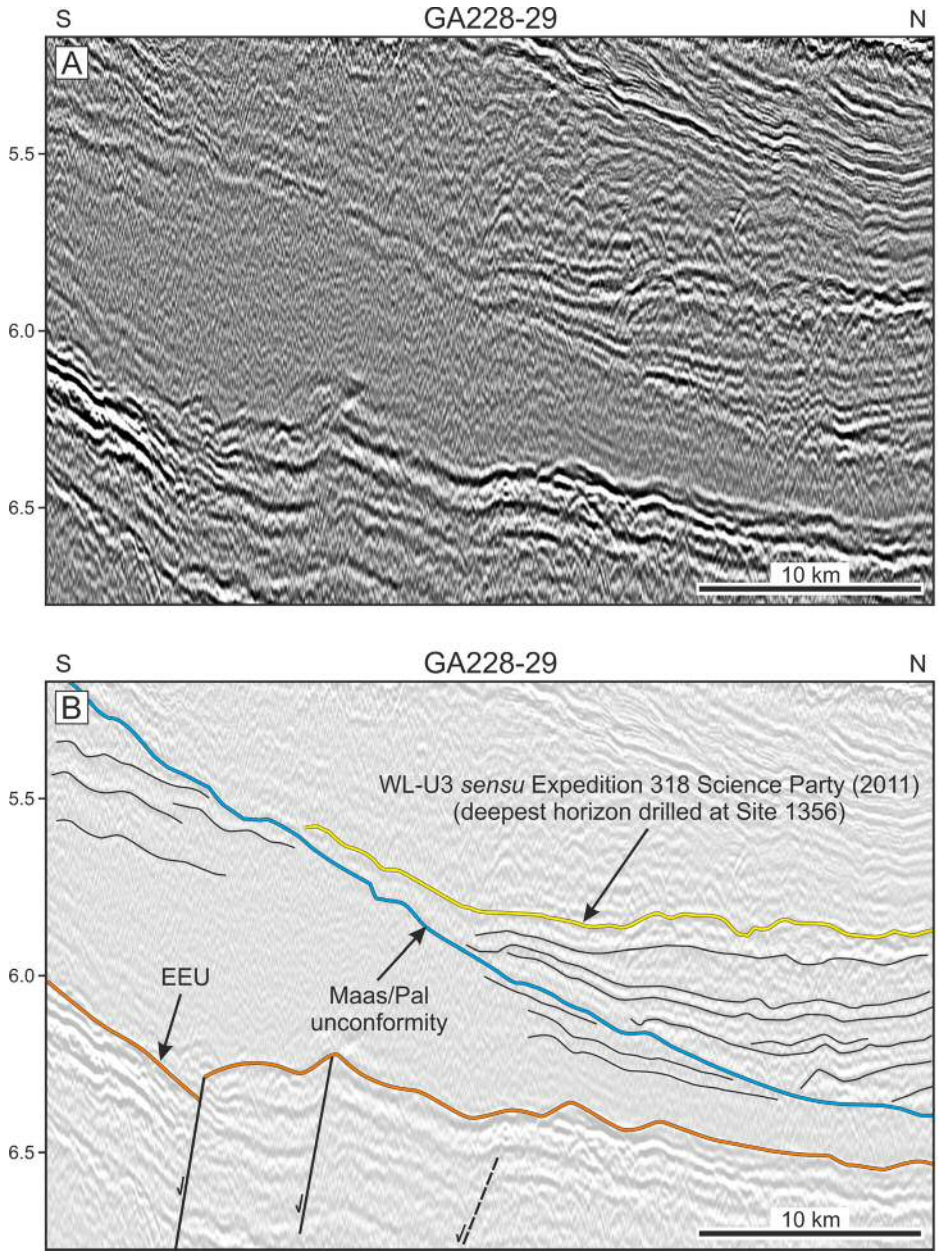


**Figure 6.21** Detail of seismic profile GA228-29 (red box in 6.19C), where one can observe in detail the discrepancy between horizon Maas/Pal and the last horizon (*WL-U3*) drilled by Expedition 318 Science Party, (2011). The strong onlap over Maas/Pal starts well below the misidentified *WL-U3* surface. EEU—end of extension surface. Location of seismic profile in Figure 6.20C.

Site 1356A total depth is not given in time, so it had to be calculated using the depth in time given for horizon *WL-U3* (6.33 s, TWT; Fig. 6.23A); the distance in meters from *WL-U3* to the bottom of the well (113.4 m) and the average sonic velocity measured on that interval (Fig. 6.23B; 2100 m/s).

With the calculated depth in time for the bottom of hole 1356A, [total depth (TD) taken from Expedition 318 Science Party, 2011] it was possible to measure the distance in time from the borehole TD to the horizon Maas/Pal (262 ms, TWT; Fig. 6.23A) and to convert it to meters (275 m; Fig. 6.23A). For this conversion was used an average velocity for the succession drilled between horizon *WL-U3* and the borehole TD (2100 m/s, Fig. 6.23A, B).

Assuming that sedimentation rates for this last part of hole 1356A (between horizon *WL-U3* and the bottom of the hole) were similar until horizon Maas/Pal, a value of 24 m/m.y. was assumed to calculate the length of time that this package took to be deposited (11.4 m.y.; Fig. 6.23A, C).

The age achieved by Expedition 318 Science Party (2011) for the bottom of hole 1356A (53.8 Ma, based on magnetostratigraphic data; Fig. 6.23C), added to the 11.4 m.y. of the remaining sediments until horizon Maas/Pal indicates an age of 65.2 Ma for this horizon. This locates the Maas/Pal horizon on the transition Cretaceous–Palaeocene, therefore calling this horizon Maas/Pal in this work.

It should be noted that these calculations carry errors related to several problems. Of these, the main source of error is related with the poor core recovery below horizon *WL-U3*, an error already acknowledged by Expedition 318 Science Party (2011). However, the absence of visible (major) erosional surfaces below the bottom of hole 1356A and the uniformity in seismic character from horizon *WL-U3* to horizon Maas/Pal, suggests that the extrapolation of the values is reliable. Therefore, the achieved age of 65.2 Ma for this surface is plausible, especially once compared with the Australian conjugate margin where an important Palaeocene unconformity is observed on the Bight Basin and on the Otway Basin (Fig. 6.2). Given the distal position of site 1356A (drilled on the continental rise, see Figure. 6.16), this unconformity would not be expected to display the same degree of erosion (or non-deposition) observed in the Bight Basin.

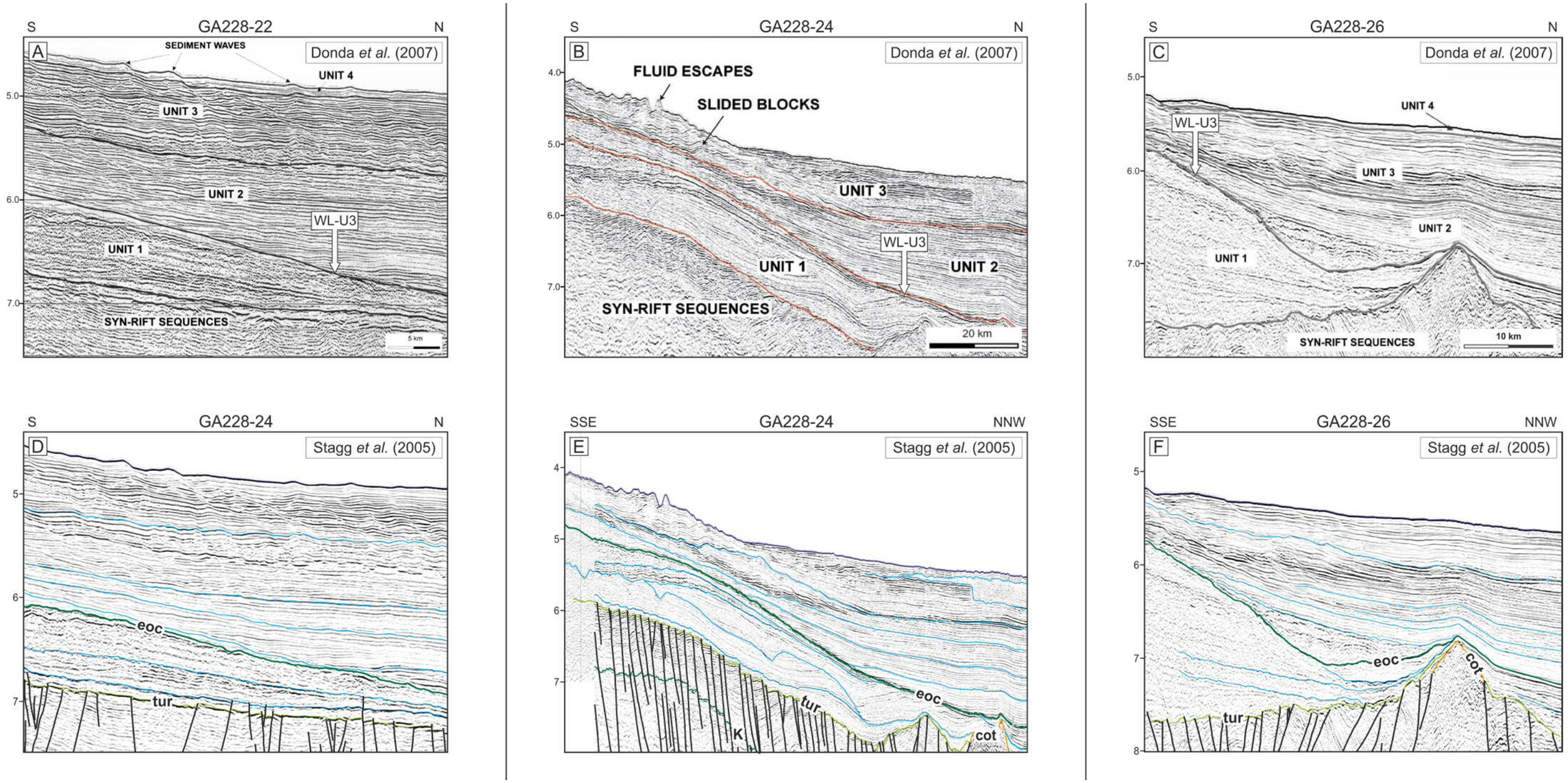


**Figure 6.22** Comparison of Donda *et al.* (2007) and Stagg *et al.* (2005) interpretation of the same horizon in different seismic profiles. On the top row (panels A, B and C) are modified figures 10, 8a and 9 respectively in Donda *et al.* (2007) (major modifications: changes in scale; B is a section of the original figure). In these panels, the *WL-U3* horizon is the bottom of Unit 2. The bottom row (panels D, E and F) are sections from plates 16 (panel D) and 17 from Stagg *et al.* (2005). The *eoc* horizon is signalled in dark green. The columns show the same seismic profile interpreted by the authors mentioned above, where it is possibly to see that the interpretation of *WL-U3* and *eoc* are coincident. The only discrepancy is between panels A and D, where Stagg *et al.* (2005) interpreted the *eoc* horizon a few milliseconds below Donda *et al.* (2007). Panels location in Figure 6.16.

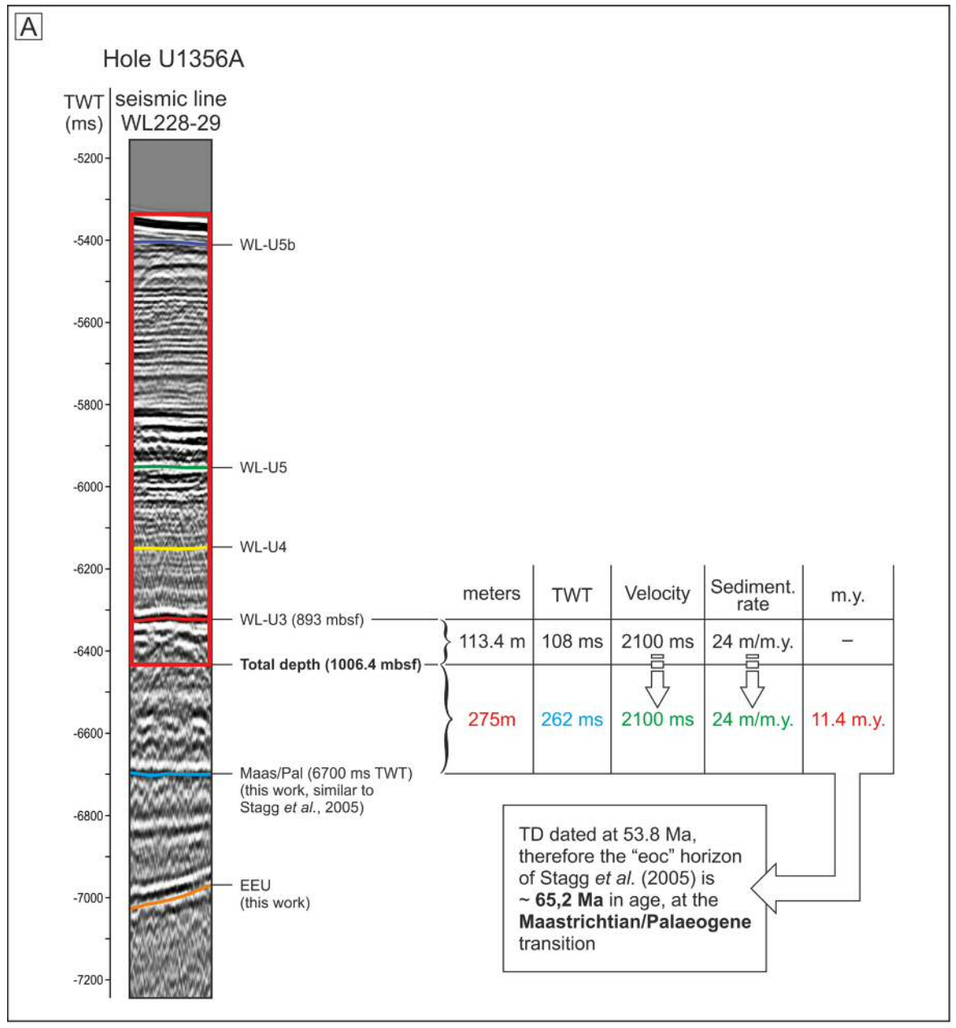


**Figure 6.23** Results and data utilised to re-assess the age of Maas/Pal horizon. A—seismic section from where IODP site 1356A was drilled (line GA228-29) with indication of the horizons described by Expedition 318 Science Party (2011) plus the horizons Maas/Pal and EEU (end of extension surface) described in this work. The table within this panel show in black the data used to calculate the age of the horizon Maas/Pal (from Expedition 318 Science Party, 2011); values in green are extrapolated from Expedition 318 Science Party (2011); in blue is shown the depth in time from the hole bottom to the Maas/Pal horizon. Values in red were calculated using data from GA228-29 seismic line and Expedition 318 Science Party (2011). See text for details. B—P-wave sonic velocities measured in cores from the last sections of hole 1356A. The average velocity of the sediments below horizon *WL-U3* (vertical green dashed line) was visually estimated as the raw data was not available). C—biomagnetostratigraphic age-depth plot for hole 1356A. Blue line represents the best-fit sedimentation rate. Panels B and C modified from Expedition 318 Science Party (2011). Site 1356 location in Figure 6.16.

## 6.6.3. Architecture of post-EEU–pre-Maas/Pal sedimentary package

Given the acoustic and stratigraphic importance of the Maas/Pal horizon, several authors opted to use this surface to define the top of a first post-rift unit, which has the EEU as its base (*e.g.* Stagg *et al.*, 2006; Donda *et al.*, 2007). In fact, the observation of seismic data from the continental slope and rise of the Antarctic margin of the SRS shows that this surface represents a natural acoustic division, separating the first post-rift sediments from younger packages deposited above it (Figs. 6.18-6.22).

With its deposition influenced by several different depositional processes, the thickness is highly variable along the area, ranging from a maximum of 1.5 s TWT (in GA228-26) to 0.75 s (in GA228-19).

### *6.6.3.1. Bottom current activity and turbiditic deposition*

Together with turbidite deposits, the stratigraphic architecture of the unit deposited between the horizons EEU and Maas/Pal suggests important bottom current activity. This is a character not previously described, and with strong similarities with West Iberia (Chapter 5). In fact, the action of bottom currents can be observed on the continental slope and rise of Wilkes Land, especially in seismic profiles GA228-24 to 26 (see Fig. 6.16). Their presence in other lines is very likely. As should be noted, most of the lines eastward of GA228-26, display poor imaging below the Maas/Pal unconformity, which hinder the identification of depositional processes (*e.g.* Fig. 6.21).

This unit, westwards of GA228-24 is usually thin (except in seismic profile GA228-18) and composed of horizontally layered, regular reflections, displaying strong progradation and suggesting that turbidite deposits predominate in the area (Figs. 6.17 and 6.18).

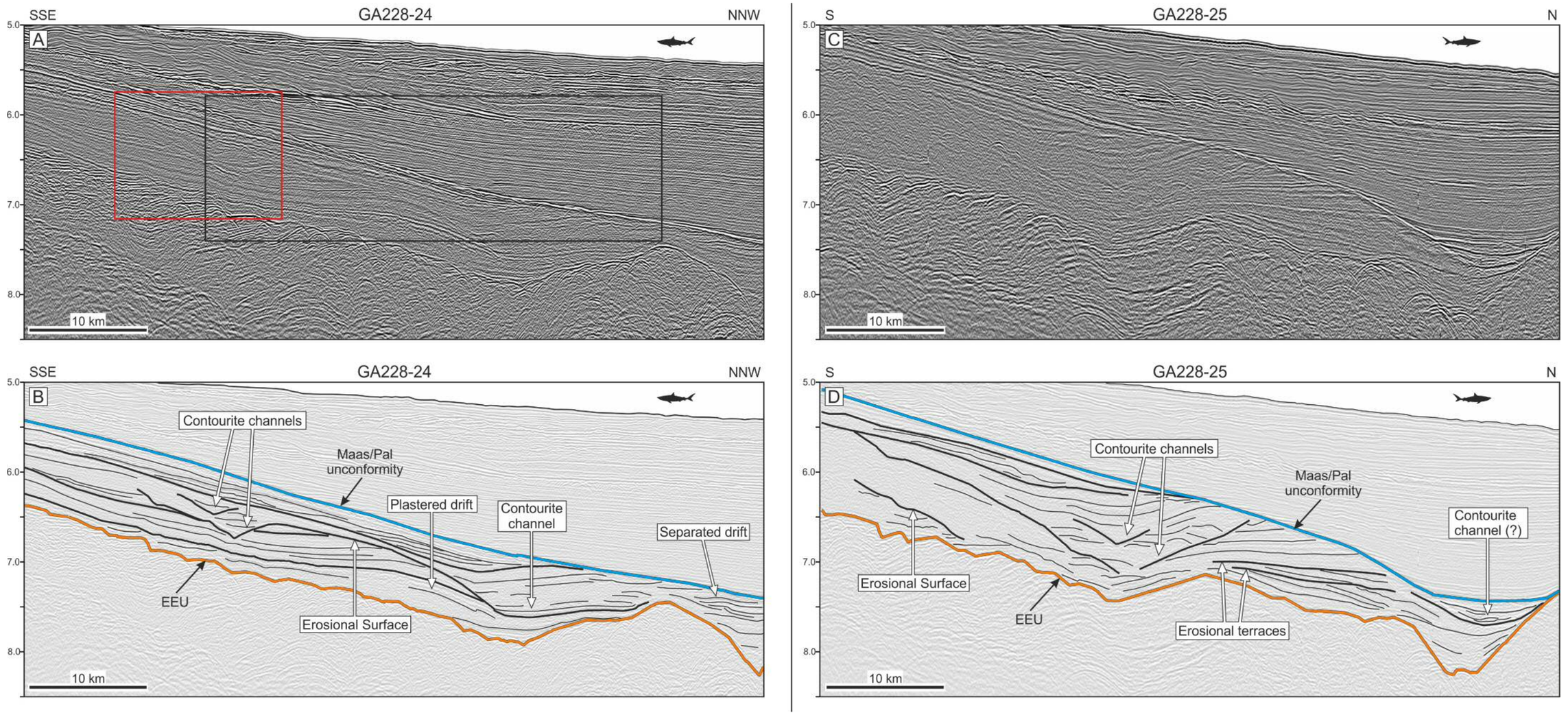


**Figure 6.24.** Cretaceous contourite drifts at east Antarctica. Section of seismic profiles GA228-24 (A) and GA228-25 (C) showing the lower slope and continental rise of the East Antarctica and line drawing interpretation (B and C respectively) of the sedimentary package between the EEU (here of Late Santonian/Early Turonian in age) and the Maas/Pal unconformity. Multiple erosional surfaces can be observed within this package along with the presence of large-scale contourite channels. In B the contourite channel on the right shows upslope migration. Several types of contourite drifts are observed. Note the characteristic stratigraphic architecture of contourites, with the deposition of large-scale mounded reflectors. In A, the black square is zoomed in Figure 6.19 and the red square in Figure 6.25. The distance between these two lines is approximately 100 km, but the large contourite channels observed in these lines seem to be continuous. EEU—end of extension unconformity. Location of seismic profiles in Figure 6.16.

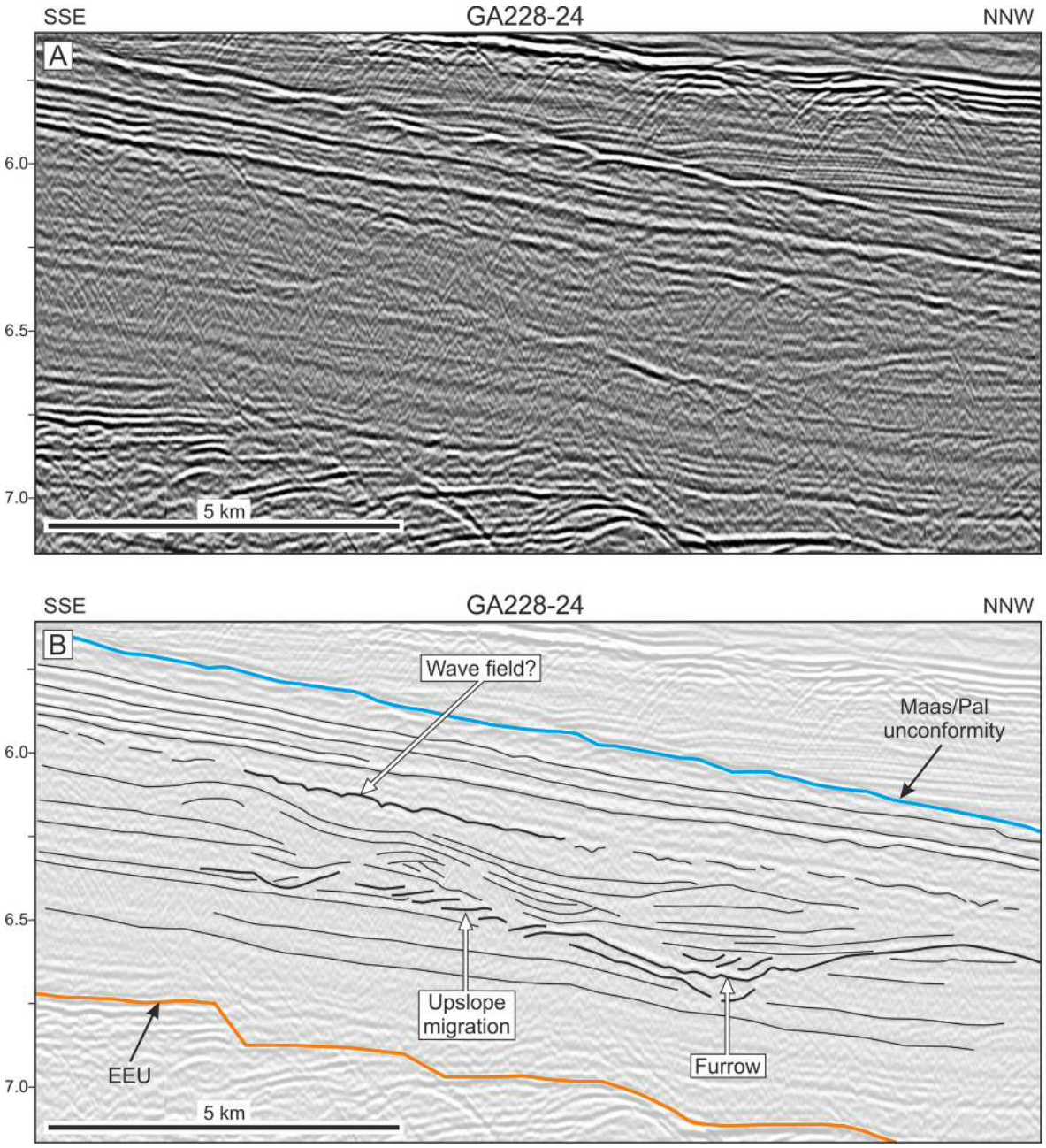


**Figure 6.25** Detail and corresponding interpretation of section from Figure 6.24. In this line a furrow is observed showing its development from an aggradational stage to a later stage with upslope migration of the current that carved it. The channel above the migrating reflections was likely carved by contourites, given the absence of other features that could indicate bottom current activity (as with the previous mentioned channel, the association with upslope migration). See Figure 6.24 for location.

Bottom current activity can be inferred from the occurrence of depositional features such as plastered drifts and separated mounded drifts (Fig. 6.24). Furthermore, areal and linear erosional features (*sensu* Rebesco *et al.*, 2014) extending for several kilometres are also observed, such as terraces, furrows and contourite channels. Although the quality of the seismic data do not allow for a detailed, small-scale characterization of the reflections that constitute these sedimentary bodies, in general they show large-scale undulating reflectors characteristic of bottom current activity (Figure 6.24).

Small scale contourite furrows on the lower slope-rise section are observed on line GA228-24, sometimes associated with erosional terraces (Fig. 6.24). Interestingly, in one of the observed furrows (located above the main channel) are observed landward migrating clinoforms of reduced dimension (Fig. 6.25).

#### *6.6.3.2. Mass-transport deposits*

The presence of mass transport deposits (MTDs) is recognized towards the top of this earliest post-rift package, in seismic profiles GA228-25, GA228-26, GA228-27 and GA228-28, where it becomes thickest (Fig. 6.16). MTDs are probably imaged in seismic profile 227-2701 (basinwards of and contiguous with 228-29), but the poor quality of this profile does not allow a detailed interpretation. Several seaward dipping faults cutting through the sediments tilt and displace several rotational blocks along the slope for several tens of kilometres (Fig. 6.26). They have irregular spacing and distally, the extensional structures seem to curve towards the horizontal, possibly converging into a (tentatively interpreted in Figure 6.26) basal detachment surface. The quality of the seismic profiles in which the MTDs are observed do not allow for an interpretation of other structures commonly associated with this type of deposit. In fact, only the headwall domain of these MTDs is observed, with the transitional and toe domains (if present) (Bull *et al.*, 2009) obscured on the interpreted seismic data.

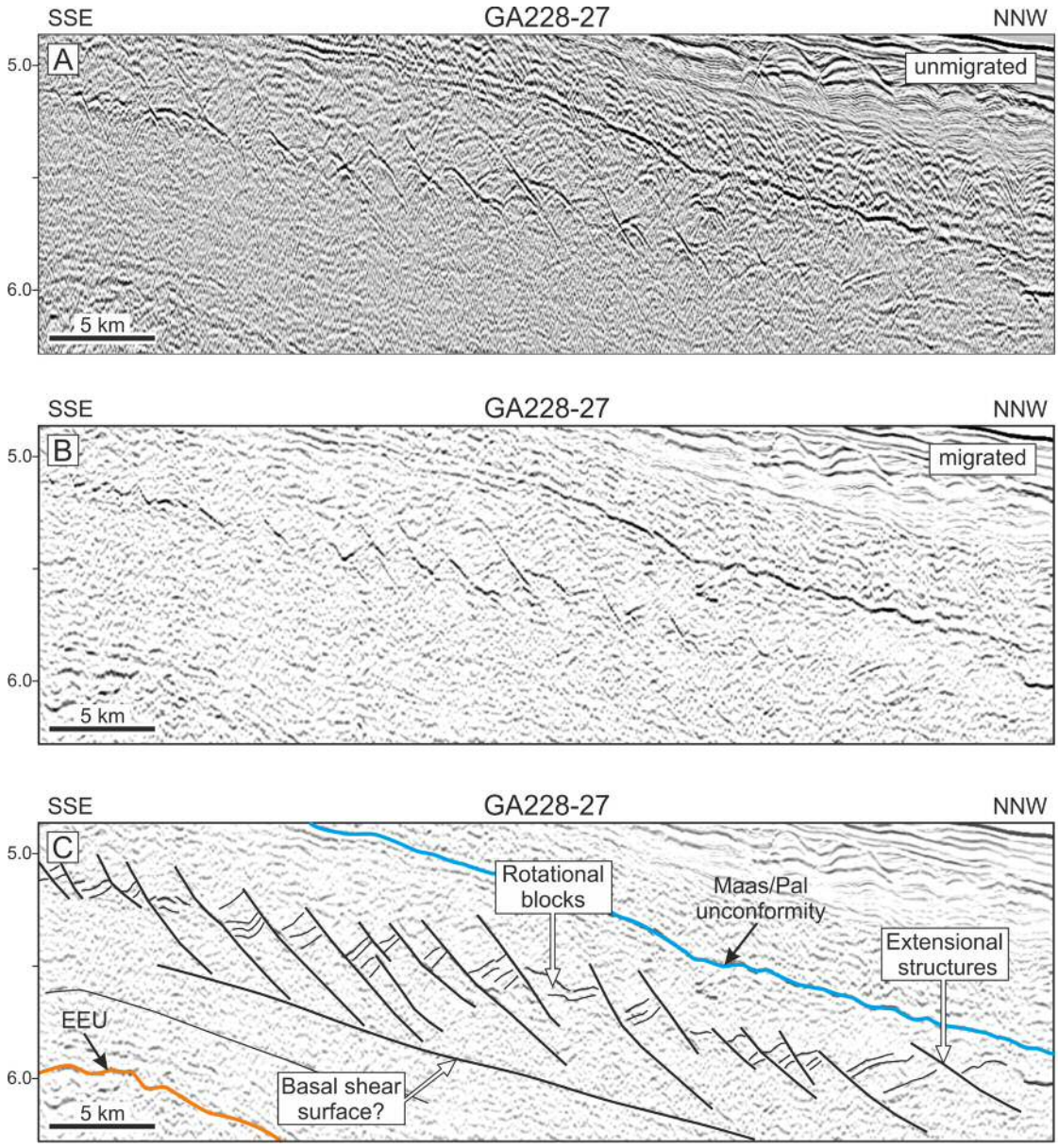


**Figure 6.26** Headwall domain of the MTD occurring on the post-rift package below the early Middle Eocene unconformity. A—stack section. B—time migrated section (from Plate 17 of Stagg *et al.,* 2005). C—line drawing interpretation. Due to the presence of artefacts (the hyperbolae), on the available non-migrated seismic data is difficult to interpret these structures, therefore the migrated seismic data from Stagg *et al.* (2005) were used instead. The downslope mass transport is made by rotation of several blocks along extensional faults. A basal shear surface is tentatively interpreted. Location of seismic profile in Figure 6.16.

These mass movements resemble the same creep-like movements associated with sediment waves documented by Donda *et al.* (2008) on Neogene sediments from the same dataset. The association of gravitational sliding and mass transport movement with sediment waves is well known and frequently one can be mistaken for the other (Correggiari *et al.*, 2001; Lee *et al.*, 2002). Donda *et al.* (2008) describe well developed sediment waves above the creep-like features, a characteristic that can tentatively be assigned to this package, as curved reflectors can be observed above the top of the gravitational faults.

## 6.7. Discussion

Important differences between the GAB and its conjugate margin Wilkes Land in Antarctica are the thickness and character of post-rift successions (Fig. 6.27). The post-rift interval is considerably thicker on the Antarctic margin than on its conjugate margin, mainly due to the fact that after post-Middle Eocene the Antarctic margin received large volumes of glacially derived sediment as turbidites and contourites, whereas the Australian margin was relatively sediment starved (Escutia *et al.*, 2000; Close *et al.*, 2007). The opposite setting occurs regarding the thickness of syn-rift units, being thinner on the Antarctic side and relatively thicker offshore Southern Australia (Direen *et al.*, 2011; Lane *et al.*, 2012) (Fig. 6.27).

### 6.7.1. The LBS in the SRS

As defined in Chapter 4 for Northwest Iberia, the LBS should be developed over divergent reflectors and sealing extensional faults towards the breakup locus, while landward a predominance of parallel reflections denoting local tectonic quiescence is likely to be observed below it (Soares *et al.*, 2012). In Northwest Iberia the existence of several wells along the margin and a good seismic coverage allow a differentiation between the LBS *sensu* Soares *et al.* (2012) and the surface showing the end of extension. Furthermore, the existence of specific characteristics of the LBS on this margin (*e.g.* commonly it is observed as a bright reflector, separating different seismic facies below and above, see Chapters 4 and 5 above) facilitates its identification on seismic data.

#### *6.7.1.1. LBS in Australia*

On the Australian side of the SRS the distinguishing characteristics of the LBS seem to change due to the varied depositional environments that occur there. It should be noted that in this work the majority of the observations of the LBS covered only the inner proximal margin, where the sedimentary environments tend to show more variability. A good example of this variability, is the change in LBS thickness and character observed along the Bremer Sub-basin. The rift-flank uplift that occurred at the time of lithospheric breakup created an angular unconformity, which is very pronounced on the west part of the Bremer Sub-basin (Fig. 6.5B). This can be due to the fact that lithospheric breakup was achieved South of the Naturaliste Plateau, west of the Bremer Sub-Basin, only around 2 Ma before (Direen *et al.*, 2012 and references within), allowing for greater mobility in the lithosphere to the west of the Bremer Sub-basin. Elsewhere on the proximal margin, the LBS develops as a moderately incising erosional surface with horizontal reflectors above, and sometimes as an erosive surface of forced regression (Fig. 6.6).

In other areas of the Bight Basin, the LBS is observed as the contact between horizontal strata without apparent erosional unconformities, particularly on the distal Recherche Sub-basin (Figs. 6.5C, 6.9A and 6.12). The presence of proximal prograding reflectors above the LBS is common on the Bight Basin. Not always they occur as the product of a forced regression but as normal progradation, although at low angle (Figs. 6.10 and 6.15).

On the Australian margin, the observed LBS fits well with the definition provided in Chapter 4 (and in Soares *et al.*, 2012). Nevertheless, on its western part this does not always occur. Here the LBS (and the Hammerhead Supersequence deposited above it) is faulted (Figs. 6.10 and 6.14B). In fact, on the Ceduma Sub-basin the proximal LBS is faulted (*e.g.* Fig. 6.10), as it develops large listric faults due to the margin collapse promoted by the massive sediment load of the Hammerhead Supersequence (Totterdell *et al.*, 2003; Macdonald *et al.*, 2012a). The same occurs in the Otway Basin, with faults cutting the LBS and the Wangerrip Supersequence above due to slope instability and sediment loading and Cenozoic compression (Blevin & Cathro, 2008; Holford *et al.*, 2014).

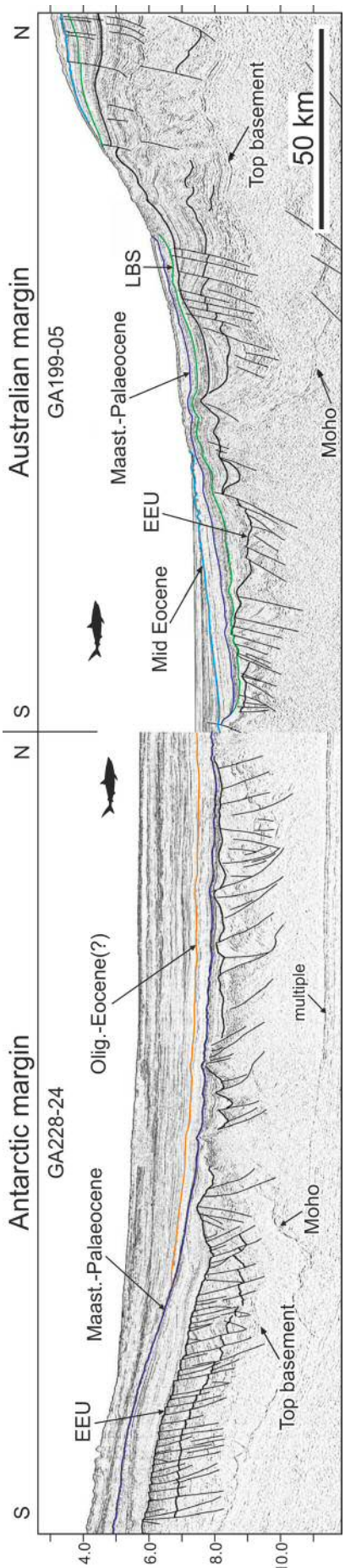


**Figure 6.27** Comparison panel across the conjugate margins of the SRS . It is possible to observe in this profile the difference in the thickness of post-rift sediments, with these being considerably thicker on the Antarctic side. Regarding the syn-rift packages, it is on the Australian side that these sediments are thicker, although the difference between margins is not as dramatic as for post-rift units. The question mark on the age of the orange horizon in Antarctica (Olig.–Eocene) is due to the uncertainty of extending its interpretation from line GA228-29 (dated in this line, where IODP Site 1356 was drilled, see section 6.6.2) without lines transverse to the continental slope. The profiles are joined at the continent–ocean boundary. LBS—lithospheric breakup surface. EEU—end of extension unconformity. Modified from Direen *et al.* (2011) with data from Direen *et al.* (2007) and this work. See Figures 6.1 and 6.16 for profile locations.

#### *6.7.1.2. LBS in Antarctica: GAB–Wilkes Land-Terre Adélie lithospheric breakup*

On the distal SRS Antarctic margin, the identification of the LBS between the GAB and the Wilkes Land-Terre Adélie poses a difficult problem (Fig. 6.2). Within the sedimentary package deposited between the horizons EEU and Maas/Pal and concerning the LBS definition, no notable reflector or obvious seismic facies transition can be correlated across the available data (Figs. 6.18, 6.19, 6.21, 6.24-26). Nevertheless, in seismic profiles GA228-22 and GA228-23 (conjugate with the eastern side of the Bight Basin) a surface was tentatively assigned to the LBS (Fig. 6.28). This surface is a strong reflector, erosive in places and it seems to separate two different seismic facies, especially towards the lower part of the continental slope (Fig. 6.28). Crucially, this reflector terminates at the continent-ocean boundary (as proposed by Stagg *et al.* 2005), as expected from a LBS.

Although the tentatively identified LBS only appears in two seismic profiles, this can be due to the fact that it was eroded by the (presumably) strong bottom currents that were triggered after the lithospheric breakup (see also Soares *et al.*, 2014). In fact, in Figure 6.28D can be observed that the development of an erosional surface truncates the LBS. In Figure 6.28A-B, the same erosional surface truncate the sediments deposited immediately above the LBS, and it is in the same position along the slope where these sediments are thinner due to erosion. Such a character strongly suggests the action of a strong, parallel to the slope bottom current carving sediments below.

The fact that the LBS does not seem to be present to the east of seismic profile GA228-23 can be explained by an increase in the erosive power of this current, completely obliterating the LBS. Strengthening this hypothesis is the large contourite channel that is observed in this same position along the slope in seismic profile GA228-24 (below the Maas/Pal unconformity, Fig. 6.24A, B). Furthermore, this large contourite channel can be observed carving pre-Maas/Pal sediments up to seismic profile GA228-26, pointing to a bottom current flowing for at least *circa* 400 km (Fig. 6.16).

In essence, several explanations can be advanced for the LBS absence in the majority of the Antarctic seismic data: the surface was eroded by strong post-lithospheric breakup bottom currents; the lithospheric breakup in this margin did not promote a change in the sediment being transported into the basin; the definition of the available seismic data is not enough to resolve the LBS. Although all these explanations can be valid per se, the above shown erosion promoted by the action of strong and persistent bottom currents seems to be the preferred cause for the almost absence of a LBS in the Antarctic side of this SRS sector.

### 6.7.2. The tectono-stratigraphic significance of the Maas/Pal unconformity

As showed in Section 6.5.1.2, the main objective of site 1356A (IODP leg 318) was to drill and date the WL-3U surface but it did not reach the targeted horizon. This horizon, equivalent to the Maas/Pal horizon in this work, was misinterpreted on the seismic lines used by Expedition 318 Science Party. Apparently, this misinterpretation was carried through from Donda *et al.* (2007), where the Maas/Pal horizon (their WL-3U) appear in an incorrect position for the first time (Fig. 6.20 and 6.21; see Table 6.1).

The oldest sediments recovered at site 1356A were dated by the Expedition 318 Science Party as Early Eocene (approximately 53.8 Ma; Fig. 6.23), resting around 275 m (262 ms TWT) above the horizon commonly accepted as early Middle Eocene (*e.g.* Stagg *et al.*, 2005; Colwell *et al.*, 2006; Close *et al.*, 2007) or Late Eocene (*e.g.* De Santis *et al.*, 2003; Donda *et al.*, 2007) (Fig. 6.20; Table 6.1).

Although this horizon was not penetrated by Site 1356, the data acquired with this well (biomagnetostratigraphy, sonic velocity, and estimated sedimentation rates) in conjunction with seismic profile GA228-29 allowed the calculation of a date for this horizon. This calculated date places it on the transition Maastrichtian-Palaeocene (~65 Ma; Fig. 6.20 and 6.23). This date has been proposed before for the same unconformity by Hampton *et al.* (1987), although on the basis of subsidence plots constructed by Eittreim & Smith (1987) where breakup in east Wilkes Land is considered as Cenomanian in age.

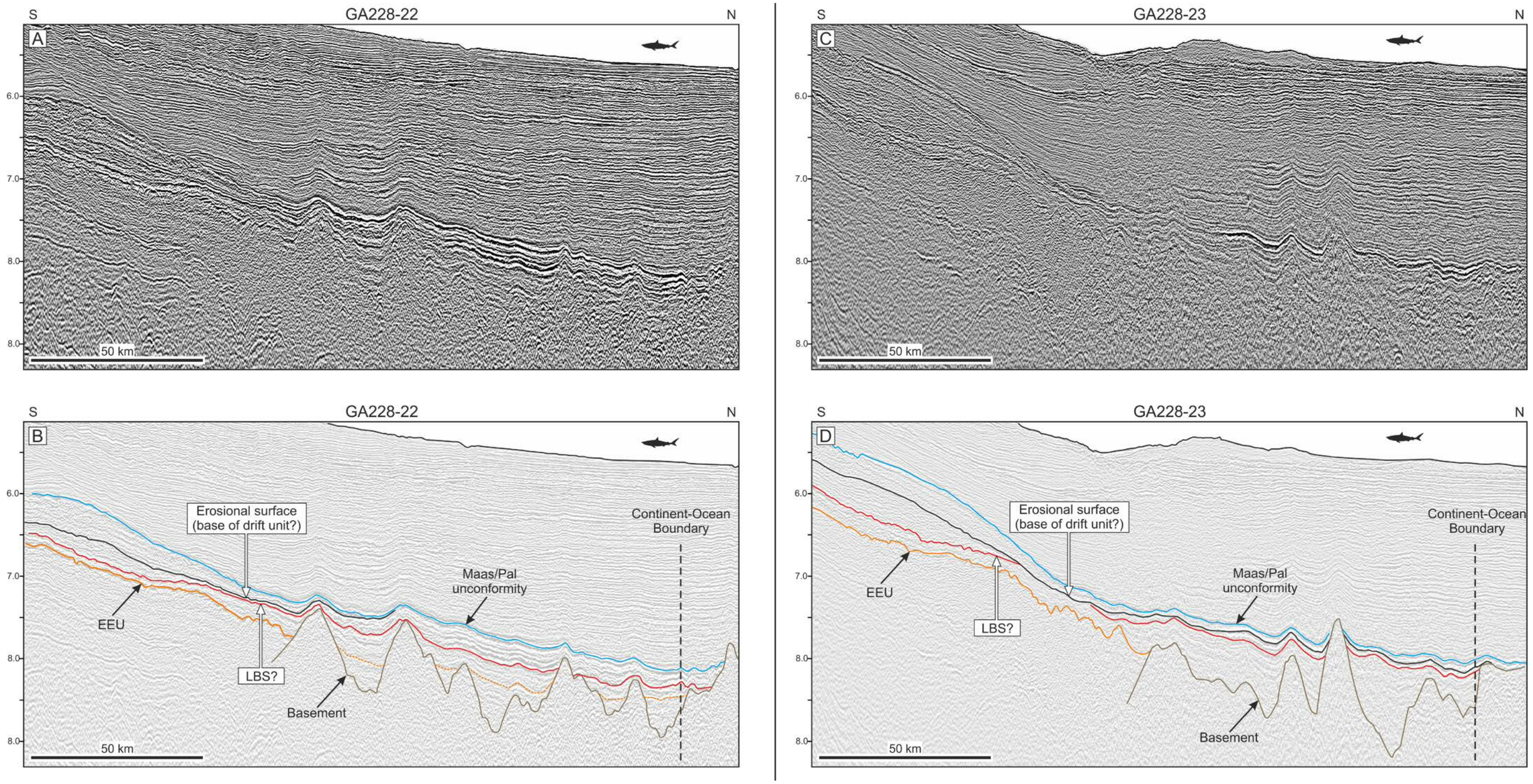


**Figure 6.28** Seismic character of the LBS in East Antarctica. The only location where a reflector can be assign to the LBS is in seismic profiles GA228-22 (A, B) and GA228-23 (C, D). The LBS here is clearly eroded in part by the action of strong bottom currents. Note that the position in D where the LBS was obliterated is the same where in in B the sediments between the LBS and the erosional surface are thinner. This is an indication of parallel to the slope bottom currents (contourite currents). Note that the LBS terminates agains the The position of the continent-ocean boundary is taken from Stagg *et al.* 2005. EEU—end of extension unconformity. Location of seismic profiles in Figure 6.16.

Given the stratigraphic importance of the Maas/Pal unconformity, several works were published where the origin of this surface is discussed. In these works, the authors advance hypotheses for its generation and importance (e.g. Eittreim & Smith, 1987; Hampton *et al.*, 1987; Tanahashi *et al.*, 1994; Escutia *et al.*, 2000; Close *et al.*, 2007). Close *et al.* (2007), discusses in depth several of these works, concluding that '(…) *at least on the deep-water part of the Antarctic margin, the eoc unconformity is primarily caused by changes in deep ocean current flow resulting from increased margin subsidence rates in response to the marked acceleration in sea-floor spreading rate in the Middle Eocene*(…)', Close *et al.* (2007, p. 51). This hypothesis was advanced by Hampton *et al.* (1987) as an alternative explanation for the age and generation of this surface. This way, Close *et al.* (2007) rejects other hypotheses, such as the idea that this surface could represent the onset of glacial derived sedimentation (Eittreim *et al.*, 1995; Escutia *et al.*, 2005; Donda *et al.*, 2007).

The previously suggested explanations for its genesis were based on the Maas/Pal unconformity being Eocene in age, and in this work it was shown that the age of this surface is instead Maastrichtian-Palaeocene. This implies that a new hypothesis is necessary to explain its generation. The calculated Maastrichtian-Palaeocene date for this surface places it very close to the age of breakup between the Otway Basin and Terre Adélie/George V Land (Falvey, 1974; Lavin, 1997; Krassay *et al.*, 2004; Direen *et al.*, 2012) (Figs. 6.1, 6.2 and 6.16). Its re-assessed age, and the fact that the Maas/Pal horizon is a surface onlaped by contourites extending for a considerable length along the Antarctic margin, strongly suggests that this surface is in fact the LBS originated by lithospheric breakup occurring in this eastern segment of the SRS. However, a question concerning the asymmetric development of this surface still arises: if this is the late Maastrichtian LBS, why it is so well developed on the Antarctic while on the Australian margin the same is not observed? A definitive answer to this question with the scarce dataset available for the Australian margin (specially the distal margin) is problematic, nevertheless some insights can be achieved.

In Figure 6.2 can be observed that an important unconformity dated as latest Maastrichtian exists across the Bight Basin (Totterdell *et al.*, 2000). Although not so

developed as in the Bight Basin, this unconformity is recognized in Otway Basin and in the west Tasmanian basins (Blevin & Cathro, 2008). Despite the geographical and temporal importance of this unconformity, its genesis is commonly attributed to eustatic variations without further considerations (Holdgate *et al.*, 1985; Totterdell *et al.*, 2000; Bradshaw, 2005). In the Otway Basin, several authors regard it as the *breakup unconformity*, promoting regional compression and truncation but do not mention its regional extension outside this basin (Lavin, 1997; Krassay *et al.*, 2004).

The existence of contourites in distal settings above the Australian latest Maastrichtian unconformity cannot be fully investigated due to a lack of data, nevertheless on the Bremer sub-basin the surface regarded as the base of the Cenozoic (top of Bremer 6; Fig. 6.2) in places is clearly onlaped by reflections that strongly suggest the action of bottom currents (Fig. 6.29). These contourites are very similar to those found onlapping the Maas/Pal unconformity in Antarctica (Fig. 6.19).

As discussed above, several authors correlate the Maas/Pal unconformity to the product of a major plate configuration occurred in the Middle Eocene due to the acceleration of seafloor spreading rate. Instead, here is proposed that this surface was generated as a response to the lithospheric breakup occurring on a pivotal point of the SRS, the western Otway Basin. In fact, the late Maastrichtian lithospheric breakup occurred in a crucial transitional segment of the SRS. The NW and central parts of the Otway Basin is where the transition from an orthogonal-oblique rifting occurs to a transform continental margin and is bounded by two important transform faults: the Spencer Fracture Zone (to the west) and the Tasman Fracture Zone (Miller *et al.*, 2002; Gibson *et al.*, 2011; Gibson *et al.*, 2012; Stacey *et al.*, 2013) (Fig. 6.1). Indeed, the Spencer Fracture Zone (George V Fracture Zone in Gibson *et al.*, 2013) is so important that it is detected by a change in shear wave velocities at up to 200 km deep and it is supposed to mark the location of the Proterozoic rift between Australia and North America (Kennett, 2000 in Miller *et al.*, 2002).

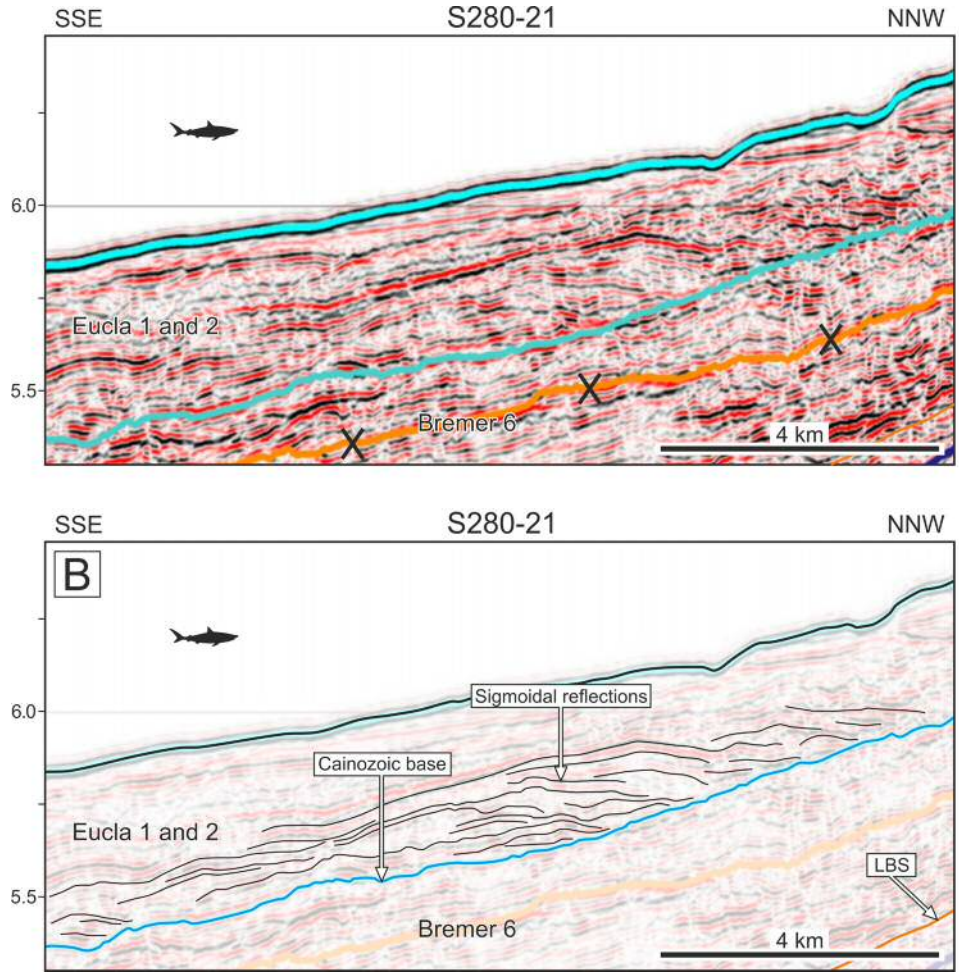


**Figure 6.29** Contourites above the base of the Cenozoic in Bremer Sub-basin. The onlaping reflections resemble very closely those found on the East Antarctic margin, compare with Figure 6.19. Unit boundaries interpretation from Bradshaw (2005) except top Bremer 5 (the LBS) which was reinterpreted (orange horizon with black X is Bradshaw, 2005 original interpretation). Contourite interpretation from this work. LBS—lithospheric breakup surface. Location of seismic profile in Figure 6.4.

Given this, lithospheric breakup occurring in this area is very likely to have triggered a major change in plate configuration. In this way, and invoking the same mechanism used to explain the triggering of currents in Iberia, the lithospheric rearrangement could have disrupted the pressure gradient balance of the water masses around the ruptured lithospheric segment, potentially triggering the installation of new bottom currents. The geographic range of this LBS suggests that this event was very strong when compared with the previous, older LBS observed in Antarctica.

Although the Maastrichtian-Palaeogene LBS is recognized along almost all extension of the SRS, it should be noticed that it does not indicate that lithospheric breakup was a mostly synchronous event along it (as suggested by Whittaker *et al.*, 2007 and in Figure 6 of Müller *et al.*, 2008). In fact, as a corollary of this analysis, the presence of older contourites and another, older surface, which can hypothetically be associated with a LBS in the Antarctic margin (probably Early Campanian in age), reinforces the hypotheses of lithospheric breakup occurring in a diachronous way across the different segments which constitute the SRS.

### 6.7.3. Contourite drifts in Antarctica

Apart from the spectacularly developed contourites above the Maas/Pal unconformity, which can be observed in almost all studied Antarctic margin, the contourites observed within the package EEU–Maas/Pal are restricted to the east part of the Wilkes Land and where the sequence is thicker (between seismic profiles GA228-22 and GA228-23). Nevertheless, after GA228-25 the quality of the seismic data decreases considerably and no clear signs of bottom current activity can be devised with confidence. Therefore, it is possible that the contourites within this package are geographically more extensive, towards Terre Adélie.

In comparison to West Iberia, where lithospheric breakup produced the sudden input of siliciclastic material directly into the basin, bypassing the continental shelf and creating an initial mixed turbidite-contourite system, in Antarctica the oldest part of this package could have been deposited by a similar process. Although good quality seismic data imaging the Antarctic continental shelf in this region is nonexistent (the presence of ice complicates the acquisition process), by comparison with the conjugate margin where a lowering of the relative sea-level is observed at lithospheric breakup with the instalment of an important deltaic system, the same process can be assumed to have acted in Antarctica. In fact, in some of the seismic lines downlaping over the LBS occurs earlier during the formation of the pre-Middle Eocene unconformity. This character can explain the absence of obvious contourites on the initial deposits, especially in the eastern Wilkes Land, since large quantities of

sediment carried to deeper parts of the margin would promote important turbiditic deposition, masking the action of deep currents on the sedimentary process, a process observed in West Iberia (see Chapter 5).

The quality of the data available and the fact that it is stacked data do not allow for detailed observations, such as a better understanding of the interaction between turbiditic and contouritic deposition in this mixed system. The fact that bottom currents create geographically more extensive evidence of their action than turbidites creates an opportunity for contourites to be better perceived in low quality seismic data. Nevertheless, this depends upon the type of contourite and the positioning of the seismic section along a contouritic body.

Between the EEU and the Maas/Pal unconformity, bottom current activity has been briefly mentioned by some authors but not described (e.g. Escutia *et al.*, 1997; De Santis *et al.*, 2003; Close, 2004). However, the interpreted seismic data shows that bottom current activity was present at the time of deposition of this sedimentary package and played an important role in its deposition. Contourites are particularly evident on several seismic lines of the survey GA228 imaging the slope and continental rise of the eastern Wilkes Land, conjugate of the Ceduna Sub-basin (Figs. 6.24 and 6.25).

In Wilkes Land and Terre Adélie the presence of contourites above the Maas/Pal unconformity (Fig. 6.19) is well know, nevertheless, as discussed above, their origin was attributed to different causes mainly due to their erroneously assumed date (*e.g.* Donda *et al.*, 2003; O'Brien *et al.*, 2006; Close *et al.*, 2007).

## 6.8. The BS in the SRS

In the SRS, apparently there are no clear signs of the presence of a BS with a well defined upper boundary for the corresponding studied lithospheric breakups. As previously discussed, not even the LBS seems to occur in all the segments once lithospheric breakup was achieved. It was suggested above that the absence of the

LBS in the Wilkes Land seems to have been caused by the action of strong bottom currents which would have erased (partially or totally) its presence (Fig. 6.28).

The absence of a recognizable top of the BS can be explained in the same way: it could have been erased or, not developed at all given the strength of the bottom currents. In fact, the evidences for bottom current activity here described suggest that they were very strong during the deposition of the sedimentary package EEU–Maas/Pal (carving wide and geographically persistent contourite channels, *cf.* Figure 6.24). Similarly, the contourite drifts found above the Maas/Pal unconformity are found in a very long stretch of the margin, and not only persistent geographically but as well in time (Fig. 6.24). This indicates that even eustatic variations recorded in more proximal environments could not have significant impact in more distal regions of the margin due to the continuous activity of bottom currents. In this way, the recognition of a BS is complicated if not impossible.

## 6.9. Conclusions

In the large geographical span of the Wilkes Land-Terre Adélie area are included several lithospheric segments that underwent breakup at different times, and therefore diachronicity plays an important role in defining the tectonic and stratigraphic architecture of the margins. Despite this diachronicity, the main conclusions of this chapter can be summarized as:

- IODP Site 1356 missed its primary objective, which was to drill the horizon *WL-3U*, here called Maas/Pal unconformity.
- Using seismic data and well data from IODP Site 1356, the age of the younger of two prominent unconformities (Maas/Pal unconformity) observed in East Antarctica was calculated as ~65.2 Ma (Maastrichtian–Palaeocene). This surface was commonly regarded as mid Eocene to early Oligocene by previous authors.
- Lithospheric breakup occurring at different segments of the SRS promoted the development of LBSs, which can be associated to these events.

- Different lithospheric breakup events in the SRS triggered episodes of increased bottom current activity with the deposition of characteristic contourite drifts.
- Bottom current activity can erode the LBS, obliterating partially or completely its presence.
- It is postulated that the last SRS lithospheric breakup event here studied (separation of Otway Basin–Terre Adélie during the Maastrichtian-Palaeocene transition), due to its location on a crucial point of the SRS, gave origin to a significant lithospheric plate rearrangement, generating the Maas-Pal surface which is in fact a LBS.
- Persistent bottom current activity can inhibit (or erase) the formation of the top of the BS hindering its identification.

This chapter shows that many similarities can be traced between the lithospheric breakup events here studied and that of Northwest Iberia–Newfoundland (Chapters 4 and 5). In the following chapter, a discussion about these similarities will be attempted, focusing on how this research can be applied to other margins.

Chapter Seven

# SUMMARY AND DISCUSSION

# 7.1. Introduction

In previous chapters, the use of multiple seismic and borehole datasets allowed the analysis of syn- to post rift transitions on two pairs of conjugate margins, Northwest Iberia–Newfoundland and South Australia–East Antarctica. These two pairs are located in distinct geographic areas, but share common characteristics in terms of rifting and lithospheric breakup processes. Significantly, the analysis developed for Northwest Iberia–Newfoundland produced results that were later confirmed in South Australia–East Antarctica. Yet, differences were found as well, as expected.

In this chapter, the main scientific results of this thesis are summarized and analyzed. Furthermore, detailed results and their applicability to other margins are discussed. Finally, recommendations for future research are suggested based on unanswered questions raised in this thesis.

# 7.2. Summary of results

## 7.2.1. Chapter 4: *The Breakup Sequence and associated Lithospheric Breakup Surface*

In Chapter 4, the characterisation of the syn- to post-rift transition in the shallow offshore Porto Basin, and in deep-offshore regions of West Iberia and Newfoundland (East Canada) was carried out by using regional (2D) seismic-reflection profiles and borehole data. Chapter 4 recognized the development of a regional stratigraphic surface at the time of complete lithospheric breakup between West Iberia and Newfoundland. This surface, commonly called *breakup unconformity*, was renamed in this thesis as the *lithospheric breakup surface* (LBS) based on two main arguments: (1) the surface it is not always developed as an unconformity on all margins and (2) the whole of the lithosphere is involved in the continental breakup process, not only the continental crust. This last point was also raised to differentiate continental crust breakup from the final lithospheric mantle breakup (which occurs after its

exhumation, following continental crust breakup), a process that occurs on multiple magma-poor conjugate margins, such as in Iberia–Newfoundland.

The generation of the LBS is, therefore, attributed to the plate readjustments verified at the moment of plate separation. Previous numerical models show that complete separation of exhumed mantle releases accumulated extensional in-plane stresses during the rifting process, in an event considered to be instantaneous at a geological scale (Braun & Beaumont, 1989; Bott, 1992b; Cloetingh & Ziegler, 2007). This release of in-plane stresses generates a flexural rebound of the lithosphere as large wavelength vertical and horizontal movements, creating localized uplift, subsidence and minor compression along a now thinned lithosphere. As result of these same plate readjustments, changes in the erosion locus (and associated sediment routes) occur during the lithospheric breakup event, altering the preceding late syn-rift stratigraphic architecture. These changes are documented in this thesis to be relevant at a basinal scale, and capable of generating a very distinct stratigraphic surface (the LBS) bounding the base of a distinct stratigraphic sequence, the breakup sequence (BS).

The BS is defined in this thesis as the sedimentary package that records the changes in sedimentation and stratigraphic architecture triggered by lithospheric breakup. Therefore, the BS represents the transitional period between lithospheric breakup and the complete establishment of thermal relaxation as the main process controlling subsidence on divergent continental margins. Thus, the BS changes in character spatially and vertically (i.e. in time) depending on differences in the way depositional systems respond to factors such as palaeodepth, distance from sediment sources, palaeotopography, and the position of depocentres relative to the main extensional locus. In such a setting, the BS can record a forced regressive systems tract on inner proximal margins (along with variations inherent to its positioning on an evolving three-dimensional sequence stratigraphic setting), and may evolve basinwards into depositional environments where turbidites and black shales predominate. The end of the BS is marked in Northwest Iberia by the deposition of a transgressive unit that constitutes a seismic-stratigraphic marker of regional

importance. On the distal margin, and outer proximal margin *pro parte*, the upper boundary of the BS is recognised as an abrupt shift from black shale deposition to barren red mudstones (Fig. 4.13).

The LBS changes in character according to its relative position on the margin, ranging from an onshore hiatus of decreasing magnitude towards the shelf edge, to a diastem or a correlative surface on the distal margin (Fig. 4.14). Nevertheless, this stratigraphic surface is ubiquitous in West Iberia, and has been crossed by deep-offshore drilling campaigns at two sites (Shipboard Scientific Party, 1979, 1987a).

As organic matter is more easily transported over long distances, compared with the heavier components of the sediment load, the forced regression recorded at the base of the BS is accompanied by the deposition and accumulation of organic matter in deep-offshore basins of West Iberia. In fact, at DSDP Site 398, the relative percentage of continental plant debris is high throughout the Albian, with a marked peak that is reached shortly after lithospheric breakup, during the Early Albian (Deroo *et al.*, 1978; Deroo *et al.*, 1979; Taugourdeau-Lantz *et al.*, 1982). This sudden increase in organic matter is likely to be linked to the Aptian–Albian OAE1b. The sluggish bottom ocean currents recorded during the Albian (Robinson *et al.*, 2010) were not able to quickly replenish the oxygen consumed by degrading organic matter accumulated during this sudden episode of terrigenous influx, leading to anoxia in large parts of the deeper continental margin. The lithospheric breakup event can thus be associated with the onset of oceanic anoxic events. Though not necessarily triggering it, the breakup event is at least one of the probable contributing mechanisms responsible for the existence of OAE1b in the North Atlantic.

### *7.2.2.* Chapter 5: *Contourite drifts as an indicator of established lithospheric breakup*

The integration of new seismic datasets with information used in Chapter 4 allowed a detailed investigation of the LBS and BS over a vast area of Northwest Iberia. The main objective of Chapter 5 was to map, describe and characterise the BS in terms of its seismic and depositional facies, with emphasis on deep-offshore areas.

Within the BS are identified three distinct seismic facies reflecting the presence of: a) black shales and fine-grained turbidites, b) mass-transport deposits (MTDs) and coarse-grained, proximal turbidites, and c) contourite drifts. Seismic and borehole data show these depositional systems to have developed as mixed carbonate-siliciclastic sediments proximally, and as organic-carbon-rich mudstones (black shales) distally on the Northwest Iberia margin. MTDs and turbidites are found on the continental slope, frequently in association with large-scale olistostromes. Distally, these mass-wasting deposits change into interbedded fine-grained turbidites and black shales showing widespread evidence of deep-water current activity towards the top of the BS.

This detailed analysis of the BS led to the discovery that contourite drifts, along with other evidence for bottom current activity (such as extensive erosional surfaces), are ubiquitous features within the BS in Northwest Iberia. The absence of bottom current activity below the LBS, and its initiation shortly after, indicates that lithospheric breakup resulted in the triggering of strong bottom currents in the study area. In fact, Chapter 5 postulates that bottom current initiation marks the establishment of fully separate continental margins and can be a useful seismic-stratigraphic indicator of this lithospheric event at a worldwide scale. In addition, such an onset of oceanic currents at a margin scale should have had important impacts in terms of palaeoclimate and faunal dispersion.

### *7.2.3.* Chapter 6: *Lithospheric breakup in South Australia–East Antarctica*

In Chapter 6, the South Australia–East Antarctica conjugate margins (or Southern Rift System—SRS) were studied in order to critically test the results found in Chapters 4 and 5 on different conjugate margins. The choice of the SRS as the region to test the concepts in this thesis results from the fact that rifting was not dissimilar to that recorded offshore Northwest Iberia–Newfoundland. In fact, both conjugate pairs share a magma-poor rift setting, with two lithospheric rifting stages (LRS), and mantle exhumation occurring during LRS2. LRS2 also records a basinwards

migration in the main extension locus. While in Northwest Iberia–Newfoundland the focus of the study was on a single lithospheric segment, the analysis undertaken in the SRS allowed the application of previous results to several crustal segments along the same conjugate margins. The SRS also experienced a diachronous lithospheric breakup along the whole length, allowing the study of interacting and overlapping lithospheric breakup surfaces and resulting breakup sequences.

According to the literature, at least three lithospheric breakup events were present in the SRS (Direen *et al.*, 2012). This thesis shows that the oldest lithospheric breakup apparently did not produce a recognizable LBS, or even a BS. In fact, seismic data from the West Wilkes Land, where lithospheric breakup was first achieved in the studied region, do not show the presence of an unequivocal LBS. Similarly, the presence of a distinct BS was not identified in this same area. Instead, the sediments deposited where the LBS and the BS would be expected to occur are a monotonous, well layered package without any perceivable seismic facies transitions within it.

The two subsequent breakup episodes record LBSs, and associated BSs. Although the first LBS to be observed appears to be truncated and/or completely obliterated by bottom current activity at places, its presence is clear in two contiguous seismic lines, where it shows its diagnostic characteristics: it is recognized in seismic data as a strong reflection, erosive in places and separating two different seismic facies (Fig. 6.28).

The re-evaluation of data from IODP Site 1356 allowed a precise dating of the most prominent seismic horizon in the region: a regional unconformity, onlapped by upslope climbing contourite drifts (the Maas/Pal unconformity, Chapter 6). The dating of this unconformity as Maastrichtian–Palaeogene allowed its identification as the LBS, corresponding to the lithospheric breakup event interpreted by several authors on the South Australian Margin (Lavin, 1997; Krassay *et al.*, 2004) and, by comparison, on other regions of the Antarctic margin (Colwell *et al.*, 2006; Close *et al.*, 2009). This event occurred at an important point of the SRS in terms of its plate configuration: the transition from an orthogonal/oblique extensional rift basin to a

transform margin. The consequent and important plate readjustment verified at this time promoted the development of a LBS and the development of important bottom current activity during the deposition of the BS.

It is in Chapter 6 that the term *end of extension unconformity* (EEU) is proposed to designate the local, diachronous surface that represents the end of the extension in a particular fault (or set of faults) in a particular area of the basin. This EEU is often interpreted on seismic data as the classical *breakup unconformity* if following the first criteria of Driscoll *et al.* (1995) for the identification of the *breakup unconformity*, a common interpretative mistake (see Chapters 1 and 4). In fact, the Driscoll *et al.* (1995, p.2) first criteria says that '*Bedding within the sedimentary succession beneath the unconformity tends to diverge toward depocentres as a result of differential subsidence due to localized block rotation during rifting. In contrast, the sediments overlying the unconformity typically have greater spatial persistence and more uniform thickness* (…)'. As not all faults are active at the same time, and there is a gradual basinward migration of extensional stresses during the rifting process (*e.g.* Reston, 2005), the *breakup unconformity* interpreted in this way is markedly diachronous and does not represent *de facto* the lithospheric breakup event between conjugate margins.

## 7.3. East Antarctica *versus* Northwest Iberia: a comparison

The study carried out on the South Australia–East Antarctica conjugate in Chapter 6 can be directly compared with results from Northwest Iberia–Newfoundland (Chapters 4 and 5). Comparisons are made in this section in terms of observed stratigraphic architectures and the factors that controlled them.

### 7.3.1. Same process, different margins

Geological variations across and within conjugate margins are a well known occurrence (Einsele, 2000; *e.g.* Allen & Allen, 2005; Catuneanu, 2006). Lithological and stratigraphical differences between conjugate margins tend to increase with ongoing rifting as they become more distant, and therefore undergoing increasingly

differentiated geological (*e.g.* differences between an upper plate and lower plate: Driscoll & Karner, 1998) and climatic processes (*e.g.* differences in latitude or oceanic currents affecting asymmetrically the climate on opposite margins: Tucholke *et al.*, 1988; Direen *et al.*, 2011). Along the same continental margin, geological variations are promoted by variations in lithospheric thickness, changes in basement fabric and structures, distinct extensional styles, diachronism in lithospheric breakup, the lithological nature of sediment sources which can contribute with different types of sediment to different areas of the same margin, variable depositional environments occurring at the basin scale—very important in shallow marine to subaerial environments.

All these factors contribute to major changes in the sedimentology and stratigraphy of conjugate margins. The Northwest Iberia and Newfoundland margins illustrate well the differences observed between two conjugate margins (see Chapter 3). Within the same margin they contribute to its compartmentalization in terms of basins and sub-basins which although share the same grand geological history, have nonetheless their particular history.

Given the particularities of each individual continental margin, a comparison between Northwest Iberia–Newfoundland and South Australia–East Antarctica, is expected not to be exact, despite the broad similarities referenced before in terms of their tectonic evolution. As shown in Chapter 6, several basins exist along the South Australian margin. As expected from a modern passive margin with a length of ~1400 km, distinct basins (and sub-basins) show important variability in their stratigraphic record. In fact, stratigraphic schemes and their nomenclature differ along the strike of the Australian margin, with a broad division between its West and the East sectors (Totterdell *et al.*, 2000; Bradshaw *et al.*, 2003) (Fig. 6.2 and 6.3).

Similar along-strike variations are expected offshore East Antarctica, but the absence of drilled wells in this region prevents the analysis of stratigraphic constraints beyond those resulting from seismic stratigraphic interpretations (Chapter 6). As a comparison, the study area in Northwest Iberia involves one single

lithospheric segment and does not record major along-strike stratigraphic variations. Nevertheless, an important change is observed when considering the presence of salt in Peniche Basin. Salt in this basin is more abundant towards the south of the study area (i.e. northwards of Aveiro Fault, see Fig. 3.1), and halokinesis disrupts and influences the stratigraphy of the areas where it is present (Alves *et al.*, 2006).

Despite the diachronism in lithospheric breakup observed along the SRS, this same lithospheric breakup event was able to generate similar stratigraphic features across the Southern Ocean Sea and in distinct crustal segments. Proximally on the Australian margin, common stratigraphic features include a prominent erosional surface truncating late syn-rift deposits (the proximal LBS, Fig. 6.2, 6.5 and 6.10) and the deposition, immediately above the LBS, of prograding reflectors denoting a forced regression or deposited with a very low trajectory angle (Figs. 6.6, 6.10 and 6.15). Basinwards, with the exception of the Bremer Sub-basin (where contourite drifts were identified, Figs. 6.8 and 6.9) limitations imposed by the lack of data did not allow a proper analysis of deep offshore regions. In Northwest Iberia, similar structures were identified above the LBS. In fact, in the proximal Porto Basin the LBS is interpreted as a basal surface of forced regression, downlaped by a forced regression wedge extending beyond the continental shelf (Figs. 4.3 and 4.4).

Given the absence of good quality data on the continental shelf and upper continental slope of East Antarctica (see Chapter 2 and Figure 6.16), it was not possible to investigate the presence of proximal diagnostic features denoting the presence of a LBS. Nevertheless, data covering the outer proximal (partially) and distal margins of East Antarctica allowed for a robust characterization of the LBS and BS in these areas (Fig. 6.16). In East Antarctica, where lithospheric breakup occurred during the Early Turonian (conjugate with the Australian Bremer Sub-basin, the SRS easternmost lithospheric segment studied), there are no diagnostic contourite drifts or even a surface correlatable with the LBS (Fig. 6.2, 6.16 and 6.17).

On the Northwest Iberia distal margin, the LBS and the BS do not always present their characteristic seismic facies. Given this, where their identification is hindered by

this lack of recognizable characteristics, their mapping is done by understanding their spatial lateral variations from adjacent seismic profiles where the LBS and the BS are identified. Nevertheless, the widely spaced seismic grid available in East Antarctic is a limiting factor on the identification of the LBS and the BS using this technique. Although the available dataset shows the transition point between the zone of exhumed continental mantle and true oceanic crust, which should be key to pinpoint the LBS or at least to significantly constrain its position (since the LBS should terminate against that point, see Fig. 7.1), the multiple interpretations concerning the position of this transition (*e.g.* see Close *et al.* 2009), do not serve as an aid in the identification of a cryptic LBS.

LBSs associated with the Early Campanian and Late Maastrichtian lithospheric breakups were, in contrast, interpreted throughout East Antarctica. Here, BSs comprise extensive contourite drift deposits and, in the case of the post-Early Campanian BS, MTDs towards its top. These MTDs occur below the modern upper continental slope in seismic profiles GA228-25 to GA228-28 (covering approximately an extension of 300 km, Figs. 6.16 and 6.26). Similarly to East Antarctica, the presence of MTDs in the BS of Northwest Iberia is limited to the continental slope area, where significant erosion and instability processes are observed during and following the syn-rift stages (Fig. 5.6). Whereas during the post-Early Campanian BS, bottom current activity can be observed ~500 km along the margin (in seismic profiles GA228-23 to GA228-28, Fig. 6.16, 6.24 and 6.25), the extent of the identifiable contourite drift deposits triggered after the Late Maastrichtian lithospheric breakup is more than 700 km. In contrast, the associated LBS spans approximately 2000 km of the same margin. This latter LBS is identified ~500 km west of the study area (in seismic profile 228/14, Plate 14 of Stagg *et al.*, 2005) and ~200 km east of seismic profile 229-06 (in Figure 7 of De Santis *et al.*, 2003).

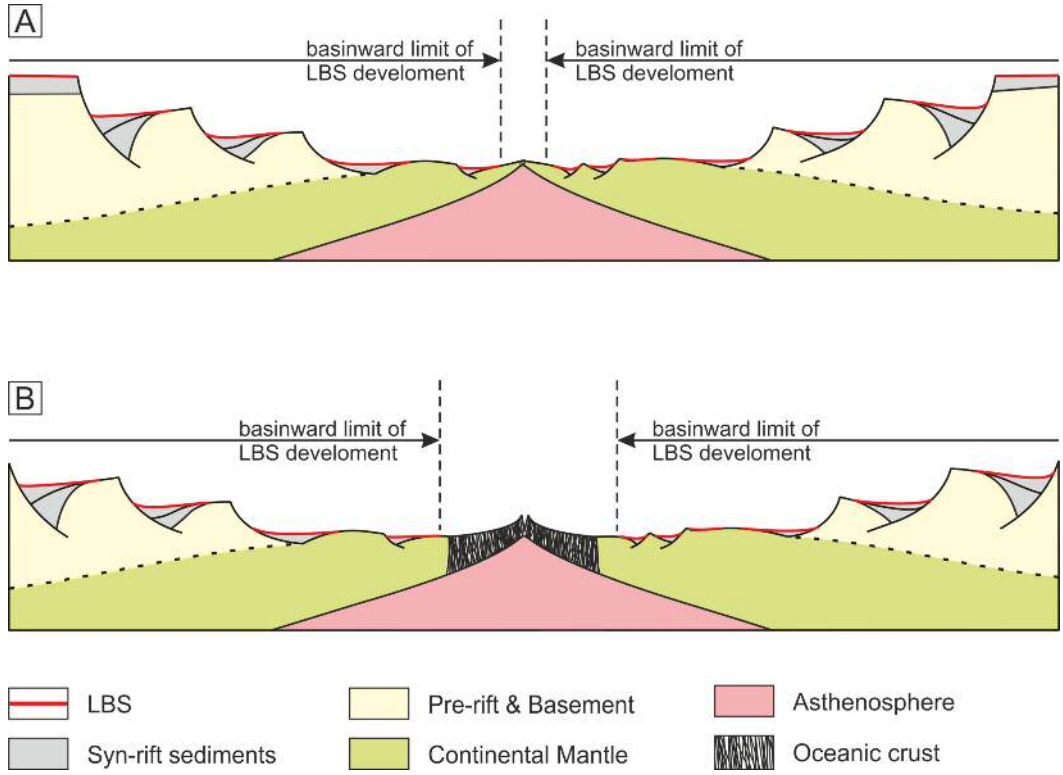


**Figure 7.1** Basinward limit of LBS development. A—moment of lithospheric breakup between conjugate margins, and formation of the LBS (line in red; note that these margins underwent a two phase lithospheric rifting with mantelic exhumation developing during LRS2). B—the same conjugate margins after undergoing oceanic crust accretion. Note that the theoretical basinward limit for the formation of the LBS is the place where the lithospheric breakup will occur. Nevertheless, the LBS may not reach this point since a certain degree of thermal uplift is likely to occur here, impeding sedimentation in these areas.

## 7.3.2. LBS and BS areal extension on a rifted margin

The large extent of the Late Maastrichtian LBS in East Antarctica (the Maas/Pal surface in Chapter 6), extending outside the lithospheric segment from which it was originated leads to two questions: (1) is there a common process to all margins for the creation of the LBS in distal areas? (2) A BS is by definition confined to the lithospheric segment in which lithospheric breakup is recorded. However, since the LBS (its basal unconformity), can extend into adjacent segments, far beyond the original segment where lithospheric breakup occurred, what happens to the BS in these areas?

A contrasting difference between the LBSs of Northwest Iberia and East Antarctica is their relative seismic reflectivity. The LBS in Northwest Iberia results from the basin wide deposition of MTDs during tectonic movements caused by the lithospheric breakup event (Chapter 4). In East Antarctica, the Late Maastrichtian LBS is the product of an increase in the intensity of bottom currents during the lithospheric breakup event. In addition, the LBS associated with Early Campanian lithospheric breakup between the GAB and the Wilkes Land-Terre Adélie shows similar characteristic to Northwest Iberia LBS: a strong reflector separating distinct seismic facies (Fig. 6.28). It should be noted, however, that at the time of the Late Maastrichtian lithospheric breakup event in East Antarctica, there was already in place a bottom current regime, which was further intensified by the lithospheric breakup event. Furthermore, on seismic data is clear that the East Antarctica margin was a well nourished margin at this time, with a relatively subdued submarine topography (*e.g.* Fig. 6.27). This setting contrasts with the multiple underfilled sub-basins that characterize the Northwest Iberia margin (Fig. 4.14). It was from the flanks of the structural highs delineating the sediment-starved sub-basins of Northwest Iberia that MTDs were sourced, creating the LBS (Shipboard Scientific Party, 197; Shipboard Scientific Party, 1987b). Despite these differences, the process that generated the LBS is similar in Iberia and SRS, with main differences between East Antarctica and Northwest Iberia being mostly derived from their palaeo sea-bottom topographies and the amount of sediment supply during the syn-rift. Mass-transport deposits are expected in East Antarctica during the Maastrichtian lithospheric breakup, especially given the fact that it was a well nourished margin, with plenty of sediment available. However, due to a lack of remnant syn-rift topography, MTDs might have been remobilized by the strong bottom current activity and redeposited as extensive contourite drifts.

In order to provide an answer to question (2) above, one should recapitulate the definition of the 'top BS' reflection as proposed in Chapter 4. The top of the BS coincides with a stratigraphic surface marking the transition from a sedimentary regime occurring under the influence of the effects of rift shoulder uplift due to the

lithospheric breakup event (sustained by erosional unloading during several millions of years), to a sedimentary regime occurring under the control of regional thermal subsidence. Given this, since rift shoulder uplift only occurs on the lithospheric segment recording final breakup, the generation of the BS *sensu stricto* is confined to this same segment (Fig. 7.2). This contrasts with what is interpreted on seismic data from East Antarctica, where the LBS extends hundreds of kilometres out of the lithospheric segment where breakup occurs, chiefly due to the lateral propagation of tectonic movements and by widespread bottom current activity along the margin (Chapter 6).

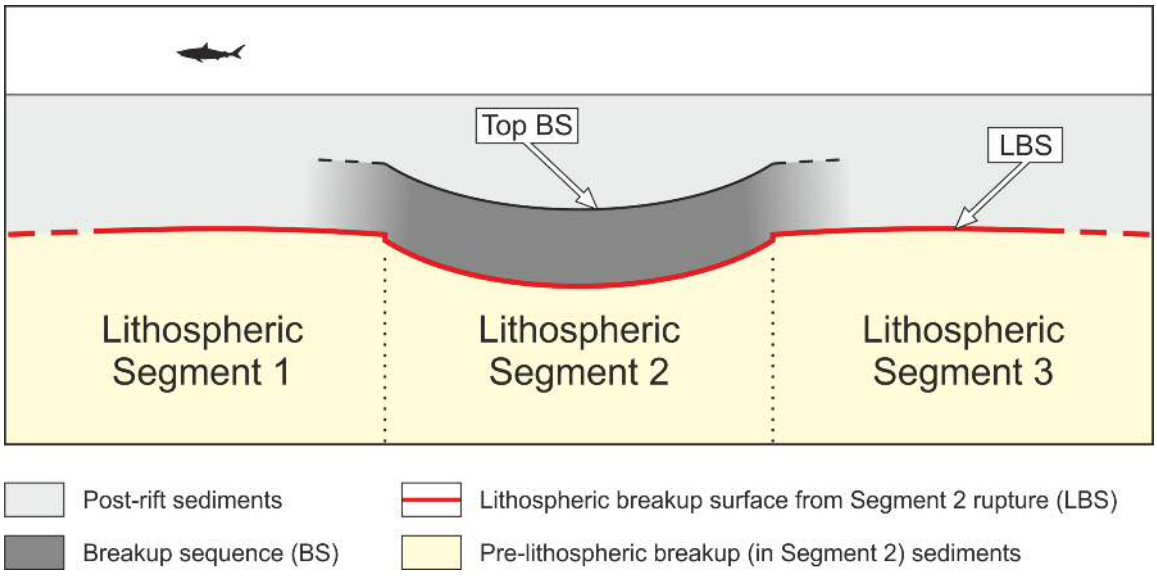


**Figure 7.2** Schematic representation of the discrepancy between the lithospheric breakup surface (LBS) and the breakup sequence (BS) when considering their spatial extension in deep sea environments. Note that Segment 2 in the Figure is the one recording lithospheric breakup. Given its definition, the BS is confined to the lithospheric segment recording the lithospheric breakup, while the LBS can extend further into neighbouring segments not recording lithospheric breakup.

### 7.3.3. Bottom current activity and black shales

An important character in the BS is the prominent bottom current activity recorded there. Nevertheless, there are differences between the types of contourite deposits found on distinct margins. In contrast to Northwest Iberia, the East Antarctica margin is much less structurally segmented, allowing the continuous development of structures associated with lithospheric breakup (*cf.* Figs. 4.14 and 6.27—the Antarctic side in Fig. 6.27). This geometry allowed the development of extensive contourite drifts that contrast with the more 'topographically confined' contourite drifts observed in Northwest Iberia (*cf.* Figs. 5.11, 5.12 6.19 and 6.24—note the differences in scale).

In South Australia, the depositional facies found above the Campanian LBS are similar to those above the LBS in the Porto Basin. Unfortunately, due to lack of deep oceanic drilling penetrating the LBSs, the distal lithologies of the BS remain unknown in the SRS. Assuming, by comparison with the South Australian margin, that deltaic facies prograding over the LBS promoted a more direct input of clastic material into deeper parts of the SRS, the presence of black shales is expected on the distal outer proximal margin by analogy with Northwest Iberia. However, in Northwest Iberia the abundance of black shales observed within the BS at DSDP Site 398 decreases with the transition from a turbidite–dominated to a contourite–dominated setting (see chapter 5, section 5.4.1). As the presence of currents strong enough to erode the Early Campanian LBS and sediments below was also observed, it is suggested that here the presence of black shales (if deposited by the same processes as in Northwest Iberia) could have been completely obliterated by the intense bottom activity. The same can apply to the Late Maastrichtian lithospheric breakup, where strong bottom currents controlling the early deposition of the BS could have eroded any hypothetical black shale deposition above the LBS (see Chapter 6).

## 7.4. Potential for BS recognition on continental margins

Changes in inplane stresses due to lithospheric breakup, promote vertical movements of the lithosphere across the margin (Braun & Beaumont, 1989; Cloetingh *et al.*, 1989; Issler *et al.*, 1989; Cathles & Hallam, 1991; Egan, 1992; Kooi & Cloetingh, 1992; van Balen *et al.*, 1998). The position where uplift and subsidence occur depends on the depth of necking in the lithosphere of the rifted margin, which will condition the initial state of flexure of the lithosphere (see Chapter 1). Not only variations on the depth of necking along the margin but as well the overall geometry of the rift basin have a close effect on the amplitude and wavelength of those vertical movements (van Balen *et al.*, 1998; Govers & Wortel, 1999). Given the existence of heterogeneities along and across strike of any given rifted margin, both at shallow and deeper levels of the lithosphere, the propagation of the in-plane stress wave (due to lithospheric breakup) and their superficial (stratigraphical, erosional) expression is conditioned by the complex architectural system of the lithosphere undergoing breakup. This implies that in a rifted margin the stratigraphic and sedimentological expression of lithospheric breakup, (the LBS and the BS) changes not only across, but also along the strike of the margin.

The recognition of a BS will therefore depend on several factors such as the lithological contrast between enveloping lithologies, its distinct stratigraphic architecture(s), the degree of erosion at its top, etc. In addition, given the variability of depositional environments observed at a given time along and across any margin, the aspect of the BS will vary accordingly. Depending on its position along the margin, the preservation potential of the BS can, and will also vary greatly. In fact, *location, location, location* could be the title of this section as the formation/preservation/observation and further recognition of the BS is directly related to the relative location (and internal character) of the BS. The potential for recognition of any given BS after its formation can depend on two major factors, both controlled by the location of the observed BS within the margin. These themes are (1) observation issues and (2) preservation issues. These will be discussed in the following sections.

## 7.4.1. Observation issues

### *7.4.1.1. Position on the inner proximal margin*

Depending on the observed area of the margin, the potential of the BS to be recognized will vary greatly. As shown and discussed previously (Chapters 4 and 6), the BS can be recognized on the inner proximal margin by presenting progradational reflections (forced regressive wedge) at its base, which result from rift shoulder uplift and associated coastline regression. Nevertheless, given the three-dimensionality of a sedimentary system at any given point in time, a forced regression wedge deposited due to lithospheric breakup should not be observed along the entire rift margin. Instead, several forced regression wedges may occur, each confined to a particular area of the margin, and separated by non-deposition areas where condensed deposits will slowly accumulate (location 5 in Figure 7.3). Lateral variation occurring both across and along the strike of a continental margin is well-known and a mandatory occurrence in non-confined (natural, opposed to artificial) sedimentary systems (Posamentier & Allen, 1999).

Potentially contributing for a decrease on the observation of the basinal deposits of the BS is the fact that sedimentary systems originated due to forced regressions have reduced lateral mobility, or may be completely absent. This occurs as their feeding channels initially tend to coalesce with the continued lowering of the relative sea-level, and predominantly incise the substrate over which they develop, fixing their position (Posamentier & Morris, 2000; Blum & Hattier-Womack, 2009). This way, the recognition of a forced regressive wedge is conditioned by the position of the observed seismic profiles (Fig. 7.3).

Considering that heterogeneities within the lithosphere promote a non-uniform propagation of in-plane stresses released during lithospheric breakup, the uplift of the inner proximal margin will surely vary in intensity from place to place (at a kilometric scale) and in some places subsidence can even be observed (Fig. 7.3). This means that the architectural expression of the BS on the outer proximal margin will vary accordingly (Fig. 7.3). Thus, depending on its location, lateral changes in the rate of uplift of rift shoulder areas can lead to a broader depositional spectrum,

ranging from non-deposition, with the creation of exclusively subaerial erosional surfaces (area located between the subaerially exposed forced regressive wedges in Figure 7.3), to forced regression wedges and enhanced depocentres, where transgressive deposits can be found. One should stress, however, that although subsidence during lithospheric breakup has not been observed in any of the studied margins in this work, according to Kooi *et al.* (1992) models (and if not considering the later refinements to this model by van Balen *et al.*, 1998), there is the possibility of downward vertical movements in rift shoulder areas upon lithospheric breakup. In the Kooi *et al.* (1992) models, the tectonic signal of vertical movements is dependent on the previous flexural state of the lithosphere, which is in turn determined by its depth of necking ($Z_{neck}$, see Chapter 1), a parameter that can vary abruptly within the same lithospheric segment (Govers & Wortel, 1999). In fact, this exact variation is observed in Northwest Iberia, which has a shallow $Z_{neck}$ on the inner proximal margin (~6 km relatively to a neutral $Z_{neck}$ of 7.5 km, Cunha, 2008) promoting uplift of the rift shoulder, changing southwards and out of the studied inner proximal margin to a relatively deep $Z_{neck}$ (~12 km, Cunha, 2008).

Inner proximal margins are very sensitive to eustatic variations (*e.g.* Catuneanu, 2006). These variations can also hinder the recognition of the base of the BS in multiple ways. Considering an inner proximal margin experiencing a relative sea-level fall due to uplift during lithospheric breakup, a eustatic sea-level drop can only add momentum to the already falling relative sea-level, promoting much wider subaerial unconformities. Conversely, a eustatic transgression can considerably mask the stratigraphic record of tectonic uplift on the rift shoulder.

**Figure 7.3** (next page) Schematic illustration of the multiplicity of aspects that the BS can assume on the inner proximal margin. A—aspect of the margin immediately before lithospheric breakup. B—same margin after lithospheric breakup. Note that the different vertical movements originated by the flexural rebound due to lithospheric breakup influence the instalment of different depositional environments.

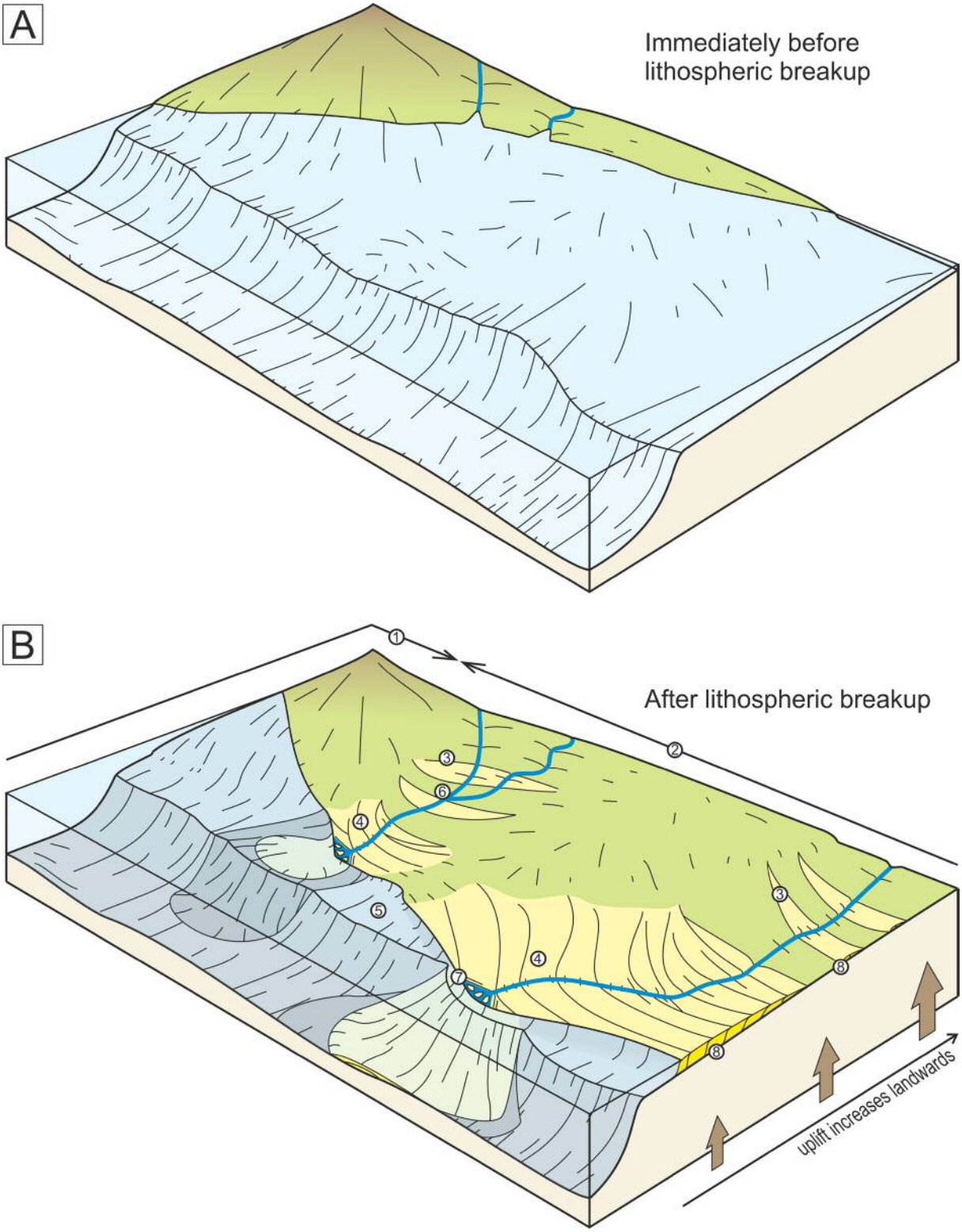


① Subsidence zone
② Uplift zone
③ Detached forced regressive wedge
④ Attached forced regressive wedge
⑤ Condensation zone between forced regressive deltas
⑥ Drainage confluence
⑦ Shelf-edge delta
⑧ Downlap and toplap characteristic of forced regressive systems tracts

To discriminate between eustatism and lithospheric uplift as the cause for the observed forced regression in the Porto Basin at the time of lithospheric breakup on the inner proximal margin, the type and degree of erosion shown by the LBS was taken in consideration. The Porto Basin, due to the basinward migration of the extensional stresses was, immediately before lithospheric breakup, in a tectonically quiescent state (at least to a certain degree). Therefore, in this area the most likely causes of accommodation space variation were sediment compaction and loading, eustatism and a certain degree of thermal subsidence. These, when excluding major eustatic sea-level drops, lead to deposits with a tabular geometry (Fig. 7.4A). In such scenario, the occurrence of a eustatic sea-level fall leads to the development of an erosional surface (cut by fair-weather waves during sea-level fall, Catuneanu, 2006) on which the age of the truncated sediments is older basinwards (Fig. 7.4B). If the sea level drop is motivated instead by a tectonic uplift of landward increasing intensity (leading to a basinward tilt of the strata, Fig. 7.4C), then the age of the exposed sediments become older landwards, and the angle between the erosional surface and the truncated sediments is likely to be very small (Fig. 7.4C). This later geometry is observed in Porto Basin, suggesting that eustatism can be dismissed as the cause for the forced regression recorded here.

Furthermore, and after the publication of Soares *et al.* 2012 (reporting the results of chapter 4), Grobe *et al.* (2014) published apatite fission track data results from onshore East Galicia area, showing that there is an indication of uplift registered close to the Aptian-Albian boundary, and related it with the lithospheric breakup event of Soares *et al.* 2012.

Another indication of inland uplift is the absence of incised channels on the forced regression wedge when observed in along strike profiles. This indicates that the amount of sediment supply was able to maintain the base level of the delta feeder and its distributary channels along with the pace of the relative sea level drop without a great amount of fluvial downcutting as it progresses along the exposed continental platform (Posamentier & Allen, 1993).

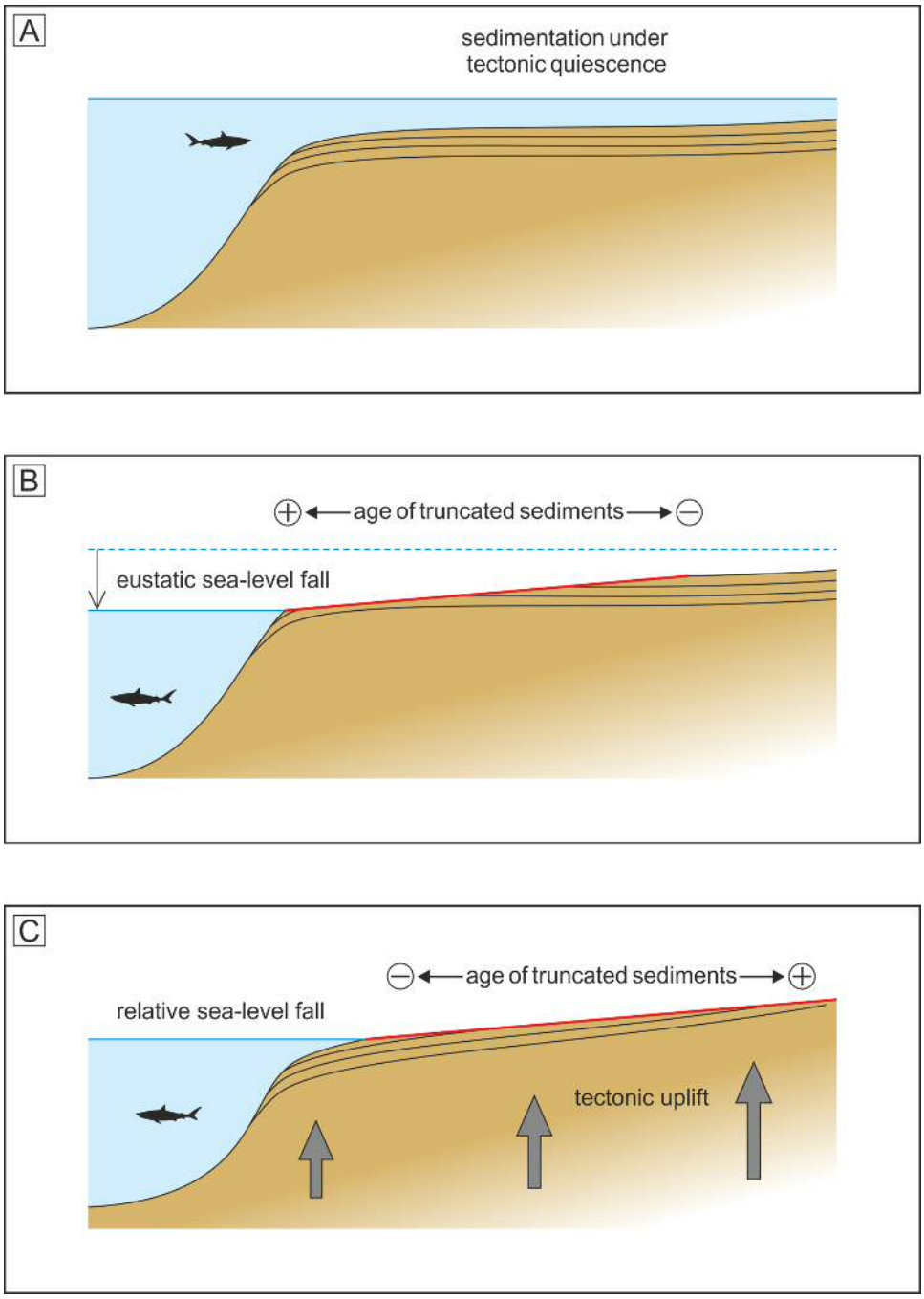


**Figure 7.4** Difference between eustatic and tectonically induced erosional surfaces on an inner proximal margin. A—horizontal deposition on a tectonically quiescent environment. B—erosional surface (in red) created due to a eustatic sea-level fall. Note that the age of the truncated sediments increases basinwards. C—erosional surface (in red) induced by tectonic uplift promoting a fall of the relative sea-level. Note that the amount of tectonic uplift increases landwards (grey arrows). In this scenario, the age of the truncated sediments increase landwards. The angle of the erosional surface (in red) is the same both in B and in C. No scale implied.

This character is even more striking given the amount of relative sea-level fall observed in Figure 4.4. It should be noted that on a fluvial system, the effect of a relative sea-level fall diminishes rapidly inland. In fact, inland of the first knickpoint, relative sea-level changes lose its influence on the fluvial system (Posamentier & Allen, 1993; Shanley, 1994). Therefore, the contribution of a relative sea-level fall on upstream sediment rejuvenation is limited (Blum & Hattier-Womack, 2009). Given this postulate, the high amount of sediment and its immature character that compose the forced regression wedge on the Porto Basin is an indication of upstream sediment sources rejuvenation, strongly suggesting the occurrence of inland tectonic uplift (Salén/Pecten, 1985; Neste, 1990; Taurus Petroleum AB, 1995).

Unfortunately, in Australia the lack of data on the inner proximal margin did not allow a full investigation of this theme. Nonetheless, upon inspection of global eustatic curves, having in mind their relative and much disputed validity, [*e.g.* Miall (1992) and Christie-Blick (1991)], no correlation between the relative sea-level drop observed at final breakup time on the different segments of this margin (Fig. 6.2) and the Haq *et al.* (1988) curve was found in this work.

From this section, one can note that the basal BS on inner proximal margins can assume multiple characteristics. Depending on the position along the margin of the acquired/studied seismic profiles and/or well data, the basal BS can assume several different aspects not covered completely on Chapter 4. Nevertheless, the expected overall uplift of the inner proximal margin during lithospheric breakup will promote the development of a group of characteristics associated with a relative sea-level drop (the forced regressive wedges) and a particular erosional pattern where the LBS develops (the LBS tectonically enhanced erosion pattern). These, in association with other indicative characteristics from other parts of the rifted margin (mentioned in previous chapters and discussed below) facilitate a robust interpretation of the LBS and its associated BS.

#### *7.4.1.2. Presence of mass-transport deposits (MTDs)*

The distribution of MTDs in the Peniche Basin shows that they are clustered in two main groups, and associated with main sediment input zones (Fig. 5.6). In contrast, in the Bremer Sub-basin the presence of MTDs was observed only on its western part (Fig. 6.7), where uplift at the time of lithospheric breakup was more intense. This resulted in the remobilisation of considerable volumes of sediment, therefore turning this latter area in an important sediment entry point to deep-offshore basins (Fig. 6.5B).

Contrasting with the Peniche Basin and Bremer Sub-basin, the presence of MTDs within the BS in Antarctica follows a different pattern. Here, they occur along a continuous, and extensive stretch of the Antarctic margin and, on each seismic profile where they were observed, share the same seismic character (occurring in seismic profiles GA228-25, GA228-26, GA228-27 and GA228-28, see Figures 6.16 and 6.26). This suggests a similar origin for these MTDs, presumably distinct from the MTDs observed on the Peniche Basin and Bremer Sub-basin.

In East Antarctica, the absence of seismic data covering the inner proximal margin does not allow for the mapping of sediment entry points. Given this, it is not possible to infer how these can influence the MTD distribution presently observed on this margin. Nevertheless, the continuity of the MTD distribution suggests that previous efficient sediment redistribution by bottom currents promoted a relatively uniform accumulation of sediment along the upper continental slope, where the MTDs will develop. Following the same reasoning used to explain the presence of MTDs on the Peniche Basin, the accumulation of sediment in an unstable zone (along the shelf edge and upper continental slope) promoted the development of favourable conditions for the occurrence of mass transport episodes. The uniformity in the internal character of MTDs along the several seismic lines where they can be observed, suggest an equal uniformity in the processes that originated them.

#### *7.4.1.3. Contourite recognition*

The model proposed in Chapter 5 relating the onset of bottom current activity to lithospheric breakup is independent of the signal of the vertical movements experienced by the lithosphere due to the inplane stress release at the time of lithospheric breakup. In fact, the disruption of the pressure gradient of the stratified water masses can occur due to either uplift or subsidence. In the absence of a well marked LBS, the presence of bottom current activity is surely the most ubiquitous indication of complete lithospheric breakup on a rifted margin. As observed in East Antarctica, the presence of the LBS is not obvious everywhere on the margin and the delimitation of the BS is not possible due to the absence of its bounding surfaces. Nevertheless, the presence of bottom current activity is ubiquitous (*e.g.* Figs. 6.19, 6,24). Of importance is the observation of extensive erosional surfaces and contourite drifts along the whole of the East Antarctic margin.

Although the observation of bottom current activity can be used as an indication of complete lithospheric breakup, the importance of bottom currents and associated contourite drifts extends far beyond ruptured lithospheric segments. This statement is corroborated by strata deposited above the Maas/Pal surface. The genesis of this surface relates to the latest Maastrichtian lithospheric breakup event recorded at the Terre Adélie–Otway Basin segment. However, the bottom current activity associated with this event extends for several hundreds of kilometres in East Antarctica (see Chapter 6). In Northwest Iberia, the extent of the available seismic data do not allow for the mapping of the full extent of the bottom current activity, but it their occurrence is likely south and northward of the study area.

As observed in NW Iberia, the uplift of the rift shoulder and the consequent onset of a forced regression systems tract resulted in bypass of large volumes of sediment over the shelf and slope, deposited basinwards as large turbidite fans (Fig. 7.5). This enhanced episode of turbidite deposition will mask the initial bottom current activity (Mulder *et al.*, 2008), hindering its observation and recognition during the initial stages of deposition of the BS. Nevertheless, basinwards into the most distal areas of the margin, the presence of bottom current activity can be observed close to the base

of the BS (Fig. 5.13B), a strong indication of its presence immediately after the lithospheric breakup event.

As discussed in Chapter 5, the recognition of contourite drifts using exclusively 2D seismic data can be complicated due to the tridimensional nature of this kind of deposits. In fact, the contourite drifts distribution map on Figure 5.9 only shows contourite drifts that could be identified with a high degree of confidence, while ambiguous contourite drifts were discarded from figuring on the map.

## 7.4.2. Preservation issues

### *7.4.2.1. Deep offshore*

In deep sea environments, the preservation the LBS and the BS can be hindered by strong bottom currents, including turbidity flows.

Erosion promoted by strong bottom current activity is observed extensively in East Antarctica (see 6.7.1.2) where the LBS seems to have been obliterated, and the horizon marking the top of the BS was not formed. As observed in Chapter 6, deep contour currents can truncate and completely obliterate the LBS in large areas of continental margins, and prevent the formation of a horizon topping the BS. On the Northwest Iberian margin, but at a much smaller scale, the top of the BS is also observed as an erosional surface and in some areas it develops as a deeply truncated horizon (Figs 5.5B, 5.10-12, 7.6).

**Figure 7.5** (next page) Turbidite fan deposited above the lithospheric breakup surface (LBS). This turbidite fan is the product of sediment bypass promoted by the forced regression associated with the lithospheric breakup event (see text for details). A and B—seismic profiles showing the turbidite fan in different sections. C—diagram showing the distance between the seismic profiles shown in A and B in several points: 1—distance between the eastern tips of the seismic profiles: ~6.1 km; 2—distance between the apex of the turbidite fan in A and B: 4.9 km; 3: —distance between the western tips of the seismic profiles: ~2.9 km. D—map with the location of the seismic profiles in A and B.

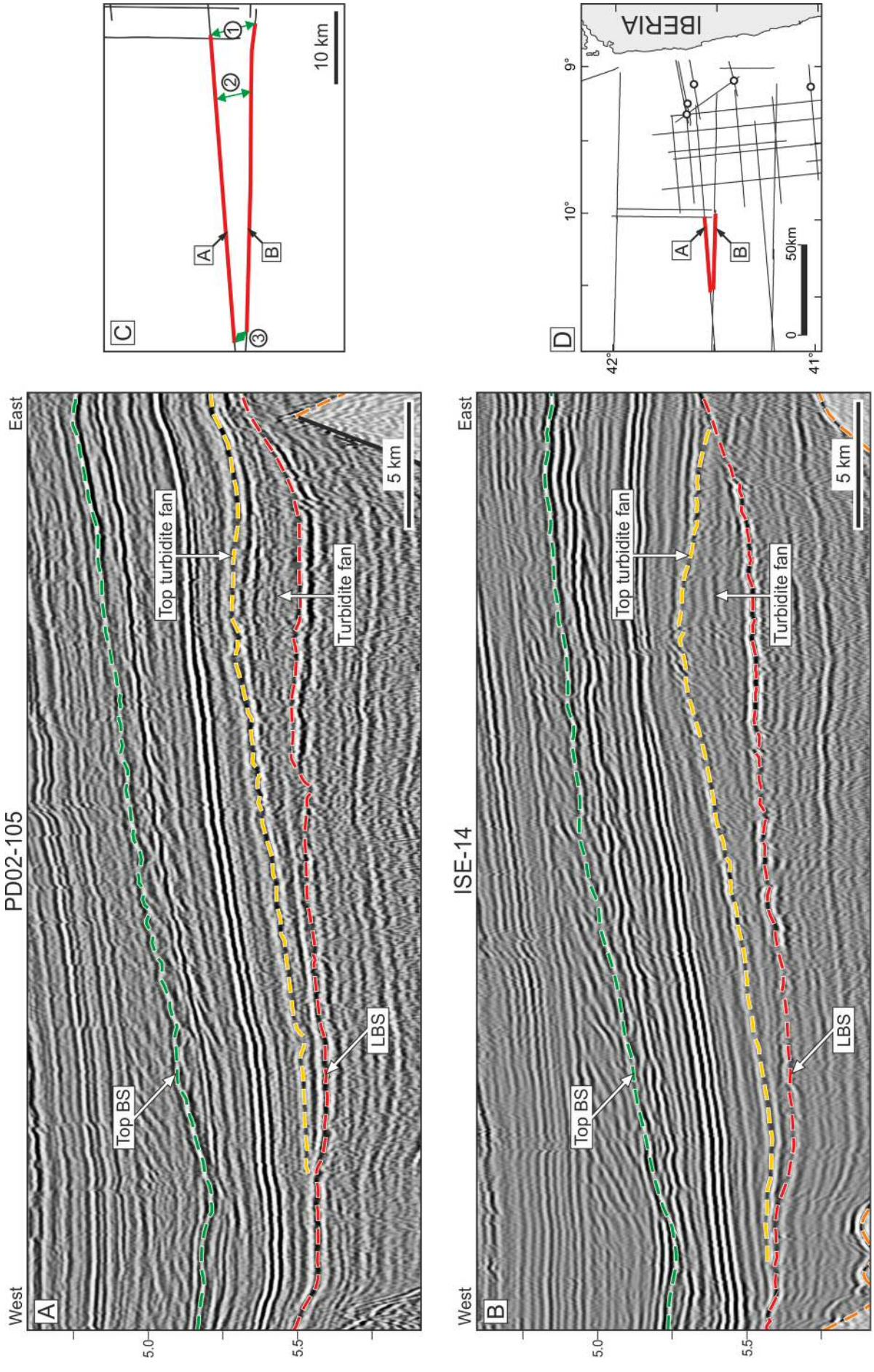
PD02-105
West
East
A
Top BS
LBS
Top turbidite fan
Turbidite fan
5 km
5.0
5.5
ISE-14
B
C
10 km
1
2
3
A
B
D
IBERIA
9°
10°
42°
41°
50km
0

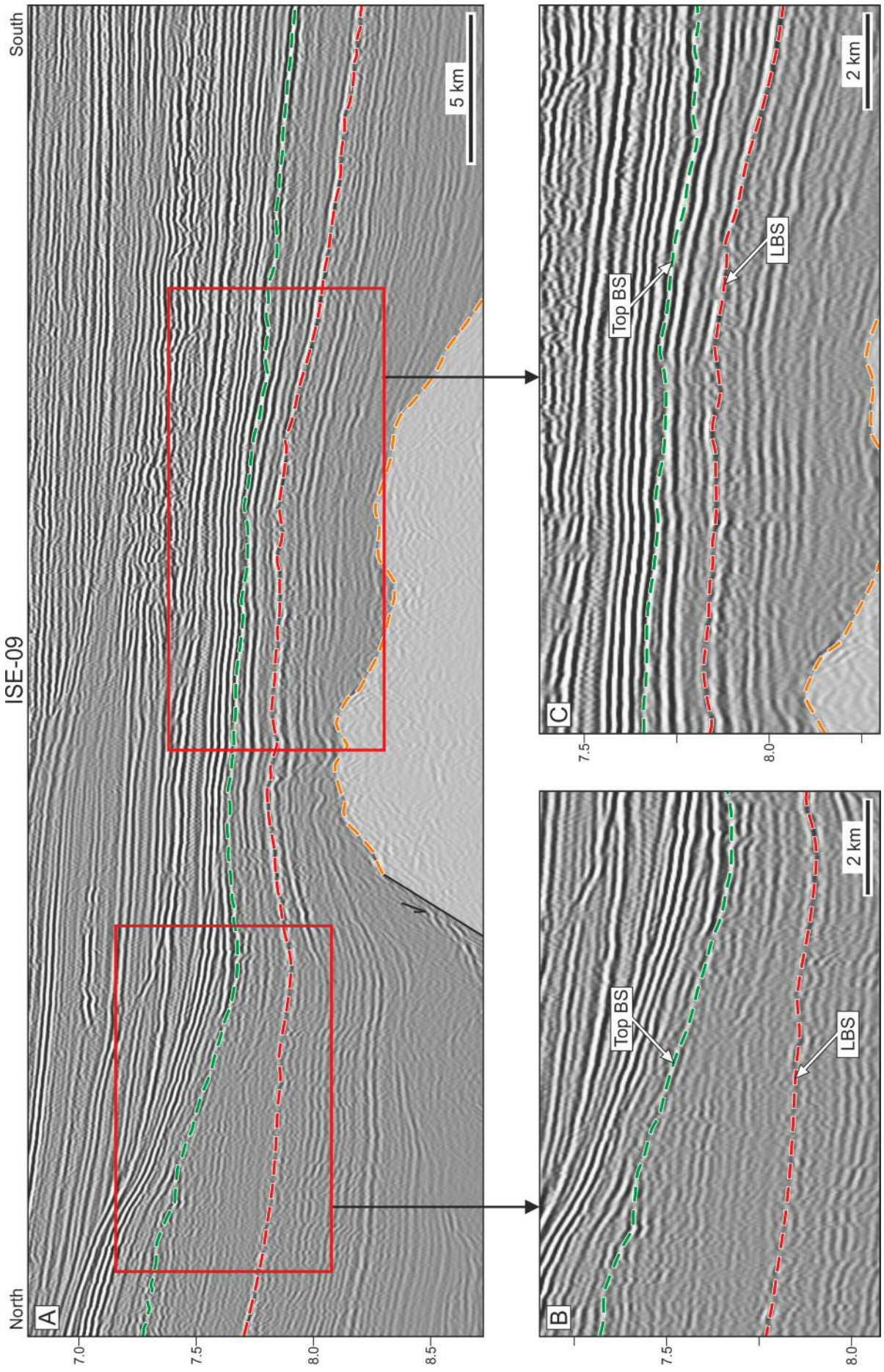
South
North
ISE-09
A
5 km
7.0
7.5
8.0
8.5
B
2 km
Top BS
LBS
7.5
8.0
C
2 km
Top BS
LBS
7.5
8.0

**Figure 7.6** (previous page) Examples of the erosive aspect the BS can display at its top. A—seismic profile showing the variability in the character of the top BS horizon in terms of its depth of erosion. B—detail of the top of the BS showing marked erosional truncation. C—detail of the BS showing a moderate erosional surface, but with deep incision observed to the northward continuation of the BS, as observed in A. Location of seismic profile in Figure 7.7

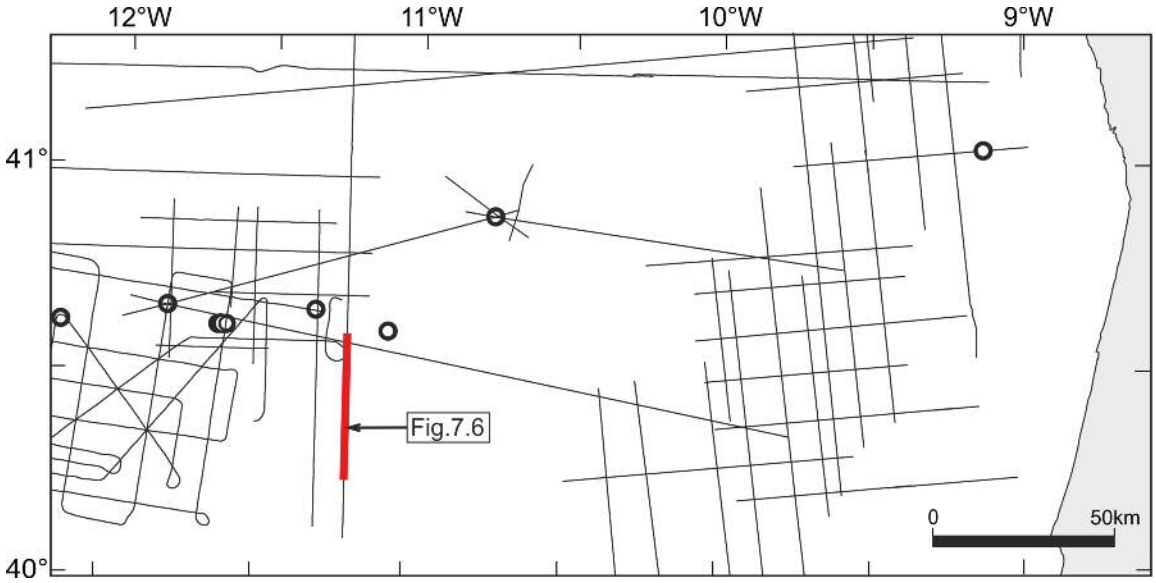


**Figure 7.7** Location of seismic profile in Figure 7.6.

### *7.4.2.2. Continental shelf*

On a continental shelf that suffered uplift due to lithospheric breakup, the preservation of sediments deposited during this event—the forced regressive wedge in Figures 4.3 and 4.4—will be a function of several variables. The overall thickness and stacking patterns of forced regressive sediments (attached or detached, *sensu* Ainsworth & Pattison, 1994) will influence their own preservation by making them more or less susceptible to erosion. The possibility of continental shelf subsidence will not be here discussed since it was not observed on the study areas.

Given the nature of the conditions promoting the deposition of a forced regressive wedge, its erosion occur at the same time of its deposition by subaerial exposure of its older parasequences. Therefore, a detached, or an attached but thin forced regressive wedge will be more likely obliterated by erosion than an attached, thick

wedge. Furthermore, a detached forced regressive wedge is not only more easily removed by erosion, but also its observation on seismic data will be more difficult due to its segmented nature, with wide sediment by-pass zones between prograding lobes, (Catuneanu, 2006).

Two strong influences on the character of forced regressive wedges triggered during lithospheric breakup are: (1) the gradient of the continental shelf and (2) the relative position of the sea-level at the start of the lithospheric breakup event (Fig. 7.8).

If the gradient of the continental shelf is very gentle, the relative sea level drop recorded during inner proximal margin uplift can expose the continental shelf so rapidly that there is no time (nor accommodation space) for the deposition of an expressive forced regressive wedge. In this case, the forced regressive sediments could be deposited as a detached forced regressive wedge with widely spaced lobes (Fig. 7.8C, F). In the case of a continental shelf with a steep gradient, its exposure will be fast, and a detached forced regressive wedge is likely to be deposited when (and where) accommodation space is widely available (Fig. 7.8A, D). The initial position of the sea-level will dictate the basinwards length of the forced regressive wedge (compare Fig. 7.8A with D). Concerning its preservation, the configuration more favourable for the deposition of a forced regressive wedge with sufficient expression to withstand erosion (after subaerial exposure due to ongoing sea-level drop) is a moderate shelf gradient and a higher initial sea-level (Fig. 7.8E). In this case, the pace of the shelf exposure and the accommodation space available will create the conditions favourable to the deposition of an attached forced regression wedge. Not considered in this analysis are variations on the amount of sediment input or the velocity of the sea-level drop, two important variables regarding the deposition of forced regressive wedges (Schlager, 1993; Ainsworth & Pattison, 1994).

The basinward accumulation of sediments over the continental slope is dominated by collapse due to sediment instability, promoting the deposition of MTDs. Another factor influencing the preservation of the lithospheric breakup-triggered forced

regressive wedge is the pace at which the uplifted rift shoulder will achieve again its pre-lithospheric breakup isostatic balance. Erosional unloading counteracts the expected rift shoulder subsidence after the lithospheric breakup uplift by promoting buoyancy of the lithosphere. The newly uplifted and exposed areas will suffer erosion and sediment removal with consequent unloading of the lithosphere promoting further uplift (Burov & Poliakov, 2003).

An example of the influence of a relatively low pre-lithospheric breakup base level is found on the Otway Basin. In this basin, the first sediments deposited over the LBS are represented by LST and TST deposits (Krassay *et al.*, 2004), implying that forced regressive deposits (if preserved) should be found only basinwards on the continental slope. Once compared with the westward South Australian basins, important differences can be observed concerning the latest syn-rift depositional environments in the Otway Basin. Here, the top of the Sherbrook Supersequence (over which the LBS develops, see Figure 6.2) comprises upper delta plain environments, deposited under a very shallow water column (Krassay *et al.*, 2004). This setting contrasts with the deeper marine environments found immediately below the LBS in the Bight Basin (Totterdell *et al.*, 2000; O'Leary *et al.*, 2005). The fact that extensive shallow depositional environments were present in the Otway Basin prior to lithospheric breakup implies that, with a further lowering of the relative sea level, the basinward movement of the active coastal plain was very fast, rapidly exposing an extensive continental shelf, similarly to what is shown in Fig. 7.8C. Forced regressive deposits should have developed not over the rapidly exposed shelf but instead over the steep basinward delta slope facies of the Sherbrook Supersequence. The fact that shelf exposure promotes drainage confluence, reducing lateral river mobility and increasing sediment bypass (Blum & Hattier-Womack, 2009) (location 6 in Figure 7.3), contributes to reduce the chances of finding preserved forced regressive sediments, as they become very localized on continental margins. Furthermore, clastic deposition over highly mobile, high-angle delta slope sediments, is very likely to be remobilised further downslope as MTDs. This would make it impossible to identify their origin as forced regressive sediments. Once the sea level rises again, only LST and TSTs are found over the LBS.

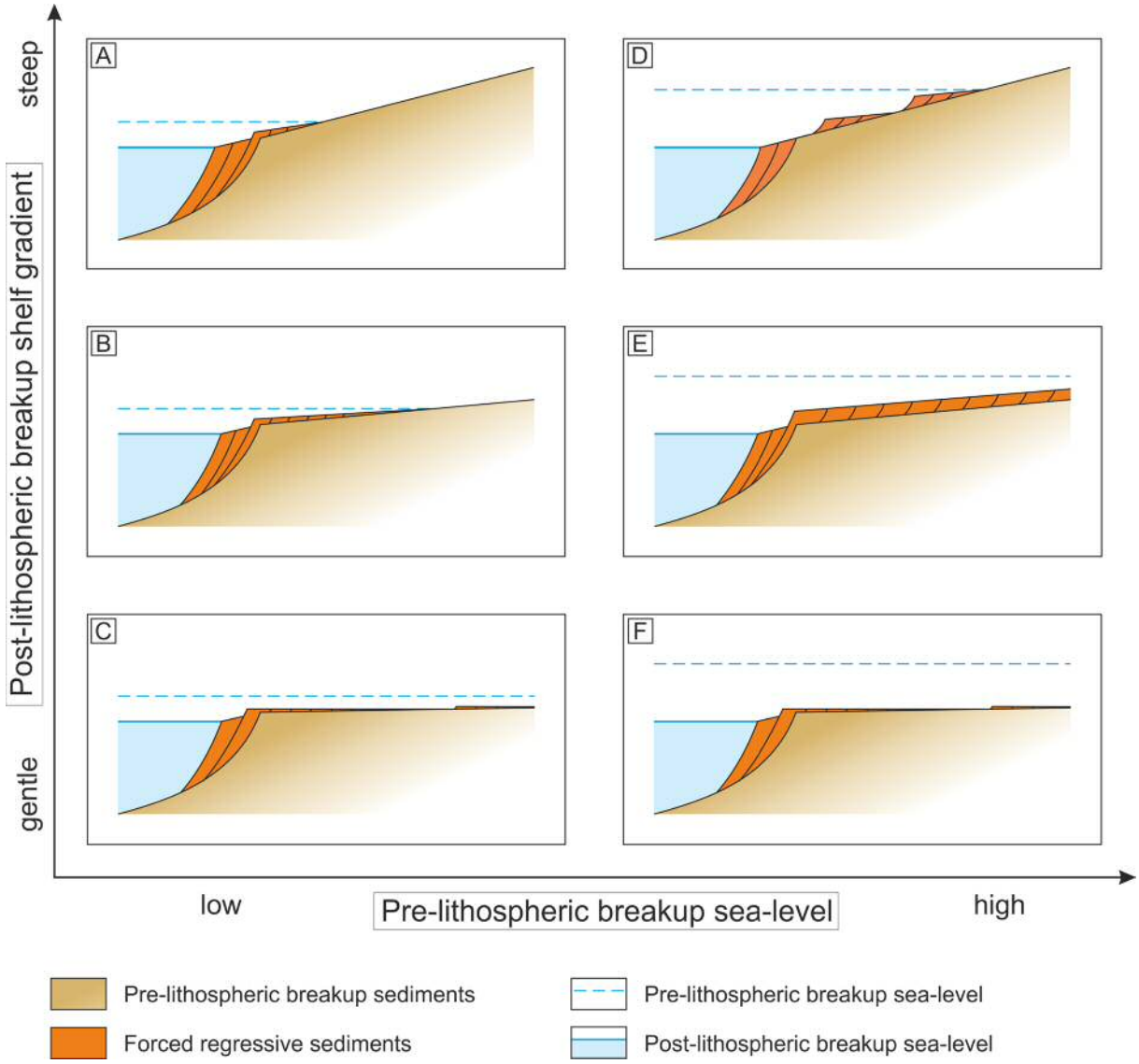


**Figure 7.8** Control of continental shelf gradient (immediately after lithospheric breakup) and sea-level (immediately before lithospheric breakup) on the morphological variation of the lithospheric breakup-triggered forced regression wedge. On the Y axis is represented the 'post-lithospheric breakup shelf gradient', which increases upwards. The X axis shows the variation on the sea-level, increasing in height to the right. The panels show the geometry of the continental shelf after rift shoulder uplift. The forced regressive wedges in each panel do not show the effects of the erosion due to subaerial exposure. The influence of changes in the amount of sediment input or on the velocity of the sea-level drop is not considered. See text for more details. The datum is the continental shelf and slope. No scale implied.

## 7.5. Research limitations in this work

The data used in this work are derived from the integration of seismic and well data. As with any study, the more data the better, and in this work, which was done at a regional scale, more seismic data would have allowed coverage of 'interpretational holes' on the produced maps and more well data would have provided with ground truth the tools for the understanding of lithological variations within the rift basin.

Unfortunately, the access to industry data (seismic and well data) is normally limited to researchers and the existing public data is frequently old and of inferior quality. Nevertheless, in this study industry data was used (the TGS-NOPEC dataset) and it provided a superior understanding of the study area in the Iberian margin.

This necessity of more data was felt in every chapter here presented. More data covering the Newfoundland margin would have provided a better comparison between this and the conjugate Iberian margin in Chapters 4 and 5. Similarly, the lack of digital data from the South Australian margin did not allow a proper comparison with the East Antarctica conjugate margin in Chapter 6. Still in Chapter 6, the lack of navigational data for the seismic surveys used in East Antarctica hindered the construction of maps. On this same margin, the lack of seismic profiles running perpendicular to the margin strike, connecting along slope seismic profiles omitted crucial data, which could allow the understanding of how the transition from different lithospheric segments is processed.

## 7.6. Further research

Every scientific work aiming to answer a specific question finishes with several other questions not initially considered. Being no exception, this work raises several questions and topics for further research. These are:

- The relationship between the EEU and the continental crust breakup;

- Numerical modelling of the lithospheric breakup event;
- The refinement of the Breakup Sequence concept;
- Contourite drifts: 3D data & palaeocurrents indicators; syn-rift bottom currents;
- A continental crust breakup surface? Can it exist?
- Lithospheric breakup diachronicity along lithospheric segments.

### 7.6.1. NW Iberia: the EEU and the presence of divergent reflectors below the LBS

An important characteristic of the syn-rift package on the Northwest Iberia distal margin, is that the presence of divergent reflections occurring against the footwalls of important faults are not common. Several explanations were proposed in the literature for the scarcity of divergent reflections on seismic data, including: a) syn-rift intervals too thin to be observed in seismic data due to low sedimentation rates, a consequence of sediment trapping in landward basins (Wilson *et al.*, 2001); b) resedimentation of syn-rift sediments towards basin centres due to the predominance of non-cohesive sediment and associated slope instability (Wilson *et al.*, 2001); c) existence of low-angle faults bounding highly rotated tilt blocks, hindering the generation of divergent reflections during syn-rift (Péron-Pinvidic *et al.*, 2007). The first explanation (a) has been favoured by recent studies on the outer proximal margin (Alves *et al.*, 2006; 2009). The last explanation (c) was invoked by Péron-Pinvidic *et al.* (2007) to explain the observed variability in stratal architecture in some of the sub-basins on the distal margin. Nevertheless, Pérez-Gussinyé *et al.* (2003) after reprocessing of line ISE17W, permitted the illumination of divergent reflections that are not visible at all in the same line used in this study Fig. 7.9). This led to the conclusion that in many places, and especially on the distal margin the presence of divergent reflections, indicating rift activity, is being overlooked. Attributing syn-rift or post-rift labels to sediment packages on the sole base of the presence or absence of divergent reflections against footwalls is not correct. If not only for the observational errors derived from seismic quality or processing, promoting overestimates of the thickness of post-rift thickness on continental margins, another issue of importance is

the diachronous activity of rift-bounding faults. In fact, faults alternate between periods of activity and inactivity while the basinward migration of the extensional locus promotes the abandonment of landward rift basins, which become relatively quiescent before lithospheric breakup is achieved (Dawers & Underhill, 2000; Reston, 2005).

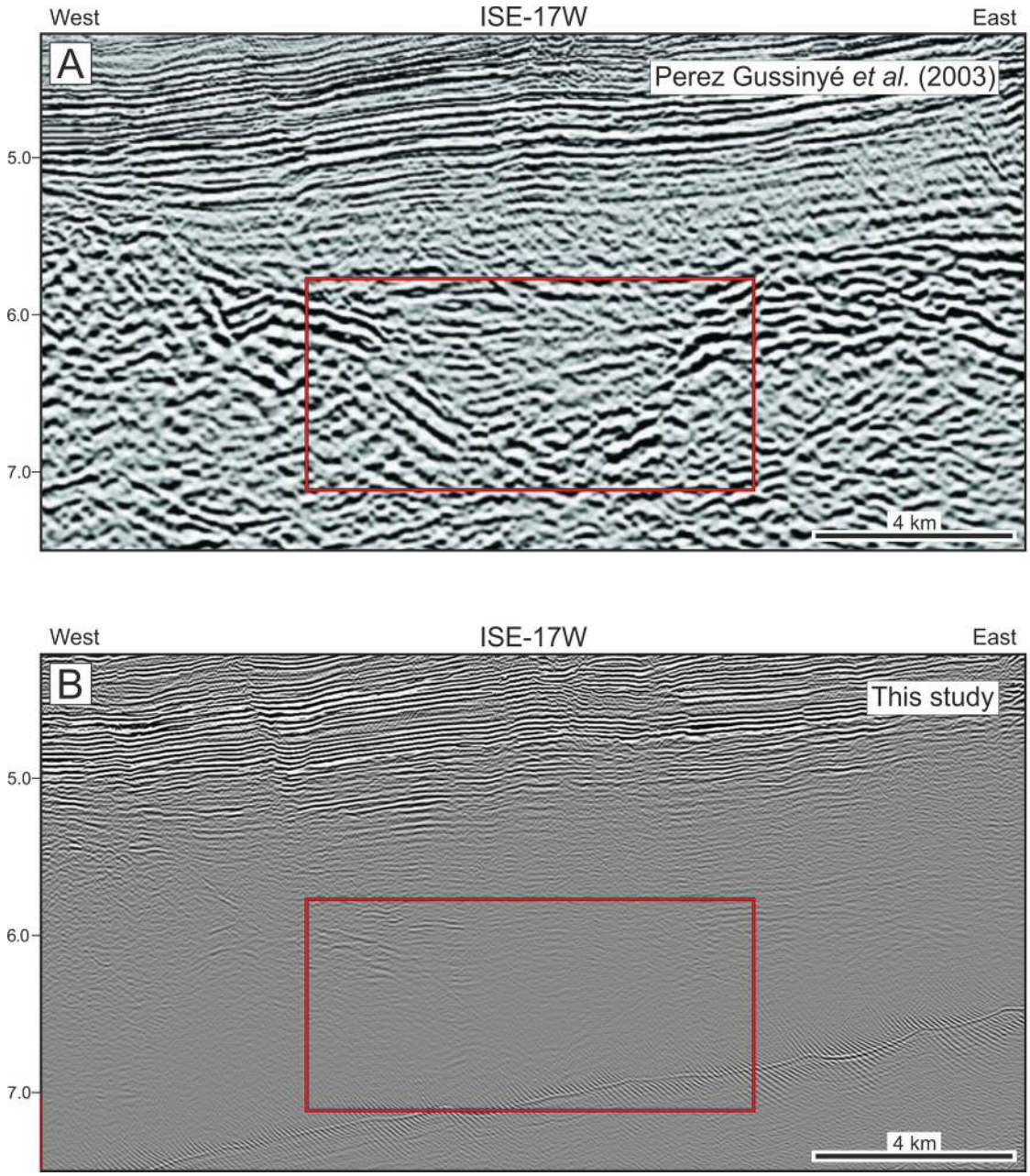


**Figure 7.9** Comparison of different processing of ISE-17 regarding the illumination of deep structures on the Iberian Margin. A—processing completed by Perez Gussinyé *et al.* (2003). B—processing available for this study. Notice in A the clear divergent reflections within the red square while in B the same area does not show the presence any divergent reflections.

Highly diachronous, the surface marking the end of fault activity on distal margin (commonly, and erroneously referred to as the *breakup unconformity*) is called in this work as the *end of extension unconformity* (EEU, see Chapter 6). Its recognition can provide important information regarding the migration of the extensional stresses along and across a continental margin. In Northwest Iberia the reprocessing of seismic data, with an emphasis on the illumination of deeper structures (as in Pérez-Gussinyé *et al.*, 2003) would allow the study of the EEU, and help to provide insights on the timings of the continental crust breakup and lithospheric breakup.

### 7.6.2. Numerical modelling of the lithospheric breakup event

The numerical modelling of the lithospheric breakup event, and the quantification of vertical movements resulting from the in-plane stress release recorded during lithospheric breakup, is an important part of future work. Another important point is the understanding of how lithospheric heterogeneity influences the physical expression of in-plane stress release. Never explored, in terms of numerical modelling is how mantelic exhumation affects lithospheric breakup.

Knowing the amount of uplift generated by the lithospheric breakup in-plane stress release and the affected area is very important for source-to-sink studies. It will allow the quantification of sediment volumes brought into the basin, with obvious consequences for the hydrocarbon industry.

Not only numerical modelling can aid at this kind of research, fission track studies can provide hard data on the amount and timing of the vertical movements suffered by rift margins during lithospheric breakup (as shown by Grobe *et al.*, 2014).

### 7.6.3. The refinement of the Breakup Sequence concept

One of the key concepts that have arisen from this work is the Breakup Sequence. Supporting this concept is the evidence shown in this work that the lithospheric breakup event triggered basin-wide structural changes, promoting the deposition of a stratigraphic sequence with distinct architectural and sedimentological

characteristics from those deposited before the breakup. Given the existence of continuous core data from the lithologies above and below the LBS in Northwest Iberia, the sedimentological characterization of the BS was possible here. The same kind of data does not exist in East Antarctica. Nevertheless, as the stratigraphic architecture of the immediate post-rift sediments in East Antarctica differs from equivalent sediments in Northwest Iberia (although both involving the presence of contourites as their main characteristic in deep water environments), their sedimentological characteristics may differ as well. Given the above, well data from East Antarctica or South Australia distal margins is necessary to further the understanding of the BS on this margin.

Another research topic concerning the BS is the lack of its upper boundary in East Antarctica. Although the reasons for this to happen were discussed in this work and its causes presumably understood (see Chapter 6), the lack of an upper boundary on a *stratigraphic sequence* goes against the concept of what a *stratigraphic sequence* is (see Catuneanu, 2006, page 4, for a discussion on the *sequence* concept). Is the presence of a top surface (being it an unconformity or a correlative conformity) defining the top of the BS a peculiarity of the Iberia–Newfoundland conjugate margins, or is the lack of it, as in East Antarctica, the norm?

Related with this topic is the duration of the deposition of the BS itself. In Chapter 4 was established that in Northwest Iberia the deposition of the BS took ~15 m.y., and its upper boundary is marked on the inner proximal margin by the top of the Cacém Formation as showing the thermal subsidence taking over the uplift caused by lithospheric breakup. Nevertheless, the chronostratigraphic position of this boundary (coinciding with the Cenomanian eustatic drowning of the continental platforms and epeiric seas), and the way it is here defined (as the moment when thermal subsidence finally takes over the uplift caused by lithospheric breakup) can suggest causality between these two events. On the other side, as the erosional unloading is what delays the thermal subsidence effects by furthering rift shoulder uplift, this could have happened earlier and without the formation of a prominent surface or reflector such as the top of the Cacém Formation. Nevertheless, this event

would be signalled (as it is, in reality, in Porto Basin) by a flooding surface landwards, and basinwards by its correlative conformity and a change in the amount of sediment sourced from fluvial input (*e.g.* Alves *et al.*, 2003; Dinis *et al.*, 2008). It should be noted that considering the particularities of each margin (for example different erosion rates between margins derived from different post-lithospheric breakup uplift rates), the duration of the BS can differ along a rifted margin. These problems deserve further investigation and it can be tackled with the use of sediment provenance studies, fission track data and numerical modelling.

### 7.6.4. Contourite drifts: 3D data & palaeocurrents indicators; syn-rift bottom currents

Although discussed, a point unanswered in this work is a definite understanding of the source of the water masses that generate the bottom current activity observed in Northwest Iberia. The use of 3D seismic data where the contourite drifts are imagined can provide the answer (or constrain it) for this question.

An interesting area to be studied with 3D seismic data in Northwest Iberia is the Northern Peniche Basin shown in Figure 7.5 (see Figure 5.11), where the presence of an elongated mounded and detached drift with a possible sediment wave field above could provide this answer.

Another interesting area, which could provide indications of the direction of the palaeo-currents with the use of 3D seismic data, is where the west side contourite imaged in Figure 5.12 develops. This elongated mounded and separated drift becomes a confined drift northwards (Fig. 5.10B), and this transition should have promoted the development of palaeocurrent indicators. If the current was flowing southwards, the transition from a constrained space (the channel in Figure 5.10B) to an unconstrained area would promote the loss of velocity of the current with a consequent drop on its erosive power. The opposite is expected if the current was flowing northwards, then the constriction of the current entering the channel would have increased its erosive power. Although intended in this thesis, it was not possible to infer the direction of the bottom currents using the reasoning above. The

indicative features of palaeocurrent direction left by the bottom currents in this area are certainly below the resolution of the 2D available seismic data. 3D seismic data have resolution enough to image very subtle features of the palaeo sea-floor (*e.g.* Posamentier *et al.*, 2007) and consequently can provide an answer for this question.

Although not clearly observed, in Northwest Iberia a certain degree of bottom current activity should have been present during the syn-rift period. As discussed in Chapter 5, the deep oceanic basin present in this area at the time of lithospheric breakup would certainly have had weak, sluggish, intermittent bottom currents compatible with the presence of the widespread black shales (which to form require very low levels of oxygen) and the lack of stratigraphic features indicative of bottom current activity. With the use of better resolution seismic data, syn-rift bottom current activity and their possible sources can be investigated. 3D seismic data can provide as well an understanding of the changes in drainage patterns promoted by the lithospheric uplift in Northwest Iberia continental shelf. This can provide important information on the variation of the vertical movements along the margin strike.

### 7.6.5. A continental crust breakup surface? Can it exist?

The continental crust breakup is very likely to be present in the stratigraphic record of Northwest Iberia. This event occurred in the lithospheric segment north of the Aveiro Fault during the Barremian (Tucholke & Sibuet, 2007), probably signalled by the presence of a Barremian condensed interval drilled offshore Galicia Bank (Boillot & Winterer, 1988).

Given the quality of the nowadays available seismic data, there is a minor probability of finding a surface that can be interpreted as contemporaneous with the continental crust separation. With better seismic resolution, the stratigraphic record of this event might be understood, possibly showing similar characteristics to the final lithospheric breakup event but with much less intensity. It will also be likely concentrated near the crustal separation locus, on the distal margin. Given the depositional characteristics of this part of the rift (deep sea, with hemipelagic

sedimentation) and the relatively minor (if any) in-plane stress release generated by this event, there is the possibility that the crustal separation event will not be identified amidst background sedimentary processes.

### 7.6.6. Lithospheric breakup diachronicity along lithospheric segments

Finally, it is very important to try to understand the diachronism of the lithospheric breakup along rifted margins. How is the transition between a completely ruptured lithospheric segment and a segment where lithospheric extension is still undergoing recorded on seismic and stratigraphic data? This is an important question that was never addressed with an extensive cross-lithospheric segments seismic dataset. The Eastern Antarctic margin seems to be a very good place to undertake such an analysis. Nevertheless, this kind of study would require a denser seismic coverage and, extremely important, biostratigraphy data of high resolution in the BS and crossing the LBS into older strata.

Chapter Eight

# CONCLUSIONS

## 8.1. Conclusions

Two new important concepts related with lithospheric breakup arise from this work, the lithospheric breakup surface and the breakup sequence.

The lithospheric breakup surface (LBS) here proposed could be regarded as merely a substitution for what is classically called *breakup unconformity*. Nevertheless, the LBS is not only a conceptual refinement of what the classical *breakup unconformity* should represent (a stratigraphic surface indicating the timing of breakup between a pair of conjugate margins), but it also reflects the unequivocal recognition of lithospheric involvement on the continental breakup process, while acknowledging at the same time the possibility of a two phase breakup process (a first crustal breakup followed by the final, lithospheric breakup). The LBS concept recognizes that lithospheric breakup is recorded not only as an unconformity, but also implies the existence of a correlative surface basin-wide. The introduction of the LBS concept also addresses questions raised by several authors concerning the validity and existence of a *breakup unconformity*.

This work shows that the classical *breakup unconformity*, a stratigraphic surface been recognized in rift basins around the world since Falvey (1974), has a geological significance that was not properly understood. In fact, the *breakup unconformity*, when interpreted on seismic data as the surface that shows the end of extensive fault activity (immediately above the divergent reflectors against the footwall), it does not represent the final breakup event, but instead it reflects the abandonment of extensional stresses on a particular fault or set of faults within a sedimentary basin. In this manner, it represents a highly diachronous surface across the rift basin, since during the rift process not all extensional faults cease their activity at the same time. Furthermore, during the rift process the extensional stresses migrate basinwards, concentrating on the breakup locus and promoting the abandonment of landward faults during the rifting process. In conjugate margins undergoing a two stage lithospheric rifting, the mantle exhumed after the separation of the continental crust will become the locus of extension, promoting an almost complete cessation of the

extensional stresses on the continental crust. Given this, the surface that often is called as *breakup unconformity* is here called end of extension unconformity (EEU).

Lithospheric breakup generates a large wavelength flexural rebound of the lithosphere, causing uplift in rift shoulder areas, and promoting the deposition of forced regressive wedges over the LBS. These forced regressive wedges constitute the inner proximal margin expression of the base of what is termed in this thesis as breakup sequence (BS). The BS is therefore a stratigraphic unit recording the expression of lithospheric breakup. Similarly to the LBS, the BS changes in character along the margin. On the inner proximal margin, the breakup sequence is composed of a series of regressive–transgressive cycles, starting with a forced regressive wedge associated with the rift-shoulder uplift observed when of lithospheric breakup. In deeper parts of the margin, the expression of the BS changes vertically (in time) and horizontally. On the outer proximal margin the BS is observed as comprising basal turbidites rich in organic matter, supplied from continental sediment sources, changing in time to deposits denoting the action of bottom current activity. Close to the continental slope MTDs are observed, themselves a product of widespread slope instability resulting from sediment accumulated on the shelf edge and upper slope during the early phases of the BS. On the distal margin, the action of bottom currents is observed early in the deposition of the BS.

An important finding during this work is the evidence of bottom current activity (contourite drifts and extensive erosional surfaces) above the LBS, *i.e.* earlier in the deposition of the BS on the distal and outer proximal margins. This character is explained in this thesis to be a consequence of the vertical tectonic movements triggered by the lithospheric breakup event. The disruption of the existing pressure gradients of the stratified water masses promoted the installation of a stronger bottom current regime, inexistent until then. The initiation of basin wide bottom current activity, above a strongly reflective surface correlated across the rift basin (the LBS) is postulated in this work to be the most important character leading to the correct positioning of the lithospheric breakup event.

The fact that the LBS and the BS (*pro parte)* can be observed on the two pairs of margins analysed (the Northwest Iberia–Newfoundland and South Australia–East Antarctica margins) suggests that these concepts can be successfully applied to other continental margins around the world. Nevertheless, some differences concerning the character of the LBS and BS were also found. These differences appear to be related with the fact that Northwest Iberia and East Antarctica (the margins more intensely studied in this work) are contrasting margins in terms of the amounts of sediment transported into their deep offshore basins. Furthermore, in East Antarctica there was the possibility to study several contiguous lithospheric segments that underwent lithospheric breakup sequentially, while in Northwest Iberia only one lithospheric segment was studied in detail. In East Antarctica, was found that the by the time of the last lithospheric breakup event (between the Otway Basin–Terre Adélie), a strong bottom current regime was already in place, and it was further increased by this last event. This promoted the generation of a genetically distinct LBS on which formation the bottom current activity is interpreted to have had a preponderant role.

An important finding from the study of the East Antarctic margin is that the surface which previously was considered as Eocene, is in fact Maastrichtian–Palaeocene in age. This allowed its correlation with the lithospheric breakup event that occurred between the Otway Basin–Terre Adélie at this time. This is a critical point of the South Australia–East Antarctica conjugate margins since it is here where the transition from an orthogonal-obliquely rifting to a transform continental margin occurs. It is postulated here that this lithospheric breakup event between the South Australia–East Antarctica conjugate margins gave origin, due to its location, to a significant lithospheric plate rearrangement, generating a LBS recorded several hundreds of kilometres away from the lithospheric segment with which can be related.

The LBS and the BS develop in non-confined and laterally-changing (both along dip and along strike) depositional environments. Therefore, their identification depends on the area of the margin in which their observation (and interpretation) are

carried out. Knowing this, their recognition can only be achieved using several of their diagnostic characteristics. Although the stratigraphical architecture can remain the same, lithological variability of a given margin will influence the sedimentological characteristics of the LBS and the BS. This is even more pronounced between the opposing margins of a conjugate pair.

The deposition, preservation and observation of the LBS and the BS depend on several factors. The LBS can be erased due to strong bottom current activity, and these same bottom currents can hinder the deposition of a distinct sequence above the LBS, the so-called BS as defined in this thesis.

# REFERENCES


AFILHADO, A., MATIAS, L., SHIOBARA, H., HIRN, A., MENDES-VICTOR, L. & SHIMAMURA, H. (2008). From unthinned continent to ocean: The deep structure of the West Iberia passive continental margin at 38°N. *Tectonophysics,* Vo. 458, p. 9-50.

AINSWORTH, R. B. & PATTISON, S. A. J. (1994). Where have all the lowstands gone? Evidence for attached lowstand systems tracts in the Western Interior of North America. *Geology,* Vo. 22, p. 415-418.

ALFARO, E. & HOLZ, M. (2014). Seismic geomorphological analysis of deepwater gravity-driven deposits on a slope system of the southern Colombian Caribbean margin. *Marine and Petroleum Geology,* Vo. 57, p. 294-311.

ALLEMAND, P. & BRUN, J.-P. (1991). Width of continental rifts and rheological layering of the lithosphere. *Tectonophysics,* Vo. 188, p. 63-69.

ALLEN, P. A. & ALLEN, J. R. (2005). *Basin Analisys: Principles and Aplications*, Blackwell, p. 549.

ALVES, T. M., GAWTHORPE, R., HUNT, D. H. & MONTEIRO, J. H. (2002). Jurassic tectono-sedimentary evolution of the Northern Lusitanian Basin (offshore Portugal). *Marine and Petroleum Geology,* Vo. 19, p. 727-754.

ALVES, T. M., MANUPPELLA, G., GAWTHORPE, R., HUNT, D. H. & MONTEIRO, J. H. (2003a). The depositional evolution of diapir- and fault-bounded rift basins: examples from the Lusitanian Basin of West Iberia. *Sedimentary Geology,* Vo. 162 p. 273-303.

ALVES, T. M., MANUPPELLA, G., GAWTHORPE, R. L., HUNT, D. H. & MONTEIRO, J. H. (2003b). Post-Jurassic tectono-sedimentary evolution of the Northern Lusitanian Basin (western Iberian margin). *Basin Research,* Vo. 15, p. 227 - 249.

ALVES, T. M., MOITA, C., CUNHA, T., MONTEIRO, J. H. & PINHEIRO, L. (2006). Meso-Cenozoic Evolution of North-Atlantic Continental Slope Basins: The Peniche Basin, Western Iberian Margin. *AAPG Bulletin,* Vo. 90, p. 31-60.

ALVES, T. M., MOITA, C., CUNHA, T., ULLNAESS, M., MYKLEBUST, R., MONTEIRO, J. H. & MANUPPELLA, G. (2009). Diachronous evolution of Late Jurassic-Cretaceous continental rifting in the northeast Atlantic (west Iberian margin). *Tectonics,* Vo. 28, p. TC4003.

ARNABOLDI, M. & MEYERS, P. A. (2006). Data report: multiproxy geochemical characterization of OAE-related black shales at Site 1276, Newfoundland Basin. *In:* TUCHOLKE, B. E., SIBUET, J.-C. & KLAUS, A. (eds.) *Proc. ODP, Sci. Results, 210.* College Station, TX (Ocean Drilling Program), p. 1-16.

ARTHUR, M. A. (1979). North Atlantic Cretaceous black shales: the record at site 398 and a brief comparison with other occurrences. *In:* SIBUET, J. C., RYAN, W. B. F. & ET AL. (eds.) *Init. Rep. DSDP, 47(2).* Washington (U.S. Government Printing Office), p. 719-751.

AUTIN, J., LEROY, S., BESLIER, M.-O., D'ACREMONT, E., RAZIN, P., RIBODETTI, A., BELLAHSEN, N., ROBIN, C. & AL TOUBI, K. (2010). Continental break-up history of a deep magma-poor margin based on seismic reflection data (northeastern Gulf of Aden margin, offshore Oman). *Geophysical Journal International,* Vo. 180, p. 501-519.

AZEVEDO, R. (2004). Paleoceanografia e a evolução do Atlântico Sul no Albiano. *Boletim de Geociências da Petrobras,* Vo. 12, p. 231-249.

BALL, P., EAGLES, G., EBINGER, C., MCCLAY, K. & TOTTERDELL, J. (2013). The spatial and temporal evolution of strain during the separation of Australia and Antarctica. *Geochemistry, Geophysics, Geosystems,* Vo. 14, p. 2771-2799.

BALLY, A. W. (ed.) (1987). *Atlas of Seismic Stratigraphy - Studies in Geology,* Tulsa, Oklahoma: AAPG Vo. 27.

BANDA, E., TORNÉ, M. & TALWANI, M. (1995). *Rifted Ocean-Continent Boundaries,* Netherlands, Springer No. 463

BARRY, K., CAVERS, D. & KNEALE, C. (1975). Recommended standards for digital tape formats *GEOPHYSICS,* Vo. 40, p. 344-352.

BASOV, V. A., B. G. LOPATIN, GRAMBERG, I. S., DANJUSHEVSKAYA, A. I., KANBAN'KOV, V. Y., LAZURKIN, V. M. & PATRUNOV, D. K. (1979). Lower Cretaceous lithostratigraphy near Galicia Bank. *In:* SIBUET, J. C., RYAN, W. B. F. & ET AL. (eds.) *Init. Rep. DSDP, 47(2).* Washington (U.S. Government Printing Office), p. 683-701.

BASSI, G. (1991). Factors controlling the style of continental rifting: insights from numerical modelling. *Earth and Planetary Science Letters,* Vo. 105, p. 430-452.

BATES, R. L. & JACKSON, J. A. (1987). *Glossary of Geology,* Alexandria, Virginia, American Geological Institute

BAUR, F., LITTKE, R., WIELENS, H., LAMPE, C. & FUCHS, T. (2010). Basin modeling meets rift analysis - A numerical modeling study from the Jeanne d'Arc basin, offshore Newfoundland, Canada. *Marine and Petroleum Geology,* Vo. 27, p. 585-599.

BEAUMONT, C., KEEN, C. E. & BOUTILIER, R. (1982). On the evolution of rifted continental margins: comparison of models and observations for the Nova Scotian margin. *Geophysical Journal of the Royal Astronomical Society,* Vo. 70, p. 667-715.

BEGLINGER, S. E., DOUST, H. & CLOETINGH, S. (2012). Relating petroleum system and play development to basin evolution: West African South Atlantic basins. *Marine and Petroleum Geology,* Vo. 30, p. 1-25.

BEIN, J. & TAYLOR, M. L. (1981). The Eyre Sub-Basin: recent exploration results. *Australian Petroleum Production and Exploration Association Journal,* Vo. 21, p. 91-98.

BELL, R., G., K. & STECKLER, M. (1988). Early Mesozoic Rift Basins of Eastern North America and their gravity anomalies: the role of detachments during extension. *Tectonics,* Vo. 7, p. 447-462.

BERTHOU, P. Y., BLANC, P. & CHAMLEY, H. (1982). Sédimentation argileuse comparée au Crétacé moyen et supérior dans le bassin occidental portugais et sur la marge voisine (site 398 DSDP): enseignements paléogéographiques et tectoniques. *Bull. Soc. Géol. France,* Vo. XXIV, p. 461-472.

BESLIER, M.-O., ASK, M. & BOILLOT, G. (1993). Ocean-continent boundary in the Iberia Abyssal Plain from multichannel seismic data. *Tectonophysics,* Vo. 218, p. 383-393.

BESLIER, M.-O., WHITMARSH, R. B., WALLACE, P. J., GIRARDEAU, J. & (EDS.) (2001a). *Proc. ODP, Sci. Results, 173*, College Station, TX (Ocean Drilling Project), No. 173

BESLIER, M.-O., ROYER, J.-Y., GIRARDEAU, J., HILL, P. J., BOEUF, E., BUCHANAN, C., CHATIN, F., JACOVETTI, G., MOREAU, A. & MUNSCHY, M. (2004a). Une large transition continent-océan en pied de marge sud-ouest australienne: premiers résultats de la campagne MARGAU/MD110. *Bulletin de la société Géologique de France,* Vo. 175, p. 629-641.

BESLIER, M.-O., ROYER, J.-Y., GIRARDEAU, J., HILL, P. J., BOEUF, E., BUCHANAN, C., CHATIN, F., JACOVETTI, G., MOREAU, A., MUNSCHY, M., PARTOUCHE, C., ROBERT, U. & THOMAS, S. (2004b). A wide ocean-continent transition along the south-west Australian margin: first results of the MARGAU/MD110 cruise. *Bulletin de la Societe Geologique de France,* Vo. 175, p. 629-641.

BESLIER, M. O., LE BIHAN, T., FERAUD, G. & GIRARDEAU, J. (2001b). Cretaceous ultra-slow spreading in the oceanic-continent transition along the southwest Australian passive margin: constraints from $^{40}Ar/^{39}Ar$ dating. *In:* European Union of Geosciences XI, Strasbourg. Cambridge Publications, p. 718.

BLACK, M., HILL, M. N., LAUGHTON, A. S. & MATTHEWS, D. H. (1964). Three non-magnetic seamounts off the Iberian coast. *Quarterly Journal of the Geological Society,* Vo. 120, p. 477-513.

BLACKMAN, D. K., CANN, J. R., JANSSEN, B. & SMITH, D. K. (1998). Origin of extensional core complexes: Evidence from the Mid-Atlantic Ridge at Atlantis Fracture Zone. *J. Geophys. Res.,* Vo. 103, p. 21315-21333.

BLEVIN, J. & CATHRO, D. (2008). *Australian Southern Margin Synthesis, Project GA707, Client report to Geoscience Australia,* Canberra, FrOG Tech Pty Ltd, p. 104.

BLEVIN, J. E. (2005). *Geological framework of the Bremer and Denmark sub-basins, southwest Australia, R/V Southern Surveyor Survey SS03/2004, Geoscience Australia Survey 265, post-survey report and GIS,* Canberra, Geoscience Australia, No. 2005/05

BLUM, M. D. & HATTIER-WOMACK, J. (2009). Climate change, sea-level change, and fluvial sediment supply to deepwater depositional systems: a review. *In:* KNELLER, B., MARTINSEN, O. J. & MCCAFFREY, B. (eds.) *External Controls on Deepwater Depositional Systems: SEPM, Special Publication.* Tulsa: SEPM (Society for Sedimentary Geology). Spec. Publ., Vo. 92, p. 15-39.

BOILLOT, G., AUXIETRE, J. L., DUNAND, J. P., DUPEUBLE, P. A. & MAUFFRET, A. (1979). The northwestern Iberian margin: A Cretaceous passive margin deformed during Eocene. *Deep Drilling Results in the Atlantic Ocean: Continental Margins and Paleoenvironment.* Washington, DC: AGU, Vo. 3, p. 138-153.

BOILLOT, G., GRIMAUD, S., MAUFFRET, A., MOUGENOT, D., KORNPROBST, J., MERGOIL-DANIEL, J. & TORRENT, G. (1980). Ocean-continent boundary off the Iberian margin: A serpentinite diapir west of the Galicia Bank. *Earth and Planetary Science Letters,* Vo. 48, p. 23-34.

BOILLOT, G., RECQ, M., WINTERER, E. L., MEYER, A. W., APPLEGATE, J., BALTUCK, M., BERGEN, J. A., COMAS, M. C., DAVIES, T. A., DUNHAM, K., *et al.* (1987a). Tectonic denudation of the upper mantle along passive margins: a model based on drilling results (ODP leg 103, western Galicia margin, Spain). *Tectonophysics,* Vo. 132, p. 335-342.

BOILLOT, G., WINTERER, E. L., MEYER, A. W. & ET AL (1987b). *Proc. ODP, Init. Reports., 103*, College Station, TX (Ocean Drilling Program)

BOILLOT, G. & MALOD, J. (1988). The north and northwest Spanish continental margin: a review. *Rev. Soc. Geol. España,* Vo. 1, p. 295-316.

BOILLOT, G. & WINTERER, E. L. (1988). Drilling on the Galicia Margin: Retrospect and Prospect. *In:* BOILLOT, G., WINTERER, E. L., MEYER, A. W. & ET AL. (eds.) *Proc. ODP, Sci. Results, 103.* College Station, TX (Ocean Drilling Program), p. 809-828.

BOILLOT, G., WINTERER, E. L., MEYER, A. W. & ET AL (1988). *Proc. ODP, Sci. Results, 103*, College Station, TX (Ocean Drilling Program)

BOILLOT, G., MOUGENOT, D., GIRARDEAU, J. & WINTERER, E. L. (1989). Rifting processes on the west Galicia margin, Spain. *In:* TANKARD, A. J. & BALKWILL, H. R. (eds.) *Extensional Tectonics and Stratigraphy of the North Atlantic Margins.* AAPG Memoir, Vo. 46, p. 363-377.

BOILLOT, G., BESLIER, M. O. & GIRARDEAU, J. (1995). Nature, Structure and Evolution of the Ocean-Continent Boundary: The Lesson of the West Galicia Margin (Spain). *In:* BANDA, E., TORNÉ, M. & TALWANI, M. (eds.) *Rifted Ocean-Continent Boundaries.* Springer Netherlands, Vo. 463, p. 219-229.

BOILLOT, G. & FROITZHEIM, N. (2001). Non-volcanic rifted margins, continental break-up and the onset of sea-floor spreading: some outstanding questions. *In:* WHITMARSH, R. B., TAYLOR, B. & FROITZHEIM, N. (eds.) *Non-Volcanic Rifting of Continental Margins: A Comparison of Evidence from Land and Sea.* London: Geological Society Special Publications, Vo. 187, p. 9-30.

BOND, G. C. & KOMINZ, M. A. (1988). Evolution of thought on passive continental margins from the origin of geosynclinal theory (~1860) to the present. *Geological Society of America Bulletin,* Vo. 100, p. 1909-1933.

BOTT, M. H. P. & KUSZNIR, N. J. (1979). Stress distributions associated with compensated plateau uplift structures with application to the continental splitting mechanism. *Geophysical Journal of the Royal Astronomical Society,* Vo. 56, p. 451-459.

BOTT, M. H. P. (1992a). Modelling the loading stresses associated with active continental rift systems. *Tectonophysics,* Vo. 215, p. 99-115.

BOTT, M. H. P. (1992b). The stress regime associated with continental break-up. *In:* STOREY, B. C., ALABASTER, T. & PANKHURST, R. J. (eds.) *Magmatism and the Causes of Continental Break-up.* London: Geological Society, Vo. 68, p. 125-136.

BOTT, M. H. P. (1993). Modelling the plate-driving mechanism. *Journal of the Geological Society,* Vo. 150, p. 941-951.

BOTT, M. H. P. (1995). Mechanisms of rifting: Geodynamic modeling of continental rift systems. *In:* OLSEN, K. H. (ed.) *Continental Rifts - Evolution, Structure, Tectonics. Developments in Geotectonics.* Elsevier, Vo. 25, p. 27- 43.

BOULT, P., WHITE, M., POLLOCK, R., MORTON, J., ALEXANDER, E. & HILL, A. (2002). Lithostratigraphy and environments of deposition. *In:* BOULT, P. J. & HIBBURT, J. E. (eds.) *The petroleum geology of South Australia, Volume 1: Otway Basin, South Australia.* Vo. 1, p. 1-98.

BRADSHAW, B. E., ROLLET, N., TOTTERDELL, J. M. & BORISSOVA, I. (2003). *A revised structural framework for frontier basins on the southern and southwestern Australian continental margin,* Canberra, Geoscience Australia, No. 2003/03

BRADSHAW, B. E. (2005). *Geology and Petroleum Potential of the Bremer Sub-basin, offshore southwestern Australia,* Canberra, Geoscience Australia, No. 2005/21

BRASS, G. W., SOUTHAM, J. R. & PETERSON, W. H. (1982). Warm saline bottom water in the ancient ocean. *Nature,* Vo. 296, p. 620-623.

BRAUN, J. & BEAUMONT, C. (1989). A physical explanation of the relation between flank uplifts and the breakup unconformity at rifted continental margins. *Geology,* Vo. 17, p. 760-764.

BRONNER, A., SAUTER, D., MANATSCHAL, G., PERON-PINVIDIC, G. & MUNSCHY, M. (2011). Magmatic breakup as an explanation for magnetic anomalies at magma-poor rifted margins. *Nature Geoscience,* Vo. 4, p. 549-553.

BROWN, B. J., MULLER, R. D., GAINA, C., STRUCKMEYER, H. I. M., STAGG, H. M. J. & SYMONDS, P. A. (2003). Formation and evolution of Australian passive margins: implications for locating the boundary between continental and oceanic crust. *Geological Society of America Special Papers,* Vo. 372, p. 223-243.

BRUN, J.-P., SOKOUTIS, D. & VAN DEN DRIESSCHE, J. (1994). Analogue modeling of detachment fault systems and core complexes. *Geology,* Vo. 22, p. 319-322.

BRUN, J. P. & BESLIER, M. O. (1996). Mantle exhumation at passive margins. *Earth and Planetary Science Letters,* Vo. 142, p. 161-173.

BRUN, J. P. (1999). Narrow rifts versus wide rifts: inferences for the mechanics of rifting from laboratory experiments. *Philosophical Transactions of the Royal Society of London. Series A: Mathematical, Physical and Engineering Sciences,* Vo. 357, p. 695-712.

BUCK, W. R. (1988). Flexural rotation of normal faults. *Tectonics,* Vo. 7, p. 959-973.

BUCK, W. R. (1991). Modes of Continental Lithospheric Extension. *J. Geophys. Res.,* Vo. 96, p. 20161-20178.

BUCK, W. R., LAVIER, L. L. & POLIAKOV, A. N. B. (1999). How to make a rift wide. *Philosophical Transactions of the Royal Society of London. Series A: Mathematical, Physical and Engineering Sciences,* Vo. 357, p. 671-693.

BUCK, W. R. (2007). Dynamic Processes in Extensional and Compressional Settings: The Dynamics of Continental Breakup and Extension. *In:* WATTS, A. B. (ed.) *Treatise in Geophysics - Volume 6, Crust and Lithosphere Dynamics.* Elsevier, Vo. 6, p. 335-376.

BULL, S., CARTWRIGHT, J. & HUUSE, M. (2009). A review of kinematic indicators from mass-transport complexes using 3D seismic data. *Marine and Petroleum Geology,* Vo. 26, p. 1132-1151.

BUROV, E. & CLOETINGH, S. (1997). Erosion and rift dynamics: new thermomechanical aspects of post-rift evolution of extensional basins. *Earth and Planetary Science Letters,* Vo. 150, p. 7-26.

BUROV, E. & POLIAKOV, A. (2003). Erosional forcing of basin dynamics: new aspects of syn- and post-rift evolution. *In:* NIEUWLAND, D. A. (ed.) *New Insights into Structural Interpretation and Modelling.* Geological Society, London, Special Publications, Vo. 212, p. 209-223.

BUSBY, C. J. & INGERSOLL, R. V. (1995). *Tectonics of Sedimentary Basins*, Blackwell, p. 579.

CAINELLI, C. & MOHRIAK, W. U. (1999). Some remarks on the evolution of sedimentary basins along the Eastern Brazilian continental margin. *Episodes,* Vo. 22, p. 206-216.

CANDE, S. C. & MUTTER, J. C. (1982). A revised identification of the oldest sea-floor spreading anomalies between Australia and Antarctica. *Earth and Planetary Science Letters,* Vo. 58, p. 151-160.

CANNAT, M., MANATSCHAL, G., SAUTER, D. & PÉRON-PINVIDIC, G. (2009). Assessing the conditions of continental breakup at magma-poor rifted margins: What can we learn from slow spreading mid-ocean ridges? *Comptes Rendus Geosciences,* Vo. 341, p. 406-427.

CATHLES, L. M. & HALLAM, A. (1991). Stress-induced changes in plate density, vail sequences, epeirogeny, and short-lived global sea level fluctuations. *Tectonics,* Vo. 10, p. 659-671.

CATUNEANU, O. (2006). *Principles of Sequence Stratigraphy,* Amsterdam, Elsevier

CATUNEANU, O., ABREU, V., BHATTACHARYA, J. P., BLUM, M. D., DALRYMPLE, R. W., ERIKSSON, P. G., FIELDING, C. R., FISHER, W. L., GALLOWAY, W. E., GIBLING, M. R., *et al.* (2009). Towards the standardization of sequence stratigraphy. *Earth-Science Reviews,* Vo. 92, p. 1-33.

CHAMLEY, H., DEBRABANT, P., J .FOULON, D'ARGOUD, G. G., LATOUCHE, C., MAILLET, N., MAILLOT, H. & SOMMER, F. (1979). Mineralogy and Geochemistry of Cretaceous and Cenozoic Atlantic Sediments off the Iberian Peninsula (Site 398, DSDP Leg 47B). *In:* SIBUET, J. C., RYAN, W. B. F. & ET AL. (eds.) *Init. Rep. DSDP, 47(2).* Washington (U.S. Government Printing Office), p. 429-449.

CHATIN, F., ROBERT, U., MONTIGNY, R. & WHITECHURCH, H. (1998). La zone Diamantine (océan Indien oriental), témoin de la séparation entre l'Australie et l'Antarctique: arguments pétrologiques et géochimiques. *Comptes Rendus de l'Académie des Sciences - Series IIA - Earth and Planetary Science,* Vo. 326, p. 839-845.

CHIAN, D., LOUDEN, K. E., MINSHULL, T. A. & WHITMARSH, R. B. (1999). Deep structure of the ocean-continent transition in the southern Iberia Abyssal Plain from seismic refraction profiles: Ocean Drilling Program (Legs 149 and 173) transect. *J. Geophys. Res.,* Vo. 104, p. 7443-7462.

CHRISTIE-BLICK, N. (1991). Onlap, offlap, and the origin of unconformity-bounded depositional sequences. *Marine Geology,* Vo. 97, p. 35-56.

CLARK, S. A., SAWYER, D. S., AUSTIN, J. A., JR., CHRISTESON, G. L. & NAKAMURA, Y. (2007). Characterizing the Galicia Bank-Southern Iberia Abyssal Plain rifted margin segment boundary using multichannel seismic and ocean bottom seismometer data. *J. Geophys. Res.,* Vo. 112, p. B03408.

CLOETINGH, S., MCQUEEN, H. & LAMBECK, K. (1985). On a tectonic mechanism for regional sealevel variations. *Earth and Planetary Science Letters,* Vo. 75, p. 157-166.

CLOETINGH, S. (1988). Intraplate Stresses: A New Element in Basin Analysis. *In:* KLEINSPEHN, K. & PAOLA, C. (eds.) *New Perspectives in Basin Analysis.* Springer New York, p. 205-230.

CLOETINGH, S., TANKARD, A. J., WELSINK, H. J. & JENKINS, W. A. (1989). Vail's coastal onlap curves and their correlation with tectonic events, offshore eastern Canada *In:* J., T. A. & BALKWILL, H. R. (eds.) *Extensional Tectonics and Stratigraphy of the North Atlantic Margins.* AAPG Memoir, Vo. 46, p. 283-293.

CLOETINGH, S. & ZIEGLER, P. A. (2007). 6.11 - Tectonic Models for the Evolution of Sedimentary Basins. *In:* EDITOR-IN-CHIEF: GERALD, S. (ed.) *Treatise on Geophysics.* Amsterdam: Elsevier, p. 485-611.

CLOSE, D. I. (2004). *A marine geophysical study of the Wilkes Land rifted continental margin, Antarctica.* DPhil, University of Oxford.

CLOSE, D. I., STAGG, H. M. J. & O'BRIEN, P. E. (2007). Seismic stratigraphy and sediment distribution on the Wilkes Land and Terre Adélie margins, East Antarctica. *Marine Geology,* Vo. 239, p. 33-57.

CLOSE, D. I., WATTS, A. B. & STAGG, H. M. J. (2009). A marine geophysical study of the Wilkes Land rifted continental margin, Antarctica. *Geophysical Journal International,* Vo. 177, p. 430-450.

COBLENTZ, D. D., RICHARDSON, R. M. & SANDIFORD, M. (1994). On the gravitational potential of the Earth's lithosphere. *Tectonics,* Vo. 13, p. 929-945.

COCKBAIN, A. E. & HOCKING, R. M. (1989). *Revised stratigraphic nomenclature in Western Australian Phanerozoic basins*, Geological Survey of Western Australia, Record 1989/15

COLWELL, J., STAGG, H. J., DIREEN, N., BERNARDEL, G. & BORISSOVA, I. (2006). The Structure of the Continental Margin off Wilkes Land and Terre Adélie Coast, East Antarctica. *In:* FÜTTERER, D., DAMASKE, D., KLEINSCHMIDT, G., MILLER, H. & TESSENSOHN, F. (eds.) *Antarctica, Contributions to Global Earth Sciences, Proceedings of the IX International Symposium on Antarctic Earth Sciences.* Berlin, Heidelberg: Springer p. 327-340.

CONEY, P. J. (1980). Cordilleran metamorphic core complexes: an overview. . *In:* CRITTENDEN, M. D., CONEY, P. J. & DAVIS, G. H. (eds.) *Cordilleran Metamorphic Core Complexes* Geological Society of America Memoirs, Vo. 153, p. 7-31.

CORREGGIARI, A., TRINCARDI, F., LANGONE, L. & ROVERI, M. (2001). Styles of Failure in Late Holocene Highstand Prodelta Wedges on the Adriatic Shelf. *Journal of Sedimentary Research,* Vo. 71, p. 218-236.

CORTI, G., BONINI, M., CONTICELLI, S., INNOCENTI, F., MANETTI, P. & SOKOUTIS, D. (2003). Analogue modelling of continental extension: a review focused on the relations between the patterns of deformation and the presence of magma. *Earth-Science Reviews,* Vo. 63, p. 169-247.

CORTI, G., BONINI, M., INNOCENTI, F., MANETTI, P., PICCARDO, G. B. & RANALLI, G. (2007). Experimental models of extension of continental lithosphere weakened by percolation of asthenospheric melts. *Journal of Geodynamics,* Vo. 43, p. 465-483.

COWARD, M. P. (1986). Heterogeneous stretching, simple shear and basin development. *Earth and Planetary Science Letters,* Vo. 80, p. 325-336.

CUNHA, T. (2008). *Gravity anomalies, flexure, and the thermo-mechanical evolution of the West Iberia Margin and its conjugate of Newfoundland.* Ph.D., Oxford University.

DAVIS, G. H. (1983). Shear-zone model for the origin of metamorphic core complexes. *Geology,* Vo. 11, p. 342-347.

DAWERS, N. H. & UNDERHILL, J. R. (2000). The Role of Fault Interaction and Linkage in Controlling Synrift Stratigraphic Sequences: Late Jurassic, Statfjord East Area, Northern North Sea. *AAPG Bulletin,* Vo. 84, p. 45-64.

DE SANTIS, L., BRANCOLINI, G. & DONDA, F. (2003). Seismo-stratigraphic analysis of the Wilkes Land continental margin (East Antarctica): influence of glacially driven processes on the Cenozoic deposition. *Deep Sea Research Part II: Topical Studies in Oceanography,* Vo. 50, p. 1563-1594.

DEAN, S. M., MINSHULL, T. A., WHITMARSH, R. B. & LOUDEN, K. E. (2000). Deep structure of the ocean-continent transition in the southern Iberia Abyssal Plain from seismic refraction profiles: The IAM-9 transect at 40°20'N. *J. Geophys. Res.,* Vo. 105, p. 5859-5885.

DEROO, G., GRACIANSKY, P. C., HABIB, D. & HERBIN, J.-P. (1978). L'origine de la matière organique dans les sédiments crétacés du site IPOD 398 (haut-fonf de Vigo): corrélations entre les données de la sédimentologie, de la géochemie organique et de la palynologie. *Bull. Soc. Géol. France,* Vo. 20, p. 465-469.

DEROO, G., HERBIN, J.-P., ROUCACHÉ, J. & TISSOT, B. (1979). Organic Geochemistry of Cretaceous Shales from DSDP Site 398, Leg 47B, Eastern North Atlantic. *In:* SIBUET, J. C., RYAN, W. B. F. & ET AL. (eds.) *Init. Rep. DSDP, 47(2).* Washington (U.S. Government Printing Office), p. 513-522.

DESMURS, L., MANATSCHAL, G. & BERNOULLI, D. (2001). The Steinmann Trinity revisited: mantle exhumation and magmatism along an ocean-continent transition: the Platta nappe, eastern Switzerland. *In:* WILSON, R. C. L., WHITMARSH, R. B., TAYLOR, B. & FROITZHEIM, N. (eds.) *Non-Volcanic Rifting of Continental Margins: A Comparison of Evidence from Land and Sea.* London: Geological Society, Special publications, Vo. 187, p. 235-266.

DESMURS, L., MÜNTENER, O. & MANATSCHAL, G. (2002). Onset of magmatic accretion within a magma-poor rifted margin: a case study from the Platta ocean-continent transition, eastern Switzerland. *Contributions to Mineralogy and Petrology,* Vo. 144, p. 365-382.

DEWEY, J. F. & BURKE, K. (1974). Hot Spots and Continental Break-up: Implications for Collisional Orogeny. *Geology,* Vo. 2, p. 57-60.

DICKIE, K., KEEN, C. E., WILLIAMS, G. L. & DEHLER, S. A. (2011). Tectonostratigraphic evolution of the Labrador margin, Atlantic Canada. *Marine and Petroleum Geology,* Vo. 28, p. 1663-1675.

DINIS, J. L. & TRINCÃO, P. (1995). Recognition and stratigraphical significance of the Aptian unconformity in the Lusitanian Basin, Portugal. *Cretaceous Research,* Vo. 16, p. 171-186.

DINIS, J. L., REY, J., CUNHA, P. P., CALLAPEZ, P. & PENA DOS REIS, R. (2008). Stratigraphy and allogenic controls of the western Portugal Cretaceous: an updated synthesis. *Cretaceous Research,* Vo. 29, p. 772-780.

DIREEN, N. G., BORISSOVA, I., STAGG, H. M. J., COLWELL, J. B. & SYMONDS, P. A. (2007). Nature of the continent–ocean transition zone along the southern Australian continental margin: a comparison of the Naturaliste Plateau, SW Australia, and the central Great Australian Bight sectors. *In:* KARNER, G. D., MANATSCHAL, G. & PINHEIRO, L. M. (eds.) *Imaging, Mapping and Modelling Continental Lithosphere Extension and Breakup.* London: Geological Society Special Publications, Vo. 282, p. 239-263.

DIREEN, N. G., STAGG, H. M. J., SYMONDS, P. A. & COLWELL, J. B. (2011). Dominant symmetry of a conjugate southern Australian and East Antarctic magma-poor rifted margin segment. *Geochemistry, Geophysics, Geosystems,* Vo. 12, p. Q02006.

DIREEN, N. G. (2012). Comment on "Antarctica — Before and after Gondwana" by S.D. Boger Gondwana Research, Volume 19, Issue 2, March 2011, Pages 335–371. *Gondwana Research,* Vo. 21, p. 302-304.

DIREEN, N. G., STAGG, H. M. J., SYMONDS, P. A. & NORTON, I. O. (2012). Variations in rift symmetry: cautionary examples from the Southern Rift System (Australia–Antarctica). *In:* MOHRIAK, W. U., DANFORTH, A., POST, P. J., BROWN, D. E., TARI, G. C., NEMČOK, M. & SINHA, S. T. (eds.) *Conjugate Divergent Margins* London: Geological Society, London, Special Publications, Vo. 369, p. 453-475.

DISCOVERY 215 WORKING GROUP (1998). Deep structure in the vicinity of the ocean-continent transition zone under the southern Iberia Abyssal Plain. *Geology,* Vo. 26, p. 743-746.

DONDA, F., BRANCOLINI, G., SANTIS, L. D. & TRINCARDI, F. (2003). Seismic facies and sedimentary processes on the continental rise off Wilkes Land (East Antarctica):

evidence of bottom current activity. *Deep Sea Research Part II: Topical Studies in Oceanography,* Vo. 50, p. 1509-1527.

DONDA, F., BRANCOLINI, G., O'BRIEN, P. E., DE SANTIS, L. & ESCUTIA, C. (2007). Sedimentary processes in the Wilkes Land margin: a record of the Cenozoic East Antarctic Ice Sheet evolution. *Journal of the Geological Society,* Vo. 164, p. 243-256.

DONDA, F., O'BRIEN, P. E., DE SANTIS, L., REBESCO, M. & BRANCOLINI, G. (2008). Mass wasting processes in the Western Wilkes Land margin: Possible implications for East Antarctic glacial history. *Palaeogeography, Palaeoclimatology, Palaeoecology,* Vo. 260, p. 77-91.

DORÉ, A. G. (1992). Synoptic palaeogeography of the Northeast Atlantic Seaway: late Permian to Cretaceous. *Geological Society, London, Special Publications,* Vo. 62, p. 421-446.

DORÉ, A. G., LUNDIN, E. R., JENSEN, L. N., BIRKELAND, Ø., ELIASSEN, P. E. & FICHLER, C. (1999). Principal tectonic events in the evolution of the northwest European Atlantic margin. *In:* FLEET, A. J. & BOLDY, S. A. R. (eds.) *Petroleum Geology of Northwest Europe: Proceedings of the 5th Conference.* London: Geological Society, Vo. 5, p. 41-61.

DOTT JR, R. H. (1978). Tectonics and sedimentation a century later. *Earth-Science Reviews,* Vo. 14, p. 1-34.

DRISCOLL, N. W., HOGG, J. R., CHRISTIE-BLICK, N. & KARNER, G. D. (1995). Extensional tectonics in the Jeanne d'Arc Basin, offshore Newfoundland: implications for the timing of break-up between Grand Banks and Iberia. *In:* SCRUTTON, R. A., STOKER, M. S., SHIMMIELD, G. B. & TUDHOPE, A. W. (eds.) *The tectonics, sedimentation and palaeogeography of the North Atlantic Region.* London: Geological Society Special Publication, Vo. 90, p. 1-28.

DRISCOLL, N. W. & KARNER, G. D. (1998). Lower crustal extension across the Northern Carnarvon basin, Australia: Evidence for an eastward dipping detachment. *J. Geophys. Res.,* Vo. 103, p. 4975-4991.

DUNBAR, J. A. & SAWYER, D. S. (1989). How Preexisting Weaknesses Control the Style of Continental Breakup. *J. Geophys. Res.,* Vo. 94, p. 7278-7292.

DUNLAP, D., WOOD, L. & MOSCARDELLI, L. (2013). Seismic geomorphology of early North Atlantic sediment waves, offshore northwest Africa. *Interpretation,* Vo. 1, p. SA75-SA91.

DUPEUBLE, P. A., REHAULT, J. P., AUXIETRE, J. L., DUNAND, J. P. & PASTOURET, L. (1976). Resultats de dragages et essai de stratigraphie des bancs de Galice, et des montagnes de Porto et de Vigo (marge occidentale Iberique). *Marine Geology,* Vo. 22, p. 37-49.

DUPRÉ, S., BERTOTTI, G. & CLOETINGH, S. (2007). Tectonic history along the South Gabon Basin: Anomalous early post-rift subsidence. *Marine and Petroleum Geology,* Vo. 24, p. 151-172.

DYKSTERHUIS, S., REY, P., MULLER, R. D. & MORESI, L. (2007). Effects of initial weakness on rift architecture. *In:* KARNER, G. D., MANATSCHAL, G. & PINHEIRO, L. M. (eds.) *Imaging, Mapping and Modelling Continental Lithosphere Extension and Breakup.* London: Geological Society Special Publications, Vo. 282, p. 443-455.

EAGLES, G. (2007). New angles on South Atlantic opening. *Geophysical Journal International,* Vo. 168, p. 353-361.

EGAN, S. S. (1992). The flexural isostatic response of the lithosphere to extensional tectonics. *Tectonophysics,* Vo. 202, p. 291-308.

EINSELE, G. (2000). *Sedimentary Basins: Evolution, Facies, and Sediment Budget,* Berlin Heidelberg, Springer-Verlag

EITTREIM, S. L., HAMPTON, M. A. & CHILDS, J. R. (1985). Seismic-Reflection Signature of Cretaceous Continental Breakup on the Wilkes Land Margin, Antarctica. *Science,* Vo. 229, p. 1082-1084.

EITTREIM, S. L. & SMITH, G. L. (1987). Seismic sequences and their distribution on the Wilkes Land margin. *In:* EITTREIM, S. L. & HAMPTON, M. A. (eds.) *The Antarctic Continental Margin Geology and Geophysics of Offshore Wilkes Land.* Houston, Texas, USA: Circum Pacific Council Publications, Vo. 5A, p. 15–43

EITTREIM, S. L., COOPER, A. K. & WANNESSON, J. (1995). Seismic stratigraphic evidence of ice-sheet advances on the Wilkes Land margin of Antarctica. *Sedimentary Geology,* Vo. 96, p. 131-156.

EMBRY, A. F. & DIXON, J. (1990). The breakup unconformity of the Amerasia Basin, Arctic Ocean: Evidence from Arctic Canada. *Geological Society of America Bulletin,* Vo. 102, p. 1526-1534.

ENGLAND, P. C. (1983). Constraints on the extension of continental lithosphere. *Journal of Geophysical Research,* Vo. 88, p. 1145-1152.

ESCUTIA, C., EITTREIM, S. L. & COOPER, A. K. (1997). Cenozoic sedimentation on the Wilkes Land continental rise, Antarctica. *In:* RICCI, C. A. (ed.) *The Antarctic Region: Geological Evolution and Processes.* Siena: Terra Antarctica, p. 791-795.

ESCUTIA, C., EITTREIM, S. L., COOPER, A. K. & NELSON, C. H. (2000). Morphology and Acoustic Character of the Antarctic Wilkes Land Turbidite Systems: Ice-Sheet-Sourced Versus River-Sourced Fans. *Journal of Sedimentary Research,* Vo. 70, p. 84-93.

ESCUTIA, C., DE SANTIS, L., DONDA, F., DUNBAR, R. B., COOPER, A. K., BRANCOLINI, G. & EITTREIM, S. L. (2005). Cenozoic ice sheet history from East Antarctic Wilkes Land continental margin sediments. *Global and Planetary Change,* Vo. 45, p. 51-81.

ESCUTIA, C., BRINKHUIS, H. & KLAUS, A. (2008). *Cenozoic East Antarctic ice sheet evolution from Wilkes Land margin sediments.* , IODP Sci. Prosp., 318

ESCUTIA, C., BRINKHUIS, H., KLAUS, A. & EXPEDITION 318 SCIENCE PARTY (2011). *Proc. IODP, Expedition Reports, 318,* Tokyo, Integrated Ocean Drilling Program Management International, Inc., No. 318

ESPURT, N., CALLOT, J.-P., TOTTERDELL, J., STRUCKMEYER, H. & VIALLY, R. (2009). Interactions between continental breakup dynamics and large-scale delta system evolution: Insights from the Cretaceous Ceduna delta system, Bight Basin, Southern Australian margin. *Tectonics,* Vo. 28, p. TC6002.

ESPURT, N., CALLOT, J.-P., ROURE, F., TOTTERDELL, J. M., STRUCKMEYER, H. I. M. & VIALLY, R. (2012). Transition from symmetry to asymmetry during continental rifting: an example from the Bight Basin–Terre Adélie (Australian and Antarctic conjugate margins). *Terra Nova,* Vo. 24, p. 167-180.

EXPEDITION 318 SCIENCE PARTY (2011a). Site U1359. *In:* ESCUTIA, C., BRINKHUIS, H., KLAUS, A. & EXPEDITION 318 SCIENCE PARTY (eds.) *Proc. IODP, Expedition Reports, 318.* Tokyo: Integrated Ocean Drilling Program Management International, Inc., Vo. 318.

EXPEDITION 318 SCIENCE PARTY (2011b). Site U1356. *In:* ESCUTIA, C., BRINKHUIS, H., KLAUS, A. & EXPEDITION 318 SCIENCE PARTY (eds.) *Proc. IODP, Expedition Reports, 318.* Tokyo: Integrated Ocean Drilling Program Management International, Inc., Vo. 318.

EXPEDITION 339 SCIENTISTS (2012). *Mediterranean outflow: environmental significance of the Mediterranean Outflow Water and its global implications. IODP Preliminary Report, 339*, Integrated Ocean Drilling Program Management International, Inc., for the Integrated Ocean Drilling Program

FALVEY, D. A. (1974). The development of continental margins in plate tectonic theory. *Journal of Australian Petroleum Exploration Association,* Vo. 14, p. 95-106.

FAUGÈRES, J.-C., STOW, D. A. V., IMBERT, P. & VIANA, A. (1999). Seismic features diagnostic of contourite drifts. *Marine Geology,* Vo. 162, p. 1-38.

FAUGÈRES, J.-C. & MULDER, T. (2011). Contour Currents and Contourite Drifts. *In:* HEIKO, H. & THIERRY, M. (eds.) *Deep-Sea Sediments.* Elsevier, Vo. Volume 63, p. 149-214.

FAVRE, P., STAMPFLI, G. & WILDI, W. (1991). Jurassic sedimentary record and tectonic evolution of the northwestern corner of Africa. *Palaeogeography, Palaeoclimatology, Palaeoecology,* Vo. 87, p. 53-73.

FEARY, D. A., HINE, A. C., MALONE, M. J. & ET AL. (2000). *Proc. ODP, Init. Reports, 182*, College Station, TX (Ocean Drilling Project)

No. 182

FLOQUET, M. (1998). Outcroup cycle stratigraphy of shallow ramp deposits: the Late Cretaceous series on the Castillian Ramp (Northern Spain). *In:* DE GRACIANSKY, P.-C., HARDENBOL, J., THIERRY, J. & VAIL, P. R. (eds.) *Mesozoic and Cenozoic Sequence Stratigraphy of European Basins.* Tulsa: SEPM (Society for Sedimentary Geology). Spec. Publ., Vo. 60, p. 343-361.

FORSYTH, D. & UYEDA, S. (1975). On the Relative Importance of the Driving Forces of Plate Motion*. *Geophysical Journal of the Royal Astronomical Society,* Vo. 43, p. 163-200.

FRANK, T. D. & ARTHUR, M. A. (1999). Tectonic forcings of Maastrichtian ocean-climate evolution. *Paleoceanography,* Vo. 14, p. 103-117.

FREY-MARTÍNEZ, J., CARTWRIGHT, J. & JAMES, D. (2006). Frontally confined versus frontally emergent submarine landslides: A 3D seismic characterisation. *Marine and Petroleum Geology,* Vo. 23, p. 585-604.

FROITZHEIM, N. & MANATSCHAL, G. (1996). Kinematics of Jurassic rifting, mantle exhumation, and passive-margin formation in the Austroalpine and Penninic nappes (eastern Switzerland). *Geological Society of America Bulletin,* Vo. 108, p. 1120-1133.

GADALLAH, M. R. & FISHER, R. (2009). *Exploration Geophysics,* Berlin Heidelberg, Springer

GANS, P. B., MILLER, E. L., MCCARTHY, J. & OULDCOTT, M. L. (1985). Tertiary extensional faulting and evolving ductile-brittle transition zones in the northern Snake Range and vicinity: New insights from seismic data. *Geology,* Vo. 13, p. 189-193.

GARCÍA, M., ERCILLA, G. & ALONSO, B. (2009a). Morphology and sedimentary systems in the Central Bransfield Basin, Antarctic Peninsula: sedimentary dynamics from shelf to basin. *Basin Research,* Vo. 21, p. 295-314.

GARCÍA, M., HERNÁNDEZ-MOLINA, F. J., LLAVE, E., STOW, D. A. V., LEÓN, R., FERNÁNDEZ-PUGA, M. C., DIAZ DEL RÍO, V. & SOMOZA, L. (2009b). Contourite erosive features caused by the Mediterranean Outflow Water in the Gulf of Cadiz: Quaternary tectonic and oceanographic implications. *Marine Geology,* Vo. 257, p. 24-40.

GIBSON, G. M., MORSE, M. P., IRELAND, T. R. & NAYAK, G. K. (2011). Arc–continent collision and orogenesis in western Tasmanides: Insights from reactivated basement structures and formation of an ocean–continent transform boundary off western Tasmania. *Gondwana Research,* Vo. 19, p. 608-627.

GIBSON, G. M., TOTTERDELL, J. M., MORSE, M. P., GONCHAROV, A., MITCHELL, C. H. & STACEY, A. R. (2012). *Basement structure and its influence on the pattern and geometry of continental rifting and breakup along Australia's southern rift margin,* Canberra, Geoscience Australia, No. 2012/47

GIBSON, G. M., TOTTERDELL, J. M., WHITE, L. T., MITCHELL, C. H., STACEY, A. R., MORSE, M. P. & WHITAKER, A. (2013). Pre-existing basement structure and its influence on continental rifting and fracture zone development along Australia's southern rifted margin. *Journal of the Geological Society,* Vo. 170, p. 365-377.

GOVERS, R. & WORTEL, M. J. R. (1999). Some remarks on the relation between vertical motions of the lithosphere during extension and the necking depth parameter inferred from kinematic modeling studies. *Journal of Geophysical Research: Solid Earth,* Vo. 104, p. 23245-23253.

GPEP GABINETE PARA A PESQUISA E EXPLORAÇÃO DE PETRÓLEO (1986). Petroleum potential of Portugal.

GRACIANSKY, P. C., MULLER, C., REHAULT, J. P. & SIGAL, J. (1978). Reconstituition de L'évolution des millieux de sedimentation sur la marge continentale ibérique au Crétacé: le flanc sud du haut-fond de Vigo et le forage DSDP-IODP 398D. *Bull. Soc. Géol. France,* Vo. XX, p. 389-399.

GRACIANSKY, P. C. & CHENET, P. Y. (1979). Sedimentological Study of Cores 138 to 56 (Upper Hauterivian to Middle Cenomanian) an Attempt at Reconstruction of Paleoenvironments. *In:* SIBUET, J. C., RYAN, W. B. F. & ET AL. (eds.) *Init. Rep. DSDP, 47(2).* Washington (U.S. Government Printing Office), p. 403-418.

GRADSTEIN, F. M., OGG, J. G. & SMITH, A. G. (2005). *A Geologic Time Scale 2004*, Cambridge University Press

GRANT, A. C., JANSA, L. F., MCALPINE, K. D. & EDWARDS, A. (1988). Mesozoic–Cenozoic geology of the eastern margin of the Grand Banks and its relation to Galicia Bank. *In:* BOILLOT, G., WINTERER, E. L., MEYER, A. W. & ET AL. (eds.) *Proc. ODP, Sci. Results, 103.* College Station, TX (Ocean Drilling Program), p. 787–808.

GROBE, R. W., ALVAREZ-MARRÓN, J., GLASMACHER, U. A. & STUART, F. M. (2014). Mesozoic exhumation history and palaeolandscape of the Iberian Massif in eastern Galicia from apatite fission-track and (U+Th)/He data. *International Journal of Earth Sciences,* Vo. 103, p. 539-561.

GROUPE GALICE (1979). The continental margin off Galicia and Portugal: Acoustical stratigraphy, dredge stratigraphy, and structural evolution. *In:* SIBUET, J. C., RYAN, W. B. F. & ET AL. (eds.) *Init. Rep. DSDP, 47(2).* Washington (U.S. Government Printing Office), p. 633 – 662.

HABIB, D. (1979). Sedimentology of palynomorphs and palynodebris in Cretaceous carbonaceous facies south of Vigo seamount. *In:* SIBUET, J. C., RYAN, W. B. F. & ET AL. (eds.) *Init. Rep. DSDP, 47(2).* Washington (U.S. Government Printing Office), p. 451-467.

HALPIN, J. A., CRAWFORD, A. J., DIREEN, N. G., COFFIN, M. F., FORBES, C. J. & BORISSOVA, I. (2008). Naturaliste Plateau, offshore Western Australia: A submarine window into Gondwana assembly and breakup. *Geology,* Vo. 36, p. 807-810.

HAMILTON, W. (1987). Crustal extension in the Basin and Range Province, southwestern United States. *In:* COWARD, M. P., DEWEY, J. F. & HANCOCK, P. L. (eds.) *Continental Extensional Tectonics.* London: Geological Society Special Publications, p. 155-176.

HAMPTON, M., EITTREIM, S. & RICHMOND, B. M. (1987). Post-Breakup Sedimentation on the Wilkes Land Margin, Antarctica. *In:* EITTREIM, S. L. & HAMPTON, M. A. (eds.) *The Antarctic Continental Margin: Geology and Geophysics of Offshore Wilkes Land.* Circum Pacific Council Publications, Vo. 5A, p. 75–88.

HANDOH, I. C., BIGG, G. R., JONES, E. J. W. & INOUE, M. (1999). An ocean modeling study of the Cenomanian Atlantic: Equatorial paleo-upwelling, organic-rich sediments and the consequences for a connection between the proto-North and South Atlantic. *Geophysical Research Letters,* Vo. 26, p. 223-226.

HAQ, B. U., HARDENBOL, J. & VAIL, P. R. (1987). Chronology of Fluctuating Sea Levels Since the Triassic. *Science,* Vo. 235, p. 1156-1167.

HAQ, B. U., HARDENBOL, J. & VAIL, P. R. (1988). Mesozoic and Cenozoic chronostratigraphy and cycles of sea-level change. *In:* WILGUS, C. K. (ed.) *Sea-Level Changes: An Integrated Approach.* Society of Economic Paleontologists and Mineralogists, Special Publication, Vo. 42, p. 71-108.

HARDENBOL, J., THIERRY, J., FARLEY, M. B., DE GRACIANSKY, P.-C. & VAIL, P. R. (1998). Mesozoic and Cenozoic sequence chronostratigraphic framework of European basins. *In:* DE GRACIANSKY, P.-C., HARDENBOL, J., THIERRY, J. & VAIL, P. R. (eds.) *Mesozoic and Cenozoic Sequence Stratigraphy of European Basins.* Tulsa: SEPM (Society for Sedimentary Geology). Spec. Publ., Vo. 60, p. 3–13.

HART, S. R. & BLUSZTAJN, J. (2006). Age and geochemistry of the mafic sills, ODP site 1276, Newfoundland margin. *Chemical Geology,* Vo. 235, p. 222-237.

HAY, W. W., DECONTO, R. M., WOLD, C. N., WILSON, K. M., VOIGT, S., SCHULZ, M., WOLD, A. R., DULLO, W.-C., RONOV, A. B., BALUKHOVSKY, A. N. & SÖDING, E. (1999). Alternative global Cretaceous paleogeography. *Geological Society of America Special Papers,* Vo. 332, p. 1-47.

HAY, W. W. (2008). Evolving ideas about the Cretaceous climate and ocean circulation. *Cretaceous Research,* Vo. 29, p. 725-753.

HAYES, D. E. (1972). *Antarctica Oceanology II: The Australian-New Zealand Sector*, American Geophysical Union, p. 364.

HEALY, D. & KUSZNIR, N. J. (2007). Early kinematic history of the Goban Spur rifted margin derived from a new model of continental breakup and sea-floor spreading initiation *In:* KARNER, G. D., MANATSCHAL, G. & PINHEIRO, L. M. (eds.) *Imaging, Mapping and Modelling Continental Lithosphere Extension and Breakup.* London: Geological Society Special Publications, Vo. 282, p. 199-215.

HENK, A. (2006). Stress and strain during fault-controlled lithospheric extension - insights from numerical experiments. *Tectonophysics,* Vo. 415, p. 39-55.

HENNING, A. T., SAWYER, D. S. & TEMPLETON, D. C. (2004). Exhumed upper mantle within the ocean-continent transition on the northern West Iberia margin: Evidence from prestack depth migration and total tectonic subsidence analyses. *J. Geophys. Res.,* Vo. 109, p. B05103.

HERMANN, J., MÜNTENER, O., TROMMSDORFF, V., HANSMANN, W. & PICCARDO, G. B. (1997). Fossil crust-to-mantle transition, Val Malenco (Italian Alps). *Journal of Geophysical Research: Solid Earth (1978–2012),* Vo. 102, p. 20123-20132.

HERNÁNDEZ-MOLINA, F. J., LLAVE, E. & STOW, D. A. V. (2008). Continental slope contourites. *In:* REBESCO, M. & CAMERLENGHI, A. (eds.) *Contourites.* Elsevier, Vo. 60, p. 379-408.

HILL, A. J. (1995). Bight Basin. *In:* DREXEL, J. F. & PREISS, W. V. (eds.) *The Geology of South Australia. Vol. 2. The Phanerozoic.* South Australian Geological Survey Bulletin 54, p. 133-149.

HILL, K. C., HILL, K. A., COOPER, G. T., O'SULLIVAN, A. J., O'SULLIVAN, P. B. & RICHARDSON, M. J. (1995). Inversion around the Bass basin, SE Australia. *In:* BUCHANAN, J. G. & BUCHANAN, P. G. (eds.) *Basin inversion.* London: Geological Society, Special Publications, Vo. 88, p. 525-547.

HISCOTT, R. N., WILSON, R. C. L., GRADSTEIN, F. M., PUJALTE, V., GARCIA-MONDEJAR, J., BOUDREAU, R. R. & WISHART, H. A. (1990). Comparative Stratigraphy and Subsidence history of Mesozoic Rift Basins of North Atlantic. *AAPG Bulletin*

Vo. 74, p. 60-76.

HOCKING, R. M. (1990). Eucla Basin. *Geology and mineral resources of Western Australia.* Australia Geological Survey, Memoir 3, p. 457-495.

HOLDGATE, G. R., MACKAY, G. H. & SMITH, G. C. (1985). The Portland Trough, Otway Basin—geology and petroleum potential. *In:* GLENIE, R. C. (ed.) *Second Southeastern Australia Oil Exploration Symposium. Technical Papers.* Melbourne: Petroleum Exploration Society of Australia (Victorian and Tasmanian Branches), p. 219-232.

HOLDGATE, G. R. & GALLAGHER, S. J. (2003). Tertiary: a period of transition to marine basin environments. *In:* BIRCH, W. D. (ed.) *Geology of Victoria*

Geological Society of Australia Special Publication 23 (Victoria Division) p. 289-335.

HOLFORD, S. P., TUITT, A. K., HILLIS, R. R., GREEN, P. F., STOKER, M. S., DUDDY, I. R., SANDIFORD, M. & TASSONE, D. R. (2014). Cenozoic deformation in the Otway Basin, southern Australian margin: implications for the origin and nature of post-breakup compression at rifted margins. *Basin Research,* Vo. 26, p. 10-37.

HOUSEMAN, G. & ENGLAND, P. (1986). Finite Strain Calculations of Continental Deformation 1. Method and General Results for Convergent Zones. *J. Geophys. Res.,* Vo. 91, p. 3651-3663.

HUISMANS, R. S. & BEAUMONT, C. (2007). Effects of initial weakness on rift architecture. *In:* KARNER, G. D., MANATSCHAL, G. & PINHEIRO, L. M. (eds.) *Imaging, Mapping and Modelling Continental Lithosphere Extension and Breakup.* London: Geological Society Special Publications, Vo. 282, p. 111-138.

HUISMANS, R. S. & BEAUMONT, C. (2011). Depth-dependent extension, two-stage breakup and cratonic underplating at rifted margins. *Nature,* Vo. 473, p. 74-78.

HUNT, D. & TUCKER, M. E. (1992). Stranded parasequences and the forced regressive wedge systems tract: deposition during base-level sea fall. *Sedimentary Geology,* Vo. 81, p. 1-9.

INGERSOLL, R. V. & BUSBY, C. J. (1995). Tectonics of Sedimentary Basins. *In:* BUSBY, C. J. & INGERSOLL, R. V. (eds.) *Tectonics of Sedimentary Basins.* Blackwell, p. 1-51.

ISSLER, D., MCQUEEN, H. & BEAUMONT, C. (1989). Thermal and isostatic consequences of simple shear extension of the continental lithosphere. *Earth and Planetary Science Letters,* Vo. 91, p. 341-358.

JAGOUTZ, O., MÜNTENER, O., MANATSCHAL, G., RUBATTO, D., PÉRON-PINVIDIC, G., TURRIN, B. D. & VILLA, I. M. (2007). The rift-to-drift transition in the North Atlantic: A stuttering start of the MORB machine? *Geology,* Vo. 35, p. 1087-1090.

JARVIS, G. T. & MCKENZIE, D. P. (1980). Sedimentary basin formation with finite extension rates. *Earth and Planetary Science Letters,* Vo. 48, p. 42-52.

JUNGSLAGER, E. H. A. (1999). Petroleum habitats of the Atlantic margin of South Africa. *In:* CAMERON, N. R., H., B. R. & CLURE, V. S. (eds.) *The Oil and Gas Habitats of the South Atlantic.* Geological Society, London, Special Publications, Vo. 153, p. 153-168.

KARSON, J. A. (1999). Geological investigation of a lineated massif at the Kane Transform Fault: implications for oceanic core complexes. *Philosophical Transactions of the Royal Society of London. Series A: Mathematical, Physical and Engineering Sciences,* Vo. 357, p. 713-740.

KEEN, C. E. (1985). The dynamics of rifting: deformation of the lithosphere by active and passive driving forces. *Geophysical Journal of the Royal Astronomical Society,* Vo. 80, p. 95-120.

KEEN, C. E., STOCKMAL, G. S., WELSINK, H., QUINLAN, G. & MUDFORD, B. (1987). Deep crustal structure and evolution of the rifted margin northeast of Newfoundland: results from LITHOPROBE East. *Canadian Journal of Earth Sciences,* Vo. 24, p. 1537 - 1549.

KEEN, M. J. & PIPER, D. J. W. (1990). Geological and historical perspective. *In:* KEEN, M. J. & WILLIAMS, G. L. (eds.) *Geology of the Continental Margin of Eastern Canada.* Geological Survey of Canada, Geology of Canada, Vo. 2, p. 5-30.

KENNETT, B. L. N. (2000). Crust and lithosphere from seismic observations. *In:* VEEVERS, J. J. (ed.) *Billion-Year Earth History of Australia and Neighbours in Gondwanaland.* Sidney: Gemoc Press, p. 74-77.

KHAIN, V. Y. (1992). The role of rifting in the evolution of the Earth's crust. *Tectonophysics,* Vo. 215, p. 1-7.

KNIES, J., MATTINGSDAL, R., FABIAN, K., GRØSFJELD, K., BARANWAL, S., HUSUM, K., DE SCHEPPER, S., VOGT, C., ANDERSEN, N., MATTHIESSEN, J., ANDREASSEN, K., JOKAT, W., NAM, S.-I. & GAINA, C. (2014). Effect of early Pliocene uplift on late Pliocene cooling in the Arctic–Atlantic gateway. *Earth and Planetary Science Letters,* Vo. 387, p. 132-144.

KOOI, H. & CLOETINGH, S. (1989). Intraplate Stresses and the Tectono-Stratigraphic Evolution of the Central North Sea. *In:* J., T. A. & BALKWILL, H. R. (eds.) *Extensional Tectonics and Stratigraphy of the North Atlantic Margins.* AAPG Memoir, Vo. 46, p. 541-558.

KOOI, H. & CLOETINGH, S. (1992). Lithospheric Necking and Regional Isostasy at Extensional Basins 2. Stress-Induced Vertical Motions and Relative Sea Level Changes. *Journal of Geophysical Research,* Vo. 97, p. 17573–17591.

KOOI, H., CLOETINGH, S. & BURRUS, J. (1992). Lithospheric Necking and Regional Isostasy at Extensional Basins 1. Subsidence and Gravity Modeling With an Application to the Gulf of Lions Margin (SE France). *Journal of Geophysical Research,* Vo. 97, p. 17553–17571.

KRASSAY, A. A. & TOTTERDELL, J. M. (2003). Seismic stratigraphy of a large, Cretaceous shelf-margin delta complex, offshore southern Australia. *AAPG Bulletin,* Vo. 87, p. 935 - 963.

KRASSAY, A. A., CATHRO, D. L. & RYAN, D. J. (2004). A regional tectonostratigraphic framework for the Otway Basin. *In:* BOULT, P. J., JOHNS, D. R. & LANG, S. C. (eds.) *Eastern Australian Basins Symposium II.* Petrol. Explor. Soc. Aust., Spec. Publ., Vo. 2, p. 97-106.

KUHNT, W. & COLLINS, E. S. (1996). Cretaceous to Paleogene Benthic Foraminifers from the Iberia Abyssal Plain. *In:* WHITMARSH, R. B., SAWYER, D. S., KLAUS, A. & MASSON, D. G. (eds.) *Proc. ODP, Sci. Results, 149.* College Station, TX (Ocean Drilling Program), p. 203-216.

KULLBERG, J. C., ROCHA, R. B., SOARES, A. F., REY, J., TERRINHA, P., AZERÊDO, A. C., CALLAPEZ, P., DUARTE, L. V., KULLBERG, M. C., MARTINS, L., MIRANDA, R., ALVES, C., MATA, J., MADEIRA, J., MATEUS, O., MOREIRA, M. & NOGUEIRA, C. R. (2013). A Bacia Lusitaniana: Estratigrafia, Paleogeografia e Tectónica. *In:* DIAS, R., ARAÚJO, A., TERRINHA, P. & KULLBERG, J. C. (eds.) *Geologia de Portugal.* Lisbon: Escolar Editora, Vo. 2.

KUSZNIR, N. J. & EGAN, S. S. (1989). Simple-shear and pure-shear models of extensional sedimentary basin formation: application to the Jeanne d'Arc basin, Grand Banks of Newfoundland. *In:* TANKARD, A. J. & BALKWILL, H. R. (eds.) *Extensional Tectonics and Stratigraphy of the North Atlantic Margins.* AAPG Memoir, Vo. 46, p. 305– 322.

KUSZNIR, N. J., MARSDEN, G. & EGAN, S. S. (1991). A flexural-cantilever simple-shear/pure-shear model of continental lithosphere extension: applications to the Jeanne d'Arc Basin, Grand Banks and Viking Graben, North Sea. *In:* M., R. A., YIELDING, G. & FREEMAN, B. (eds.) *The Geometry of Normal Faults.* London: Geological Society Special Publications, Vo. 56, p. 41-60.

KUSZNIR, N. J. & ZIEGLER, P. A. (1992). The mechanics of continental extension and sedimentary basin formation: A simple-shear/pure-shear flexural cantilever model. *Tectonophysics,* Vo. 215, p. 117-131.

KUSZNIR, N. J. & KARNER, G. D. (2007). Continental lithospheric thinning and breakup in response to upwelling divergent mantle flow: application to the Woodlark, Newfoundland and Iberia margins. *In:* KARNER, G. D., MANATSCHAL, G. & PINHEIRO, L. M. (eds.) *Imaging, Mapping and Modelling Continental Lithosphere Extension and Breakup.* London: Geological Society Special Publications, Vo. 282, p. 389-419.

KYRKJEBØ, R., GABRIELSEN, R. H. & FALEIDE, J. I. (2004). Unconformities related to the Jurassic-Cretaceous synrift-post-rift transition of the northern North Sea. *Journal of the Geological Society,* Vo. 161, p. 1-17.

LANE, H., MÜLLER, R. D., TOTTERDELL, J. M. & WHITTAKER, J. M. (2012). Developing a consistent sequence stratigraphy for the Wilkes Land and Great Australian Bight margins. *In:* PESA Eastern Australasian Basins Symposium IV. p. 1-13.

LAVIER, L. L. & MANATSCHAL, G. (2006). A mechanism to thin the continental lithosphere at magma-poor margins. *Nature,* Vo. 440, p. 324-328.

LAVIN, C. (1997). The Maastrichtian breakup of the Otway Basin margin - a model developed by integrating seismic interpretation, sequence statigraphy and thermochronological studies. *Exploration Geophysics,* Vo. 28, p. 252-259.

LE PICHON, X. & SIBUET, J.-C. (1981). Passive Margins: A Model of Formation. *J. Geophys. Res.,* Vo. 86, p. 3708-3720.

LE PICHON, X., ANGELIER, J. & SIBUET, J.-C. (1982). Plate boundaries and extensional tectonics. *Tectonophysics,* Vo. 81, p. 239-256.

LEE, H. J., SYVITSKI, J. P. M., PARKER, G., ORANGE, D., LOCAT, J., HUTTON, E. W. H. & IMRAN, J. (2002). Distinguishing sediment waves from slope failure deposits: field examples, including the 'Humboldt slide', and modelling results. *Marine Geology,* Vo. 192, p. 79-104.

LEEDER, M. R. (1995). Continental Rifts and Proto-Oceanic Rift Troughs. *In:* BUSBY, C. J. & INGERSOLL, R. V. (eds.) *Tectonics of Sedimentary Basins. , Blackwell: 53-117.*: Blackwell, p. 119-148.

LEINFELDER, R. R. & WILSON, R. C. (1998). Third-order sequences in an upper Jurassic rift-related second-order sequence, Central Lusitanian Basin, Portugal. *In:* DE GRACIANSKY, P.-C., HARDENBOL, J., THIERRY, J. & VAIL, P. R. (eds.) *Mesozoic and Cenozoic Sequence Stratigraphy of European Basins.* Tulsa: SEPM (Society for Sedimentary Geology), Special Publication, Vo. 60, p. 507-525.

LESNE, O., CALAIS, E. & DEVERCHÈRE, J. (1998). Finite element modelling of crustal deformation in the Baikal rift zone: new insights into the active-passive rifting debate. *Tectonophysics,* Vo. 289, p. 327-340.

LISTER, G. S., ETHERIDGE, M. A. & SYMONDS, P. A. (1986). Detachment faulting and the evolution of passive continental margins. *Geology,* Vo. 14, p. 246-250.

LISTER, G. S. & DAVIS, G. A. (1989). The origin of metamorphic core complexes and detachment faults formed during Tertiary continental extension in the northern Colorado River region, U.S.A. *Journal of Structural Geology,* Vo. 11, p. 65-94.

LISTER, G. S., ETHERIDGE, M. A. & SYMONDS, P. A. (1991). Detachment models for the formation of passive continental margins *Tectonics,* Vo. 10, p. 1038-1064.

MACDONALD, D., GOMEZ-PEREZ, I., FRANZESE, J., SPALLETTI, L., LAWVER, L., GAHAGAN, L., DALZIEL, I., THOMAS, C., TREWIN, N., HOLE, M. & PATON, D. (2003). Mesozoic break-up of SW Gondwana: implications for regional hydrocarbon potential of the southern South Atlantic. *Marine and Petroleum Geology,* Vo. 20, p. 287-308.

MACDONALD, J., BACKÉ, G., KING, R., HOLFORD, S. & HILLIS, R. (2012a). Geomechanical modelling of fault reactivation in the Ceduna Sub-basin, Bight Basin, Australia. *In:* HEALY, D., BUTLER, R. W. H., SHIPTON, Z. K. & SIBSON, R. H. (eds.) *Faulting, Fracturing and Igneous Intrusion in the Earth's Crust.* Geological Society, London, Special Publications, Vo. 367, p. 71-89.

MACDONALD, J., HOLFORD, S. & KING, R. (2012b). Structure and Prospectivity of the Ceduna Delta—Deep-Water Fold-Thrust Belt Systems, Bight Basin, Australia. *New Understanding of the Petroleum Systems of Continental Margins of the World: 32nd Annual.* SEPM, Vo. 32, p. 779-816.

MACLEOD, C. J., SEARLE, R. C., MURTON, B. J., CASEY, J. F., MALLOWS, C., UNSWORTH, S. C., ACHENBACH, K. L. & HARRIS, M. (2009). Life cycle of oceanic core complexes. *Earth and Planetary Science Letters,* Vo. 287, p. 333-344.

MALDONADO, A. (1979). Upper Cretaceous and Cenozoic depositional processes and facies in the distal north Atlantic continental margin off Portugal, DSDP site 398. *In:* SIBUET, J. C., RYAN, W. B. F. & ET AL. (eds.) *Init. Rep. DSDP, 47(2).* Washington (U.S. Government Printing Office), p. 373-401.

MALDONADO, A., BARNOLAS, A., BOHOYO, F., ESCUTIA, C., GALINDO-ZALDÍVAR, J., HERNÁNDEZ-MOLINA, J., JABALOY, A., LOBO, F. J., NELSON, C. H., RODRÍGUEZ-FERNÁNDEZ, J., SOMOZA, L. & VÁZQUEZ, J.-T. (2005). Miocene to Recent contourite drifts development in the northern Weddell Sea (Antarctica). *Global and Planetary Change,* Vo. 45, p. 99-129.

MALDONADO, A., BOHOYO, F., GALINDO-ZALDÍVAR, J., HERNÁNDEZ-MOLINA, J., JABALOY, A., LOBO, F. J., RODRÍGUEZ-FERNÁNDEZ, J., SURIÑACH, E. & VÁZQUEZ, J. T. (2006). Ocean basins near the Scotia–Antarctic plate boundary: Influence of tectonics and paleoceanography on the Cenozoic deposits. *Marine Geophysical Researches,* Vo. 27, p. 83-107.

MANATSCHAL, G. & NIEVERGELT, P. (1997). A continent-ocean transition recorded in the Err and Platta nappes (Eastern Switzerland). *Eclogae Geologicae Helvetiae,* Vo. 90, p. 3-27.

MANATSCHAL, G. & BERNOULLI, D. (1998). Rifting and early evolution of ancient ocean basins: the record of the Mesozoic Tethys and of the Galicia-Newfoundland margins. *Marine Geophysical Researches,* Vo. 20, p. 371-381.

MANATSCHAL, G., FROITZHEIM, N., RUBENACH, M. & TURRIN, B. D. (2001). The role of detachment faulting in the formation of an ocean-continent transition: insights from the Iberia Abyssal Plain. *Geological Society, London, Special Publications,* Vo. 187, p. 405-428.

MANATSCHAL, G. (2004). New models for evolution of magma-poor rifted margins based on a review of data and concepts from West Iberia and the Alps. *International Journal of Earth Sciences,* Vo. 93, p. 432-466.

MANATSCHAL, G., MÜNTENER, O., LAVIER, L. L., MINSHULL, T. A. & PÉRON-PINVIDIC, G. (2007). Observations from the Alpine Tethys and Iberia–Newfoundland margins pertinent to the interpretation of continental breakup. *In:* KARNER, G. D., MANATSCHAL, G. & PINHEIRO, L. M. (eds.) *Imaging, Mapping and Modelling Continental Lithosphere Extension and Breakup.* London: Geological Society Special Publications, Vo. 282, p. 291-324.

MARTÍN-CHIVELET, J., FREGENAL-MARTÍNEZ, M. A. & CHACÓN, B. (2008). Traction structures in contourites. *In:* REBESCO, M. & CAMERLENGHI, A. (eds.) *Contourites.* Elsevier, Vo. 60, p. 159-182.

MARTINSEN, O. J. (1994). Mass movements. *In:* MALTMAN, A. (ed.) *The Geological Deformation of Sediments.* London: Chapman & Hall, p. 127-165.

MASSON, D. G., CARTWRIGHT, J. A., PINHEIRO, L. M., WHITMARSH, R. B., BESLIER, M. O. & ROESER, H. (1994). Compressional deformation at the ocean–continent transition in the NE Atlantic. *Journal of the Geological Society,* Vo. 151, p. 607-613.

MCKENZIE, D. (1978). Some remarks on the development of sedimentary basins. *Earth and Planetary Science Letters,* Vo. 40, p. 25-32.

MEIJER, P. T., SLINGERLAND, R. & WORTEL, M. J. R. (2004). Tectonic control on past circulation of the Mediterranean Sea: A model study of the Late Miocene. *Paleoceanography,* Vo. 19, p. PA1026.

MIALL, A. D. (1992). Exxon global cycle chart: An event for every occasion? *Geology,* Vo. 20, p. 787-790.

MILLER, J. M., NORVICK, M. S. & WILSON, C. J. L. (2002). Basement controls on rifting and the associated formation of ocean transform faults—Cretaceous continental extension of the southern margin of Australia. *Tectonophysics,* Vo. 359, p. 131-155.

MIRANDA, R., VALADARES, V., TERRINHA, P., MATA, J., AZEVEDO, M. R., GASPAR, M., KULLBERG, J. C. & RIBEIRO, C. (2009). Age constraints on the Late Cretaceous alkaline magmatism on the West Iberian Margin. *Cretaceous Research,* Vo. 30, p. 575-586.

MITCHELL, A. H. & READING, H. G. (1969). Continental margins, Geosynclines and ocean floor spreading. *Journal of Geology,* Vo. 77, p. 629--645.

MITCHUM, R. M., VAIL, P. R. & SANGREE, J. B. (1977). Seismic stratigraphy and global changes in sea level. Part 6. Stratigraphic interpretation of seismic reflection patterns in depositional sequences. *In:* PAYTON, C. E. (ed.) *Seismic Stratigraphy - appplications to hidrocarbon exploration.* AAPG Memoir, Vo. 26, p. 117-133.

MOHRIAK, W., NEMČOK, M. & ENCISO, G. (2008). South Atlantic divergent margin evolution: rift-border uplift and salt tectonics in the basins of SE Brazil. *In:* PANKHURST, R. J., TROUW, R. A. J., BRITO NEVES, B. B. & DE WIT, M. J. (eds.) *West Gondwana: Pre-Cenozoic Correlations Across the South Atlantic Region.* London: Geological Society, Special Publications, Vo. 294, p. 365-398.

MOHRIAK, W. U., DANFORTH, A., POST, P. J., BROWN, D. E., TARI, G. C., NEMČOK, M. & SINHA, S. T. (2012). *Conjugate Divergent Margins,* London, Geological Society, London, Special Publications, No. 369

MOHRIAK, W. U. & FAINSTEIN, R. (2012). 7 - Phanerozoic regional geology of the eastern Brazilian margin. *In:* ROBERTS, D. G. & BALLY, A. W. (eds.) *Regional Geology and Tectonics: Phanerozoic Passive Margins, Cratonic Basins and Global Tectonic Maps.* Boston: Elsevier, p. 222-282.

MONTADERT, L., WINNOCK, E., DELTEIL, J. R. & GRAU, G. (1974). Continental margins of Galicia - Portugal and Bay of Biscay. *In:* BURK, C. A. & DRAKE, C. L. (eds.) *The geology of continental margins.* New York: Springer, p. 323-342.

MOORE, J. G. (1992). A syn-rift to post-rift transition sequence in the Main Porcupine Basin, offshore western Ireland. *Geological Society, London, Special Publications,* Vo. 62, p. 333-349.

MORGAN, P. & BAKER, B. H. (1983). Introduction - processes of continental rifting. *Tectonophysics,* Vo. 94, p. 1-10.

MORTON, J. G. G., HILL, A. J., PARKER, G. & TABASSI, A. (1994). Towards a unified stratigraphy for the Otway Basin. *In:* FINLAYSON, D. M. (ed.) *NGMA/PESA Otway Basin Symposium Otway Basin Symposium, Melbourne, 20 April 1994: extended abstracts* Melbourne: Australian Geological Survey Organisation, Vo. 1994/14, p. 7-12.

MOULIN, M., ASLANIAN, D. & UNTERNEHR, P. (2010). A new starting point for the South and Equatorial Atlantic Ocean. *Earth-Science Reviews,* Vo. 98, p. 1-37.

MOULLADE, M. & GUÉRIN, S. (1982). Le Probleme des relations de l'Atlantique Sud et de l'Atlantique Central au Crétacé moyen: nouveles donnés microfaunistiques d'apres les forages DSDP. *Bull. Soc. Géol. France,* Vo. XXIV, p. 511-517.

MOULLADE, M. & BOILLOT, G. (1988). Subsidence and deepening of the Galicia Margin: the paleoenvironmental control. *In:* BOILLOT, G., WINTERER, E. L., MEYER, A. W. & ET AL. (eds.) *Proc. ODP, Sci. Results, 103.* College Station, TX (Ocean Drilling Program), p. 733-740.

MULDER, T., FAUGÈRES, J. C. & GONTHIER, E. (2008). Chapter 21 Mixed Turbidite–Contourite Systems. *In:* REBESCO, M. & CAMERLENGHI, A. (eds.) *Developments in Sedimentology.* Elsevier, Vo. Volume 60, p. 435-456.

MULDER, T. (2011). Gravity Processes and Deposits on Continental Slope, Rise and Abyssal Plains. *In:* HÜNEKE, H. & MULDER, T. (eds.) *Deep-Sea Sediments. Developments in Sedimentology.* Amsterdam: Elsevier, Vo. 63, p. 25-148.

MÜLLER, R. D., GAINA, C. & CLARK, S. (2000). Seafloor spreading around Australia. *In:* VEEVERS , J. J. (ed.) *Billion-year earth history of Australia and neighbours in Gondwanaland.* Sydney: GEMOC Press, p. 18-28.

MÜLLER, R. D., SDROLIAS, M., GAINA, C. & ROEST, W. R. (2008). Age, spreading rates, and spreading asymmetry of the world's ocean crust. *Geochemistry, Geophysics, Geosystems,* Vo. 9, p. Q04006.

MÜNTENER, O. & HERMANN, J. (2001). The role of lower crust and continental upper mantle during formation of non-volcanic passive margins: evidence from the Alps. *Geological Society, London, Special Publications,* Vo. 187, p. 267-288.

MÜNTENER, O., DESMURS, L., PETTKE, T., MEIER, M. & SCHALTEGGER, U. (2002). Melting and melt/rock reaction in extending mantle lithosphere: trace element and isotopic constraints from passive margin peridotites. *Geochimica and Cosmochimica Acta,* Vo. 66, p. A536.

MURILLAS, J., MOUGENOT, D., BOULOT, G., COMAS, M. C., BANDA, E. & MAUFFRET, A. (1990). Structure and evolution of the Galicia Interior Basin (Atlantic western Iberian continental margin). *Tectonophysics,* Vo. 184, p. 297-303, 305, 307-319.

MUTTER, J. C., A. HEGARTY, K., CANDE, S. C. & WEISSEL, J. K. (1985). Breakup between Australia and Antarctica: A brief review in the light of new data. *Tectonophysics,* Vo. 114, p. 255-279.

NERES, M., BOUCHEZ, J. L., TERRINHA, P., FONT, E., MOREIRA, M., MIRANDA, R., LAUNEAU, P. & CARVALLO, C. (2014). Magnetic fabric in a Cretaceous sill (Foz da Fonte, Portugal): flow model and implications for regional magmatism. *Geophysical Journal International,* Vo. 199, p. 78-101.

NESTE (1990). Final Well Report Lima-1. DPEP (Divisão para Pesquisa e Exploração de Petróleo), Portugal.

NICHOLSON, C. J. & RYAN, D. J. (2005). Structural framework. *In:* BRADSHAW, B. E. (ed.) *Geology and Petroleum Potential of the Bremer Sub-basin, offshore southwestern Australia.* Canberra: Geoscience Australia, Vo. 2005/21, p. 43-75.

NIELSEN, T., KNUTZ, P. C. & KUIJPERS, A. (2008). Seismic expression of contourite depositional systems. *In:* REBESCO, M. & CAMERLENGHI, A. (eds.) *Contourites.* Elsevier, Vo. 60, p. 301-321.

NORVICK, M. & SMITH, M. (2001). Southeast Australia-Mapping the plate tectonic reconstruction of southern and southeastern Australia and implications for petroleum systems. *APPEA Journal-Australian Petroleum Production and Exploration Association,* Vo. 41, p. 15-34.

NØTTVEDT, A., GABRIELSEN, R. H. & STEEL, R. J. (1995). Tectonostratigraphy and sedimentary architecture of rift basins, with reference to the northern North Sea. *Marine and Petroleum Geology,* Vo. 12, p. 881-901.

O'DRISCOLL, D., HOLCOMBE, B. B., ROSE, P. T. & JONES, D. J. (1995). Cretaceous and Tertiary unconformities in the Atlantic margin basins. *The Petroleum Geology of Ireland's Offshore Basins.* London: Geological Society, Vo. 93, p. 341.

O'BRIEN, P., STANLEY, S. & PARUMS, R. (2006). Post-Rift Continental Slope and Rise Sediments from 38° E to 164° E, East Antarctica. *In:* FÜTTERER, D., DAMASKE, D., KLEINSCHMIDT, G., MILLER, H. & TESSENSOHN, F. (eds.) *Antarctica, Contributions to Global Earth Sciences, Proceedings of the IX International Symposium on Antarctic Earth Sciences.* Berlin, Heidelberg: Springer, p. 341-347.

O'LEARY, R. P. D., BRADSHAW, B. E. & RYAN, D. J. (2005). Stratigraphic framework. *In:* BRADSHAW, B. E. (ed.) *Geology and Petroleum Potential of the Bremer Sub-basin, offshore southwestern Australia.* Canberra: Geoscience Australia, Vo. 2005/21, p. 12-42.

OLLIER, C. D. & PAIN, C. F. (1997). Equating the basal unconformity with the palaeoplain: a model for passive margins. *Geomorphology,* Vo. 19, p. 1-15.

OLSEN, K. H. & MORGAN, P. (1995). Introduction: Progress in understanding continental rifts. *In:* OLSEN, K. H. (ed.) *Continental Rifts - Evolution, Structure, Tectonics. Developments in Geotectonics.* Elsevier, Vo. 25, p. 3-26.

PALAIN (1976). *Une série détritique terrigène. Les 'Grès de Silves': Trias et Lias inférieur du Portugal,* Lisbon, Mem. Serv. Geol. Portugal, No. 25, p. 377.

PARRISH, J. T., ZIEGLER, A. M. & SCOTESE, C. R. (1982). Rainfall patterns and the distribution of coals and evaporites in the Mesozoic and Cenozoic. *Palaeogeography, Palaeoclimatology, Palaeoecology,* Vo. 40, p. 67-101.

PAYTON, C. E. (1977). *Seismic stratigraphy: applications to hydrocarbon exploration,* Tulsa, Oklahoma, AAPG Memoir, No. 26, p. 516

PENROSE CONFERENCE PARTICIPANTS (1972). Penrose field conference on ophiolites. . *Geotimes,* Vo. 17, p. 24-25.

PEREIRA, R. & ALVES, T. M. (2011). Margin segmentation prior to continental break-up: A seismic-stratigraphic record of multiphased rifting in the North Atlantic (Southwest Iberia). *Tectonophysics,* Vo. 505, p. 17-34.

PÉREZ-GUSSINYÉ, M., RANERO, C. R., RESTON, T. J. & SAWYER, D. (2003). Mechanisms of extension at nonvolcanic margins: Evidence from the Galicia interior basin, west of Iberia. *J. Geophys. Res.,* Vo. 108, p. 2245.

PERINCEK, D. & COCKSHELL, C. (1995). The Otway basin: early Cretaceous rifting to Neogene inversion. *Australian Petroleum Eexploration Association Journal,* Vo. 35, p. 451-451.

PÉRON-PINVIDIC, G., MANATSCHAL, G., MINSHULL, T. A. & SAWYER, D. S. (2007). Tectonosedimentary evolution of the deep Iberia-Newfoundland margins: Evidence for a complex breakup history. *Tectonics,* Vo. 26, p. TC2011.

PÉRON-PINVIDIC, G., SHILLINGTON, D. J. & TUCHOLKE, B. E. (2010). Characterization of sills associated with the U reflection on the Newfoundland margin: evidence for widespread early post-rift magmatism on a magma-poor rifted margin. *Geophysical Journal International,* Vo. 182, p. 113-136.

PICKUP, S. L. B., WHITMARSH, R. B., FOWLER, C. M. R. & RESTON, T. J. (1996). Insight into the nature of the ocean-continent transition off West Iberia from a deep multichannel seismic reflection profile. *Geology,* Vo. 24, p. 1079-1082.

PINHEIRO, L. M., WHITMARSH, R. B. & MILES, P. R. (1992). The ocean–continent boundary off the western continental margin of Iberia—II. Crustal structure in the Tagus Abyssal Plain. *Geophysical Journal International,* Vo. 109, p. 106-124.

PINHEIRO, L. M., WILSON, R. C. L., REIS, R. P., WHITMARSH, R. B. & RIBEIRO, A. (1996). The western Iberian margin: A geophysical and geological overview. *In:* WHITMARSH, R. B., SAWYER, D. S., KLAUS, A. & MASSON, D. G. (eds.) *Proc. ODP, Sci. Results, 149.* College Station, TX (Ocean Drilling Program), p. 3–23.

PLATT, N. H. (1995). Sedimentation and Tectonics of a Synrift Succession: Upper Jurassic Alluvial Fans and Palaeokarst at the Late Cimmerian Unconformity, Western Cameros Basin, Northern Spain. *In:* PLINT, A. G. (ed.) *Sedimentary Facies Analysis.* Oxford: Special Pub. International Association of Sedimentologists, Vo. 22, p. 219-236.

POSAMENTIER, H. W. & ALLEN, G. P. (1993). Variability of the sequence stratigraphic model: effects of local basin factors. *In:* POSAMENTIER, H. W., SUMMERHAYES, C. P., HAQ, B. U. & ALLEN, G. P. (eds.) *Sequence Stratigraphy and Facies Associations.* Special Pub. International Association of Sedimentologists, Vo. 18, p. 3-18.

POSAMENTIER, H. W. & ALLEN, G. P. (1999). *Siliciclastic sequence stratigraphy: concepts and applications*, SEPM Concepts in Sedimentology and Paleontology, No. 7, p. 210.

POSAMENTIER, H. W. & MORRIS, W. R. (2000). Aspects of the stratal architecture of forced regressive deposits. *In:* HUNT, D. & GAWTHORPE, R. L. (eds.) *Sedimentary Responses to Forced Regressions.* London: Geological Society Special Publications, Vo. 172, p. 19–46.

POSAMENTIER, H. W. & WALKER, R. G. (2006). Deep-Water Turbidites and Submarine Fans. *Facies Models Revisited.* SEPM (Society for Sedimentary Geology), Vo. 84, p. 399-520.

POSAMENTIER, H. W., DAVIES, R. J., CARTWRIGHT, J. A. & WOOD, L. (2007). Seismic geomorphology – an overview. *In:* DAVIES, R. J., POSAMENTIER, H. W., WOOD, L. & CARTWRIGHT, J. A. (eds.) *Seismic geomorphology – Applications to Hydrocarbon Exploration and Production.* Geological Society, London, Special Publications, Vo. 277.

POULSEN, C. J., GENDASZEK, A. S. & JACOB, R. L. (2003). Did the rifting of the Atlantic Ocean cause the Cretaceous thermal maximum? *Geology,* Vo. 31, p. 115-118.

PROSSER, S. (1993). Rift-related linked depositional systems and their seismic expression. *In:* WILLIAMS, G. D. & DOBB, A. (eds.) *Tectonics and seismic sequence stratigraphy.* London: Geological Society Special Publications, Vo. 71, p. 35-66.

RANERO, C. R. & RESTON, T. J. (1999). Detachment faulting at ocean core complexes. *Geology,* Vo. 27, p. 983-986.

RANERO, C. R. & PÉREZ-GUSSINYÉ, M. (2010). Sequential faulting explains the asymmetry and extension discrepancy of conjugate margins. *Nature,* Vo. 468, p. 294-299.

RASMUSSEN, E. S., LOMHOLT, S., ANDERSEN, C. & VEJBÆK, O. V. (1998). Aspects of the structural evolution of the Lusitanian Basin in Portugal and the shelf and slope area offshore Portugal. *Tectonophysics,* Vo. 300 p. 199 - 255.

REBESCO, M. & STOW, D. (2001). Seismic expression of contourites and related deposits: a preface. *Marine Geophysical Researches,* Vo. 22, p. 303-308.

REBESCO, M. & CAMERLENGHI, A. (2008). *Contourites*, Elsevier No. 60

REBESCO, M., CAMERLENGHI, A. & VAN LOON, A. J. (2008). Contourite Research: A Field in Full Development. *In:* REBESCO, M. & CAMERLENGHI, A. (eds.) *Contourites.* Elsevier, Vo. 60, p. 1-10.

REBESCO, M., HERNÁNDEZ-MOLINA, F. J., VAN ROOIJ, D. & WÅHLIN, A. (2014). Contourites and associated sediments controlled by deep-water circulation processes: State-of-the-art and future considerations. *Marine Geology,* Vo. 352, p. 111-154.

REEMST, P. & CLOETINGH, S. (2000). Polyphase rift evolution of the Vøring margin (mid-Norway): Constraints from forward tectonostratigraphic modeling. *Tectonics,* Vo. 19, p. 225-240.

RÉHAULT, J.-P. & MAUFFRET, A. (1979). Relationships between Tectonics and Sedimentation around the Northwestern Iberian Margin. *In:* SIBUET, J. C., RYAN, W. B. F. & ET AL. (eds.) *Init. Rep. DSDP, 47(2).* Washington (U.S. Government Printing Office), p. 663-681.

RESTON, T. & PÉREZ-GUSSINYÉ, M. (2007). Lithospheric extension from rifting to continental breakup at magma-poor margins: rheology, serpentinisation and symmetry. *International Journal of Earth Sciences,* Vo. 96, p. 1033-1046.

RESTON, T. & MCDERMOTT, K. (2014). An assessment of the cause of the 'extension discrepancy' with reference to the west Galicia margin. *Basin Research,* Vo. 26, p. 135-153.

RESTON, T. J. (2005). Polyphase faulting during the development of the west Galicia rifted margin. *Earth and Planetary Science Letters,* Vo. 237, p. 561-576.

RESTON, T. J. (2007). The formation of non-volcanic rifted margins by the progressive extension of the lithosphere: the example of the West Iberian margin. *In:* KARNER, G. D., MANATSCHAL, G. & PINHEIRO, L. M. (eds.) *Imaging, Mapping and Modelling Continental Lithosphere Extension and Breakup.* London: Geological Society Special Publications, Vo. 282, p. 77-110.

REY, J. (1979). Le crétacé inférieur de la marge atlantique Portugaise: biostratigraphie, organisation séquentielle, évolution paléogéographique. *Ciências da Terra,* Vo. 5, p. 1-16.

REY, J., DINIS, J. L., CALLAPEZ, P. & CUNHA, P. P. (2006). *Da rotura continental à margem passiva. Composição e evolução do Cretácico de Portugal. Cadernos de Geologia de Portugal*

REY, P., VANDERHAEGHE, O. & TEYSSIER, C. (2001). Gravitational collapse of the continental crust: definition, regimes and modes. *Tectonophysics,* Vo. 342, p. 435-449.

RING, U. (1994). The influence of preexisting structure on the evolution of the Cenozoic Malawi rift (East African rift system). *Tectonics,* Vo. 13, p. 313-326.

ROBERTS, D. G. & BALLY, A. W. (eds.) (2012). *Regional Geology and Tectonics: Phanerozoic Rift Systems and Sedimentary Basins,* Boston: Elsevier, Vo.

ROBINSON, S. A., MURPHY, D. P., VANCE, D. & THOMAS, D. J. (2010). Formation of "Southern Component Water" in the Late Cretaceous: Evidence from Nd-isotopes. *Geology,* Vo. 38, p. 871-874.

ROSENBAUM, G., REGENAUER-LIEB, K. & WEINBERG, R. (2005). Continental extension: From core complexes to rigid block faulting. *Geology,* Vo. 33, p. 609-612.

ROSENBAUM, G., WEINBERG, R. F. & REGENAUER-LIEB, K. (2008). The geodynamics of lithospheric extension. *Tectonophysics,* Vo. 458, p. 1-8.

ROSENDAHL, B. R. (1987). Architecture of Continental Rifts with Special Reference to East Africa. *Annual Review of Earth and Planetary Sciences,* Vo. 15, p. 445-503.

ROTH, P. H. (1986). Mesozoic palaeoceanography of the North Atlantic and Tethys Oceans. *Geological Society, London, Special Publications,* Vo. 21, p. 299-320.

ROUBY, D., BRAUN, J., ROBIN, C., DAUTEUIL, O. & DESCHAMPS, F. (2013). Long-term stratigraphic evolution of Atlantic-type passive margins: A numerical approach of interactions between surface processes, flexural isostasy and 3D thermal subsidence. *Tectonophysics,* Vo. 604, p. 83-103.

ROWLEY, D. B. & SAHAGIAN, D. (1986). Depth-dependent stretching: A different approach. *Geology,* Vo. 14, p. 32-35.

ROYDEN, L. & KEEN, C. E. (1980). Rifting process and thermal evolution of the continental margin of Eastern Canada determined from subsidence curves. *Earth and Planetary Science Letters,* Vo. 51, p. 343-361.

RUPPEL, C. (1995). Extensional processes in continental lithosphere. *J. Geophys. Res.,* Vo. 100, p. 24187-24215.

RUSSELL, S. M. & WHITMARSH, R. B. (2003). Magmatism at the west Iberia non-volcanic rifted continental margin: evidence from analyses of magnetic anomalies. *Geophysical Journal International,* Vo. 154, p. 706-730.

SALÉN/PECTEN (1985). Final Well Report Lula-1. DPEP (Divisão para Pesquisa e Exploração de Petróleo), Portugal.

SALLARÈS, V., MARTÍNEZ-LORIENTE, S., PRADA, M., GRÀCIA, E., RANERO, C., GUTSCHER, M.-A., BARTOLOME, R., GAILLER, A., DAÑOBEITIA, J. J. & ZITELLINI, N. (2013). Seismic evidence of exhumed mantle rock basement at the Gorringe Bank and the adjacent Horseshoe and Tagus abyssal plains (SW Iberia). *Earth and Planetary Science Letters,* Vo. 365, p. 120-131.

SAUNDERS, A. D., STOREY, M., KENT, R. W. & NORRY, M. J. (1992). Consequences of plume-lithosphere interactions. *In:* STOREY, B. C., ALABASTER, T. & PANKHURST, R. J. (eds.) *Magmatism and the Causes of Continental Break-up*

London: Geological Society, Vo. 68, p. 41-60.

SAWYER, D. S., WHITMARSH, R. B., KLAUS, A., BESLIER, M. O. & COLLINS, E. S. (1994). *Proc. ODP, Init. Reports, 149*, College Station, TX (Ocean Drilling Program)

SAYERS, J., SYMONDS, P. A., DIREEN, N. G. & BERNARDEL, G. (2001). Nature of the continent-ocean transition on the non-volcanic rifted margin of the central Great Australian Bight. *Geological Society, London, Special Publications,* Vo. 187, p. 51-76.

SCHLAGER, W. (1993). Accommodation and supply—a dual control on stratigraphic sequences. *Sedimentary Geology,* Vo. 86, p. 111-136.

SCHMELING, H. (2010). Dynamic models of continental rifting with melt generation. *Tectonophysics,* Vo. 480, p. 33-47.

ŞENGÖR, A. M. C. & BURKE, K. (1978). Relative timing of rifting and volcanism on Earth and its tectonic implications. *Geophysical Research Letters,* Vo. 5, p. 419– 421.

ŞENGÖR, A. M. C. (1995). Sedimentation and Tectonics of Fossil Rifts. *In:* BUSBY, C. J. & INGERSOLL, R. V. (eds.) *Tectonics of Sedimentary Basins.* Blackwell, p. 53-117.

SHANLEY, K. W. P., J. MC. (1994). Perspectives on the Sequence Stratigraphy of Continental Strata *AAPG Bulletin,* Vo. 78, p. 544-568.

SHANMUGAM, G. (2008). Deep-water Bottom Currents and their Deposits. *In:* REBESCO, M. & CAMERLENGHI, A. (eds.) *Contourites.* Elsevier, Vo. 60, p. 59-81.

SHILLINGTON, D. J., WHITE, N., MINSHULL, T. A., EDWARDS, G. R. H., JONES, S. M., EDWARDS, R. A. & SCOTT, C. L. (2008). Cenozoic evolution of the eastern Black Sea: A test of depth-dependent stretching models. *Earth and Planetary Science Letters,* Vo. 265, p. 360-378.

SHIPBOARD SCIENTIFIC PARTY (1975). Site 268. *In:* HAYES, D. E., FRAKES, L. A. & ET AL. (eds.) *Init. Rep. DSDP, 28.* Washington (U.S. Government Printing Office), p. 153-177.

SHIPBOARD SCIENTIFIC PARTY (1979). Site 398. *In:* SIBUET, J. C., RYAN, W. B. F. & ET AL. (eds.) *Init. Rep. DSDP, 47(2).* Washington (U.S. Government Printing Office), p. 25-233.

SHIPBOARD SCIENTIFIC PARTY (1987a). Site 641. *In:* BOILLOT, G., WINTERER, E. L., MEYER, A. W. & ET AL. (eds.) *Proc. ODP, Init. Repts., 103.* College Station, TX (Ocean Drilling Program), p. 571-649.

SHIPBOARD SCIENTIFIC PARTY (1987b). Introduction, objectives, and principal results: Ocean Drilling Program Leg 103, west Galicia Margin. *In:* BOILLOT, G., WINTERER, E. L., MEYER, A. W. & ET AL. (eds.) *Proc. ODP, Init. Repts., 103.* College Station, TX (Ocean Drilling Program), p. 3–17.

SHIPBOARD SCIENTIFIC PARTY (1998). Site 1070. *In:* WHITMARSH, R. B., BESLIER, M.-O., WALLACE, P. J. & ET AL. (eds.) *Proc. ODP, Init. Reports, 173.* College Station, TX (Ocean Drilling Project), Vo. 173, p. 265-294.

SHIPBOARD SCIENTIFIC PARTY (2004a). Leg 210 summary. *In:* TUCHOLKE, B. E., SIBUET, J.-C., KLAUS, A. & ET AL. (eds.) *Proc. ODP, Init. Repts., 210.* College Station TX (Ocean Drilling Program), p. 1-78.

SHIPBOARD SCIENTIFIC PARTY (2004b). Site 1276. *In:* TUCHOLKE, B. E., SIBUET, J.-C., KLAUS, A. & ET AL. (eds.) *Proc. ODP, Init. Repts., 210.* College Station TX (Ocean Drilling Program), p. 1-358.

SHIPLEY, T., GAHAGAN, L., JOHNSON, K. & DAVIS, M. (2005). *Seismic Data Center, University of Texas Institute for Geophysics* [Online]. Available: http://www.ig.utexas.edu/sdc/ [Accessed 2010-Dec-14].

SIBUET, J.-C., SRIVASTAVA, S., ENACHESCU, M. E. & KARNER, G. (2007a). Early Cretaceous motion of Flemish Cap with respect to North America: implications on the formation of Orphan Basin and SE Flemish Cap-Galicia Bank conjugate margins. *In:* KARNER, G. D., MANATSCHAL, G. & PINHEIRO, L. M. (eds.) *Imaging, Mapping and Modelling Continental Lithosphere Extension and Breakup.* London: Geological Society Special Publications, Vo. 282, p. 63–76.

SIBUET, J.-C., SRIVASTAVA, S. & MANATSCHAL, G. (2007b). Exhumed mantle-forming transitional crust in the Newfoundland-Iberia rift and associated magnetic anomalies. *J. Geophys. Res.,* Vo. 112, p. B06105.

SIBUET, J.-C. & TUCHOLKE, B. E. (2012). The geodynamic province of transitional lithosphere adjacent to magma-poor continental margins. *In:* MOHRIAK, W. U., DANFORTH, A., POST, P. J., BROWN, D. E., TARI, G. C., NEMČOK, M. & SINHA, S. T. (eds.)

*Conjugate Divergent Margins* Geological Society, London, Special Publications, Vo. 369, p. 429– 452.

SIBUET, J., SRIVASTAVA, S. P. & SPAKMAN, W. (2004). Pyrenean orogeny and plate kinematics. *J. Geophys. Res.* , Vo. 109.

SIBUET, J. C. & RYAN, W. B. F. (1979). Site 398: Evolution of the West Iberian Passive Continental Margin in the Framework of the Early Evolution of the North Atlantic Ocean. *In:* SIBUET, J. C., RYAN, W. B. F. & ET AL. (eds.) *Init. Rep. DSDP, 47(2).* Washington (U.S. Government Printing Office), p. 761-775.

SIBUET, J. C., RYAN, W. B. F. & ET AL. (1979). *Init. Rep. DSDP, 47(2)*, Washington (U.S. Govt. Printing Office)

SIGAL, J. (1979). Chronostratigraphy and Ecostratigraphy of Cretaceous Formations Recovered on DSDP Leg 47B, Site 398. *In:* SIBUET, J. C., RYAN, W. B. F. & ET AL. (eds.) *Init. Rep. DSDP, 47(2).* Washington (U.S. Government Printing Office), p. 287-326.

SINCLAIR, I. K. (1988). Evolution of Mesozoic-Cenozoic sedimentary basins in the Grand Banks area of Newfoundland and comparison with Falvey's (1974) rift model. *Bulletin of Canadian Petroleum Geologists,* Vo. 36, p. 255-273.

SOARES, D. M., ALVES, T. M. & TERRINHA, P. (2012). The breakup sequence and associated lithospheric breakup surface: Their significance in the context of rifted continental margins (West Iberia and Newfoundland margins, North Atlantic). *Earth and Planetary Science Letters,* Vo. 355–356, p. 311-326.

SOARES, D. M., ALVES, T. M. & TERRINHA, P. (2014). Contourite drifts on early passive margins as an indicator of established lithospheric breakup. *Earth and Planetary Science Letters,* Vo. 401, p. 116-131.

SONDER, L. & ENGLAND, P. C. (1989). Effects of a Temperature-Dependent Rheology on Large-Scale Continental Extension. *Journal of Geophysical Research,* Vo. 94, p. 7603-7619.

SPOHN, T. & SCHUBERT, G. (1982). Convective Thinning of the Lithosphere: A Mechanism for the Initiation of Continental Rifting. *J. Geophys. Res.,* Vo. 87, p. 4669-4681.

SRIVASTAVA, S. P., SIBUET, J. C., CANDE, S., ROEST, W. R. & REID, I. D. (2000). Magnetic evidence for slow seafloor spreading during the formation of the Newfoundland and Iberian margins. *Earth and Planetary Science Letters,* Vo. 182, p. 61-76.

STACEY, A. R., MITCHELL, C. H., STRUCKMEYER, H. I. M. & TOTTERDELL, J. M. (2013). *Geology and hydrocarbon prospectivity of the deepwater Otway and Sorell basins, offshore southeastern Australia,* Canberra, Geoscience Australia, Record 2013/02

STAGG, H. & WILLCOX, J. (1991). Structure and hydrocarbon potential of the Bremer Basin, southwest Australia. *Bureau of Mineral Resources Journal of Australian Geology and Geophysics,* Vo. 12, p. 327-337.

STAGG, H., COLWELL, J., BORISSOVA, I., ISHIHARA, T. & BERNARDEL, G. (2006). The Bruce Rise area, East Antarctica: Formation of a continental margin near the greater India-Australia-Antarctica triple junction. *Terra Antartica,* Vo. 13, p. 3.

STAGG, H. M. J., WILLCOX, J. B., NEEDHAM, D. J. L., O'BRIEN, G. W., COCKSHELL, C. D., HILL, A. J., THOMAS, B. & HOUGH, L. P. (1990). *Basins of the Great Australian Bight region: geology and petroleum potential. Continental Margins Folio, 5*, Bureau of Mineral Resources, Geology and Geophysics Department of Mines and Energy, South Australia

STAGG, H. M. J., COLWELL, J. B., DIREEN, N. G., O'BRIEN, P. E., BROWN, B. J., BERNARDEL, G., BORISSOVA, I., CARSON, L. & CLOSE, D. B. (2005). *Geological framework of the continental margin in the region of the Australian Antarctic Territory,* Canberra, Geoscience Australia, No. 2004/25

STAPEL, G., CLOETINGH, S. & PRONK, B. (1996). Quantitative subsidence analysis of the Mesozoic evolution of the Lusitanian basin (western Iberian margin). *Tectonophysics,* Vo. 266, p. 493-507.

STILLE, P., STEINMANN, M. & RIGGS, S. R. (1996). Nd isotope evidence for the evolution of the paleocurrents in the Atlantic and Tethys Oceans during the past 180 Ma. *Earth and Planetary Science Letters,* Vo. 144, p. 9-19.

STOREY, B. C. (1995). The role of mantle plumes in continental breakup: case histories from Gondwanaland. *Nature,* Vo. 377, p. 301-308.

STOW, D. A. V. & PIPER, D. J. W. (1984). Deep-water fine-grained sediments: Facies models. *In:* STOW, D. A. V. & PIPER, D. J. W. (eds.) *Fine grained sediments Deep-Water processes and facies.* London: Geological Society, Special Publications, Vo. 15, p. 611–646.

STOW, D. A. V., FAUGÈRES, J. C., HOWE, J. A., PUDSEY, C. J. & VIANA, A. R. (2002). Bottom currents, contourites and deep-sea sediment drifts: Current state-of-the-art. *In:* STOW, D. A. V., PUDSEY, C. J., HOWE, J. A., FAUGÈRES, J.-C. & VIANA, A. R. (eds.) *Deep-Water Contourite Systems: Modern Drifts and Ancient Series, Seismic and Sedimentary Characteristics.* London: Geological Society, London, Memoirs, 22, Vo. 22, p. 7–20.

SUMMERHAYES, C. P. (1987). Organic-rich Cretaceous sediments from the North Atlantic. *In:* BROOKS, J. & FLEET, A. J. (eds.) *Marine Petroleum Source Rocks.* London: Geological Society, Vo. 26, p. 301-316.

SURLYK, F. & LYKKE-ANDERSEN, H. (2007). Contourite drifts, moats and channels in the Upper Cretaceous chalk of the Danish Basin. *Sedimentology,* Vo. 54, p. 405-422.

SYMONDS, P. A., PLANKE, S., FREY, O. & SKOGSEID, J. (1998). Volcanic evolution of the Western Australian continental margin and its implications for basin development. *In:* PURCELL, P. G. & PURCELL, R. R. (eds.) *The sedimentary basins of Western Australia 2. Proceedings of Petroleum Exploration Society of Australia Symposium.* Perth, Vo. 2, p. 33-54.

TALWANI, M., EWING, J., SHERIDAN, R., HOLBROOK, W. S. & GLOVER, L., III (1995). The Edge Experiment and the U.S. East Coast Magnetic Anomaly. *In:* BANDA, E., TORNÉ, M. & TALWANI, M. (eds.) *Rifted Ocean-Continent Boundaries.* Springer Netherlands, Vo. 463, p. 155-181.

TANAHASHI, M., EITTREIM, S. & WANNESON, J. (1994). Seismic stratigraphic sequences of the Wilkes Land margin. *Terra Antarctica,* Vo. 1, p. 391-393.

TANKARD, A. J. & WELSINK, H. J. (1987). Extensional Tectonics and Stratigraphy of Hibernia Oil Field, Grand Banks, Newfoundland. *AAPG Bulletin,* Vo. 71, p. 1210-1232.

TANKARD, A. J. & WELSINK, H. (1989). Mesozoic Extension and Styles of Basin Formation in Atlantic Canada. *In:* TANKARD, A. J. & BALKWILL, H. R. (eds.) *Extensional Tectonics and Stratigraphy of the North Atlantic Margins.* AAPG Memoir, Vo. 46, p. 175-195.

TAUGOURDEAU-LANTZ, J., AZÉMA, C., HASENBOEHLER, B., MASURE, E. & MORON, J. M. (1982). Évolution des domaines continentaux et marins de la marge portugaise (Leg 47 B, site 398 D) au cours du Crétacé: essai d'interprétation par l'analyse palynologique comparée. *Bull. Soc. Géol. France,* Vo. XXIV, p. 447-459.

TAURUS PETROLEUM AB (1995). Final Well Report Touro-1. DPEP (Divisão para Pesquisa e Exploração de Petróleo), Portugal.

TER VOORDE, M. & CLOETINGH, S. (1996). Numerical modelling of extension in faulted crust: effects of localized and regional deformation on basin stratigraphy. *Geological Society, London, Special Publications,* Vo. 99, p. 283-296.

TEXACO (1979). Final Well Report Cavala-4. DPEP (Divisão para Pesquisa e Exploração de Petróleo), Portugal.

THUROW, J. & KUHNT, W. (1986). Mid-Cretaceous of the Gibraltar Arch Area. *In:* SUMMERHAYES, C. P. & SHACKLETON, N. J. (eds.) *North Atlantic Palaeoceanography.* London: Geological Society, Special Publications, Vo. 22, p. 423-445.

TIKKU, A. A. & CANDE, S. C. (1999). The oldest magnetic anomalies in the Australian-Antarctic Basin: Are they isochrons? *Journal of Geophysical Research: Solid Earth,* Vo. 104, p. 661-677.

TIKKU, A. A. & CANDE, S. C. (2000). On the fit of Broken Ridge and Kerguelen plateau. *Earth and Planetary Science Letters,* Vo. 180, p. 117-132.

TIKKU, A. A. & DIREEN, N. G. (2008). Comment on "Major Australian-Antarctic Plate Reorganization at Hawaiian-Emperor Bend Time". *Science,* Vo. 321, p. 490.

TOTTERDELL, J., BRADSHAW, B. & WILLCOX, J. (2003). Structural and tectonic setting. *In:* O'BRIEN, G. W., PARASCHIVOIU, E. & HIBBURT, J. E. (eds.) *Petroleum geology of South Australia, Volume 5: The Great Australian Bight.* p. 1-57.

TOTTERDELL, J. M., BLEVIN, J. E., STRUCKMEYER, H. I. M., BRADSHAW, B. E., COLWELL, J. B. & KENNARD, J. M. (2000). A new sequence framework for the Great Australian Bight: starting with a clean slate. *Australian Petroleum Production and Exploration Association Journal,* Vo. 40, p. 95-117.

TOTTERDELL, J. M. & KRASSAY, A. A. (2003a). The role of shale deformation and growth faulting in the Late Cretaceous evolution of the Bight Basin, offshore southern Australia. *In:* VAN RENSBERGEN, P., R.R., H., MALTMAN, A. & MORLEY, C. K. (eds.) *Subsurface Sediment Mobilization.* London: Geological Society, London, Special Publications, Vo. 216, p. 429-442.

TOTTERDELL, J. M. & KRASSAY, A. A. (2003b). *Sequence stratigraphic correlation of onshore and offshore Bight Basin successions,* Canberra, Geoscience Australia, No. 2003/02

TOTTERDELL, J. M., MITCHELL, C. & RECORD, B. G. A. (2009). *Bight Basin geological sampling and seepage survey: RV Southern Surveyor Survey SS01/2007,* Canberra, Geoscience Australia, No. 2009/24

TRABUCHO ALEXANDRE, J., VAN GILST, R. I., RODRÍGUEZ-LÓPEZ, J. P. & DE BOER, P. L. (2011). The sedimentary expression of oceanic anoxic event 1b in the North Atlantic. *Sedimentology,* Vo. 58, p. 1217-1246.

TUCHOLKE, B. E. & VOGT, P. R. (1979). Western North Atlantic: Sedimentary evolution and aspects of tectonic history. *In:* TUCHOLKE, B. E., VOGT, P. R. & ET AL. (eds.) *Init. Rep. DSDP, 43.* Washington (U.S. Government Printing Office), Vo. 43, p. 791-825.

TUCHOLKE, B. E. & MCCOY, F. W. (1986). Paleogeographic and paleobathymetric evolution of the North Atlantic Ocean. *In:* VOGT, C. & TUCHOLKE, B. E. (eds.) *The western North Atlantic region.* Boulder, Colorado: Geological Society of America, p. 589-602.

TUCHOLKE, B. E., , I. G. A. O. T. N., ATLANTIC BETWEEN 50 Ø TO 72 Ø N AND 0 Ø TO 65 Ø W, E. B. S. P., SFIVASTAVA, D. V., AND B. TUCHOLKE, PP. , DSCH. HYDROG. & INST., 1988. (1988). Sediment distribution. *In:* SRIVASTAVA, S., VOPPEL, D. & TUCHOLKE, B. E. (eds.) *Geophysical Atlas of the North Atlantic between 50° to 72° N and 0° to 65° W.* Hamburg: Dtsch. Hydrogr. Inst., p. 9-12.

TUCHOLKE, B. E., AUSTIN, J. A. & UCHUPI, E. (1989). Crustal Structure and Rift-Drift Evolution of the Newfoundland Basin *In:* J., T. A. & BALKWILL, H. R. (eds.) *Extensional Tectonics and Stratigraphy of the North Atlantic Margins.* AAPG Memoir, Vo. 46, p. 247-263.

TUCHOLKE, B. E. & HOLBROOK, W. S. (2001). Cruise Report EW-0007 Newfoundland Basin - SCREECH: Study of continental rifting and extension on the Eastern Canadian Shelf.

TUCHOLKE, B. E., SIBUET, J.-C., KLAUS, A. & ET AL. (2004). *Proc. ODP, Init. Reports, 210*, College Station, TX (Ocean Drilling Project), No. 210

TUCHOLKE, B. E., SAWYER, D. S. & SIBUET, J.-C. (2007a). Breakup of the Newfoundland-Iberia rift. *In:* KARNER, G. D., MANATSCHAL, G. & PINHEIRO, L. M. (eds.) *Imaging, Mapping and Modelling Continental Lithosphere Extension and Breakup.* London: Geological Society Special Publications, Vo. 282, p. 9-46.

TUCHOLKE, B. E. & SIBUET, J.-C. (2007). Leg 210 synthesis: tectonic, magmatic, and sedimentary evolution of the Newfoundland-Iberia rift. *In:* TUCHOLKE, B. E., SIBUET, J.-C. & KLAUS, A. (eds.) *Proc. ODP, Sci. Results, 210.* College Station, TX (Ocean Drilling Project), Vo. 210, p. 1-56.

TUCHOLKE, B. E., SIBUET, J.-C., KLAUS, A. & (EDS.) (2007b). *Proc. ODP, Sci. Results, 210*, College Station, TX (Ocean Drilling Project), No. 210

TUCHOLKE, B. E. & SIBUET, J.-C. (2012). Problematic plate reconstruction. *Nature Geosci,* Vo. 5, p. 676-677.

TUCHOLKE, B. E. & WHITMARSH, R. B. (2012). 10 - The Newfoundland–Iberia conjugate rifted margins. *In:* ROBERTS, D. G. & BALLY, A. W. (eds.) *Regional Geology and Tectonics: Phanerozoic Passive Margins, Cratonic Basins and Global Tectonic Maps.* Boston: Elsevier, p. 342-382.

TURCOTTE, D. L. & EMERMAN, S. H. (1983). Mechanisms of active and passive rifting. *Tectonophysics,* Vo. 94, p. 39-50.

URQUHART, E., GARDIN, S., LECKIE, R. M., WOOD, S. A., PROSS, J., GEORGESCU, M. D., LADNER, B. & TAKATA, H. (2007). A paleontological synthesis of ODP Leg 210, Newfoundland Basin. *In:* TUCHOLKE, B. E., SIBUET, J.-C. & KLAUS, A. (eds.) *Proc. ODP, Sci. Results, 210.* College Station, TX (Ocean Drilling Program), p. 1-53.

VAN BALEN, R. T., VAN DER BEEK, P. A. & CLOETINGH, S. A. P. L. (1995). The effect of rift shoulder erosion on stratal patterns at passive margins: Implications for sequence stratigraphy. *Earth and Planetary Science Letters,* Vo. 134, p. 527-544.

VAN BALEN, R. T., PODLADCHIKOV, Y. Y. & CLOETINGH, S. A. P. L. (1998). A new multilayered model for intraplate stress-induced differential subsidence of faulted lithosphere, applied to rifted basins. *Tectonics,* Vo. 17, p. 938-954.

VANNEY, J. R. & MOUGENOT, D. (1981). *La plateforme continentale du Portugal et les provinces adjacentes: analyse géomorphologique,* Lisbon, Mem. Serv. Geol. Portugal, 28

VEEVERS, J. J. (1981). Morphotectonics of Rifted Continental Margins in Embryo (East Africa), Youth (Africa-Arabia), and Maturity (Australia). *The Journal of Geology,* Vo. 89, p. 57-82.

VEEVERS , J. J. (1984). *Phanerozoic Earth History of Australia,* Oxford, Clarendon Press

VEEVERS, J. J. (1986). Breakup of Australia and Antarctica estimated as mid-Cretaceous (95 ± 5 Ma) from magnetic and seismic data at the continental margin. *Earth and Planetary Science Letters,* Vo. 77, p. 91-99.

VEEVERS, J. J. & LI, Z. X. (1991). Review of seafloor spreading around Australia. II. Marine magnetic anomaly modelling. *Australian Journal of Earth Sciences,* Vo. 38, p. 391-408.

VEEVERS, J. J. (2012). Reconstructions before rifting and drifting reveal the geological connections between Antarctica and its conjugates in Gondwanaland. *Earth-Science Reviews,* Vo. 111, p. 249-318.

VINCENT, E., ČEPEK, P., SLITER, W. V., WESTBERG, M. J., GARTNER, S. & DOI:10.2973/DSDP.PROC.50.141.1980 (1979). Biostratigraphy and Depositional History of the Moroccan Basin, Eastern North Atlantic. *In:* LANCELOT, Y., WINTERER, E. L. & ET AL. (eds.) *Init. Rep. DSDP, 50.* Washington (U.S. Government Printing Office), p. 775-800.

VISSERS, R. L. M. & MEIJER, P. T. (2012). Mesozoic rotation of Iberia: Subduction in the Pyrenees? *Earth-Science Reviews,* Vo. 110, p. 93-110.

VOIGT, S., GALE, A. S. & FLÖGEL, S. (2004). Midlatitude shelf seas in the Cenomanian-Turonian greenhouse world: Temperature evolution and North Atlantic circulation. *Paleoceanography,* Vo. 19, p. PA4020.

VOIGT, S., JUNG, C., FRIEDRICH, O., FRANK, M., TESCHNER, C. & HOFFMANN, J. (2013). Tectonically restricted deep-ocean circulation at the end of the Cretaceous greenhouse. *Earth and Planetary Science Letters,* Vo. 369–370, p. 169-177.

VON RAD, U., RYAN, W. B. F. & SIBUET, J.-C. (2004). Physical properties of Hole 47-398D. DOI: 10.1594/PANGAEA.221455.

VON RAD, U., RYAN, W. B. F. & SIBUET, J.-C. (2005). Sound velocity of Hole 47-398D. DOI: 10.1594/PANGAEA.229561.

WANNESSON, J., PELRAS, M., PETITPERRIN, B., PERRET, M. & SEGOUFIN, J. (1985). A geophysical transect of the Adélie Margin, East Antarctica. *Marine and Petroleum Geology,* Vo. 2, p. 192-200.

WANNESSON, J. (1991). Geology and petroleum potential of the Adelie Coast margin, East Antarctica. *In:* JOHN, W. S. (ed.) *Antarctica as an Exploration Frontier--Hydrocarbon Potential, Geology, and Hazards.* American Association of Petroleum Geologists, Studies on Geology, p. 77-87.

WEISSEL, J. K. & HAYES, D. E. (1972). Magnetic Anomalies in the Southeast Indian Ocean. *In:* HAYES, D. E. (ed.) *Antarctica Oceanology II: The Australian–New Zealand Sector.* American Geophysical Union, p. 165-196.

WEISSEL, J. K. & KARNER, G. D. (1989). Flexural Uplift of Rift Flanks Due to Mechanical Unloading of the Lithosphere During Extension. *J. Geophys. Res.,* Vo. 94, p. 13919-13950.

WELFORD, J. K. & HALL, J. (2007). Crustal structure of the Newfoundland rifted continental margin from constrained 3-D gravity inversion. *Geophysical Journal International,* Vo. 172, p. 890-908.

WERNICKE, B. (1981). Low-angle normal faults in the Basin and Range Province: nappe tectonics in an extending orogen. *Nature,* Vo. 291, p. 645-648.

WERNICKE, B. & BURCHFIEL, B. C. (1982). Modes of extensional tectonics. *Journal of Structural Geology,* Vo. 4, p. 105-115.

WERNICKE, B. (1985). Uniform-sense normal simple shear of the continental lithosphere. *Canadian Journal of Earth Sciences,* Vo. 22, p. 108-125.

WERNICKE, B. & TILKE, P. G. (1989). Extensional Tectonic Framework of the U.S. Central Atlantic Passive Margin. *In:* TANKARD, A. J. & BALKWILL, H. R. (eds.) *Extensional Tectonics and Stratigraphy of the North Atlantic Margins.* AAPG Memoir, Vo. 46, p. 7-21.

WHITE, L. T., GIBSON, G. M. & LISTER, G. S. (2013). A reassessment of paleogeographic reconstructions of eastern Gondwana: Bringing geology back into the equation. *Gondwana Research,* Vo. 24, p. 984-998.

WHITE, R. & MCKENZIE, D. (1989). Magmatism at Rift Zones: The Generation of Volcanic Continental Margins and Flood Basalts. *J. Geophys. Res.,* Vo. 94, p. 7685-7729.

WHITE, R. S. (1992). Magmatism during and after continental break-up. *In:* STOREY, B. C., ALABASTER, T. & PANKHURST, R. J. (eds.) *Magmatism and the Causes of Continental Break-up.* London: Geological Society, Vo. 68, p. 1-16.

WHITMARSH, R. B. & MILES, P. R. (1995). Models of the development of the West Iberia rifted continental margin at 40°30'N deduced from surface and deep-tow magnetic anomalies. *J. Geophys. Res.,* Vo. 100, p. 3789-3806.

WHITMARSH, R. B. & SAWYER, D. (1996). The ocean/continent transition beneath the Iberia Abyssal Plain and continental-rifting to seafloor-spreading processes. *In:* WHITMARSH, R. B., SAWYER, D. S., KLAUS, A. & MASSON, D. G. (eds.) *Proc. ODP, Sci. Results, 149.* College Station, TX (Ocean Drilling Program), p. 713-733.

WHITMARSH, R. B., SAWYER, D. S., KLAUS, A., MASSON, D. G. & (EDS.) (1996a). *Proc. ODP, Sci. Results, 149*, College Station, TX (Ocean Drilling Program)

WHITMARSH, R. B., WHITE, R. S., HORSEFIELD, S. J., SIBUET, J.-C., RECQ, M. & LOUVEL, V. (1996b). The ocean-continent boundary off the western continental margin of Iberia: Crustal structure west of Galicia Bank. *Journal of Geophysical Research: Solid Earth,* Vo. 101, p. 28291-28314.

WHITMARSH, R. B., BESLIER, M.-O., WALLACE, P. J. & ET AL. (1998). *Proc. ODP, Init. Reports, 173*, College Station, TX (Ocean Drilling Project), No. 173

WHITMARSH, R. B., MANATSCHAL, G. & MINSHULL, T. A. (2001). Evolution of magma-poor continental margins from rifting to seafloor spreading. *Nature,* Vo. 413, p. 150-154.

WHITMARSH, R. B. & WALLACE, P. J. (2001). The rift-to-drift development of the West Iberia nonvolcanic margin: a summary and review of the contribution of Ocean Drilling Project Leg 173. *In:* BESLIER, M.-O., WHITMARSH, R. B., WALLACE, P. J. & GIRARDEAU, J. (eds.) *Proc. ODP, Sci. Results, 173.* College Station TX (Ocean Drilling Project), Vo. 173, p. 1-36.

WHITTAKER, J. M., MÜLLER, R. D., LEITCHENKOV, G., STAGG, H., SDROLIAS, M., GAINA, C. & GONCHAROV, A. (2007). Major Australian-Antarctic Plate Reorganization at Hawaiian-Emperor Bend Time. *Science,* Vo. 318, p. 83-86.

WHITTAKER, J. M., MÜLLER, R. D. & GONCHAROV, A. (2008). Australian-Antarctic rifting. *In:* PESA Eastern Australasian Basins Symposium III. p. 271-274.

WHITTAKER, J. M., WILLIAMS, S. E. & MÜLLER, R. D. (2013). Revised tectonic evolution of the Eastern Indian Ocean. *Geochemistry, Geophysics, Geosystems,* Vo. 14, p. 1891-1909.

WILLCOX, J. B. & STAGG, H. M. J. (1990). Australia's southern margin: a product of oblique extension. *Tectonophysics,* Vo. 173, p. 269-281.

WILLIAMS, B. E., SHANNON, E. & SINCLAIR, I. K. (1999). Comparative Jurassic and Cretaceous tectono-stratigraphy and reservoir development in the Jeanne d'Arc and Porcupine basins. *In:* FLEET, A. J. & BOLDY, S. A. R. (eds.) *Petroleum Geology of Northwest Europe: Proceedings of the 5th Conference.* London: Geological Society, p. 487-499.

WILLIAMS, S. E., WHITTAKER, J. M. & MÜLLER, R. D. (2011). Full-fit, palinspastic reconstruction of the conjugate Australian-Antarctic margins. *Tectonics,* Vo. 30, p. TC6012.

WILLIAMSON, P. E., SWIFT, M. G., O'BRIEN, G. W. & FALVEY, D. A. (1990). Two-stage Early Cretaceous rifting of the Otway Basin margin of southeastern Australia: Implications for rifting of the Australian southern margin. *Geology,* Vo. 18, p. 75-78.

WILSON, J. T. (1965). A New Class of Faults and their Bearing on Continental Drift. *Nature,* Vo. 207, p. 343-347.

WILSON, R. C. L. (1975). Atlantic opening and Mesozoic continental margin basins of Iberia. *Earth and Planetary Science Letters,* Vo. 25, p. 33-43.

WILSON, R. C. L. (1988). Mesozoic development of the Lusitanian Basin, Portugal. *Rev. Soc. Geol. España,* Vo. 1, p. 393-407.

WILSON, R. C. L., HISCOTT, R. N., WILLIS, M. G. & GRADSTEIN, F. M. (1989). The Lusitanian basin of west-central Portugal: Mesozoic and Tertiary tectonic, stratigraphy, and subsidence history. *In:* A.J.TANKARD & BALKWILL, H. R. (eds.) *Extensional Tectonics and Stratigraphy of the North Atlantic*

*Margins.* AAPG Memoir, Vo. 46, p. 341-361.

WILSON, R. C. L., SAWYER, D. S., WHITMARSH, R. B., ZERONG, J. & CARBONELL, J. (1996). Seismic stratigraphy and tectonic history of the Iberia Abyssal Plain. *In:* WHITMARSH, R. B., SAWYER, D. S., KLAUS, A. & MASSON, D. G. (eds.) *Proc. ODP, Sci. Results, 149.* College Station, TX (Ocean Drilling Program), p. 617-633.

WILSON, R. C. L., MANATSCHAL, G. & WISE, S. (2001). Rifting along non-volcanic passive margins: stratigraphic and seismic evidence from the Mesozoic successions of the Alps and western Iberia. *In:* WILSON, R. C. L., WHITMARSH, R. B., TAYLOR, B. & FROITZHEIM, N. (eds.) *Non-Volcanic Rifting of Continental Margins: A Comparison of Evidence from Land and Sea.* London: Geological Society, London, Special Publications, Vo. 187, p. 429-452.

WITHJACK, M. O., SCHLISCHE, R. W. & OLSEN, P. E. (1998). Diachronous Rifting, Drifting, and Inversion on the Passive Margin of Central Eastern North America: An Analog for Other Passive Margins. *AAPG Bulletin,* Vo. 82, p. 817-835.

WITT, W. G. (1977). Stratigraphy of the Lusitanian Basin. Shell Prospex Portuguesa, unpublished report.

WOOD, R. J. (1981). The subsidence history of Conoco well 15/30-1, central North Sea. *Earth and Planetary Science Letters,* Vo. 54, p. 306-312.

ZEYEN, H., NEGREDO, A. & FERNÀNDEZ, M. (1996). Extension with lateral material accommodation - 'active' vs. 'passive' rifting. *Tectonophysics,* Vo. 266, p. 121-137.

ZIEGLER, P. A. (1975). Outline of the geological history of the North Sea. *In:* WOODLAND, A. W. (ed.) *Proceedings of the 4th Conference Petroleum Geology, Petroleum and the Continental Shelf of North-West Europe.*: John Wiley & Sons, New York, Vo. 1, p. 165–187.

ZIEGLER, P. A. (1988). *Evolution of the Artic-North Atlantic and the Western Tethys-A visual presentation of a series of paleogeographic-paleotectonic maps,* Tulsa, Oklahoma, AAPG Memoir, No. 43, p. 198.

ZIEGLER, P. A. (1993). Plate-moving mechanisms: their relative importance: William Smith Lecture 1992. *Journal of the Geological Society,* Vo. 150, p. 927-940.

ZIEGLER, P. A. & CLOETINGH, S. (2004). Dynamic processes controlling evolution of rifted basins. *Earth-Science Reviews,* Vo. 64, p. 1-50.

ZOBACK, M. L. (1992). First- and Second-Order Patterns of Stress in the Lithosphere: The World Stress Map Project. *J. Geophys. Res.,* Vo. 97, p. 11703-11728.

ZUBER, M. T. & PARMENTIER, E. M. (1986). Lithospheric necking: a dynamic model for rift morphology. *Earth and Planetary Science Letters,* Vo. 77, p. 373-383.

# APPENDIX

## Time-structure and isopach maps

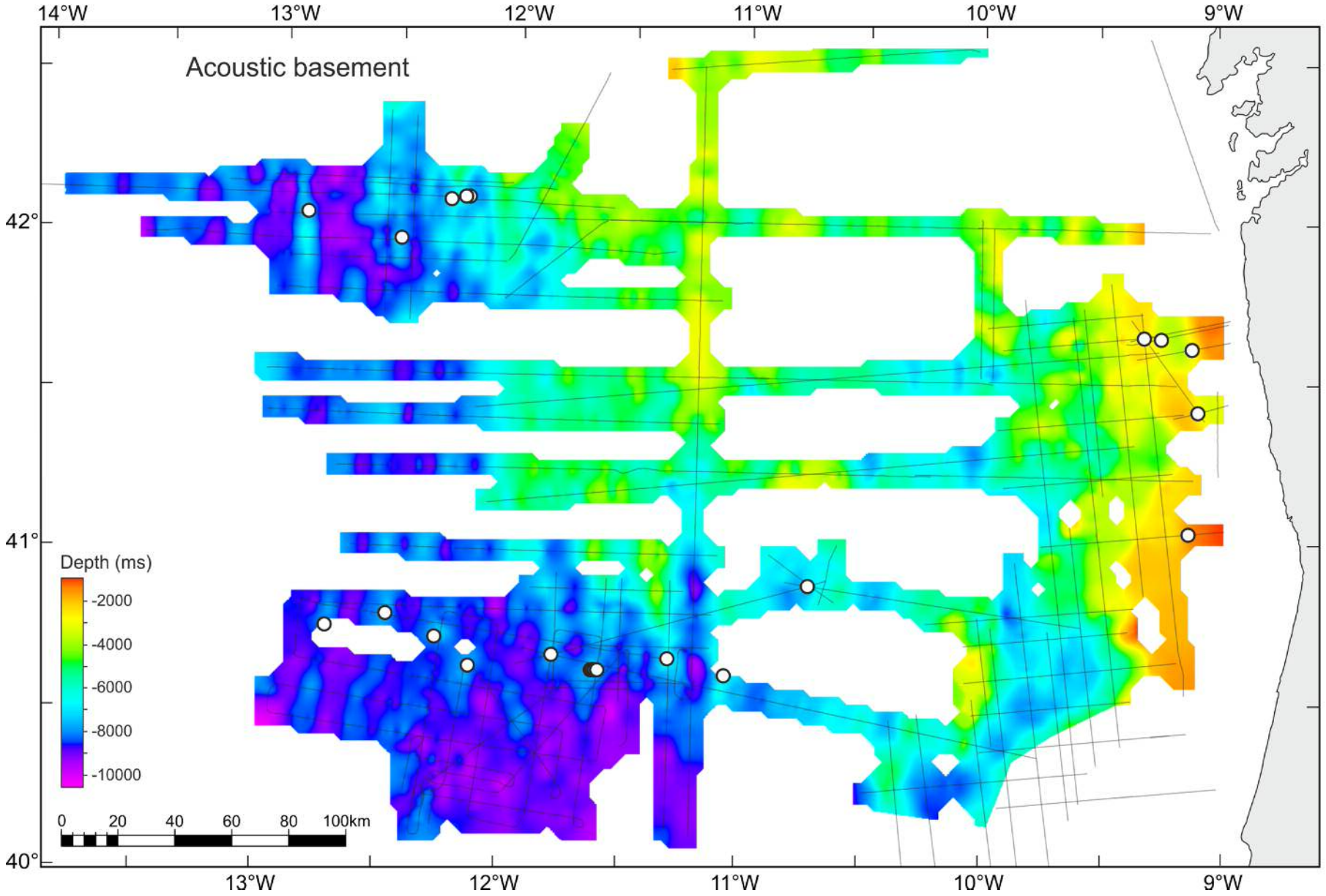
Acoustic basement
14°W
13°W
12°W
11°W
10°W
9°W
42°
41°
40°
Depth (ms)
-2000
-4000
-6000
-8000
-10000
0
20
40
60
80
100km

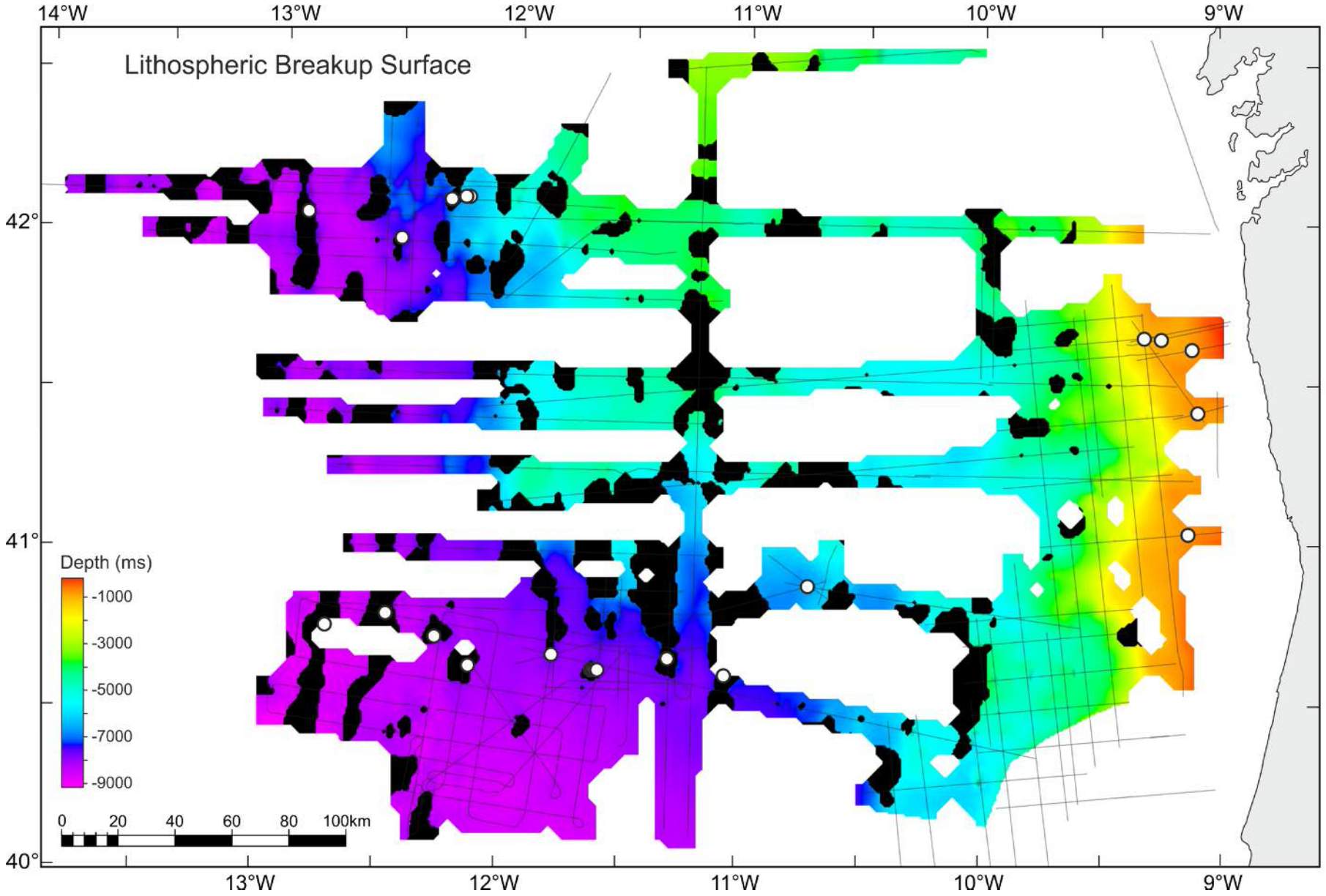
Lithospheric Breakup Surface
14°W
13°W
12°W
11°W
10°W
9°W
42°
41°
40°
Depth (ms)
-1000
-3000
-5000
-7000
-9000
0
20
40
60
80
100km

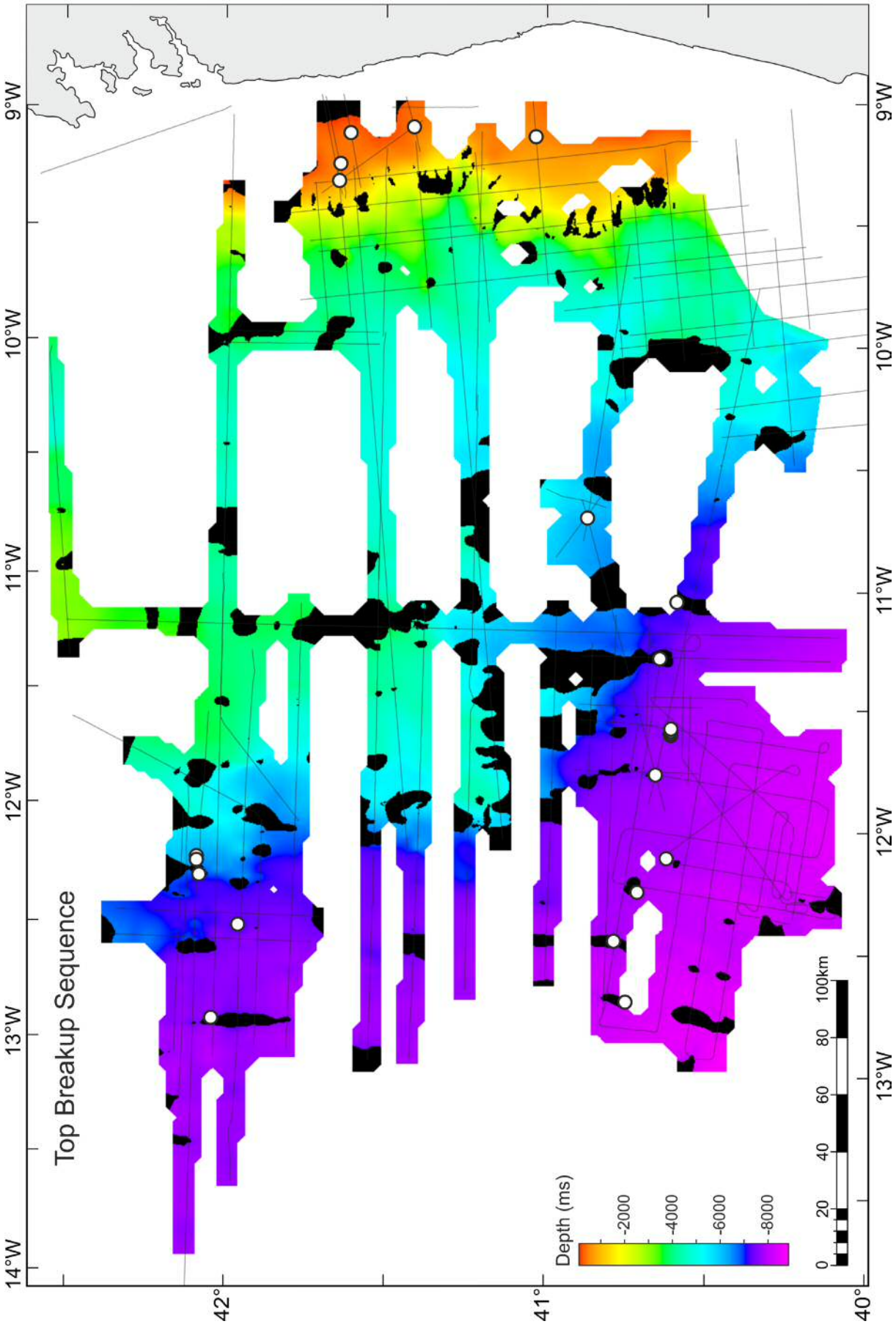
Top Breakup Sequence
Depth (ms)
-2000
-4000
-6000
-8000
0
20
40
60
80
100km
9°W
10°W
11°W
12°W
13°W
14°W
42°
41°
40°

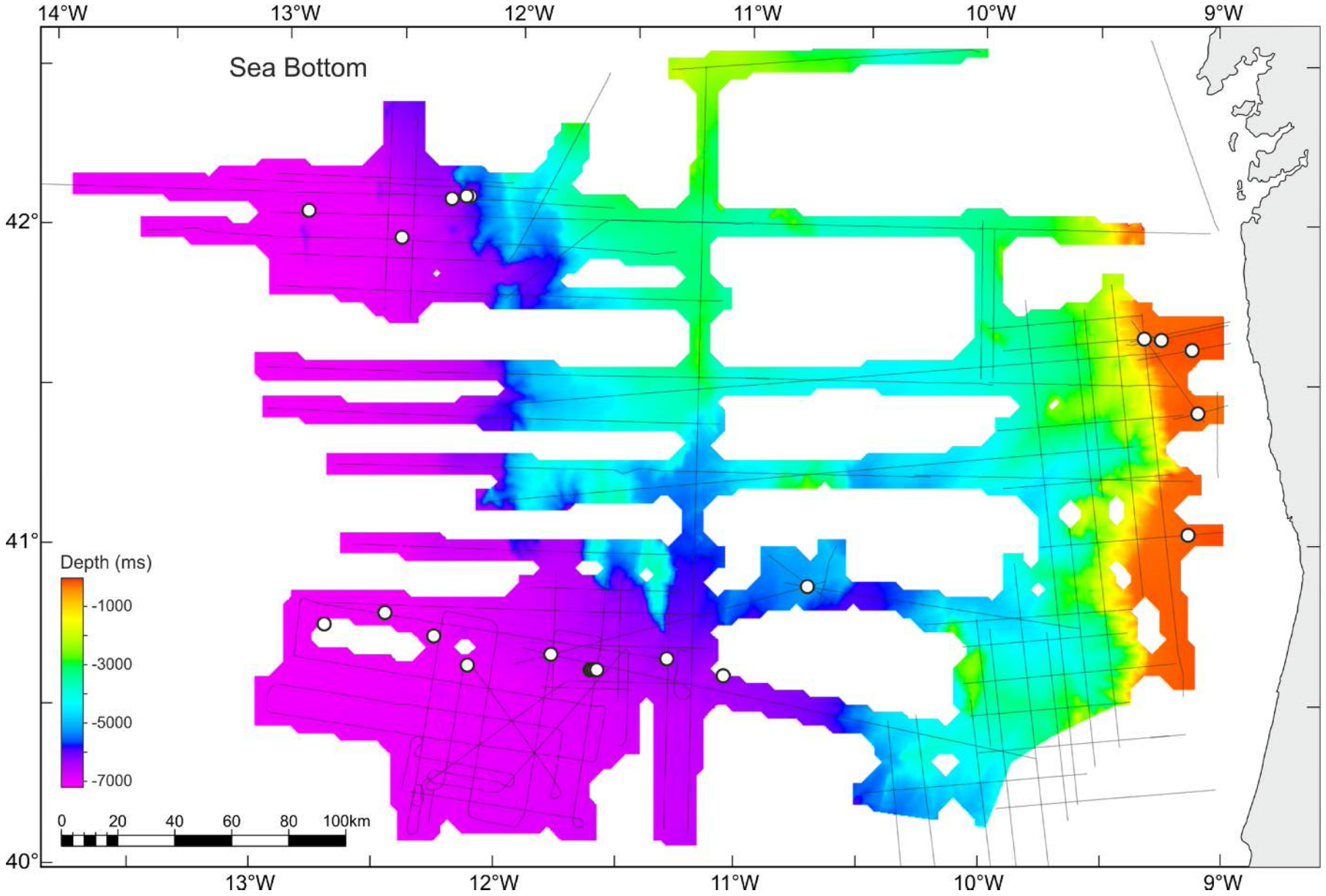
Sea Bottom
14°W
13°W
12°W
11°W
10°W
9°W
42°
41°
40°
Depth (ms)
-1000
-3000
-5000
-7000
0
20
40
60
80
100km

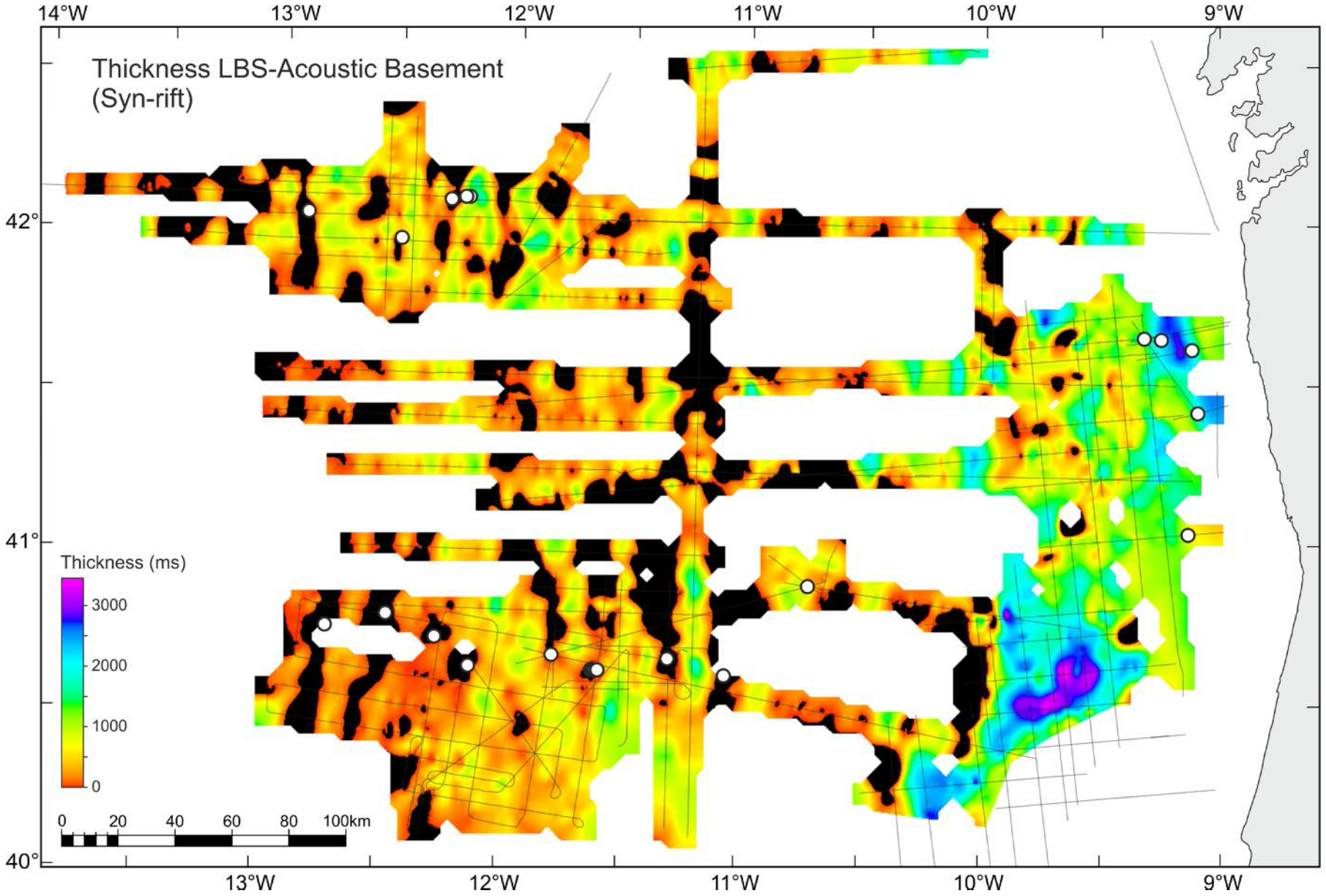
Thickness LBS-Acoustic Basement
(Syn-rift)
14°W
13°W
12°W
11°W
10°W
9°W
42°
41°
40°
Thickness (ms)
3000
2000
1000
0
0
20
40
60
80
100km

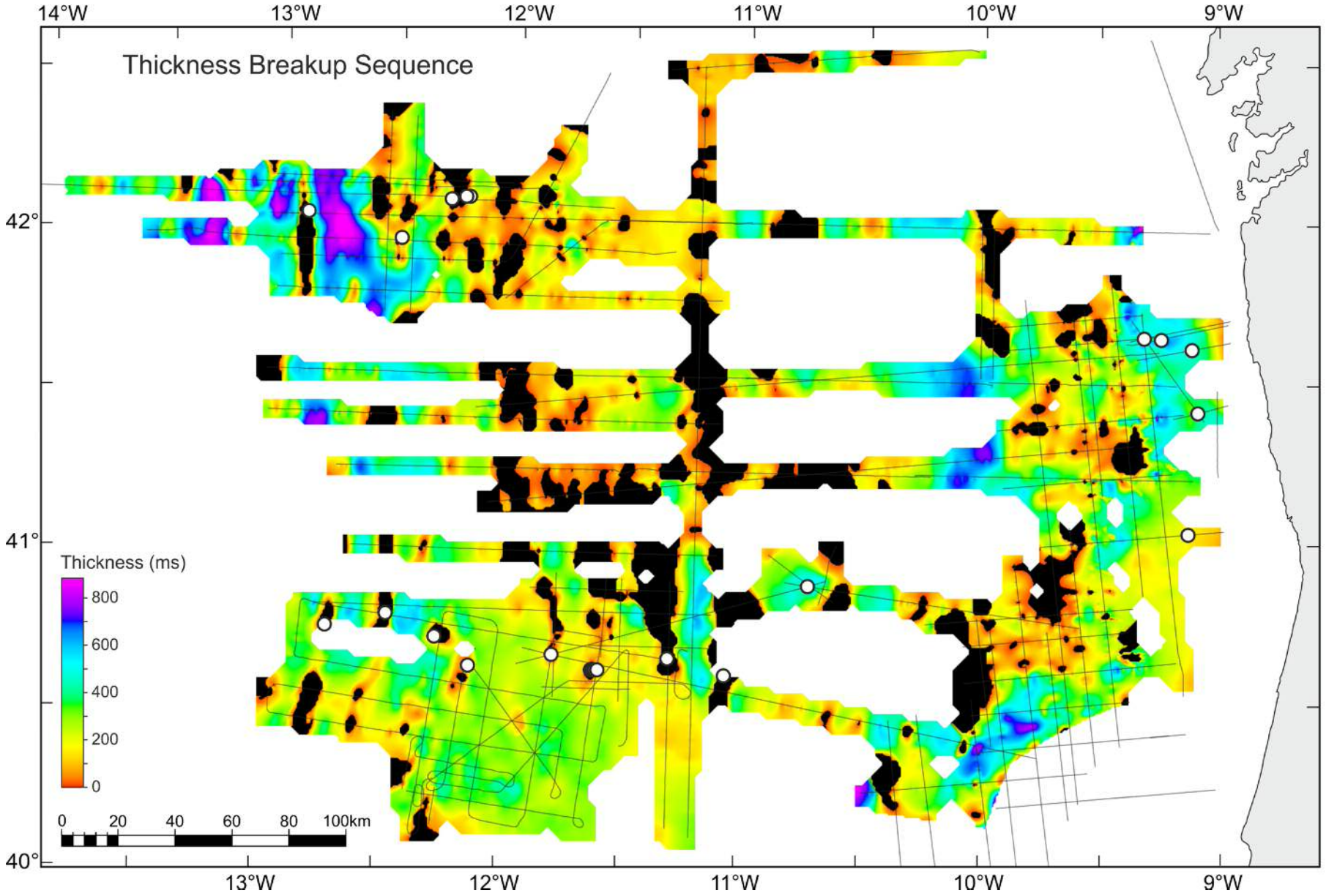
Thickness Breakup Sequence
14°W
13°W
12°W
11°W
10°W
9°W
42°
41°
40°
Thickness (ms)
800
600
400
200
0
0
20
40
60
80
100km

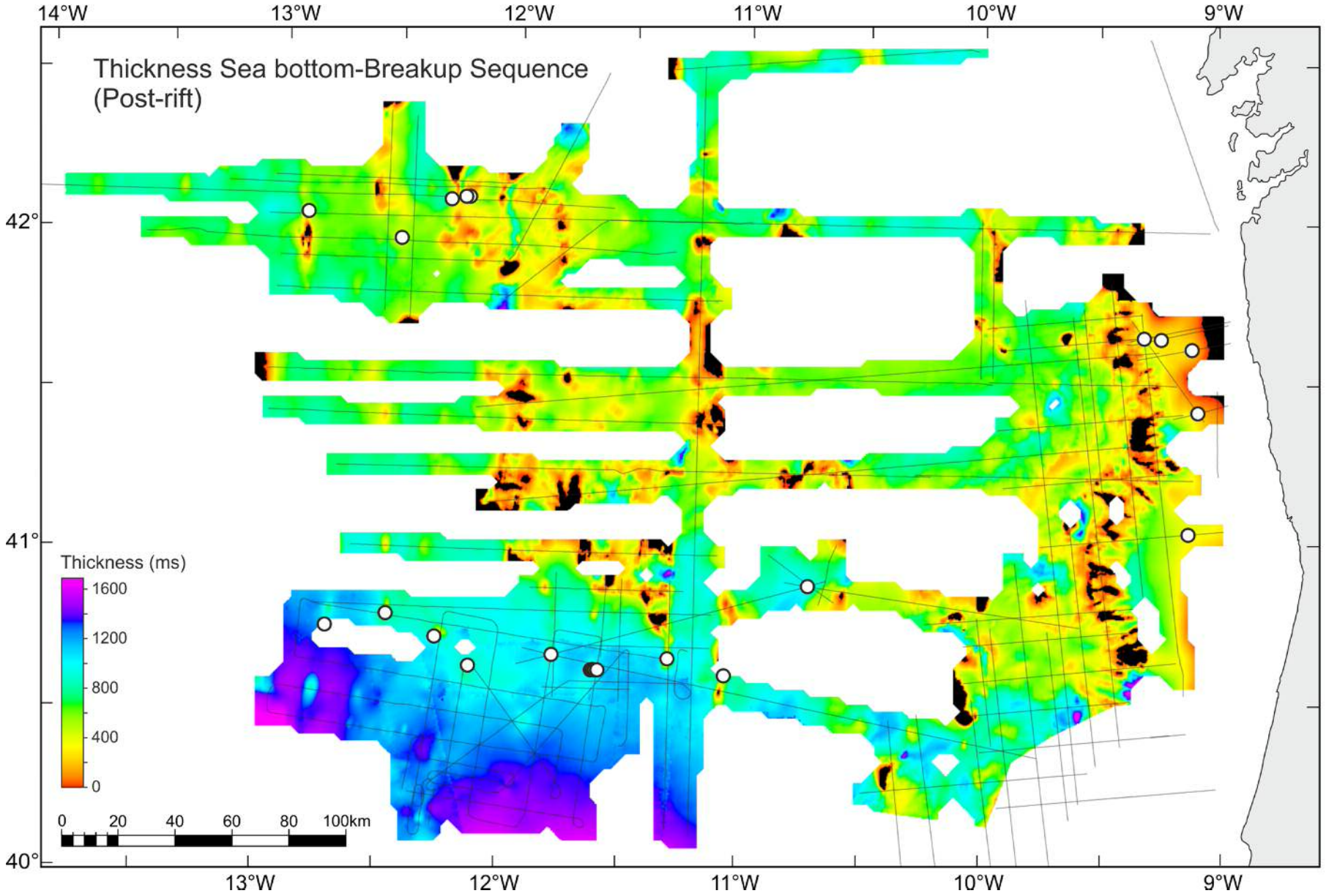
Thickness Sea bottom-Breakup Sequence
(Post-rift)
14°W
13°W
12°W
11°W
10°W
9°W
42°
41°
40°
Thickness (ms)
1600
1200
800
400
0
0
20
40
60
80
100km